



universität
wien

DISSERTATION

Titel der Dissertation

„Studies on Poplar-Endophyte-Interactions with Plant-
Growth-Promoting Effects“

Verfasserin

Mag. Anne Mette Hanak

angestrebter akademischer Grad

Doktorin der Naturwissenschaften (Dr. rer. nat.)

Wien, 2014

Studienkennzahl lt. Studienblatt: A 091 438

Dissertationsgebiet lt. Studienblatt: Dr.-Studium der Naturwissenschaften Botanik

Betreuer: Univ.-Prof. Dr. Wolfram Weckwerth

TABLE OF CONTENTS

1	INTRODUCTION.....	10
1.1	POPULUS AS A MODEL SYSTEM PLANT	10
1.2	POLYPLOIDY IN PLANTS	11
1.3	ENDOPHYTES AND THEIR HOSTS	13
1.4	NITROGEN ASSIMILATION, THE NITROGEN CYCLE AND NITROGEN USE EFFICIENCY (NUE)	16
1.5	SALT-STRESS	19
1.6	AIMS OF THE PHD THESIS	20
2	MATERIAL AND METHODS.....	21
2.1	THE ENDOPHYTES <i>PAENIBACILLUS</i> SP. P22 AND <i>PAENIBACILLUS DURUS</i>	21
2.1.1	Culturing <i>Paenibacillus</i> sp. P22 and <i>Paenibacillus durus</i>	23
2.1.2	Microscopic analyses of <i>Paenibacillus</i> sp. P22 and <i>Paenibacillus durus</i>	23
2.1.3	Genome annotation of <i>Paenibacillus</i> sp. P22.....	24
2.2	BIOMASS PRODUCTION WITH POPLAR HYBRID AF2, AF8 AND MONVISO	25
2.2.1	Experiment on Hydroponics	26
2.2.1.1	Cultivation and inoculation	26
2.2.2	Experiment on vermiculite / perlite.....	28
2.2.2.1	Inoculation after rooting.....	28

2.2.2.2 Direct inoculation	28
2.3 DIFFERENT EXPERIMENTS ON <i>IN-VITRO</i> CULTURED POPLAR HYBRIDS	29
2.3.1 Culturing of poplar hybrid 741 under <i>in-vitro</i> conditions.....	29
2.3.2 Bacterial inoculation of poplar hybrid 741 with <i>Paenibacillus</i> sp. P22	30
2.3.3 Allocation of bacteria using different microscopic techniques	31
2.3.3.1 REM / TEM / ESEM / TISH	31
2.3.4 Media screening of poplar hybrid 741, poplar Hybrid Esch 5 2N, 4N and 2N4N	33
2.3.5 <i>In-vitro</i> culturing of poplar clones AF2, AF8 and Monviso.....	33
2.3.5.1 Surface sterilization and micropropagation	33
2.4 ACCLIMATIZATION OF DIFFERENT POPLAR CLONES.....	34
2.5 DIFFERENT EXPERIMENTS WITH POPLAR HYBRID OF VARIOUS PLOIDY LEVELS	35
2.5.1 Flow cytometric measurements and microscopic analysis	35
2.5.2 Proteomic profiling using LTQ-Orbitrap MS/MS shotgun.....	35
2.5.2.1 Protein extraction	35
2.5.2.2 Protein digestion and desalting.....	36
2.5.2.3 LTQ-Orbitrap MS/MS shotgun proteomics.....	36
2.5.2.4 Data mining	37
2.5.2.5 Statistical analysis	37
2.6 <i>CHLAMYDOMONAS REINHARDTII</i> CC503 CW92 MT+	38

2.6.1	Culturing <i>C. reinhardtii</i>	38
2.6.2	Lipid staining	39
2.7	<i>MEDICAGO TRUNCATULA</i> `JEMALONG A17`	40
2.7.1	Cultivation of <i>Medicago truncatula</i> and <i>Sinorhizobium meliloti</i>	40
2.7.2	Microscopic analysis of shoot, root and leaves under different growth conditions	41
3	RESULTS.....	43
3.1	<i>PAENIBACILLUS</i> SP. P22 AND <i>PAENIBACILLUS DURUS</i> UNDER DIFFERENT CULTUR CONDITIONS	43
3.1.1	Microscopic analyses of <i>Paenibacillus</i> sp. P22 and <i>Paenibacillus durus</i>	49
3.1.2	Genome annotation of <i>Paenibacillus</i> sp. P22.....	51
3.2	EXPERIMENT OF BIOMASS WITH POPLAR HYBRID AF2, AF8 AND MONVISO	52
3.2.1	Hydroponic culture experiment.....	52
3.2.1.1	Poplar hybrid AF2	52
3.2.1.2	Poplar hybrid Monviso.....	55
3.2.1.3	Poplar hybrid AF8	57
3.2.2	Vermiculite / perlite culture with inoculation after rooting.....	60
3.2.2.1	Poplar hybrid AF2	60
3.2.2.2	Poplar hybrid Monviso	64
3.2.2.3	Poplar hybrid AF8	68

3.2.3 Vermiculite / perlite culture with direct inoculation.....	72
3.2.3.1 Poplar hybrid AF2	72
3.2.3.2 Poplar hybrid Monviso.....	73
3.2.3.3 Poplar hybrid AF8	74
3.3 DIFFERENT EXPERIMENTS IN <i>IN-VITRO</i> CULTURED POPLAR HYBRIDS.....	77
3.3.1 Growth promoting effects of <i>Paenibacillus</i> sp. P22 inoculated in poplar hybrid 741 in <i>in-vitro</i> culture	77
3.3.2 Allocation of bacteria in <i>in-vitro</i> poplar hybrid 741	82
3.3.3 Media screening on different poplar clones	84
3.4 <i>IN-VITRO</i> GROWTH OF POPLAR CLONE AF2, AF8 AND MONVISO	87
3.5 ACCLIMATIZATION OF DIFFERENT POPLAR HYBRIDS.....	88
3.6 MICROSCOPIC, FLOW CYTOMETRIC AND PROTEOMIC MEASUREMENTS ON FIELD GROWN 2N, 4N AND 2N4N POPLAR HYBRIDS	92
3.6.1 Flow cytometric measurement.....	92
3.6.2 Anatomic studies.....	94
3.6.3 Chloroplast counts in stomata cells	98
3.6.4 Proteome analysis of leaf samples.....	100
3.6.4.1 PCA and ICA using log ¹⁰ - and z-transformation	100
3.6.4.2 Data analysis using ProtMAX	105
3.6.4.3 Data analysis using UniProt.....	106
3.6.4.4 Diploid poplar hybrid L447.....	109

3.6.4.5	Tetraploid poplar hybrid L447	112
3.6.4.6	Mixoploid poplar hybrid L447	113
3.6.4.7	PCA, Heat map and Anova analysis of selected proteins I	115
3.6.4.8	PCA, Heat map and Anova analysis of selected proteins II	121
3.7	SYNCHRONIZATION OF <i>CHLAMYDOMONAS REINHARDTII</i> CC 503 M ⁺	142
3.7.1	Lipid experiments of <i>Chlamydomonas reinhardtii</i>	143
3.8	<i>MEDICAGO TRUNCATULA</i> `JEMALONG A17`	145
3.8.1	Morphology and stomata imprint.....	145
3.8.2	Anatomic analyses of vegetative organs of <i>Medicago truncatula</i>	
	150
4	DISCUSSION	154
4.1	COMPARISON OF <i>PAENIBACILLUS</i> SP. P22 AND <i>PAENIBACILLUS DURUS</i>	154
4.2	BIOMASS OF AF2, AF8 AND MONVISO	155
4.3	LOCALIZATION OF <i>PAENIBACILLUS</i> SP. P22 IN <i>IN-VITRO</i> GROWN POPLAR HYBRID 741.....	
	156
4.4	MEDIA-SCREENING	156
4.5	ANATOMIC SECTIONS OF 2N, 4N AND 2N4N LEAVES	157
4.6	CHLOROPLAST COUNTS IN STOMATA CELLS.....	157
4.7	PROTEOME PROFILING OF POPLAR HYBRID L447	157
4.8	ANALYSIS OF <i>CHLAMYDOMONAS REINHARDTII</i>	159
4.9	STRESS-RELATED EXPERIMENTS ON <i>MEDICAGO TRUNCATULA</i>	159

5	LIST OF ABBREVIATIONS	160
6	LITERATURE.....	162
7	ACKNOWLEDGEMENTS.....	185
8	APPENDIX.....	186
8.1	ZUSAMMENFASSUNG	186
8.2	ABSTRACT	188
8.3	CURICULUM VITAE	190

1 Introduction

1.1 POPULUS AS A MODEL SYSTEM PLANT

Published molecular data (116, 173) estimated the age of the angiosperms as 200 - 420 mya years. Bell et al. (16) established new gene analysis and discovered that the angiosperms have their origins in the early Jurassic to early Cretaceous time (139 mya). Angiosperms can be found in any terrestrial ecosystem. They have colonized both fresh- and saltwater habitats over the last thousand years. The understanding of the major branching patterns and clades within the angiosperms has been based on analyses of multiple genes sampled from multiple genomes, analyses of morphology and duplicated genes (16). Once a full genome has been assembled, the main challenge lies in its annotation, the identification of the protein-coding genes and other functional units that are encoded in the genome (134). Based on the fact that woody plants are one of the largest and oldest living organisms, they are inimitably objects for biological studies (111). After the genus *Pinus* (Gymnospermae), *Populus* (Angiospermae) has been the second most studied tree in biotechnology and the most in genetic modification so far (108). The completion of the genome sequence (208) of *Populus trichocarpa* now offers various genetic, genomic and biochemical tools for researchers to understand tree physiology and apply this knowledge also in biotechnology as poplar is a major energy crop (101, 235).

Poplar belongs to the genus of the Salicaceae and is located over the northern hemisphere but there are differences in ecological requirements at species level. It has emerged about 40 - 65 million years ago (101). Beside the presence of naturally occurring hybrids, poplar can be organized into nearly 75 species (38, 52, 166). These species are arranged into six sections based on morphological and ecological characteristics (174). Among these sections, there are balsam poplars, black poplars, aspen and white poplars which have increasing importance for plant breeding, especially for the current biomass production in temperate climates (123). *Populus tremuloides* is the most widespread tree species in North America. Its rapid growth originates the most wood-based biomass out of any other plant species (38). Poplar is widely used for timber, pulp and paper (167). Because of the initiating adventitious

roots of poplar stem cuttings, they have been established by large-scale propagation of hardwood cuttings (85).

Down to the present day the demand for forest products increased dramatically and the high energy prices lead to reconsider in providing wood as a source of biofuel (203). Resultant to this the forest industry cannot continue to rely on the depletion of natural forests. It is crucial to find another way to replace the natural population of trees with cultivated varieties (149). Concerning the new energy sources genetic improvements in poplar species has been studied in China over the past 10 years (126). For Italian farmers the short rotation forests (SRF) plantations of hybrid poplars are very attractive because of the producing wood chips for energy production. In 2003 a field experiment was conducted across northern Italy with new clones for SRF on 3 different soils. Preliminary results showed that in all sites, survival was high for almost all clones (165). Wood boilers for homeowners or business are already in use. In longer term, wood can serve as a source of lignocellulose to produce bioethanol and proposed for the production of biofuel (203). In addition to the ethanol production there are hybrid poplars which are chosen for plantation because they are very fast growing trees (63). Bioenergy or biofuel crops are annual or perennial plants which are cultivated to produce liquid, solid or gaseous forms of energy. Poplar is a bioenergy crop which is already used worldwide. It can be cultivated on low quality soils, including contaminated soils, floodplain habitats as well as nutrient poor and saline habitats (224).

1.2 POLYPLOIDY IN PLANTS

Polyploidy is the heritable condition of possessing more than two complete sets of chromosomes (Fig. 1). Polyploids are common among plants, as well as some groups of amphibians and fish. Recent findings in genome research indicate that many species, that are currently diploid, evolved from polyploidy ancestors (228). These species are then called paleopolyploids. The highest incidence of polyploidy known can be found in Hawaiian flora, and most Hawaiian species are paleopolyploid, which have evolved polyploidy prior to the dispersal of their ancestors to Hawaii (27). Polyploidy in particular has become a major focus of biosystematic research and has already been long recognized as an inseparable part of angiosperm biology (130, 204). It is a main factor in higher plant evolution leading to the formation of new species (3). Polyploidy can show new phenotypes, new niche

invasion and ecological diversification. Polyploidy have a state of fixed heterocygosity that raise a big reservoir of new alleles for mutation, selection and gene evolution (4). Out of evolutionary sight polyploidy is a major feature of many plants, at temporal scales ranging from ancient to contemporary and with profound effects at scales ranging from molecular to ecological (5). Comparative and genome sequence analyses show, that some plant species e.g. Poplar or *Arabidopsis thaliana* are recent diploidized polyploids (23). Polyploid genomes may undergo changes in genome structure through genetic and epigenetic changes, so that over the time polyploids have become diploidizes. This means that they react like diploids in cytogenetically and genetically manner (33). The cell volume is proportional to the amount of DNA which can be found in the nucleus of the cell. If there is a doubling of the cell's genome there is a 1.6 fold increase in the surface area of the nuclear envelope (144). This fact can disrupt the positioning of telomeric and centromeric heterochromatin and so disturb the mediate interaction between the chromosomes and nuclear components (69). In the 1930's it has become a new breeding aim to produce triploid trees out of tetraploide explants. They showed a high growth performance and resistance traits (121, 157, 161). To become a triploid plant there are different methods but the method with suitable results is the colchicine treatment (62). Colchicine is a mitotic poison which inhibits microtubule polymerization and so disturbs the chromosome segregation during meiosis. Polyploidy arises through mitotic or meiotic misdivisions and unreduced gametes by nondisjunction of chromosomes in the germ line (120) whereby the entire chromosome set is multiplied. This genomic plasticity has a gradient effect on the proteome and the metabolome (32).

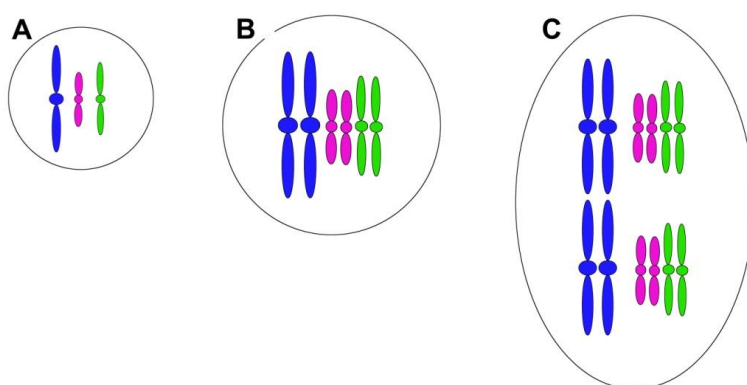


Figure 1: Number of chromosomes in nucleus. (A) Haploid = N. (B) Diploid = 2N. (C) Tetraploid = 4N.

1.3 ENDOPHYTES AND THEIR HOSTS

In the last years the interest studying bacterial population structure in soil, rhizosphere has increased because of the positive response of many plants to inoculation with suitable plant growth promoting bacterial strains (180). Organisms with photosynthetic activity evolved symbioses with a wide range of microorganisms (88). About 300 000 higher plant species existing on earth has at least one individual host living endophyte. Only a handful has ever been fully studied of their endophytic biology (209, 239). Endophytic bacteria were also detected in trees like elm, pine, oak, citrus, coffee (8, 18, 73, 153, 231) and poplar and not only in horticultural plant (109, 122) species where the focus of interest had turned.

Endophytic bacteria are bacteria that reside in the living cells of the host plant without causing any harm (79, 82, 99, 139, 150, 197). It has been shown that they have several mechanisms by which they can support plant growth by providing phytohormones, low-molecular compounds or enzymes (70, 80, 115). They can also improve plant growth via the fixation of nitrogen (diazotroph) (46, 223, 229). Plant growth promoting mechanisms, which comes directly from the endophytic bacteria may involve the production of growth regulators, nitrogen fixation and the production of sugar sensing mechanisms in plants (10, 19, 72, 195). Many well-known plant pathogens had been identified to be typical endophytic bacteria that cause no disease symptoms, but could become pathogenic under certain conditions or within different host genotypes (150). Some endophytes can be more aggressive colonizers than others in the host plant and as a result they can displace others. Sessitsch et al. investigated that potato plants suffering from light deficiency compared to healthy robust plants show similar endophytic populations. Nevertheless is the diversity of endophytes significantly higher in healthy plants then in stressed plants (196).

Beside, as a bioenergy resource, poplar became interesting for phytoremediation purposes and a target species for genetic transformations (227). Inoculation species used for bioenergy are therefore an attractive option to increase productivity of biofuel feedstocks. Rogers et al. investigated the effect of inoculating hard wood cuttings of *Populus deltoides* Bart. x *Populus nigra* L. clone OP367 with *Enterobacter* sp. 638 (178). They could show that after 17 weeks inoculated plants had a greater, 55% in total, biomass than non-inoculated control plants.

The bacteria enter the plants via germination radicles (71), stomatas (179) at sites of the epidermal / exodermal damage, that naturally occurs due to development of lateral roots, through for e.g. root hairs (206). It is believed that root adhesion of plant associated bacteria occurs in different steps since the end of the roots are the primary target for endophytic invasion of plants. Inside the plant the endophytes colonize the plant systematically by allocating through the vascular system or the apoplast (95, 100, 172, 181). The endophytic populations in the inside of the host have been observed to grow between 2.0 and 7.0 log¹⁰ cells per gram of fresh tissue (74). The maximum bacterial population is near the root surface or in the root interior and decrease from the roots to the stem and the leaves where bacterial density is lowest (83, 114, 124, 135, 156, 171). After the bacteria have entered the plant, they have to establish themselves, so that they can produce several plant regulating compounds (9, 112, 184). The variety of bacteria that has been reported as endophytes includes genera of Alpha-, Beta- and Gammaproteobacteria, Actinobacteria, Firmicutes and Bacterioidetes (13, 57, 103, 129, 151, 219). Scientists at the U. S. Brookhaven National Laboratory have decoded the genome of a plant-dwelling microbe which could increase plant growth by 40 percent (217). It is believed that root adhesion of plant associated bacteria occurs in different steps because the end of the roots, are the primary target for endophytic invasion of plants. True endophytes may also be identified by their capacity to reinfect disinfected seedlings (181). Several genes were detected from *Enterobacter* sp. 638 which are encoding proteins involved in the putative adhesion to the root (218).

Growth promoting bacteria (GPB) are frequently artificially applied on seeds. It is not known precisely whether the applied microorganisms stay on the seed surface or reside the inner seed tissue (83). The isolation can be done by surface disinfection or internal plant tissue extraction (226).

Tissue culture has been used to reduce or to eliminate endophytes in their host for a re-inoculation. Inoculants seem to be successful in micropropagated plants, if there are few or no other microorganisms inside. There could be and there already are plantlets which are inoculated, so they are more vigorous and have increased drought-resistance and increased resistance to pathogens, less transplanting shock and lower mortality (15, 136, 185).

It is assumed that long living plants like trees create their own kind of endophytic spectra accordingly to the environmental condition which leads to a higher effectivity of the phenotypic plasticity in bad environmental situations (114, 156, 171). These plant-microbe interactions have already been main subjects of different studies (30, 183, 200). Seeds from Norway spruce had been collected to detect the presence of endophytes. This was carried out with culturing methods and direct amplification of the 16S rDNA gene. *Pseudomonas* and *Rhizobium* bacteria, knowing plant-associated bacteria with growth promoting potential, were located in Norway spruce seeds. It is possible that the plant seeds could serve as a vector for transmission of beneficial bacteria (26). First in the late 1980's evidence has been found that some Brazilian varieties of sugarcane are able to be long term cultivated with low N-fertilizers inputs because of N₂-fixing bacteria which are associated with the plants (21). In sweet potato plants have been several tests on identifying bacteria with different abilities for e.g. fixing nitrogen, producing indole-acetic-acid and exhibit stress tolerance. They found different bacteria and could distinguish whether they are able to fix nitrogen or produce IAA: They tested them on potato cuttings and these studies indicated that endophytes of sweet potato plants are beneficial to plant growth (107). Some species of the genus *Paenibacillus* are known plant hormone producers such as auxins and cytokinins. They can also produce peptide antibiotics as well as different hydrolyzing enzymes (189). Auxin is a known plant hormone and synthesized by all higher plants (128). The predominant form of auxin in plants is indole-3-acetic-acid (IAA). Many plant-associated soil bacteria are known to synthesize auxin, especially IAA which leads to the suggestion that this could be part of a strategy to manipulate the growth of host plants (205). Some bacteria probably use the exuded tryptophane from the plants as a precursor for auxin synthesis (106). There is evidence that auxin synthesis by bacteria influence root architecture in non-nodulating plants (140). For example, endophytic bacteria of red clover seem to be responsible for the allelopathic effects over maize, causing reduced plant emergence and plant height (210).

1.4 NITROGEN ASSIMILATION, THE NITROGEN CYCLE AND NITROGEN USE EFFICIENCY (NUE)

Nitrogen gas comprises about 78% of the earth's atmosphere. Plants must absorb nitrogen in form of ammonium ions and nitrate ions to build amino acids and building blocks of proteins. Each nitrogen molecule has strong triple bond holding the two atoms together and this bond is very hard to break. Breaking this atmospheric nitrogen is only possible at high temperatures or by bacteria in the soil. But plants and animals need a continual supply of nitrogen since this is an essential macronutrient. Since nitrogenase is very oxygen-sensitive it is obvious that some endophytes need a microaerobic environment for an efficient nitrogen fixation. Doty et al. have shown that some endophytes need an association with the plant before nitrogen fixation occurs (49). Ammonium and Nitrate are absorbed active into root cells through some high-affinity transport systems for NO_3^- and NH_4^+ (78). Millard et al. (148) suppose that the N acquisition from the soil by tree roots is regulated to the current nitrogen demand of the plant which is needed for growth and development. As well as the nitrogen storage the whole plant requires. Internal factors (201) such as leaf and root development, senescence and external factors, like heat, drought, salinity (77) and atmospheric CO_2 and O_3 concentrations (190) determine these requirements. Storage and re-mobilization of nitrogen during the growing season is both in annual and perennial plants possible (174).

The plant life cycle with attention to nitrogen can be roughly divided into two main phases which can overlap in some species. The vegetative phase where the leave and root development occurs and they behave like sink organs for assimilation of inorganic nitrogen and the synthesis of amino acids (87). A later stage of plant development, generally starting after flowering, the remobilization of the nitrogen accumulated by the plant takes place (137) which also can occur before flowering for the synthesis of new proteins in developing organs (118). The assimilatory phase where the ammonium incorporated into free amino acids has to be immediately re-assimilated into glutamine and glutamate (162). In trees, nitrogen can be stored in form of proteins like vegetative storage proteins (37) and amino acids such as arginine, glutamine and asparagine, which are of particular significances soluble storage amino compounds. Plants are able to use chemical nitrogen in different forms like simple inorganic compounds or polymeric N forms (159).

The doubling of agricultural food production over the last decades has multiplied the increase in the use of nitrogen fertilizers. This has a tremendous impact on the diversity and functioning of the on-agricultural neighboring bacterial, animal and plant ecosystem (86). The highest impacts are the eutrophication of marine (146) and freshwater ecosystems (76) when the nitrogen fertilizers are leaching into the water. Therefore it is of major importance to identify the critical steps to control plant nitrogen use efficiency (NUE). To maximize the nitrogen use efficiency and to prevent the loss of nitrogen to the environment it is essential to understand the nitrogen release from fertilizers relative to plant growth (Fig. 2).

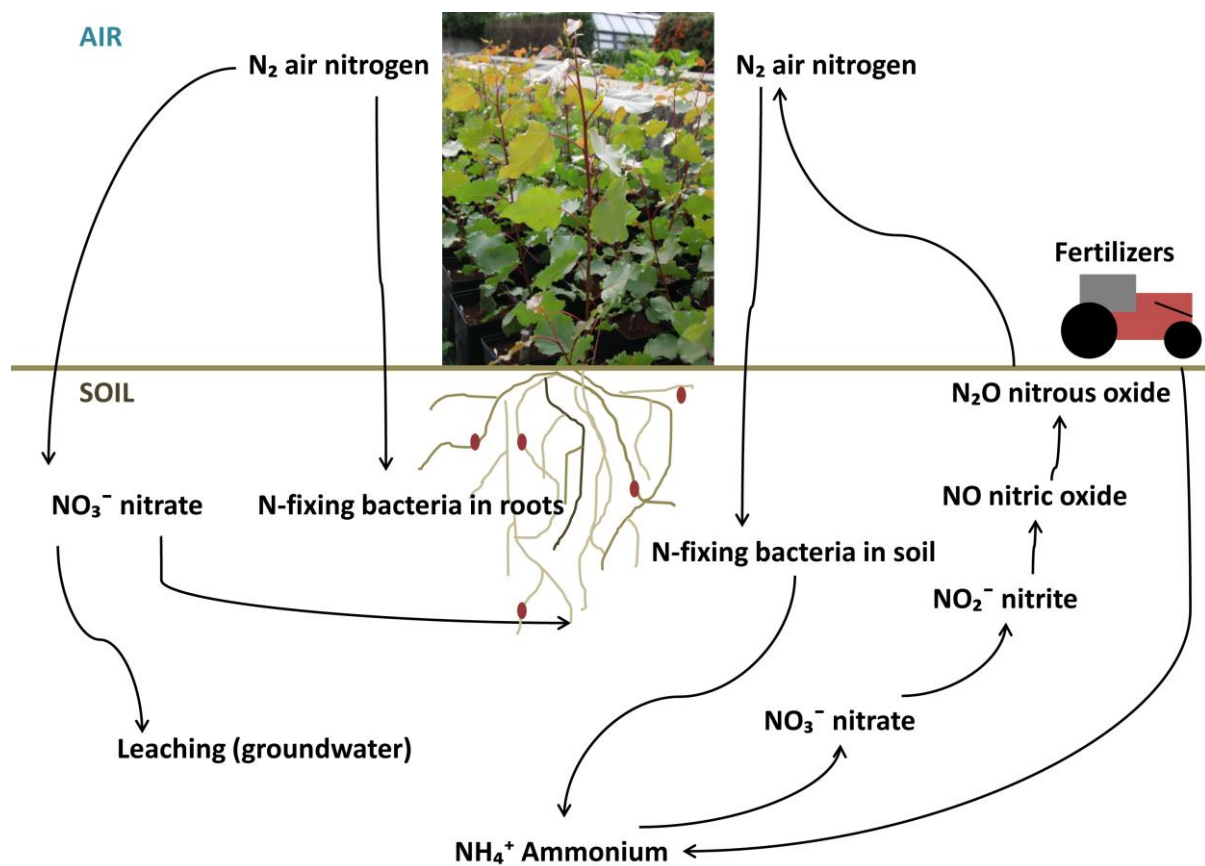


Figure 2: Nitrogen cycle

In 1982 Moll et al. (155) defined NUE as being the benefit of grain per unit of available nitrogen in the soil, including the N present in soil and the fertilizers (G_w/N_s).

$$NUE = G_w/N_s$$

This NUE consists of two steps: the uptake efficiency, which is the ability of the plant to take up the nitrogen from the soil and the utilize efficiency which is the ability to use the nitrogen for biomass production. Still this way of calculating the NUE is difficult because of several factors. All applied fertilizers N are not available to the plant and additional to the applied fertilizer N there is the N from the soil. For calculating the NUE of a crop it should be considered as a function of climate conditions, soil texture, interactions between soil and bacterial processes (25) and the nature of organic or inorganic nitrogen sources (192). Huggins et al. (93) modified the formula of NUE of Moll. They added the term N_{av} to represent plant available nitrogen as the difference between N supply and N losses associated with volatilization, de-nitrification, leaching and immobilization. The N supply is the available N to plants that season (N_{av}/N_s).

$$N = N_{av}/N_s$$

If there is a higher N uptake in plants, there is less soluble N in the soil that could be immobilized or lost (64). Therefore in field experiments the plant available N may be calculated as the total N in plant tissues plus the remaining inorganic soil nitrogen within the root zone NUE (G_w/N_{av}) without N losses.

$$G_w/N_{av}=N_{av}/N_s$$

There is also a possibility of measuring the grain nitrogen accumulation efficiency (GNACE), which is the amount of N in the grain divided by the N supply (N_g/N_s).

$$GNACE = N_g/N_s$$

Another important factor is the nitrogen harvest index, which is the ratio of N present in grain to total plant N content (N_g/N_t). This is analogue to the harvest index (HI), the ration of grain to total biomass. This is a measurement of N placing efficiency. The main components to contribute the overall NUE are N uptake efficiency and N utilization efficiency (40). The N release from such fertilizers depends on the microbial processes of N mineralization and nitrification, which on the other hand are influenced by the environmental conditions, soil properties, C/N ratio of the fertilizer and the lignin content of the plant itself. The common method is the measuring of the net change in nitrate and nitrite concentrations. But it does not account for the inorganic N immobilized in microbial biomass or lost through denitrification during soil

incubation (132). There are some grass species which appear to be able to obtain fixed nitrogen through symbiotic relations with bacteria. This way of nitrogen fixation is a characteristic in plants which can be found on infertile soils that have less available nitrogen. This host-bacteria association is best studied in dune grass (*Ammophilla arenaria* and the bacteria *Gluconoacetobacter*). A ^{15}N isotope dilution experiment indicated that up to 80% of the plant's nitrogen was supplied by nitrogen fixation from the endophyte (39). Renneberg et al. (174) published that poplar plants reduced total biomass when they were treated with a medium containing ammonium as a nitrogen source.

1.5 SALT-STRESS

One major environmental factor which is limiting plant growth and productivity is salinity (164) which is visible in molecular, biochemical and physiological level in plants (45, 56, 84). A high salt-stress can disrupt homeostasis in water potential and ion distribution in plants. To define the term 'stress' in plants it is safe to say that salt is provided in any external factor that influences plant growth, productivity, reproducible capacity and survival negatively. These factors can be divided into two main categories: abiotic or environmental stress factors and biotic or biological stress factors (176). Abiotic stress such drought, salinity and temperature are the most affected stress terms in plant growth and productivity, while drought the major limitation to plant growth has (96). The plant responses to different stresses can be found in cellular, physiological and on transcriptome levels (12). Analyses of gene expression has indicated that salt can stimulate the expression of nitrate transporters (168). Currently because of the high interest of plant stress response there are used large-scale genomics approaches to identify which genes are involved in different regulating processes (2). There have been some transgenic strategies to avoid these problems with reactive oxygen species (ROS) or osmolytes (241). Elthing et al. (55) tested the interaction of nitrogen nutrition and salinity in grey poplar and discovered that the N nutrition dependent effects of salt exposure were more intensive in leaves and roots. So they suppose that poplar plantations which were nitrate fertilized should grow on saline soil. High salinity concentration can also trigger an increase the level of plant hormones such as ABA and cytokines (220).

1.6 AIMS OF THE PHD THESIS

Poplar is an important energy crop and currently one of the most investigated model systems for tree biology. Furthermore, poplar plants have been used as a model system for tree-endophyte-interaction studies with the purpose to understand mechanisms of bacterial plant-growth-promotion. As already mentioned endophytic bacteria colonize the internal tissue of their host plants and are able to build root nodules in some legumes. They have been detected in nearly all plants studied under field conditions as well as in many tissue cultures without showing any signs of pathogen infection. The function and effects of endophytes on host plants are manifold, including plant growth promoting effects, capacity of controlling pathogens and increased stress resistance. The mechanism of poplar-endophyte-interaction was investigated by studying a recently isolated poplar-specific endophyte, *Paenibacillus* sp. P22. Scherling et al. (188) have published that *Paenibacillus* sp. P22 has a beneficial effect on the growth of a poplar hybrid 741 ($\text{♀}[\textit{Populus alba} \times (\textit{P. davidiana} + \textit{P. simonii}) \times \textit{P. tomentosa}]$) grown under *in-vitro* conditions.

The aim of the thesis is to understand the molecular mechanisms of these growth promoting effects in more detail by sequencing the genome of this endophyte. Furthermore the effect of *Paenibacillus* sp. P22 on the growth and anatomical parameter of different poplar hybrids (AF2, AF8, Monviso) cuttings is studied. Additional studies on poplar as an important energy crop are conducted on the effects of polyploidy on the proteome level. Furthermore *Medicago truncatula* and *Chlamydomonas reinhardtii* are investigated with respect to abiotic stress conditions.

2 Material and Methods

2.1 THE ENDOPHYTES *PAENIBACILLUS* SP. P22 AND *PAENIBACILLUS*

DURUS

Molecular biological methods have suggested that the genus *Bacillus* is a phylogenetically heterogeneous taxon (6). Until it was reclassified into a separate genus in 1993 by Ash et al. on basis of the analysis of the 16S rRNA gene sequences of group 3 bacilli, *Paeanibacillus* belonged to the genus *Bacillus* (11). The rod-shaped cells are motile, have peritrichous flagella and show a negative gram staining and are forming ellipsoidal endospores (230). In *in-vitro* some of these species of *Paenibacillus* show a great ability to fix atmospheric nitrogen. Nearly all of the described nitrogen-fixing *Paenibacillus* species were isolated from the rhizosphere or roots of Graminaeaceos plants (134).

The strain *Paenibacillus* which was used for these different experimental set-ups was *Paenibacillus* sp. P22. It had been isolated from the aspen hybrid 741 and received from Dr. Dietrich Ewald from the Institute for Genetic Forestry in Waldsieversdorf, Germany. The phylogenetic analyses of P22 were based on 16S rDNA sequencing and described by Ulrich et al. (225). The 16S rRNA gene sequences obtained in this study was deposited in the EMBL nucleotide sequence database under the Accession No. AM906085 or on NCBI following link: <http://www.ncbi.nlm.nih.gov/nuccore/160858168>.

Paenibacillus sp. P22 shows a strong similarity to *Paenibacillus humicus* (Fig. 3) (99.5%) (225). It is a gram-negative, facultative anaerobic and endospore-forming bacterium that can be found in a variety of environments. Former Experiments have shown that *in-vitro* grown explants of poplar hybrid 741 inoculated with the bacterial strain *Paenibacillus* sp. 22 show a significant increase in biomass compared to non inoculated explants (225).

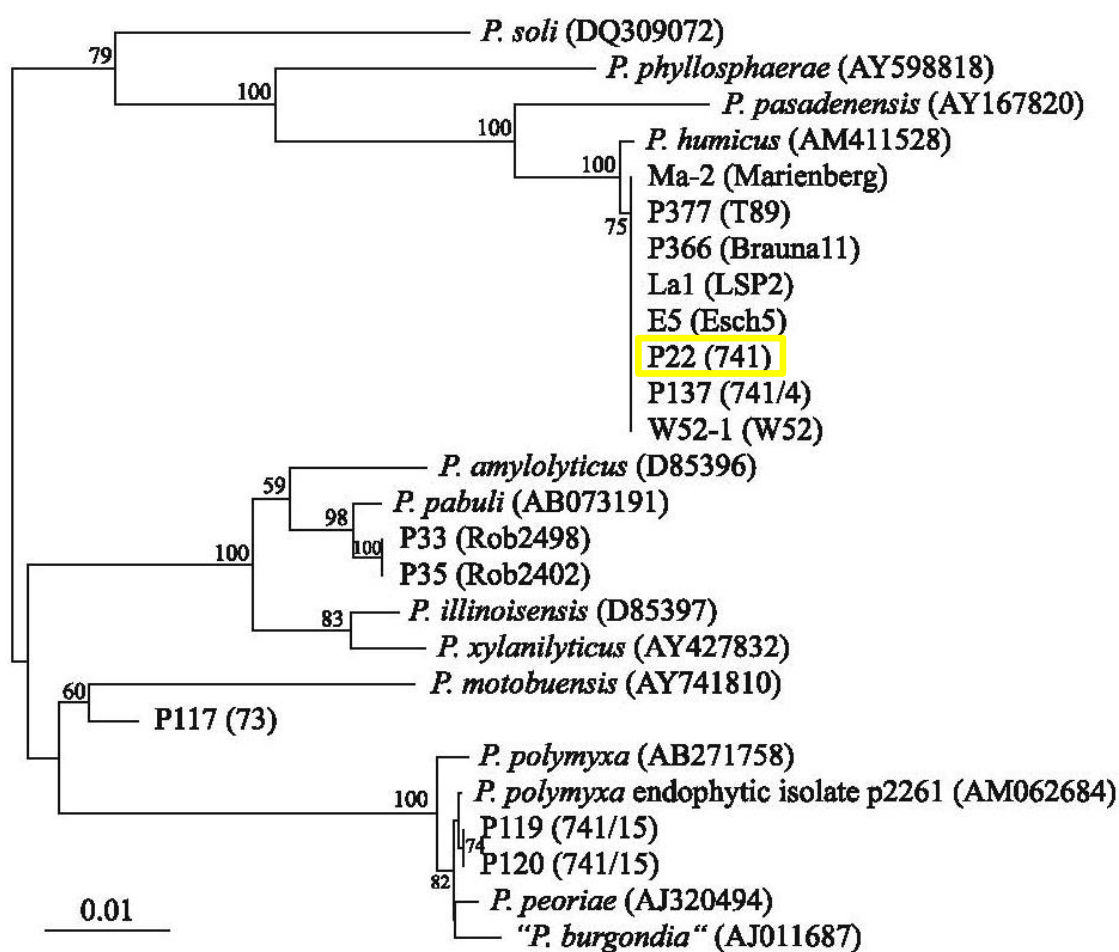


Figure 3: Phylogenetic tree based on 16S rRNA gene sequences of *Paenibacillus* isolates. Yellow marked isolate is *Paenibacillus* sp. P22 that was used in these experimental studies (225).

The other bacterial strain which had been used in these experiments was *Paenibacillus durus* ATCC 35681 which had been received from DSMZ (DSMZ-German Collection of Microorganisms and Cell Cultures, Leibniz Institute). *Paenibacillus durus* has been isolated from the rhizosphere, soils and plant roots and had only been found in Brazilian and Hawaiian soils (20). It is a gram-positive, facultative anaerobic diazotroph that falls into the broad cluster of nitrogen fixers (36). *Paenibacillus durus* (syn., *azotofixans*) ATCC 35681 is able to fix atmospheric dinitrogen with high efficiency which is not affected by the presence of nitrate. There are three DNA regions containing genes involved in nitrogen fixation.

2.1.1 CULTURING *PAENIBACILLUS* SP. P22 AND *PAENIBACILLUS DURUS*

Both *Paenibacillus* strains were cultured on different media, liquid and solid. For 500 ml solid medium, which has also been used as the storage method of the bacterial strains at 4°C, following materials were used: tryptone (8 g), yeast extract (1 g), agar-agar (4 g) and sodium-chloride (0.5 g). The other storage method was done by preparing three different freezing media. Freezing medium 1 comprised (double conc.): K₂HPO₄ (12.6 g), Na-Citrate (0.9 g), MgSO₄*7 H₂O (0.18 g), (NH₄)₂ SO₄ (1.80 g), KH₂PO₄ (3.6 g) and glycerol (88.0 g). All substances were filled up to 71 ml and mixed in a ratio of 1:1 with bacteria in log-phase. The culture was directly plunged into liquid nitrogen and frozen at – 80°C. Freezing medium 2 had a mixture of 25% glycerol and TSB-medium (Fluka Analytik, 22092) and was also stored at minus 80°C. The third freezing medium included 50% glycerol and TSB-medium.

For different growth analyses under various temperature conditions, *Paenibacillus* sp. P22 and *P. durus* were grown in 50 ml TY-solution: tryptone (8 g), yeast extract (1 g), NaCl (0.5 g) and glucose (4 M) in the Innova 44 incubator shaker (New Brunswick). For one experiment both *Paenibacillus* strains were grown under nitrogen starvation and for the other experiment acetate was added to the growth medium.

2.1.2 MICROSCOPIC ANALYSES OF *PAENIBACILLUS* SP. P22 AND *PAENIBACILLUS DURUS*

For the transmission electron microscopic analysis the bacteria were grown on tryptic soy agar plates: peptone (16 g/l), yeast extract (2 g/l), NaCl (5.6 g), glucose (1 g/l) and agarose (8 g/l). Three days after inoculation a colony of bacteria was placed with a sterile spatula into a small amount of 1% low melting agarose. After hardening of the agarose the sample was placed into the fixation solution I (sodium-cacodylatbuffer 0.2 M, glutaraldehyde 25%), for 3 hours and afterwards washed gently 3 times for 15 minutes with a washing solution (sodium-cacodylatbuffer : aquabidest; v / v). Afterwards the samples were transferred into fixation solution II (osmium solution 1%) for 3 - 4 hours. Again they were washed 3 times for 15 minutes with the washing solution. The dehydration of the object started with a 30% EtOH for 15 minutes and had been continued up to 50%, 70%, 80%, 90% and 100% EtOH.

A constant transfer of the objects into EtOH in acetonitrile (1 : 1) for 10 minutes and further into 100% pure acetonitrile was carried out. The objects were placed in a hard agar low viscosity resin and polymerized at 60°C. The polymerized blocks were cut on the Reichert Ultracut S with a diamond knife from DIATOME (45°). The ultra-thin sections with a thickness of 70 nm were put on a 200 Mesh Hexagonal copper grid from Agar Scientific. Subsequent the samples were investigated with the Zeiss EM 902.

2.1.3 GENOME ANNOTATION OF *PAENIBACILLUS* SP. P22

Paenibacillus sp. P22 was grown under aerobic conditions on tryptic soy broth agar plates. The DNA extraction was performed with a DNA GeneJET™ Gel Extraction Kit: agarose (0.4 g), H₂O (45 ml), sodium-tetraborate buffer (5 ml). The gel slice was excised containing the DNA fragment by adding 1:1 volume of binding buffer to the gel slice. The gel slice was dissolved at 50 - 60°C for about 10 minutes with 800 µl of the solubilized gel solution and transferred to the Gene Jet™ purification column and centrifuged for 1 minute. The flow-through was discarded and the column was placed into the same collection tube. 700 µl of wash buffer was added to the Gene Jet purification column and centrifuged for 1 minute. Again the flow-through was discarded and placed into the column and centrifuged for 1 minute. The flow-through was discarded the column was again placed back into the same collection tube. The empty gene Jet™ purification column for an additional was centrifuged for 1 min. to remove residual wash buffer completely. The Gene jet purification column was transferred into a clean 1.5 ml microcentrifuge tube. 50 µl of elution buffer was added to the center of the purification column membrane and centrifuged for 1 minute.

The DNA content was measured with the Spectrophotometer ND-1000 Nanodrop. The genome sequencing was conducted with the 454® and Ion Torrent™ PGM technologies. Coding sequences (CDS) were predicted based on a house-internal workflow that integrates a initio predictions from Glimmer (41), Genemark (133), Prodigal (97) and Critica (14) with homology information derived from a BLAST search against NCBI NR (186). Noncoding RNAs were identified by tRNAscanSE (131), RNAmmer (113), and Infernal (81). Predicted CDS were compared to the databases InterPro (94), Swissprot (22) and trEMBL (22) for functional annotation and mapped to KEGG pathways.

2.2 BIOMASS PRODUCTION WITH POPLAR HYBRID AF2, AF8 AND

MONVISO

For field condition experiments, shoot cuttings of poplar clones named AF8, AF2 and Monviso, received from Josef Schweinberger of Saatzucht Probstdorf, Austria were used (1, 25.2.2012) (2, 162, 161). The origin of these clones is the Alasia New Clones Company in Italy. This company deals with the marketing of clones produced by Alasia Franco Vivai and the creation of agroenergetic chain on an international level (7) (25.2.2012).

The clone AF2 was chosen by Alasia Franco. It belongs to the species *Populus x canadensis*. It was constituted in 1994 and is a male plant. The mother plant is *Populus deltoides* 145 - 86 from Illinois – USA and the father plant *Populus nigra* 40 from Piemonte – Italia. Its appearance is linear, with a cylindrical shoot and continuous branches with an outstanding dominant to the top. The start of vegetation is around the 5th of April and the senescence of the leaves about the 2nd of December. The biological nutrient media can be from sand to clays with a good water supply. It has a high tolerance over some special pathogens and wind. The adversity tolerance against following pathogens is high: *Ventura* sp., *Melampsora* sp., *Marssonina* sp., *Dothichiza populea*, *Phleomyzus passerinii* and very high against the poplar mosaic virus. The gravity is about 0.28 g/cm³ and it is used for biomass for energy, chipboards, paper industry- and pellets.

The clone AF8 was chosen by Alasia Franco. It belongs to the species (*Populus generosa*) x *Populus trichocarpa* and was invented in 1993 and is a female specimen. The mother plant is *P. x generosa* 103-86 [*P. deltoides* 583 (Iowa - USA) x *P. trichocarpa* 196 (Oregon -U.S.A.)] and the father plant *P. trichocarpa* PEE (Washington - USA). The tolerance against *Venturia* sp., Poplar mosaic virus and wind is very high and high against *Melampsora* sp., *Marssonina* sp., *Dothichiza populea*, *Phleomyzus passerinii* high. The gravity is 0.28 g/cm³ and it is used as biomass for energy, chipboards, paper industry- and pellets. It's habit is a linear shoot with half open leaves. Start of vegetation is around the 13th of April the end is around the 30th of November.

Monviso was chosen by Alasia Franco and is a species of *Populus x generosa* x *Populus nigra*. It is female and was bred in 1991. The mother plant is *P. x generosa* 103-86 [*P. deltoides* 583 (Iowa - USA) x *P. trichocarpa* 196 (Oregon -U.S.A.)] and the father plant *P. nigra* 715 - 86 [*P. nigra* 12 (Piemonte -Italia-) x *P. nigra* 7 (Umbria – Italia)]. It's habit is a little circular shoot with a lot of branches. The vegetation starts on the 11th of April and ends around the 25th of November. It shows no tolerance for different water levels but shows a very high tolerance for *Venturia* sp., *Melampsora* sp., *Marssonina* sp., *Dothichiza populea*, Poplar mosaic virus as well as sufficient tolerance against *Phleomyzus passerinii* and wind. The gravity is about 0.31 g/cm³ and it is used as biomass for energy, chipboards, paper industry- and pellets.

Filat et al. (66) tested four Italian clones from Alasia relative to their biomass in short rotation coppiced (SRC) in five different experimental cultures and locations. They have found significant differences of plants survival and height. Furthermore, different diameters have been calculated among the clones (variants). Site conditions and culture techniques have produce large variation among the plantations.

For all three experiments 10 explants of each clone excluding the negative control were used. (In the results only 9 of the replicas are shown). Field grown explants of poplar clones AF8, AF2 and Monviso had been harvested in November and cut into approximately 20 - 25 cm length and directly stored at 4°C in a climate chamber under dark conditions. The biomass experiment started with three different experimental designs. One design for hydroponic culture and the other for direct field condition experiments inoculated with *Paenibacillus* sp. P22 and *Paenibacillus durus*. The plants were placed in one selected section of the greenhouse at the biocenter in Vienna. The ericarium which is one out of four sections of the greenhouse that has a temperate, frost-protected zone with temperatures from 7 – 25C° and a relative air humidity of > 30%.

2.2.1 EXPERIMENT ON HYDROPONICS

2.2.1.1 CULTIVATION AND INOCULATION

The shoot cuttings for the hydroponics were placed into 1000 ml beakers (Fig. 4 A) containing 500 ml of a half-strength Hoagland's nutrient solution which was refreshed every 3rd day and prepared as followed: HOAGLAND solution,

Ca(NO₃)₂*4H₂O (236.1 g/l), KNO₃ (101.1 g/l), KH₂PO₄ (136.1 g/l), MgSO₄*7H₂O (246.5 g/l), trace elements: H₃BO₃ (2.8 g/l), MnCl₂*4H₂O (1.8 g/l), ZnSO₄*5H₂O (0.1 g/l), NaMoO₄ (0.025 g/l), FeEDTA (367.1 g/l) (90, 198). The shoots were watered with a ½-strength Hoagland solution with 210 ppm nitrogen content in 1 l solution. The cuttings stayed for about 4 weeks in the beakers until the roots had a length of 5 - 10 cm. After reaching the required root length the shoot cuttings were inoculated for 3 days with 25 ml of the inoculum solution with either *Paenibacillus* sp. P22 or *Paenibacillus durus*. This solution was prepared by growing the different bacterial strains in 250 ml TY-solution until the concentration reached an OD of 1.109 CFU/ml measured at 660 nm. Then the samples were centrifuged and washed twice in a 10 mM MgSO₄ solution and re-suspended in 1/10 volume (25 ml) 10 mM MgSO₄. The resulted concentration of inoculum was 1.108 - 1.1010 CFU/ml and again washed three times in ½-strength S&H-medium (Hildebrandt-Schenk medium: KNO₃ (2500 mg/l), CaCl₂*2H₂O (200 mg/l), NH₄H₂PO (300 mg/l), MgSO₄*7H₂O (400 mg/l), FeNaEDTA (19.8 mg/l), H₃BO₃ (5.0 mg/l), MnSO₄*H₂O (10 mg/l), ZnSO₄*7H₂O (1.0 mg/l), KJ (1.0 mg/l), Na₂MoO₄ (0.1 mg/l), CuSO₄*5H₂O (0.2 mg/l), CoCl₂*6H₂O (0.1 mg/l), myo-inositol (100 0mg/l), thiamin-HCl (5.0 mg/l), nicotin-acid (5.0 mg/l), pyridoxin-HCl (0.5 mg/l) with pH 5.7) (187). Due to emerging nutrition deficits 6 weeks after the experiment had started, the Hoagland solution was raised from a ½-strength- to a ¾-strength composition (Fig. 4 B).

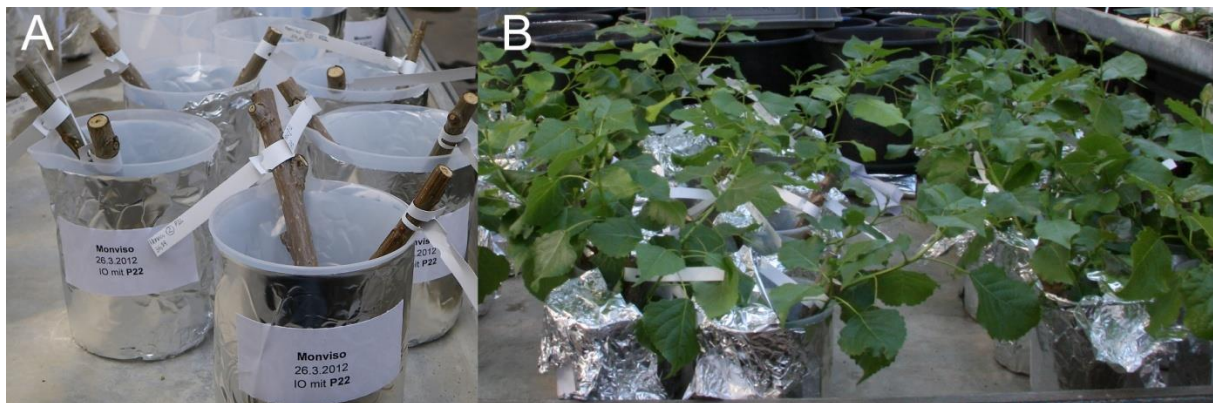


Figure 4: (A) Initiation of hydroponic culture of shoot cuttings placed in 500 ml beakers. (B) 4 weeks old shoot cuttings of Monviso placed in 500 ml beakers. Method of experiment described in chapter 2.2.1.

2.2.2 EXPERIMENT ON VERMICULITE / PERLITE

2.2.2.1 INOCULATION AFTER ROOTING

The first experiment started with weighting the shoot cuttings and placing them into 18 d pot filled with a vermiculite / perlite mixture and directly watered with normal water (Fig. 5 A). After 2 weeks of growth they were tested for root growth. After the root growth had started the shoot cuttings were inoculated with 15 ml of the inoculation solution of *Paenibacillus* sp. P22 or *Paenibacillus durus* which had been prepared as described in chapter 2.2.1.1.

2.2.2.2 DIRECT INOCULATION

Inoculation of the cuttings started with the preparation of the inoculation solution (*Paenibacillus* sp. P22 / *Paenibacillus durus*) which was a mixture with ½-strength Hoagland solution and the bacterial inoculums to a concentration of 1.108-1.1010 CFU/ml. After 3 days of incubation the shoot cuttings were weight and planted in non-sterile vermiculite / perlite (8:2) 2 l (18 Ø) pots. The pots were placed in the greenhouse at a constant temperature of 22°C and 14 h light and 10 h dark with a photosynthetic active radiation of 165 mmol/m²s (Fig. 5 A and B). Pictures were taken every four days and the plants harvested after 10 weeks to weight their total biomass (217).



Figure 5: (A) Initiation of greenhouse experiment of poplar shoot cuttings placed in vermiculite / perlite mixture. (B) Picture taken couple of weeks after pique. Method of experiment described in chapter 2.2.2.

2.3 DIFFERENT EXPERIMENTS ON *IN-VITRO* CULTURED POPLAR HYBRIDS

The used plant material for *in-vitro* experiments was poplar hybrid 741 received from Dr. Dietrich Ewald of the Institute for Genetic Forestry in Waldsiedersdorf, Germany (Fig. 6 A and B). Poplar 741 is a hybrid of ($\text{♀}[\textit{Populus alba} \times (\textit{P. davidiana} + \textit{P. simonii}) \times \textit{P. tomentosa}]$) and was originally invented in China (211). This hybrid is able to develop female blossoms with a reduced amount of seeds. Furthermore, it is a perfect model organism and has been tested for transgenic experiments, for insect-resistant and insectal protein expression in Bt genes (*Bacillus thuringiensis*) (211, 234).

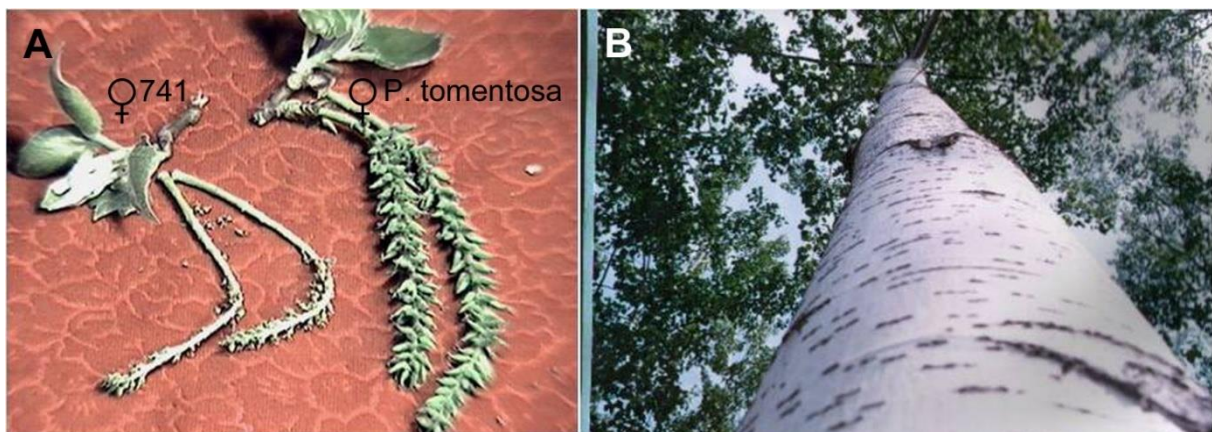


Figure 6: (A) Shown on the left side the sterile blossom of poplar hybrid 741 compared to the fertile blossom of *P. tomentosa* on the right side. (B) This image shows a 23 year old poplar hybrid 741. Both pictures were received from Ulrich K. Institute for Genetic Forestry and taken from Prof. M. S. YANG, College of Forestry, Agricultural University of Hebei, Baoding, China.

To see differences in the species-species interaction between bacterial endophytes and their host plants, two bacterial strains were used for the inoculation experiment of the described poplar hybrids. The selected strains are described in chapter 2.1.

2.3.1 CULTURING OF POPLAR HYBRID 741 UNDER *IN-VITRO* CONDITIONS

Explants of polar explants inoculated with endophytes and some free from cultivable endophytes via root meristematic micropropagation by Kristina Ulrich (225), had been micropropagated in *in-vitro* cultures. The inoculation of the plants had been done via two different methods. The first method consisted of applying the inoculation solution on the fresh cut poplar shoot. The other method was by putting the new built root system into this bacterial solution for approximately 20 minutes.

Cuttings of poplar 741 with and without cultivable endophytes were precultured in test tubes including 13.5 ml of a ½-strength Linsmayer and Skoog medium (127) without growth promoting hormones for about 4 weeks in a diurnal cycle 12 h dark and 12 h light.

This medium was prepared as followed: L&S-medium (Duchefa Biochemie L0230.0005) (2.2 g/l), sucrose (20 g/l), gelrite (4.3 g/l), with pH 5.7.

The bacterial strain *Paenibacillus* sp. P22 was cultivated on a minimal-medium consisted of: sucrose (20 g/l), K₂HPO₄ (0.1 g/l), KH₂PO₄ (0.4 g/l), MgSO₄*7H₂O (0.2 g/l), NaCl (0.1 g/l), FeCl₃ (0.01 g/l) and Na₂MoO₄ (0.002 g/l) (92).

2.3.2 BACTERIAL INOCULATION OF POPLAR HYBRID 741 WITH *PAENIBACILLUS* SP.

P22

For one inoculation method via the roots, half of the grown explants was transferred into test tubes containing 13.5 ml of ½-strength solid woody plant medium which was prepared as followed: NH₄NO₃ (400 mg/l), CaCl₂*2H₂O (96 mg/l), Ca(NO₃)₂ (386 mg/l), MgSO₄*7H₂O (370 mg/l), KH₂PO₄ (170 mg/l), K₂SO₄ (990 mg/l), Na₂EDTA (37.3 mg/l), FeSO₄*7H₂O (85 mg/l), H₃BO₃ (6.2 mg/l), MnSO₄*H₂O (22.3 mg/l), ZnSO₄*7H₂O (8.6 mg/l), Na₂MoO₄*2H₂O (0.25 mg/l), KI (0.83 mg/l), CuSO₄ (0.25 mg/l), myo-Inosit (100 mg/l), thiamine-HCl (1.0 mg/l), nicotin-acid (0.5 mg/l), pyridoxin-HCl (0.5 mg/l), glycine (2.0 mg/l), sucrose (20 g/l), 0.1 M IBA, (0.1 mg/l), 0.1 M NAA (0.01 mg/l) and gelrite (4.3 g/l) with pH set to 5.7 (141), for about 2 weeks until first roots (approximately 1 cm length) were visible.

The other half was used for the inoculation method with the direct application of the bacteria on the stem.

For the inoculation of the root system a liquid medium of a 1/8 concentrated Murashige and Skoog solution was used and prepared as followed: KNO₃ (190 g/l), CaCl₂*2H₂O (44 g/l), NH₄NO₃ (165 g/l), MgSO₄*7H₂O (37 g/l), KH₂PO₄ (17 g/l), Na₂EDTA (3.7 g/l), FeSO₄*7H₂O (2.78 g/l), H₃BO₃ (6.2 g/l), MnSO₄*H₂O (16.9 g/l), ZnSO₄*7H₂O (8.6 g/l), KJ (0.83 g/l), Na₂MoO₄*2H₂O (0.25 g/l), CuSO₄*5H₂O (0.025 g/l), CoC₂*6H₂O (0.025 g/l), thiamine-HCl (10 mg per 0.5 l), nicotin-acid (5.0 mg per 0.5 l), pyridoxine-HCl (50 mg per 0.5 l), glycine (200 mg per 0.5 l), myo-inositol (100 mg/l) and sucrose (30 g/l) with pH set to 5.7 (158), where the roots were kept for about 20 minutes.

Rooted poplar explants as well as shoot cuttings were placed on Hildebrandt-Schenk medium which was prepared as followed: KNO_3 (250 mg/l), $\text{CaCl}_2 \cdot 2\text{H}_2\text{O}$ (200 mg/l), $\text{NH}_4\text{H}_2\text{PO}_4$ (300 mg/l), $\text{MgSO}_4 \cdot 7\text{H}_2\text{O}$ (400 mg/l), FeNaEDTA (19.8 mg/l), H_3BO_3 (5.0 mg/l), $\text{MnSO}_4 \cdot \text{H}_2\text{O}$ (10 mg/l), $\text{ZnSO}_4 \cdot 7\text{H}_2\text{O}$ (1.0 mg/l), KJ (1.0 mg/l), Na_2MoO_4 (0.1 mg/l), $\text{CuSO}_4 \cdot 5\text{H}_2\text{O}$ (0.2 mg/l), $\text{CoCl}_2 \cdot 6\text{H}_2\text{O}$ (0.1 mg/l), myo-inositol (100 mg/l), thiamin-HCl (5.0 mg/l), nicotin-acid (5.0 mg/l), pyridoxin-HCl (0.5 mg/l) and gelrite (4.4 g/l), with a pH set to 5.7 and including glass pearls for a stabilization of the plant (187).

20 rooted poplar explants were inoculated and placed in test tubes including 13.5 ml of liquid ½-strength S&H-medium including glass pearls. Another 6 rooted poplar explants were not inoculated and placed in a ½-strength S&H-medium as a control.

20 fresh cut and inoculated explants from poplar L741 were placed in half-strength solid S&H-medium and another 6 non inoculated explants were placed in test tubes including 13.5 ml of solid a ½-strength S&H-medium as a control. Every 3rd to 4th day pictures were taken of the samples. The data collection from the test tubes of both inoculation methods last about 6 weeks.

2.3.3 ALLOCATION OF BACTERIA USING DIFFERENT MICROSCOPIC TECHNIQUES

The appearance and the allocation of the bacteria in poplar 741 were investigated at cell level by using different microscopic techniques.

Some explants of poplar were inoculated with endophytes and some were free of endophytes via root meristematic micropropagation. The inoculation of the plants was done by direct application of the bacterial solution on the fresh shoot cutting and by putting the new built root system into a bacterial solution.

2.3.3.1 REM / TEM / ESEM / TISH

The allocation of bacteria in the tissue and outside of the epidermis was investigated with the REM Philips XL 30 ESEM. Fresh poplar cuttings were carefully placed on already prepared small stubs with cole sticker and immediately analyzed.

The transmission electron microscopic (TEM) analysis was done with the TEM ZEISS 902. The sampling started with the control at 0 h then every 6 hours for 1 day, followed by one sampling once a week over a period of 4 weeks. The plants were harvested and cut in small pieces of approximately 3 mm length.

To prevent the cellular sap from leaking the bacteria were put into the nearly solid agar and directly in a fixation solution I (0.2 M sodium-cacodylate-buffer, 25% glutaraldehyde) for 3 hours and afterwards they were washed gently 3 times for 15 minutes with a washing solution (sodium-cacodylate-buffer:aquabidest; v/v). The objects were transferred into fixation solution II (1% osmium solution) for 3 - 4 hours. Again they were washed 3 times for 15 minutes with the washing solution. The dehydration of the object started with a 30% EtOH for 15 minutes and was continued up with 50%, 70%, 80%, 90% and 100% EtOH. The objects were transferred constantly into EtOH /acetonitrile (1:1) for 10 minutes and further into 100% pure acetonitrile. For the direct dehydration step the objects were placed into a hard agar low viscosity resin and polymerized at 60°C. The polymerized blocks were cut on the microtome ultra S with a diamond knife from DIATOME and the ultra-thin section with a thickness of 70 nm will be put on a 200 Mesh Hexagonal copper grid from Agar Scientific.

For tissue in-situ hybridization the procedure started with placing the plant pieces in a 1% low melting agarose and cutting them into small pieces. Directly after hardening they were fixed for 10 minutes in 70% EtOH. The samples were fixed in EtOH because of they were gram-positive bacteria. Afterwards the samples were transferred into 90% EtOH for another 10 minutes and then directly transferred into a 100% EtOH. There they were fixed for 30 minutes and the EtOH was refreshed 3 times. After the last step of 100% EtOH the samples were transferred in new Eppendorf tubes filled with LR-White with no accelerator (Gröpl R1291). The LR-White was renewed 8 times every 60 minutes. After the 8th change the samples were placed in new test tubes and stored overnight for approximately 12 h at room temperature. After this time the samples were placed in gelatin capsules filled with fresh LR-White (Gröpl, G292-03, G292-08) and polymerized in a heating chamber (Heraeus) for 2 days. The vacuum oven had a temperature of about 46°C. Higher temperatures would cause the ribosomes to denature. After the polymerization the capsules were opened and the samples were cut with an ultra-microtome (Ultracut S). The semi-thin sections were about 100 µm thick and were placed on Silane-Prep Slides (Sigma-Aldrich S4651-72EA) and Poly-Prep Slides (PO425-72EA). Four sections per drop of double distilled water were mounted on the slide and then air dried. After drying the square was labeled by drawing a ring with a PAP-pen (Sigma-Aldrich Z67258-1EA).

2.3.4 MEDIA SCREENING OF POPLAR HYBRID 741, POPLAR HYBRID ESCH 5 2N, 4N AND 2N4N

Poplar hybrid 741, diploid Esch 5, tetraploid Esch 5 and mixoploid Esch 5 were cultivated on different growth media to test the different growth behavior. Following media were tested:

- Full-strength L&S-medium with growth promoting hormones: L&S-medium (4.4 g/l), glucose (20 g/l), 6-benzylammonipurine (5 ml/l) (stock solution 10 mg per 100 ml), 1-naphthalene acetic acid (0.5 ml/l) (stock solution 10 mg per 100 ml), kinetin (0.1 ml/l) (stock solution 10 mg per 100 ml).
- Half-strength L&S-medium with growth promoting hormones: L&S-medium (2.2 g/l), glucose (20 g/l).
- Half-strength L&S-medium without growth promoting hormones

2.3.5 *IN-VITRO* CULTURING OF POPLAR CLONES AF2, AF8 AND MONVISO

Field grown plants are typically more contaminant than those grown in a greenhouse or even sterile in a growth chamber. Additionally splashing soils during watering will increase the contamination of the plants. Sometimes it is advisable to treat the plants with fungicides or bactericides to avoid these contaminations.

2.3.5.1 SURFACE STERILIZATION AND MICROPROPAGATION

The surface sterilization of 10 fresh and young, non-woody, shoot pieces with an approximate length of 2 cm were taken from each clone. The shoots were rinsed with 10% EtOH. The surface sterilization was done by stirring the explants for 15 minutes in a 10% sodium-hypochlorite solution, which is the most frequent choice for surface sterilization. Because of phytotoxicity the concentration and time have to be determined empirically for each type of explants. For this reason it is important to determine the concentration of the sodium-hypochlorite solution. The bleach was decanted and the shoots were directly washed with sterile water which also was decanted immediately. Then the shoots were washed with sterile water 3 times for 10 minutes each. All these steps were done under the lamina. Directly after the last step of washing the shoot cuttings were placed in a Hipp glass with full-strength L&S-medium. This full-strength medium was changed into a ½-strength medium because of visible aggravation of the cuttings.

2.4 ACCLIMATIZATION OF DIFFERENT POPLAR CLONES

The successful acclimatization of *in-vitro* grown plants heavily depends on the ability to transfer the plants out of the culture on a large scale. During the transfer from *in-vitro* to *ex-vitro* plantlets do not have any defense mechanism against microbes in the soil or can cope with the environmental conditions (29). During the *in-vitro* culture, plantlets grow under controlled conditions e.g. the air humidity is higher than in conventional culture. Furthermore, while growing *in-vitro* the plantlets show abnormal morphology, anatomy and physiologic signs because the plantlets are usually supplied with large doses of growth regulators (110). For example the stomata on leaves and stem do not have any mechanism of opening or closing and little epicuticular and cuticular wax, resulting in excess evapotranspiration after micropropagation. Fila et al. discovered that the hydraulic conductivity at both root and shoot-root connection levels was low in micropropagated plantlets (65). These abnormalities have to be corrected by placing the plants into a climate chamber for a period of time where the air humidity is lower and the irradiance is much higher (169). For further field experiments the poplar clones 741 with *Paenibacillus* sp. P22 and *Paenibacillus durus*, poplar hybrid L447 (diploid, tetraploid and mixoploid) were acclimatized. This was performed by piquing sterile explants of poplar clones with and without roots (with callus) into pots filled with a mixture of peat and perlite. Then they were placed thoroughly in the Heraeus acclimatization chamber. They were watered with 0.1% Pervicur which is a fungicide to avoid any pathogens on the plants. At the beginning air humidity was at 85% for 2 weeks, then it was continuously decreased every 2nd day. After 2 weeks in the climate chamber they were transferred into the greenhouse with a light cycle of 16 hours of light and 8 hours of darkness. The temperature was constant at about 22°C with a photosynthetic active radiation of 165 mmol/m²s.

2.5 DIFFERENT EXPERIMENTS WITH POPLAR HYBRID OF VARIOUS PLOIDY LEVELS

2.5.1 FLOW CYTOMETRIC MEASUREMENTS AND MICROSCOPIC ANALYSIS

The flow cytometric analyses of diploid, tetraploid and mixoploid fresh poplar leaves was estimated using the CyFlow® Ploidy Analyser (Partec, Germany) equipped with a 365 nm LED. The flow cytometer measures emerging light from cells or particles which pass through a laser beam. This data is captured and measured statistically. The samples were prepared using DAPI (4'-6-diamidino-2-phenylindole) which served as DNA-selective stain. Only histograms with coefficients of variation (CVs) < 5% for the G0/G1 peak of the analyzed sample were allowed (47).

For the microscopic analysis 15 fresh leave samples were taken from three 2 year old poplar trees (2N, 4N, 2N4N) and placed into a square of polystyrol. After correct adjustment of the sample in the Neapler-crank, it was cut with a C-knife positioned in a microtome from Reichert with a thickness of about 40 µm. After cutting the sections the leaves were placed on a glas-slide and investigated under the light microscope.

2.5.2 PROTEOMIC PROFILING USING LTQ-ORBITRAP MS/MS SHOTGUN

2.5.2.1 PROTEIN EXTRACTION

A pool of young and old diploid, tetraploid and mixoploid lyophilized poplar leaves were prepared for proteomic analyzes. Three biological replicates were taken from each sample and extracted as followed. The freeze dried material was grinded with the retsch mill (MM400, RETSCH) until it was completely homogenized. An integrative protein and metabolite extraction protocol was used as previously described experiment. 7.5 mg of dry weight was homogenized with 1 ml of extraction buffer (methanol/chloroform/water, 2.5:1:0.5 [v/v/v]) and incubated for 8 minutes on ice. After 4 minutes of centrifugation at 4°C with 14.000 g the supernatant was transferred into new tubes for later metabolite extraction. Another 400 µl of the extraction buffer was added to the protein containing pellet and incubated for another 8 minutes to wash remaining metabolites off the protein pellet. After centrifugation the second supernatant was added to the first for metabolomic analysis and the resulted

white pellet was taken for further protein extraction. The pellet was diluted in 1.5 ml urea buffer (50 mM HEPES, 8 M urea, pH 7.8) and centrifuged at 10.000 g for 10 minutes at 4°C. The supernatant was transferred into new tubes and mixed with precooled (- 20°C) precipitation buffer (acetone containing 0.5% β -mercaptoethanol) and stored over night at - 20°C. After centrifugation with 4.000 g at 4°C for 15 minutes the protein-pellet was washed once in 2 ml ice-cold methanol (- 20°C) and again centrifuged (4.000 g, 4°C, 10 min.). The resulted pellet was air dried at room temperature.

2.5.2.2 PROTEIN DIGESTION AND DESALTING

The air dried protein pellets were dissolved in 8 M urea buffer (50 mM Hepes, pH 8.0). To determine the protein content a coomassie blue colorimetric method using BSA as standard was conducted. Protein samples (100 μ g) were digested with 1 μ l of the sequencing grade endoproteinase Lys-C (1:100, v/w μ g prot) Roche, Mannheim, Germany) for 5 h at 37°C to cut the peptide bonds C-terminally at lysine. For the second digestion trypsin buffer (10% ACN, 2 mM CaCl_2 , 50 mM AmBic) was added to obtain a final urea concentration of 2 M. The protein samples were placed in the hybridization oven over night at 37°C with porozyme immobilized trypsin beads (1:10, v/w, Applied Biosystems, Darmstadt). The digested proteins were desalted with the C18-SPEC 96-well plates (Varian, Darmstadt, Germany) following the manufacturer's manual. Afterwards the peptides were eluted with methanol, and split into two technical replicates and vacuum dried (Scanvac).

2.5.2.3 LTQ-ORBITRAP MS/MS SHOTGUN PROTEOMICS

The complete vacuum dried peptides were dissolved in 5% acetonitrile and 0.1% formic acid resulting in a final concentration of 0.1 μ l. A total of 0.5 μ g proteins of each sample were randomly loaded on an RP column (ascensis HTC PAL, CTC Analytics) and separated during a 90 min. gradient from 80% solvent A (0.1% formic acid) to 90% of solvent B (80 % acetonitrile). Mass spectral analysis was performed on an LTQ Orbitrap (Thermo Scientific Fisher) in an acquisition cycle of 9 scan events: the full range scan (Orbitrap) was from 350 to 1800 m/z followed by 8 dependent MS2 scans in the (linear ion trap) of the most abundant m/z in the full scan. An exclusion mass list was set to 500 to an exclusion time of 60 s and a width of 10 ppm. The repeat count was set to 1 with the duration of 20 s. The Minimum

signal threshold counts were set to 1000 and the charge state screening was enabled with rejection of +1 and unassigned charge states.

2.5.2.4 DATA MINING

The mass spectral analysis was done by using the SEQUEST search-algorithm combined with Proteome Discoverer (v 1.4, Thermo Fisher Scientific Inc.) to search MS data against a fasta file. The UniProt-Knowledgebase (<http://www.uniprot.org/>) contained about 43.000 sequences in April 2013 was used. *In-silico* peptide lists were compiled with trypsin as digestion enzyme, methionine oxidation and acetylation as dynamic modification and a maximum of 2 missed cleavages. The tolerance for mass was set to 5 ppm for precursor ions and for fragment ions 0.8 Da. To exclude false positive matches the quality of protein identifications was assessed by a search against a decoy database which contains reverse sequences. Only peptides with a FDR of high confidence ($\leq 0.01\%$) identification and a minimum Xcorr of 2.2 and proteins with at least two different peptides were considered valid. Additionally a mass accuracy precursor alignment (MAPA) approach (91) using the software ProtMAX (53) was conducted. A data conversion of .raw to .mzXML files was performed and a target list, containing the m/z values of the peptides and the retention time (RT) was obtained by the previous database dependent approach. The resulted data were used as a search filter to analyze peptide abundance in precursor scans. The intensity of the threshold was set to percentages.

2.5.2.5 STATISTICAL ANALYSIS

The identified proteins were assembled to a database depended matrix including the spectral counts of each sample. For quantitative analysis only those proteins were used, identified at least 4 out of 6 replicates. Remaining missing values were replaced with 0.1 and \log^2 -transformation. A principal component analysis (PCA) was conducted with the COVAIN toolbox, which was designed for uni-and multivariate statistics (213). A t-test with a p-value ≤ 0.05 was performed shown in the results.

The PCA transforms a d-dimensional sample vector to a vector of lower dimensionality where the first two principal components comprise a two-dimensional subspace explaining the highest variance of the data set. Furthermore, the information about the contribution of the original variable to a corresponding PC are given by the loadings or weight which are the elements of the transformation vector (191).

Fold-change was calculated as relative changes in protein abundance compared to young and old leaves. The \log^2 -transformation was performed simply to obtain symmetric values around zero instead of asymmetric values (< 0.5 and > 2).

2.6 *CHLAMYDOMONAS REINHARDTII* CC503 CW92 MT+

Algae are one of the most important biofactories on earth based on their photosynthesis and CO_2 -fixation capacity (237). Green algae are capable of accumulating large amounts of lipid droplets as a source of biodiesel (glycerides and fatty acids) and can grow rapidly under modest culture conditions. *Chlamydomonas reinhardtii* is a biflagellate, photosynthetic unicellular organism with an easily cultivated haploid vegetative stage. It is the first algae subject to a full scale genome project and has been the object of numerous other morphological, physiological, and genetic studies (170). Many microalgae accumulate oils, special under growth limiting conditions and thus have gained renewed attention as a potentially sustainable feedstock for biofuel production (154). In 2007 the genome of *Chlamydomonas reinhardtii* was published. It developed into a model organism for plant systems biology and was called from now on “the green yeast” (145). In the last years there has started to be great interest in the development of technologies to harvest lipids from microalgae and convert them into diesel fuel (35, 51, 177). When *Chlamydomonas* is growing under nitrogen deprivation after entering the stationary phase, it is producing lipid bodies, as well as abundant starch.

2.6.1 CULTURING *C. REINHARDTII*

Chlamydomonas reinhardtii CC503 cw93 mt+ was received by www.chlamy.org and had to be precultured before starting the experiment. The medium for *Chlamydomonas reinhardtii* was prepared as followed: $\text{K}_2\text{HPO}_4 \cdot 3\text{H}_2\text{O}$ (288 g/l), KH_2PO_4 (144 g/l), NH_4Cl (15 g/l), $\text{MgSO}_4 \cdot 7\text{H}_2\text{O}$ (4 g/l), $\text{CaCl}_2 \cdot 2\text{H}_2\text{O}$ (2 g/l). The Hutner's trace-medium was prepared by mixing $\text{ZnSO}_4 \cdot 7\text{H}_2\text{O}$ (22 g per 100 ml), $\text{MnCl}_2 \cdot 4\text{H}_2\text{O}$ (5.06 g per 50 ml), $\text{CuSO}_4 \cdot 5\text{H}_2\text{O}$ (1.61 g per 50 ml), $(\text{NH}_4)_6\text{Mo}_7\text{O}_{24} \cdot 4\text{H}_2\text{O}$ (1.1 g per 50 ml), H_3BO_3 (11.4 g per 200 ml), $\text{CoCl}_2 \cdot 6\text{H}_2\text{O}$ (1.61 g per 50 ml) and at last $\text{FeSO}_4 \cdot 7\text{H}_2\text{O}$ (4.99 g per 50 ml) together. 50 g of EDTA disodium salt was dissolved in 250 ml water under high temperature separately. The first solution was brought to boil and the EDTA was added to it. The mixture turned

green immediately. After dissolving all substances the solution had to be cooled down to 70°C and a pH of 6.7 had to be adjusted with about 80 - 90 ml of 20% KOH. The final solution was finally filled up to 1 l. The flask was closed with a cotton plug and stored for 1 - 2 weeks and shook once a day. The solution should eventually turn purple and can precipitate a rust-brown substance, which can be removed by filtering through two layers of Whatman #1 filter paper. Aliquots of the Hutner trace solution had been stored at - 20°C.

300 ml of the final medium had been inoculated with cell cultures with a size of 6 - 8 mm Ø of *Chlamydomonas reinhardtii*. The cell cultures were incubated in an Innova 44 incubator shaker (New Brunswick) at 110 rpm with a light intensity of 110 µE/m²s. After approximately 2 days density of the culture constituted about 5 x 10⁶ cells/ml. 200 ml of fresh medium was inoculated with 75 ml of the new grown *Chlamydomonas* culture. Liquid solutions as well as a solid solution were prepared. The nutrients for liquid media are suitable for plate cultures with addition of 1.5% agar and for slants in test tubes with 1.5% or 2.0% agar. Cells were suspended by mixing them softly in 2.5 - 4.0 ml of melted soft agar (0.7% agar) at 45°C and immediately poured onto the surface of previously prepared plates.

2.6.2 LIPID STAINING

As *Chlamydomonas reinhardtii* is known for an increase of lipid production under nitrogen starvation a monitoring of the lipid accumulation inside the cells via fluorescence microscopy was used. The lipid staining of *C. reinhardtii* cells was done by mixing 100 µl of cell culture with 2 µl Nile red (10 mg Nile red in 0.01% acetone) in an Eppendorf tube. Directly after staining the cells were investigated with a Nikon Microphot-SA. The starch staining was done by mixing 10 µl of *Chlamydomonas reinhardtii* cell culture with 10 µl Iugol solution (10 times diluted stock solution) with immediately investigating the sample under bright field.

2.7 *MEDICAGO TRUNCATULA* 'JEMALONG A17'

Beside poplar as a woody plant for bioenergy, *Medicago truncatula* as a Legume plays a central role in the development of agriculture and civilization and is also a system model plant. Nowadays this Legume counts for approximately 1/3 of the world's primary crop production (17). Plants are able to adapt to environmental changes of their habitat. However, perturbations may result in a physiologically and/or anatomically visible reaction. *Medicago truncatula* is an annual forage plant in the Mediterranean area, autogamous self-fertile with a small diploid genome and a short life cycle (42). *Medicago truncatula* can establish symbiosis with the bacteria *Sinorhizobium meliloti*. These bacteria colonize the meristematic tissue of the root tip, whereby nodule development is induced. This bacteroid-plant interaction plays a key role enabling nitrogen fixation of the plant. The total number of formed nodules depends upon the size and degree of consequence of the root system at the time of inoculation (58). The symbiosis between the legumes and the rhizobia is initiated by the exchange of signal molecules, like flavonoid compounds, between the plant and the microbe (222).

2.7.1 CULTIVATION OF *MEDICAGO TRUNCATULA* AND *SINORHIZOBIUM MELILOTI*

The seed germination was conducted by scarification of the seeds with soaking them into 5 volumes of conc. H_2SO_4 for 5 - 10 minutes with continuous vortexing. The next step was the 4 time rinse with milli-Q before the surface sterilization. This was done by leaving the seeds in 5 volumes of 5% sodium-hypochlorite for 3 minutes. The seeds were decanted and washed 8 times with sterile water under the laminar and placed in 4°C for 36 h in about 3 volumes of sterile water. The last step was the germination where the seeds were washed about 6 - 8 times with sterile water and placed on petri dishes with wet filter paper closed with foil and placed into a dark place at room temperature. The germination took about 20 h. The seedlings were placed in pots filled with a vermiculite/perlite mixture (2 : 5) and placed in a climate chamber with a 14 h day and 10 h night rhythm (Fig. 7). The light intensity was by $600 \mu\text{mol m}^{-2}\text{s}^{-1}$, temperature day 22°C / night 16°C and the relative humidity was at 70-60%. 3 weeks after pique of *Medicago truncatula* some plants were inoculated with *Sinorhizobium meliloti* while the control pants were not inoculated. 7 weeks after piquing the results of the experiment were estimated. The plants were watered with

EVANS solution (60) consisting of following elements: $\text{MgSO}_4 \cdot \text{H}_2\text{O}$ (0.493 g/l), K_2SO_4 (0.279 g/l), KH_2PO_4 (0.023 g/l), CaCl_2 (0.056 g/l), EDTA-Fe (0.017 g/l), K_2HPO_4 (0.145 g/l), $\text{MnSO}_4 \cdot \text{H}_2\text{O}$ (0.77 mg/l), H_3BO_3 (1.43 mg/l), $\text{ZnSO}_4 \cdot 7\text{H}_2\text{O}$ (0.22 mg/l), $\text{CuSO}_4 \cdot 5\text{H}_2\text{O}$ (0.08 mg/l), $\text{CoCl}_2 \cdot 6\text{H}_2\text{O}$ (0.117 g/l), $\text{NaMoO}_4 \cdot 2\text{H}_2\text{O}$ (0.05 mg/l) and CaSO_4 (1.033 g/l). Inoculated explants were watered without nitrogen while the control plants were watered with a solution including 0.5 mM NH_4NO_3 for three weeks which afterwards was decreased to 2.5 mM.

Salt treated plants were watered with Evans solution added with 100 mM NaCl.

For both experiments the time table was set to day 0 which was the day before stress, sample 3 was the 3rd day of drought- or salt-stress, day 6 was the 6th day of drought- or salt-stress and day 8 was the 2nd day of re-watering.



Figure 7: Drought-stress experiment of *Medicago truncatula* growing in a climate chamber. Left side nitrogen fixing *M. truncatula* explants compared to the nitrogen assimilating plants to the right. The method and the results for this experiment are shown in chapter 2.7 and 3.8.

2.7.2 MICROSCOPIC ANALYSIS OF SHOOT, ROOT AND LEAVES UNDER DIFFERENT GROWTH CONDITIONS

For microscopic analysis the harvested samples were placed in a FAA solution even though it is a very harsh fixative. The used FAA solution consisted of EtOH (50 ml), glacial acetic-acid (5 ml), formaldehyde 37 - 40% (10 ml) and distilled H_2O (35 ml) which was mixed up to 100 ml. The leaves were fixed for about 6 h while the root, stem and nodules were fixed for 12 - 24 h. Directly after the first fixation step the next steps was the fixation in Technovit 7100 which is a cold-polymerizing resin for embedding. The pre-infiltration was done by mixing in equal ratio parts 96% EtOH with Technovit 7100 and placing the plant samples in small glass vials with the solution for about 1 - 2 hours, according to the size of the explants. The infiltration of

the samples was done by preparing infiltration solution which consists of 1 g hardener dissolved in 100 ml base liquid. The specimens were placed in the infiltration solution for about 12 hours until the color of the samples disappeared completely. The last step was to put the plant tissue in a polymerizing solution. 1 ml of the hardener was added with 15 ml of the preparation solution and stirred for some seconds. 1 - 3 ml of the solution was poured into histoforms and the plant specimens were placed in to the form and positioned as required. The time of workability at room temperature was about 2 - 5 minutes. The samples hardened after max. 2 hours. After polymerization the samples were taken out with special Histosec blocks which were also the attachment for the microtome. After cutting with the microtome (Polycut S) the slides were stained with safranine and astrablue. The objects were prepared in 5 - 10 μm slices and investigated with the microscope Nikon Eclipse 55i.

The counting of stomata was done by following steps: The single leaves were sampled and immediately pressed on a drop of cellulose-di-acetate which had been put on a polymethyl-metacrylate slide (143). After removing the leaf from the slide the stomata imprint was investigated with a microscope from Reichert Austria Nr. 255 625. An area of 0.049 mm^2 was counted and the average was calculated out of four different places of the leaf.

3 Results

3.1 *PAENIBACILLUS* SP. P22 AND *PAENIBACILLUS DURUS* UNDER DIFFERENT CULTUR CONDITIONS

Figures 8 to 14 show the endophytes *Paenibacillus* sp. P22 and *Paenibacillus durus*, grown under different conditions of cultivation.

Images (A) and (B) of figure 8 show solid cultures of *Paenibacillus* sp. P22 and *Paenibacillus durus* grown on TY agar plates over a period of 4 days at a temperature of 28°C. The isolate *Paenibacillus* sp. P22 evolves flat, white, opaque, smooth and entire colonies on the agar plate. Contrary to P22, *Paenibacillus durus* also evolves flat, but yellow colored, smooth, entire and single colonies on spread over the agar plate.

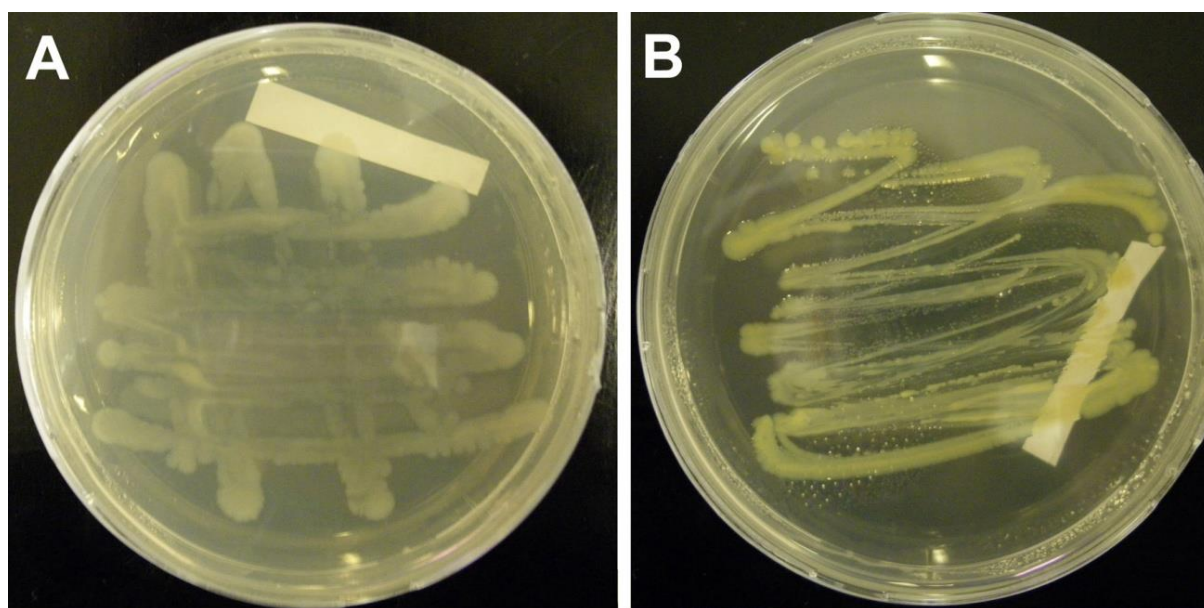


Figure 8: (A) Solid culture of *Paenibacillus* sp. P22 inoculated on a TY agar plate growing over a period of 4 days at 28°C. (B) Solid culture of *Paenibacillus durus* inoculated on a TY agar plate growing over a period of 4 days at 28°C. Method of experiment described in chapter 2.1.1.

Figure 9 (A) shows a liquid culture of *Paenibacillus* sp. P22 and (B) a culture of *Paenibacillus durus* grown in a liquid medium including glucose and sodium-chloride. The visible difference can be determined in the color which is much lighter in the P22 culture than in the liquid culture of *P. durus*. Additional to that, *P. durus* develops solid colonies at the bezel (red circle). The added growth curve was measured with the Multiskan Spectrum Reader (Thermo Scientific) with an intensity of 660 nm. It

shows that *Paenibacillus durus* growth starts 13 h and P22's 15 h after inoculation of the growth-medium. Both strains show a significant growth between 20 h and 50 h after inoculation. Furthermore, in both strains the stationary phase start at about 50 h after inoculation and the phase of cell dying is about 65 h after inoculation.

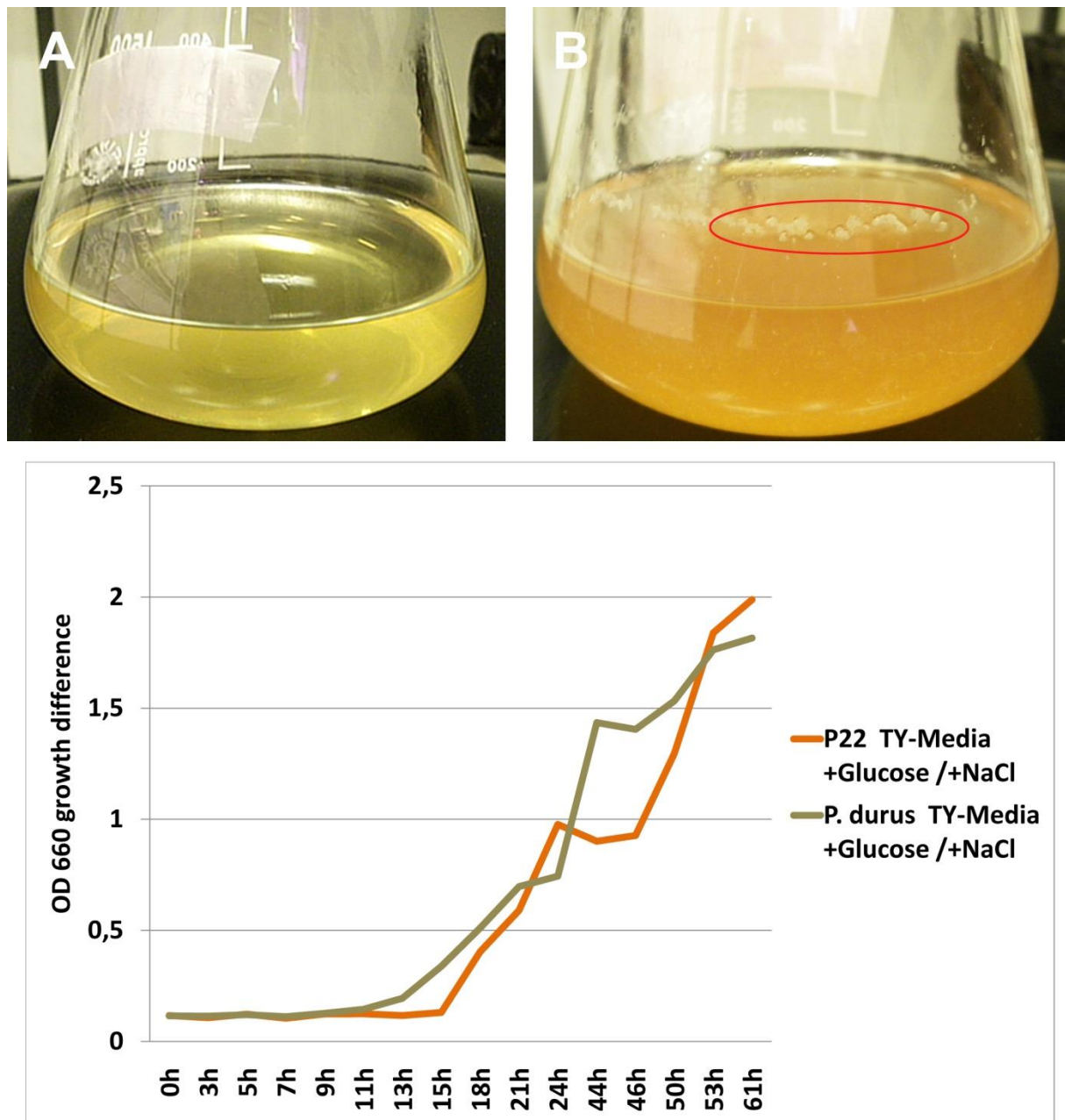


Figure 9: (A) Liquid culture of *Paenibacillus* sp. P22 grown in a liquid TY-medium including NaCl and glucose over a period of 4 days. (B) Liquid culture of *Paenibacillus durus* grown in a liquid TY- medium including NaCl and glucose over a period of 4 days. The growth curve of P22 (orange) and *Paenibacillus durus* (brown) is described in chapter 2.1.1.

In figure 10 (A) and (B) both strains were grown in liquid medium without glucose and without sodium-chloride. Again the difference between both strains can be seen in their color. Without any sugar, the color of both strains is darker than those grown

including sugar and sodium-chloride. *P. durus* growth starts 13 h after inoculation and P22 approximately 22 h after inoculation with the liquid medium. Both strains have a stable phase of about 4 h. After this stable phase the growth starts again with an exponential phase. After 53 h after inoculation *Paenibacillus durus* stops growing while *Paenibacillus* sp. P22 still kept on growing for about 8 h and then it stops and the dying phase of the bacterial cultures starts.

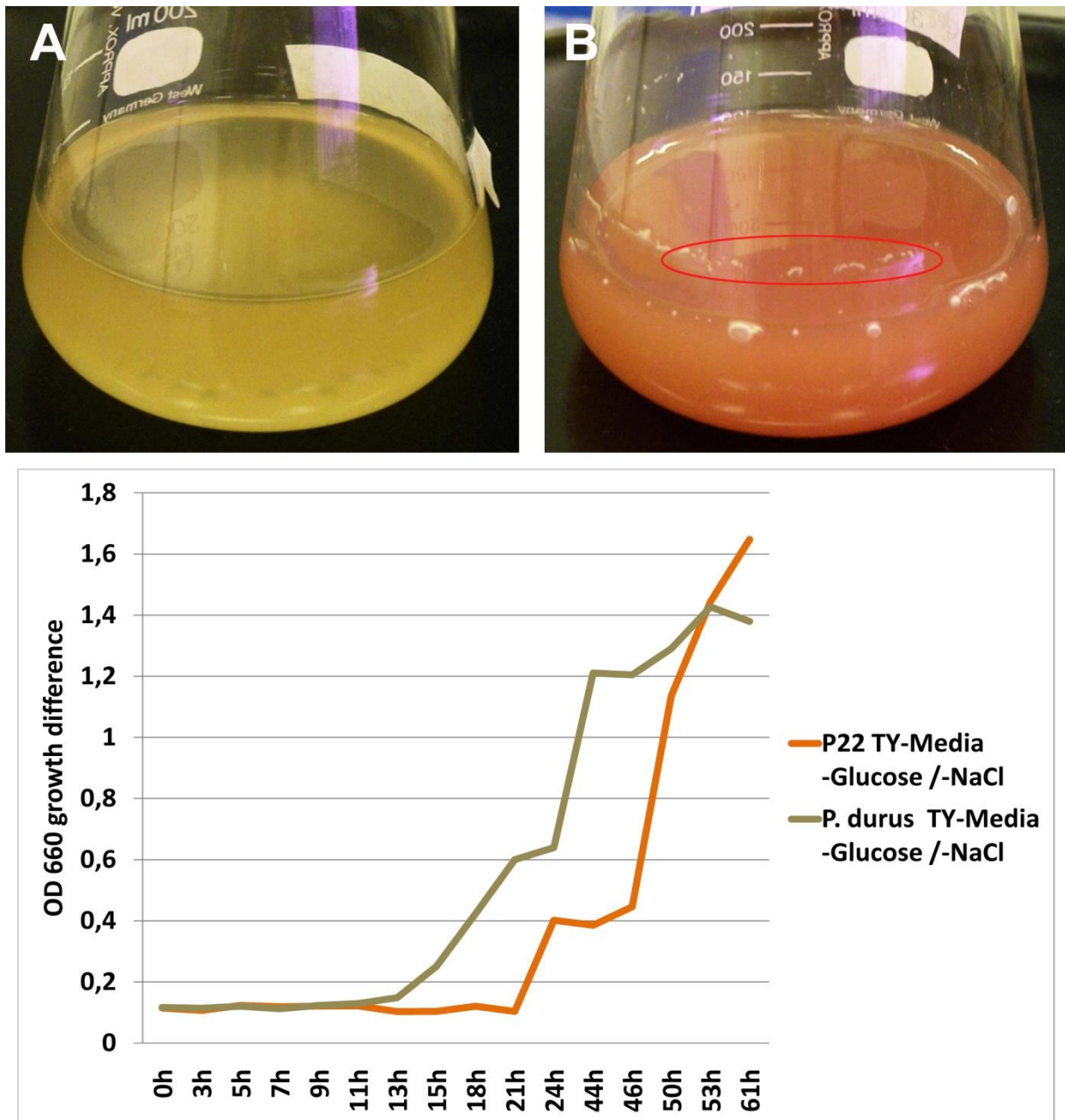


Figure 10: (A) Liquid culture of *Paenibacillus* sp. P22 grown in a liquid TY-medium without NaCl and glucose over a period of 4 days. (B) Liquid culture of *Paenibacillus durus* grown in a liquid TY-medium without NaCl and glucose over period of 4 days. The growth curve of P22 (orange) and *Paenibacillus durus* (brown) is described in chapter 2.1.1.

The growth of *Paenibacillus* sp. P22 was tested under different temperature conditions over a period of 3 days. Figure 11 (A) shows that P22 was not able to grow at 4°C, while a growth at 37°C could still be estimated (B). The best growth can be observed at 27°C (C) which has already been investigated in former experiments. The image (D) shows an agar plate inoculated with P22 grown at 50°C where no growth could be distinguished as well at 70°C, where no data are shown.

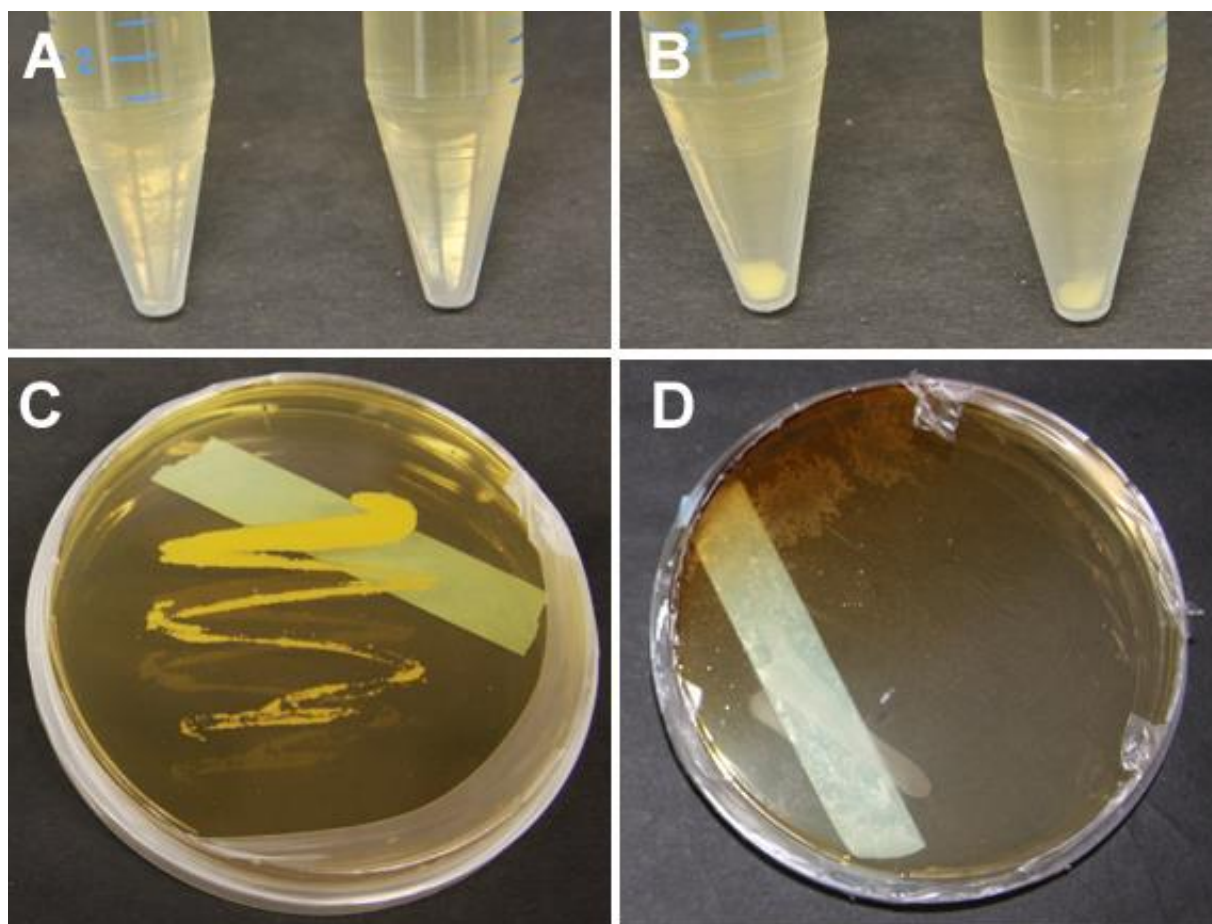


Figure 11: Testing of bacterial growth under different temperature conditions. (A) At 4°C no growth can be observed. (B) At 37°C a minimal growth can be observed. (C) 27°C a good growth of P22 can be estimated. (D) At 50°C *Paenibacillus* sp. P22 is not able to grow. Method of experiment described in chapter 2.1.1.

In figure 12 (A) *Paenibacillus* sp. P22 was grown on a nitrogen free-medium and successfully reinoculated into a liquid TY-medium. In figure 11 (B), P22 was grown on TSB-medium and re-inoculated in TY-medium. The difference is strongly visible in the density of the cultures of *Paenibacillus* sp. P22. But in both methods the bacteria started to grow very well.

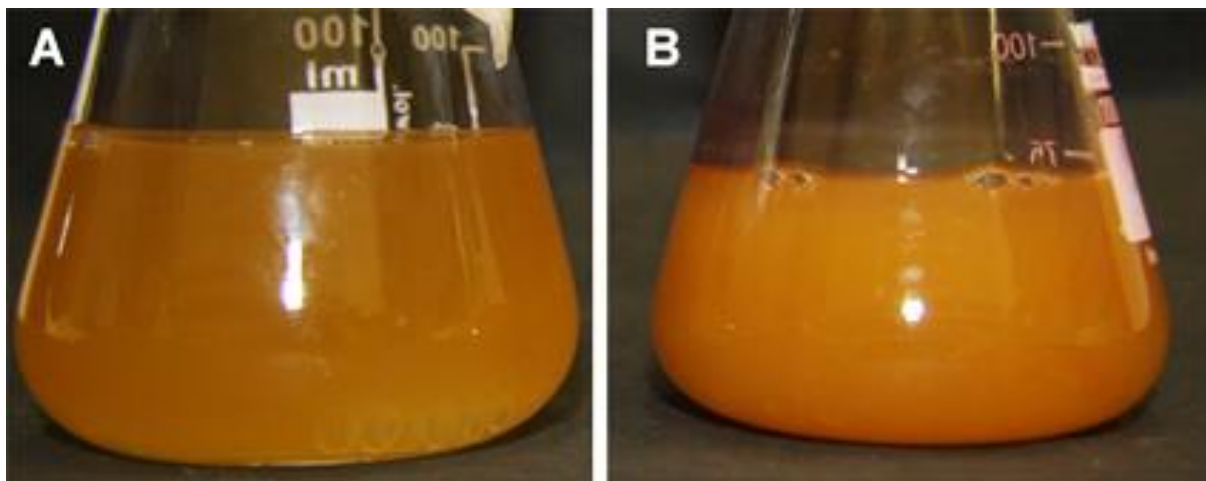


Figure 12: (A) *Paenibacillus* sp. P22 pre-cultivated on solid nitrogen free-medium (not shown) and re-inoculated into liquid TSB-medium. (B) *Paenibacillus* sp. P22 pre-cultivated on solid TY-medium (not shown) and re-inoculated into liquid TSB-medium. Method of re-inoculation described in chapter 2.1.1.

The results for freezing-medium 1 are not shown because no *Paenibacillus* cultures are grown. Freezing-medium 2 (Fig. 13 and 14) with 25% glycerol shows a growth of bacteria cultures after 2 days of incubation on TY agar plates. The medium including 50% glycerol shows a growth of P22 three days after inoculation.

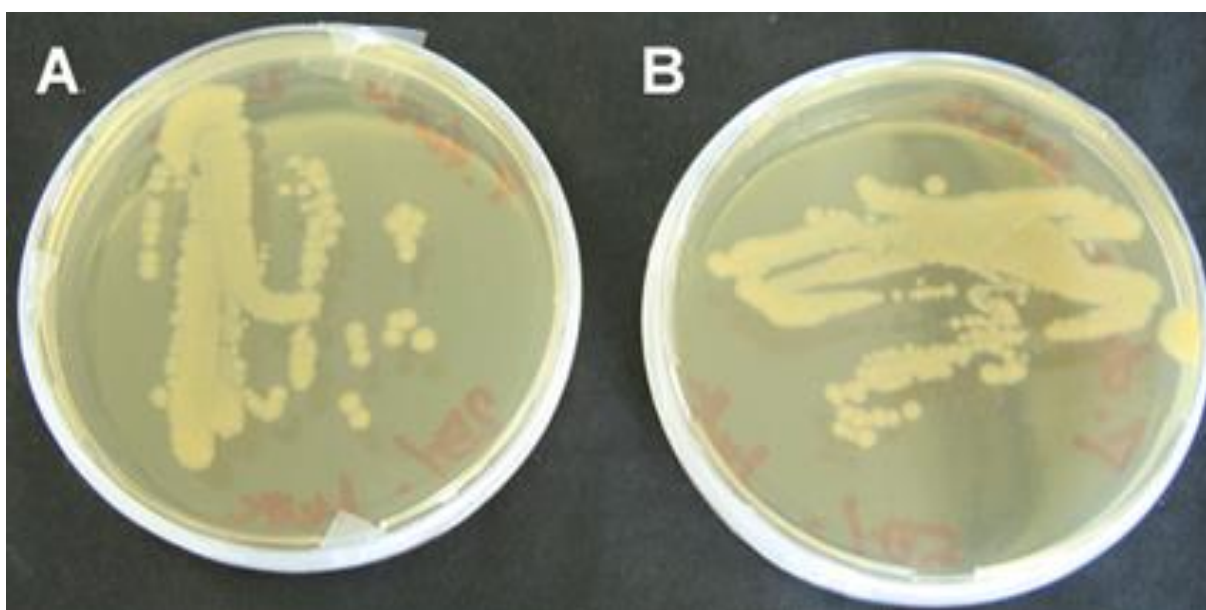


Figure 13: *Paenibacillus* sp. P22 cultures grown 3 days on TY agar plates after the bacteria had been stored at - 80°C. (A) P22 growing on TY agar plates after the storage in a freezing-medium including 25% Glycerol. (B) P22 growing on TY agar plates after the storage in a freezing-medium including 50% Glycerol. Method of experiment described in chapter 2.1.1.

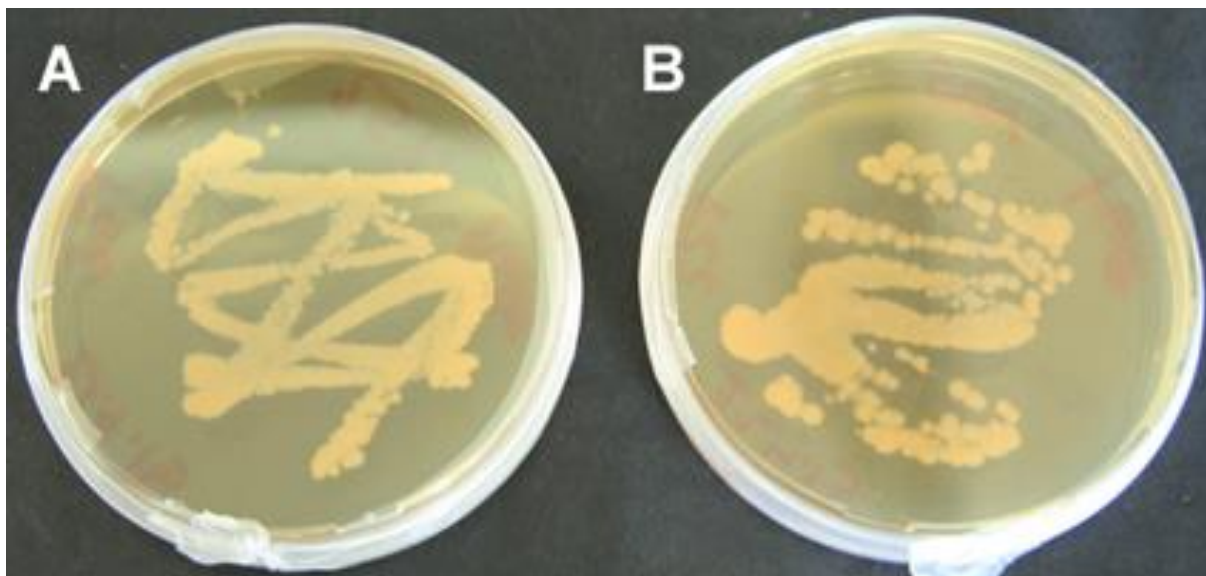


Figure 14: *Paenibacillus durus* cultures grown 3 days on TY agar plates after the bacteria had been stored at - 80°C. (A) *Paenibacillus durus* growing on TY agar plate after the storage in a freezing-medium including 25% Glycerol. (B) *Paenibacillus durus* growing on TY agar plate after the storage in a freezing-medium including 50% Glycerol. Method of experiment described in chapter 2.1.1.

In all the liquid cultures the pH-values did not vary a lot even between the different colored cultures. The pH of *Paenibacillus durus* was at 6.62 while the pH of *Paenibacillus* sp. P22 was at about 7.07.

3.1.1 MICROSCOPIC ANALYSES OF *PAENIBACILLUS* SP. P22 AND *PAENIBACILLUS*

DURUS

Figure 15 shows different microscopic analyses of *Paenibacillus* sp. P22 and *Paenibacillus durus*. Picture (A) shows *Paenibacillus* sp. P22 in a 100 fold magnification pictured with light microscopy methods. The morphology of P22 shows the elongated bacteria with no flagella. In the red circle different stages of cleavage can be observed. The size of these bacteria is about 1 μm . Image (B) shows a longitudinal section of this gram-negative bacterium taken with a transmission electron microscope. The red rectangle marks the thick cell wall which is typical for this bacterium. The length of the bacteria is about 1.5 μm . Additional to this TEM image (C) shows a square section ($\sim 800 \mu\text{m}$) of the endosporic form of P22 with 7 - 8 spikes (red square) surrounded by a rests of the spore coat of its mother cell. Endospores are usually formed when a population of vegetative cells passes out of the exponential phase of growth. The mature spore is released by lysis of the mother cell in which it was formed. Picture (D) shows a confocal laser scan microscope picture of a pure bacteria culture of P22 which has been treated with TISH (tissue *in-situ* hybridization) using the FISH probe EUB 338 green / red. Another method of investigating the bacterium *Paenibacillus* sp. P22 was chosen in image (E), the ESEM method (environmental laser scanning microscopy). A piece (4 mm) of root from poplar hybrid 741 grown in *in-vitro* tissue culture was placed on a stub and directly investigated with the ESEM. The red circles show the bacteria that resided on the root surface of these explants and in the growth media where the shoot cuttings were placed. Similar to (B) and (C), image (F) shows a TEM picture of *Paenibacillus durus*. Like *Paenibacillus* sp. P22 it is a gram-negative bacterium with a size of $\sim 600 \mu\text{m}$ in square section. *P. durus* does not have any flagella (not shown).

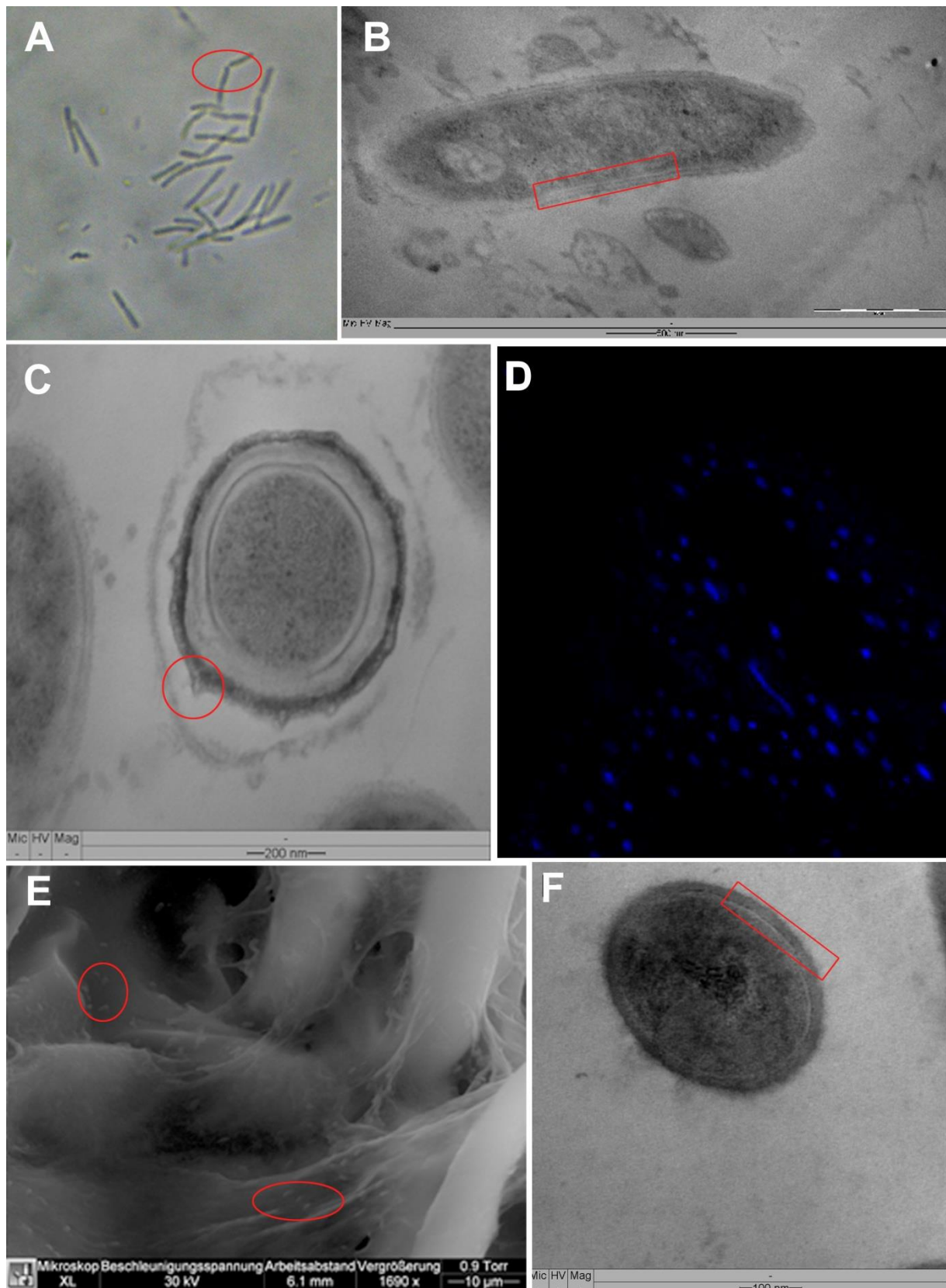


Figure 15: (A) 100 fold light microscopy of *Paenibacillus* sp. P22, cleavage of the cells is visible (red). (B) TEM shot of P22, red colored rectangle shows the cell wall of these gram-negative bacteria. (C) TEM picture of P22, endosporic form with 7 - 8 forming spikes. (D) *Paenibacillus* sp. P22 in the CLSM fluorescence method which let the bacteria shine blue, treated with the TISH-method. (E) Root of poplar 741 investigated in ESEM shows bacteria (red circles) located in the media at the root surface. (F) TEM image of *Paenibacillus durus*.

3.1.2 GENOME ANNOTATION OF *PAENIBACILLUS* SP. P22

Application of the 454[®] sequencing technology resulted in 561.213 reads and 61.143.112 nucleotides. In an Ion Torrent[™] PGM sequencing approach 1.978.332 reads and 343.311.791 nucleotides were gathered. Consensus assembly using MIRA (34) yielded in 5.443.257 bp in 297 contigs (< 300 bp) with an overall GC content of 58%. The genome of *Paenibacillus* sp. P22 contains 5.224 protein-coding genes, 65 tRNAs and 1 16S rRNA. Presence of tRNAs for all 20 proteinogenic amino acids as well as 31 out of 31 phylogenetic marker proteins (Software AMPHORA2 (238)) that are essential in prokaryotes indicate an estimated completeness of the genome of about 99%.

Further investigation of the metabolic capabilities of *Paenibacillus* sp. P22 yielded two particularly interesting elucidations. We found a gene encoding a nitrogenase [EC:1.19.6.1] for nitrogen fixation. This coincides with the observation that *Paenibacillus* sp. P22 is able to grow without nitrogen in the medium (189). Furthermore the metabolite profiles of the poplar plants which were inoculated with *Paenibacillus* sp. P22 showed a strongly altered C/N homeostasis directly pointing to a changed nitrogen assimilation pathway as a result of the endophyte-plant interaction (189). Further genes of nitrate assimilation in *Paenibacillus* sp. P22 were identified, e.g. a nitrate reductase [NAD(P)H] large subunit [EC:1.7.1.4]. Both enzymes the nitrogenase and the nitrate reductase were described also in *Paeanibacillus polymyxa* E681 (105) a nitrogen fixing bacterium (http://www.genome.jp/dbget-bin/www_bget?pathway+ppy01230). Furthermore, we were able to detect genes of the auxin-pathway, e.g. the tryptophane synthase beta chain [EC:4.2.1.20] suggesting growth-promoting effects by hormone secretion.

The accession numbers CBRA010000001-CBRA010000571 which has been deposited in the 'European Nucleotide Archive' show the genome sequence of *Paenibacillus* sp. P22 detected with the Ion Torrent[™] PGM sequencing approach. A new number which compares the data of Ion Torrent[™] PGM sequencing and the 454[®] sequencing technology will be available in January 2014.

3.2 EXPERIMENT OF BIOMASS WITH POPLAR HYBRID AF2, AF8 AND MONVISO

All figures for this chapter are numbered as followed: (A) control (no inoculation), (B) inoculation with *Paenibacillus* sp. P22, (C) inoculation with *Paenibacillus durus*, 1 number of replica, (a) 0 days, start of experiment, (b) day of inoculation, (c) 10 days, 28 days, 70 days after inoculation. The t-test was set with two variances with a p-value ≤ 0.05 , hypothetic difference of mean value = 0.

3.2.1 HYDROPONIC CULTURE EXPERIMENT

3.2.1.1 POPLAR HYBRID AF2

The hydroponic experimental setup did not show the results that have been expected. As shown in figure 16, poplar clone AF2 does not show any significance in biomass 10 days after inoculation neither with *Paenibacillus* sp. P22 nor inoculated with *Paenibacillus durus* compared to the control explants. In none of the shoots of the control and the shoots inoculated with *Paenibacillus durus* the rooting had started. Only the explants that were inoculated with *Paenibacillus* sp. P22 have a beginning root growth.

28 days (Fig. 17) after inoculation the root growth has started of inoculated shoots with *Paenibacillus durus* and *Paenibacillus* sp. P22 while the control was still rootless. A difference of growth is visible but a control with the t-test could not measure any significance between all three experimental setups. 70 days after IO, shown in figure 18, 19 and 20 (A), the control does not grow well anymore which can be seen in the diagram. There has also been a drop out of one sample of the inoculated explants with P22. The comparison of the inoculated shoot to the control is difficult, nearly impossible. Already 6 weeks after planting a severe deficiency of macronutrients can be observed which was tried to be replaced by a change of the pouring solution. This deficit could be distinguished by the yellow colored leafs of the explants.

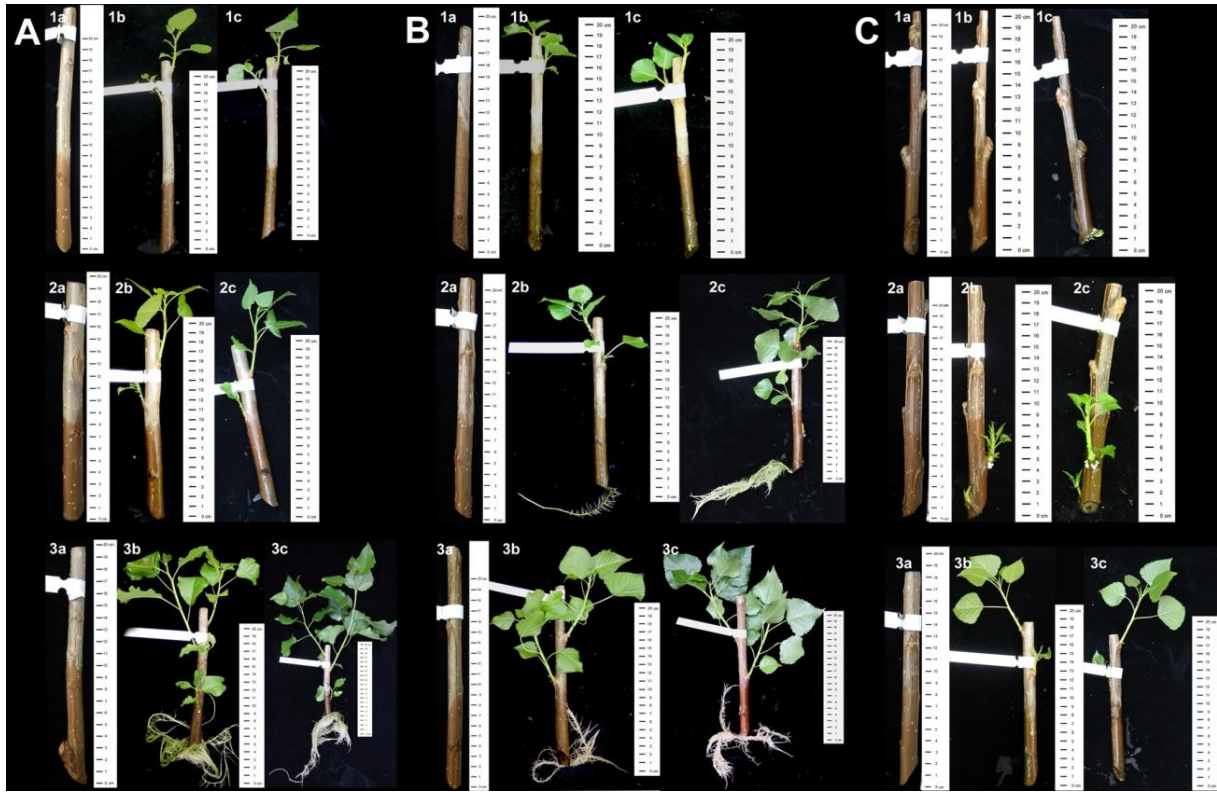


Figure 16: Harvest of poplar hybrid AF2 10 days after IO with *Paenibacillus* sp. P22 and *Paenibacillus durus*. (A) Control (1-3: number of replica, a: day 0, b: day of inoculation, c: day 10 after IO). (B) IO with *Paenibacillus* sp. P22 (1-3: number of replica, a: day 0, b: day of inoculation, c: day 10 after IO). (C) IO with *Paenibacillus durus* (1-3: number of replica, a: day 0, b: day of inoculation, c: day 10 after IO).

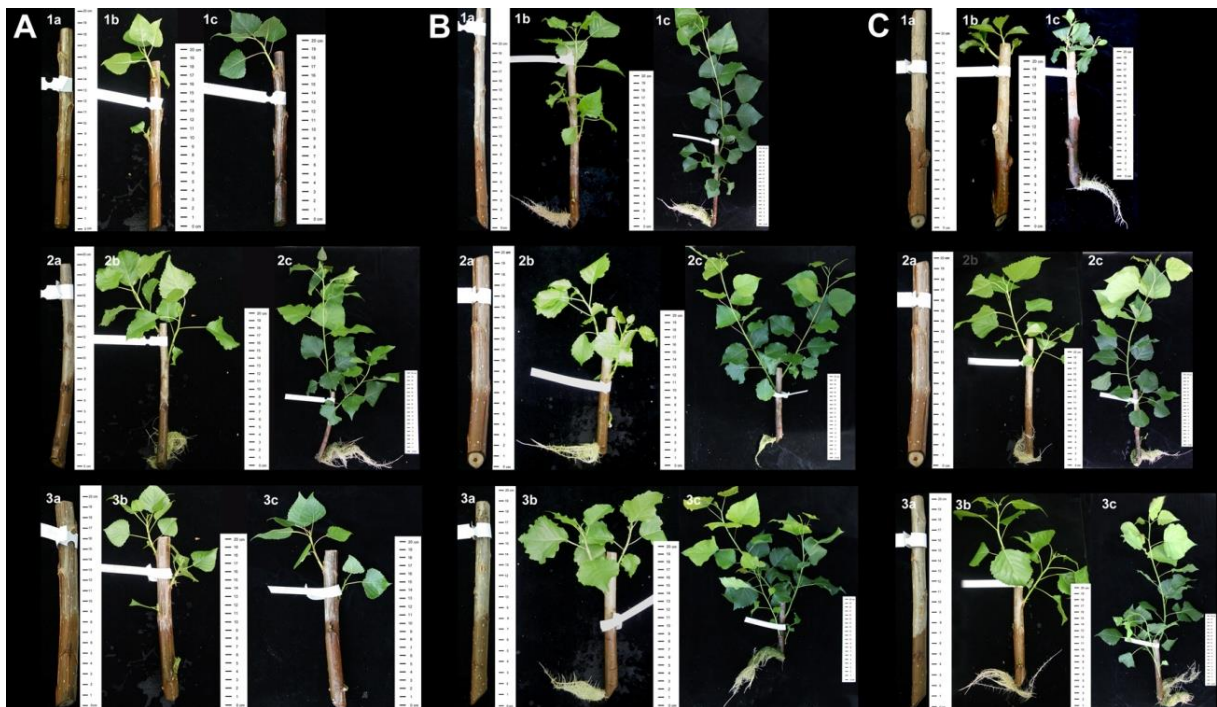


Figure 17: Harvest of poplar hybrid AF2 28 days after IO. (A) Control (1-3: number of replica, a: day 0, b: day of inoculation, c: day 28 after IO). (B) IO with *Paenibacillus* sp. P22 (1-3: number of replica, a: day 0, b: day of inoculation, c: day 28 after IO). (C) IO with *Paenibacillus durus* (1-3: number of replica, a: day 0, b: day of inoculation, c: day 28 after IO).

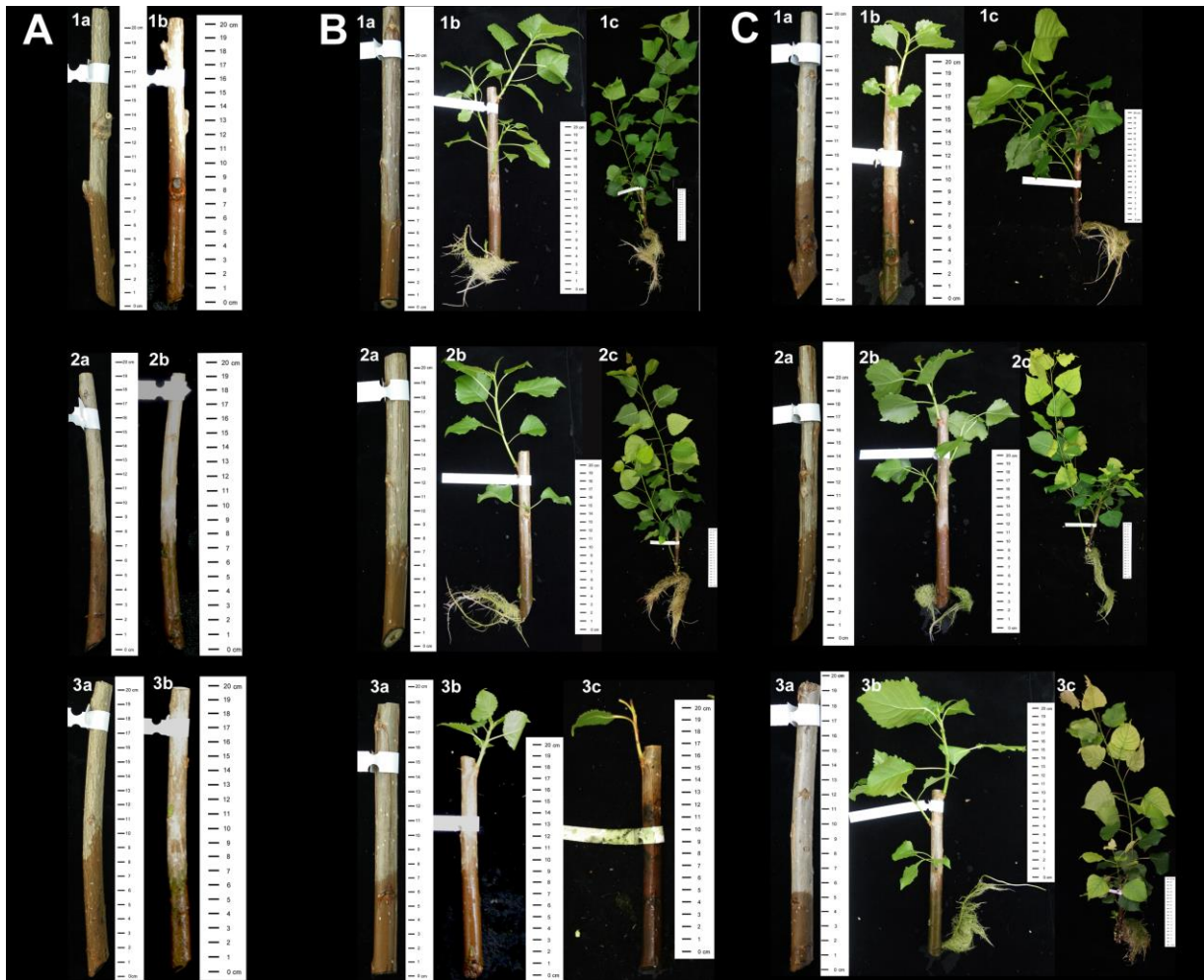


Figure 18: Harvest of poplar hybrid AF2 70 days after IO. (A) Control (1-3: number of replica, a: day 0, b: day of inoculation, c: day 70 after IO). (B) IO with *Paenibacillus* sp. P22 (1-3: number of replica, a: day 0, b: day of inoculation, c: day 70 after IO). (C) IO with *Paenibacillus durus* (1-3: number of replica, a: day 0, b: day of inoculation, c: day 70 after IO).

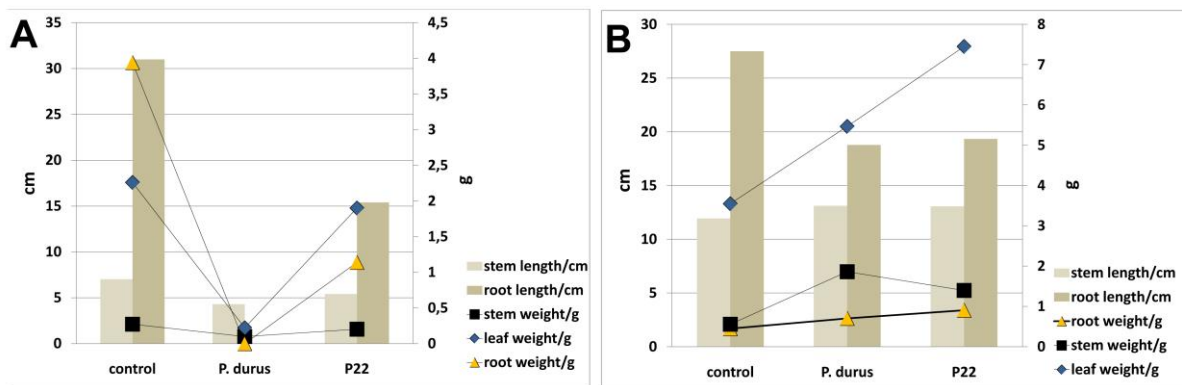


Figure 19: Schemata of all measured data of poplar hybrid AF2. (A) Harvest 10 days after IO. (B) Harvest 28 days after IO; e.g. the p-value of the stem weight between control and the explants inoculated with *Paenibacillus* sp. P22 was $p \leq 0.0886$ and the root weight between the control and inoculated with *Paenibacillus durus* $p \leq 0.6733$.

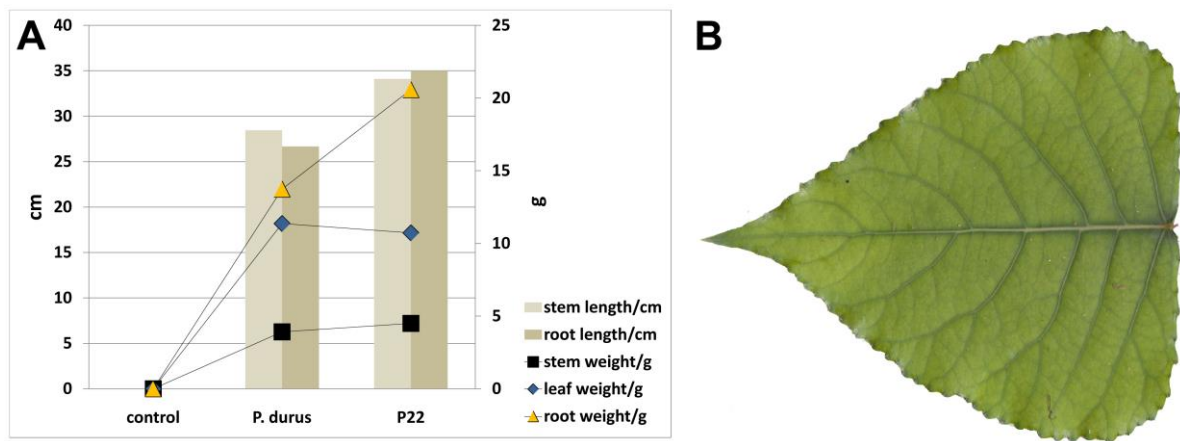


Figure 20: (A) Schemata of all measured data of poplar hybrid AF2, Harvest 70 days after IO; e.g. the p-value of the stem weight between control and the explants inoculated with *Paenibacillus* sp. P22 was $p \leq 0.0886$ and the root weight between control and inoculated with *Paenibacillus durus* $p \leq 0.6733$. (B) Leaf of a young poplar hybrid AF2.

3.2.1.2 POPLAR HYBRID MONVISO

The poplar clone Monviso had a much faster growth compared to AF2, and AF8. But still, no significance in biomass 10 days after inoculation could be measured. The same result could be estimated for the harvest 28 - and 70 days after inoculation with both bacterial strains (Figure 21, 22, 23, 24 and 25). There are no drop-outs for this clone in this experiment. A deficiency of some macromolecules can also be investigated in this hybrid.

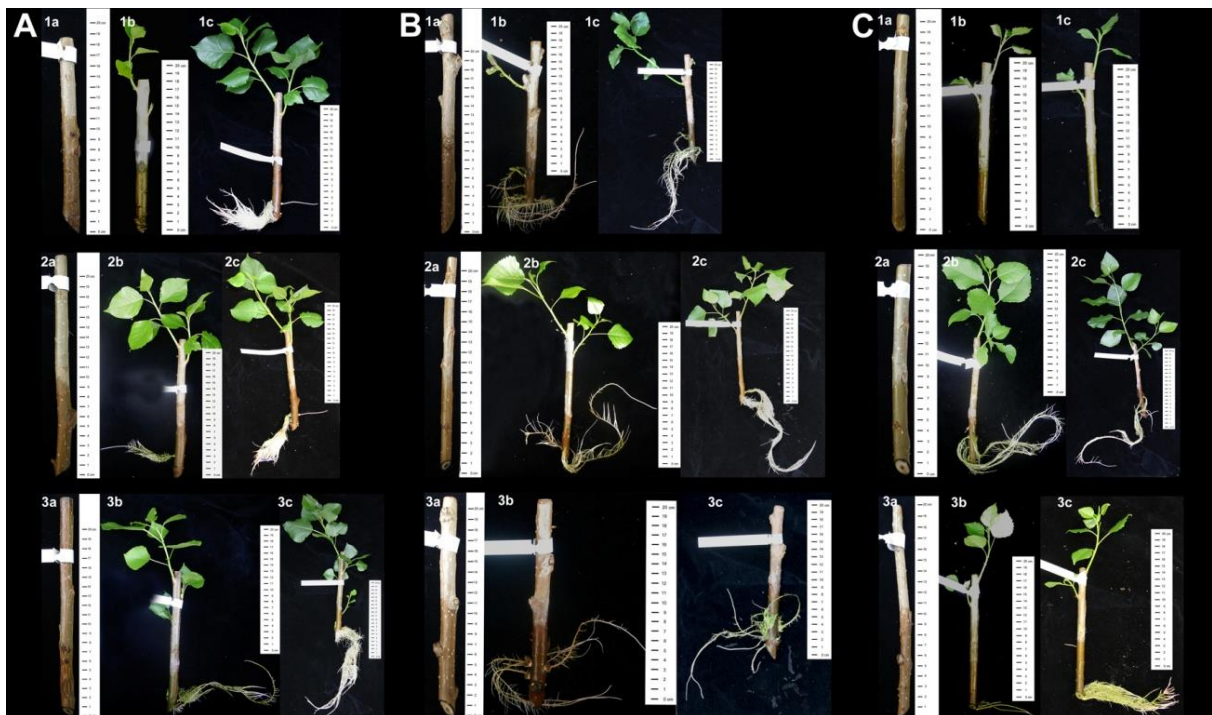


Figure 21: Harvest of Monviso 10 days after IO with *Paenibacillus* sp. P22 and *Paenibacillus durus*. (A) Control (1-3: number of replica, a: day 0, b: day of inoculation, c: day 10 after IO). (B) IO with *Paenibacillus* sp. P22 (1-3: number of replica, a: day 0, b: day of inoculation, c: day 10 after IO). (C) IO with *Paenibacillus durus* (1-3: number of replica, a: day 0, b: day of inoculation, c: day 10 after IO).

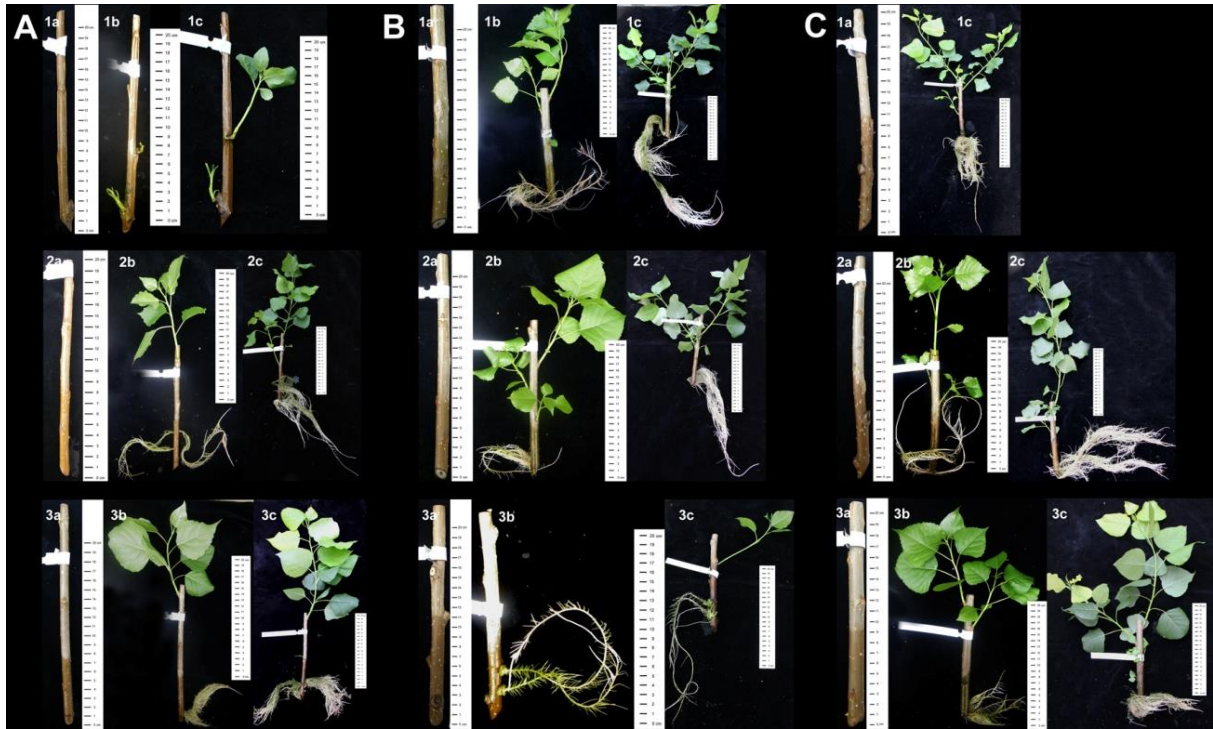


Figure 22: Harvest of poplar hybrid Monviso 28 days after IO. (A) Control (1-3: number of replica, a: day 0, b: day of inoculation, c: day 28 after IO). (B) IO with *Paenibacillus* sp. P22 (1-3: number of replica, a: day 0, b: day of inoculation, c: day 28 after IO). (C) IO with *Paenibacillus durus* (1-3: number of replica, a: day 0, b: day of inoculation, c: day 28 after IO).



Figure 23: Harvest of poplar hybrid Monvsio 70 days after IO. (A) Control (1-3: number of replica, a: day 0, b: day of inoculation, c: day 70 after IO). (B) IO with *Paenibacillus* sp. P22 (1-3: number of replica, a: day 0, b: day of inoculation, c: day 70 after IO). (C) IO with *Paenibacillus durus* (1-3: number of replica, a: day 0, b: day of inoculation, c: day 70 after IO).

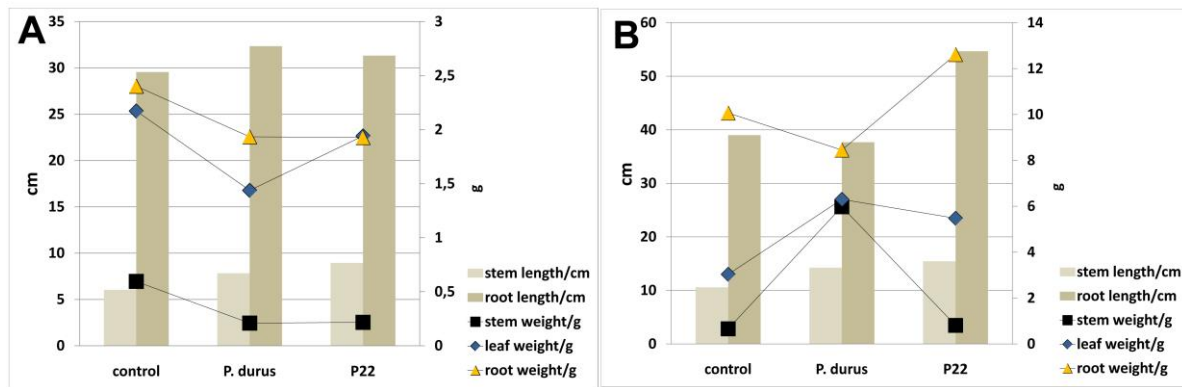


Figure 24: Schemata of all measured data of poplar hybrid Monviso. (A) Harvest 10 days after IO. (B) Harvest 28 days after IO. Significances in stem weight of inoculated shoot cuttings with *Paenibacillus durus* compared to the control and the other inoculated shoot cuttings.

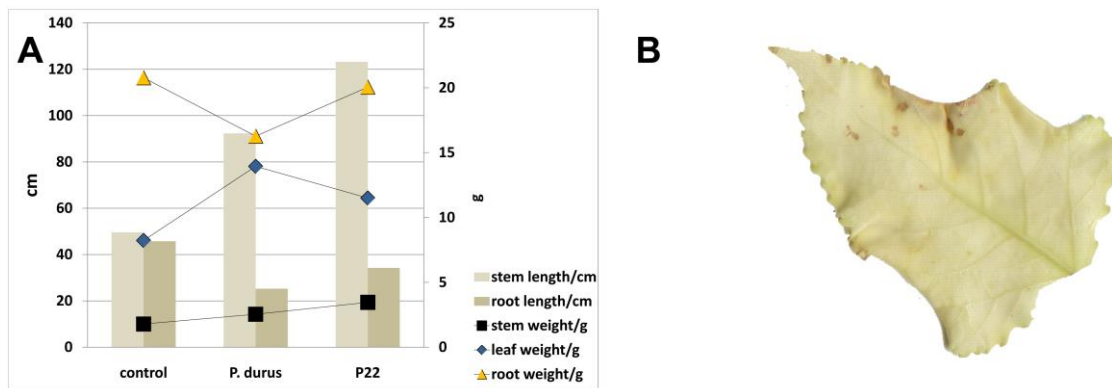


Figure 25: (A) Schemata of all measured data of poplar hybrid Monviso, Harvest 70 days after IO; t-test done with the data 70 days after inoculation shows that the stem weight between control and IO with P22 was $p \leq 0.2376$ and leaf weight between control and *P. durus* was $p \leq 0.1329$. (B) Leaf of poplar hybrid Monviso with nutrient starvation signs of infection.

3.2.1.3 POPLAR HYBRID AF8

The poplar clone AF8 does not show any significant differences in biomass 10 days (data not shown). 28 days (Fig. 26 and 28) after inoculation with the two different bacterial strains show minor growth promoting effects in root and stem weight in the explants inoculated with *Paenibacillus durus*. In figure 28 C, 70 days (Fig. 27) after inoculation, a difference in root weight and stem length of the shoot cuttings inoculated with *Paenibacillus* sp. P22 be distinguished.

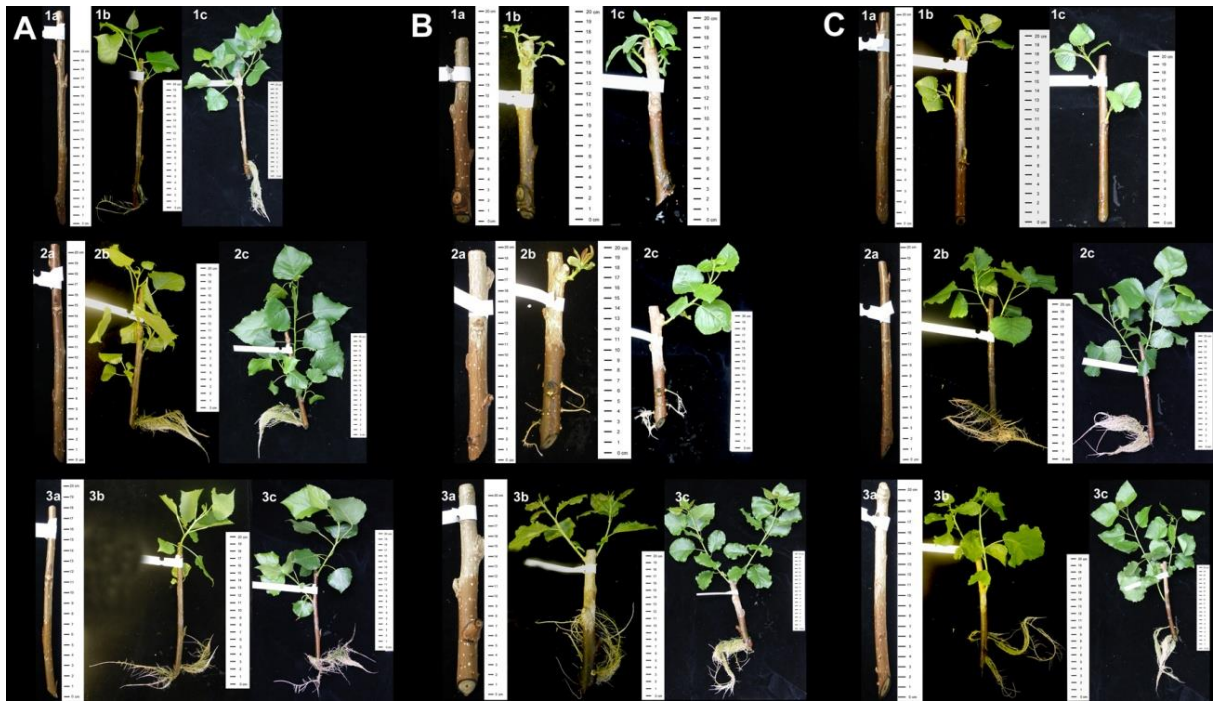


Figure 26: Harvest of poplar hybrid AF8 28 days after IO. (A) Control (1-3: number of replica, a: day 0, b: day of inoculation, c: day 10 after IO). (B) IO with *Paenibacillus* sp. P22 (1-3: number of replica, a: day 0, b: day of inoculation, c: day 10 after IO). (C) IO with *Paenibacillus durus* (1-3: number of replica, a: day 0, b: day of inoculation, c: day 10 after IO).



Figure 27: Harvest of poplar hybrid AF8 70 days after IO. (A) Control (1-3: number of replica, a: day 0, b: day of inoculation, c: day 28 after IO). (B) IO with *Paenibacillus* sp. P22 (1-3: number of replica, a: day 0, b: day of inoculation, c: day 28 after IO). (C) IO with *Paenibacillus durus* (1-3: number of replica, a: day 0, b: day of inoculation, c: day 28 after IO).

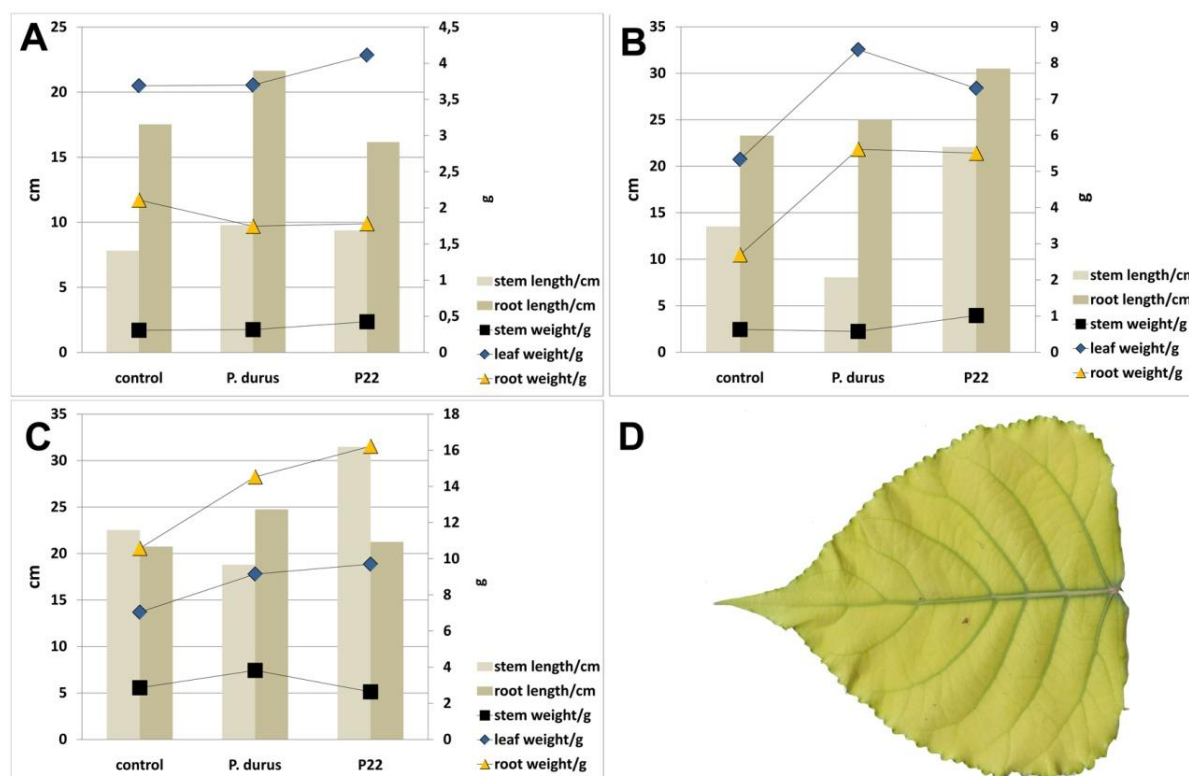


Figure 28: Schemata of all measured data of poplar hybrid AF8. (A) Harvest 10 days after IO. (B) Harvest 28 days after IO. (C) Harvest 70 days after IO. (D) Young leaf of poplar hybrid AF8 with signs of nutrient starvation.

3.2.2 VERMICULITE / PERLITE CULTURE WITH INOCULATION AFTER ROOTING

3.2.2.1 POPLAR HYBRID AF2

Poplar hybrid AF2 shows a difference of root length 10 days after inoculation with *Paenibacillus* sp. P22 and *P. durus* (Fig. 29 and 31 A). The root length and the root weight show a significant growth rate 28 days after inoculation with *Paenibacillus* sp. P22 compared to the control. Also the stem weight, leaf weight and the area leaf index show positive results compared to the control plants (Fig. 30 and 32). 70 days (Fig. 33, 34 and 35) after inoculation the gain of biomass can be distinguished by the shoots inoculated with *Paenibacillus durus* as well.

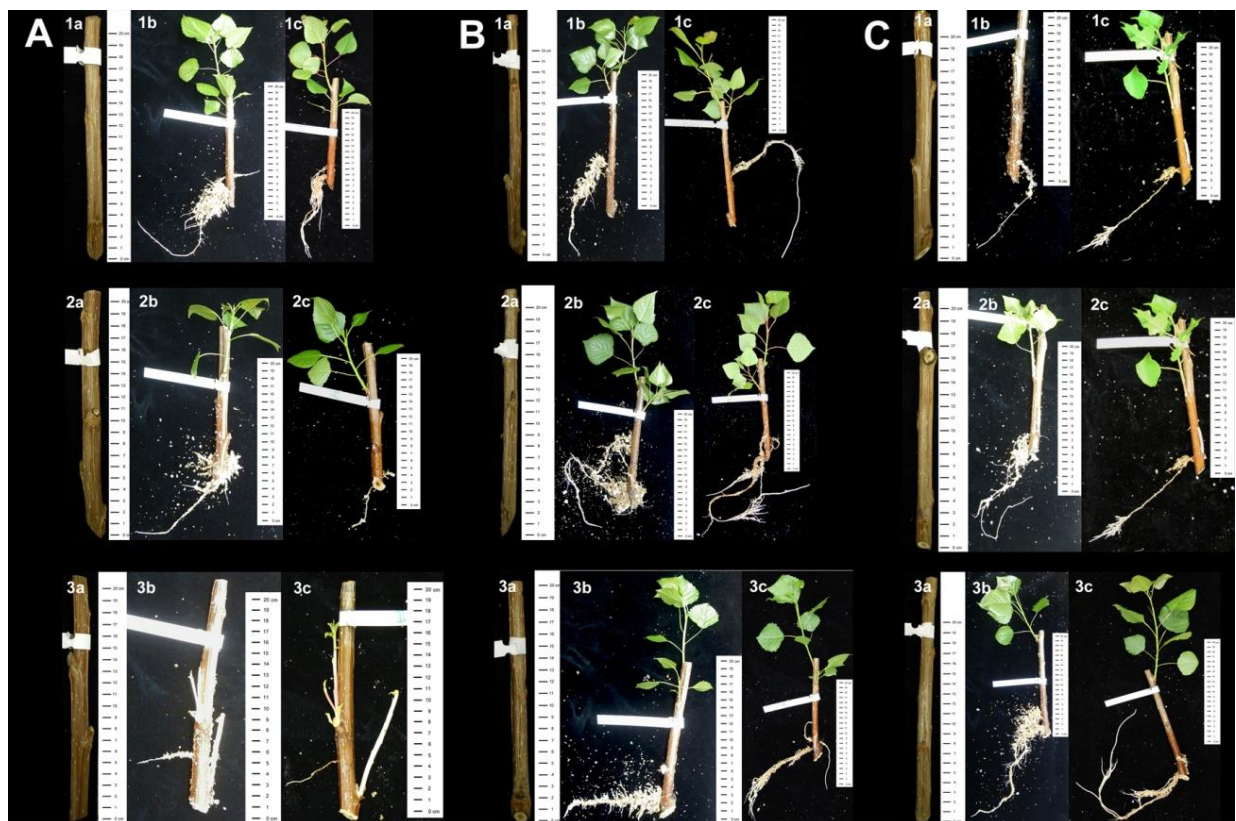


Figure 29: Harvest of AF2 10 days after IO with *Paenibacillus* sp. P22 and *Paenibacillus durus*. (A) Control (1-3: number of replica, a: day 0, b: day of inoculation, c: day 10 after IO). (B) IO with *Paenibacillus* sp. P22 (1-3: number of replica, a: day 0, b: day of inoculation, c: day 10 after IO). (C) IO with *Paenibacillus durus* (1-3: number of replica, a: day 0, b: day of inoculation, c: day 10 after IO).

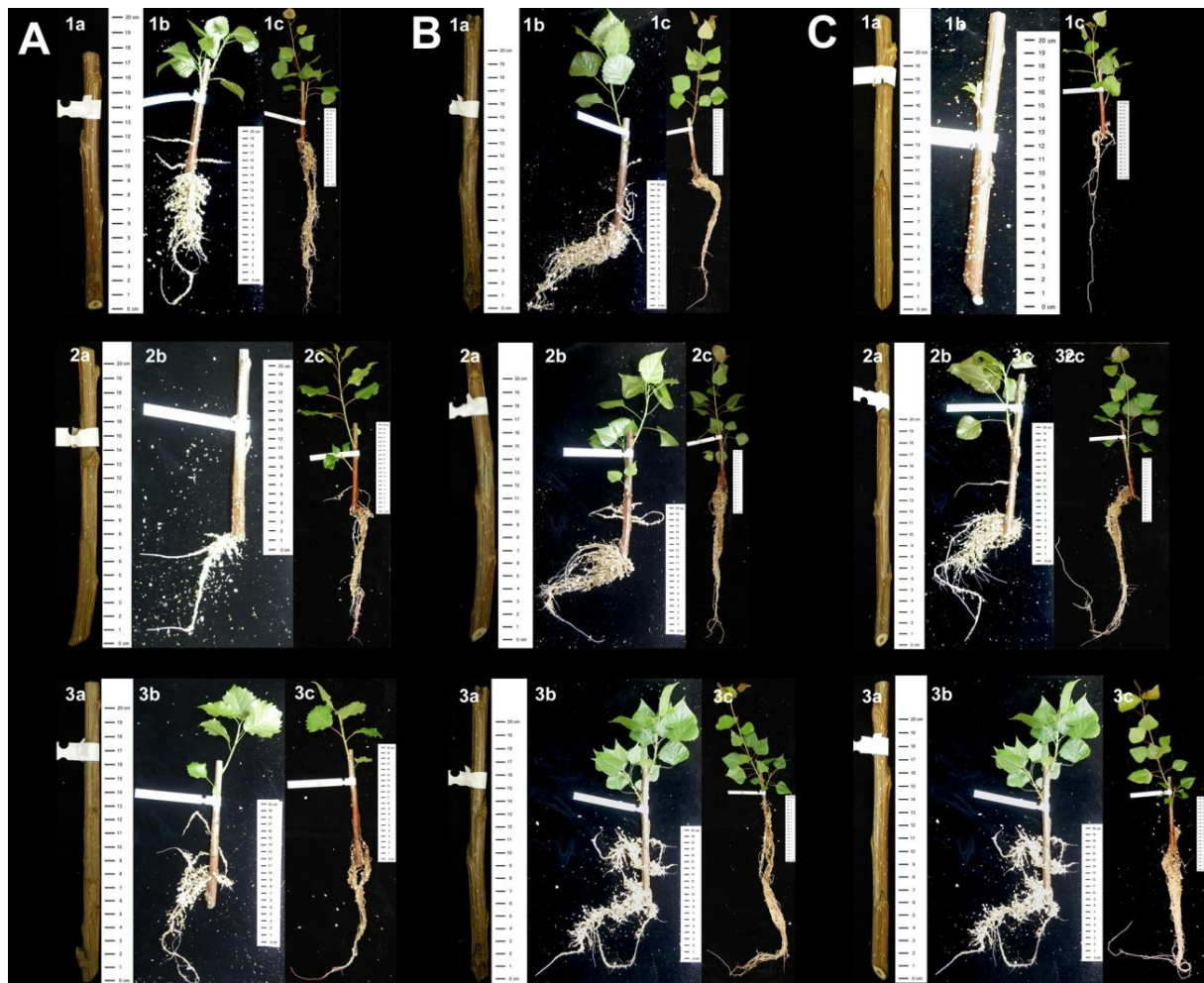


Figure 30: Harvest of poplar hybrid AF2 28 days after IO. (A) Control (1-3: number of replica, a: day 0, b: day of inoculation, c: day 28 after IO). (B) IO with *Paenibacillus* sp. P22 (1-3: number of replica, a: day 0, b: day of inoculation, c: day 28 after IO). (C) IO with *Paenibacillus durus* (1-3: number of replica, a: day 0, b: day of inoculation, c: day 28 after IO).

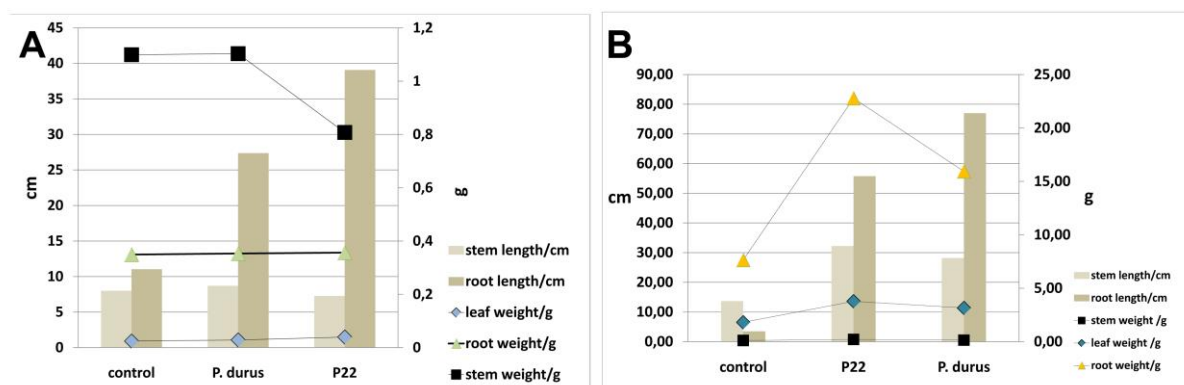


Figure 31: Schemata of different data of AF2. (A) Harvest 10 days after IO; no significance between the control and the inoculated explants. (B) Harvest 28 days after IO; significance in root weight between control and inoculated shoot with *Paenibacillus* sp. P22 but no significances between control and shoot inoculated with *Paenibacillus durus*.

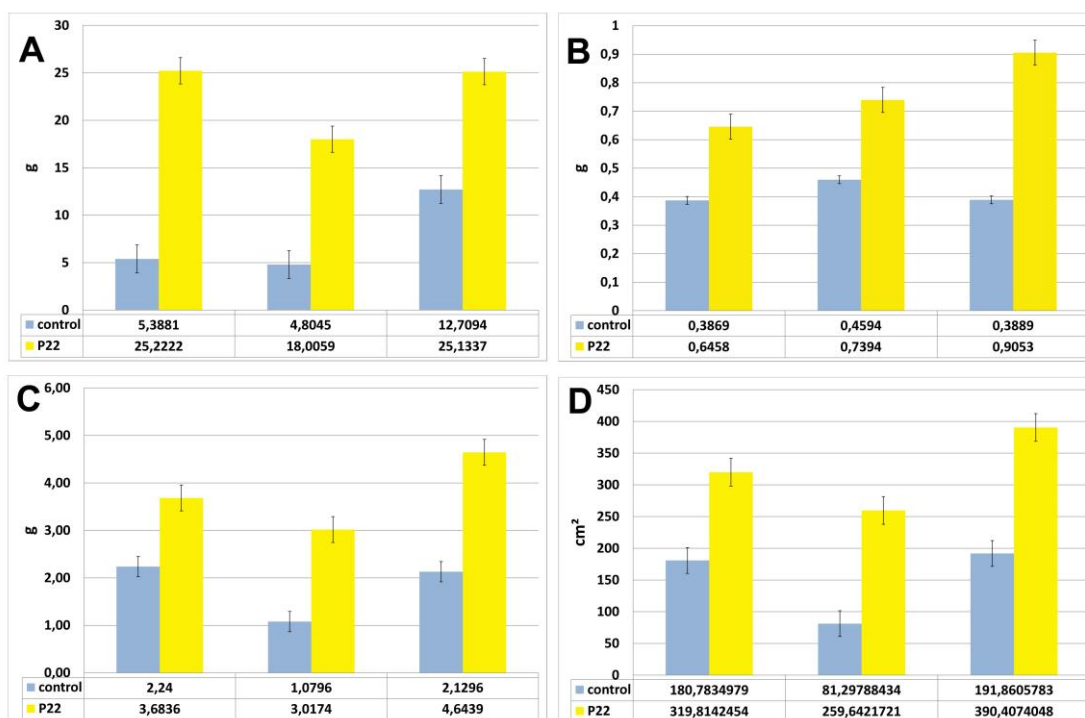


Figure 32: Schemata of different data of AF2. (A) Root weight 28 days after inoculation; significance $p \leq 0.0122418$ between control and IO P22. (B) Stem weight 28 days after IO; significance $p \leq 0.048$ between control and IO P22. (C) Leaf weight 28 days after IO, significance $p \leq 0.030$. (D) Area leaf index 28 days after IO, p-value ≤ 0.0290 between control and IO P22.

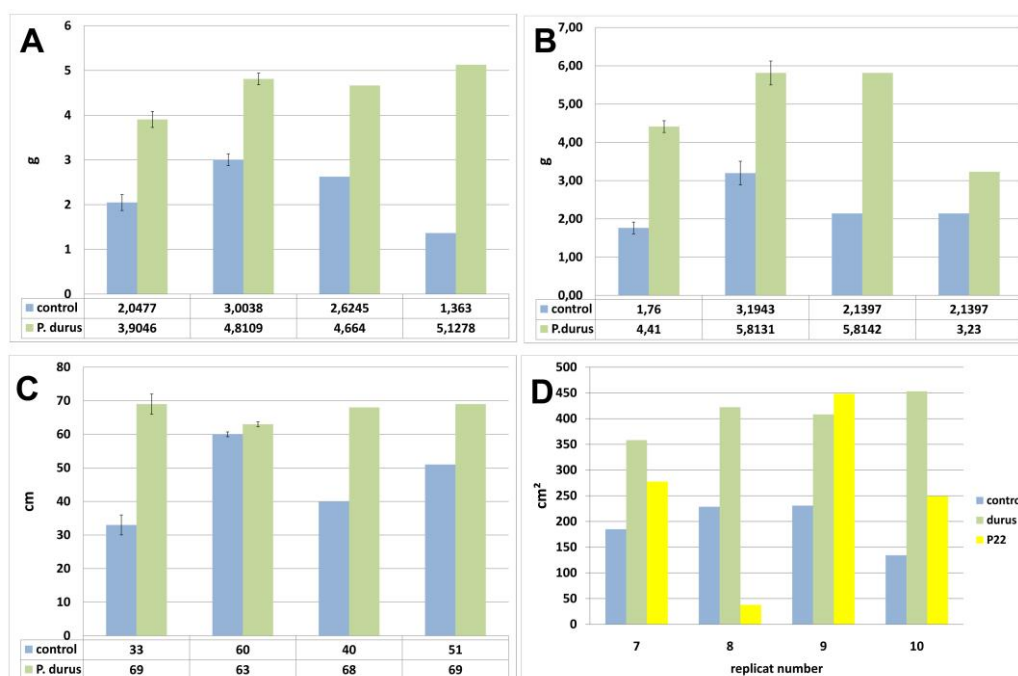


Figure 33: Schemata of different data of AF2. (A) Leaf weight 70 days after IO; for e.g. control / *P. durus* $p \leq 0.0030487$. (B) Stem weight 70 days after IO. (C) Root length 70 days after IO. (D) Leaf area index 70 days after IO for e.g. significance between the control and *P. durus* inoculated stem $p \leq 0.00037453$.

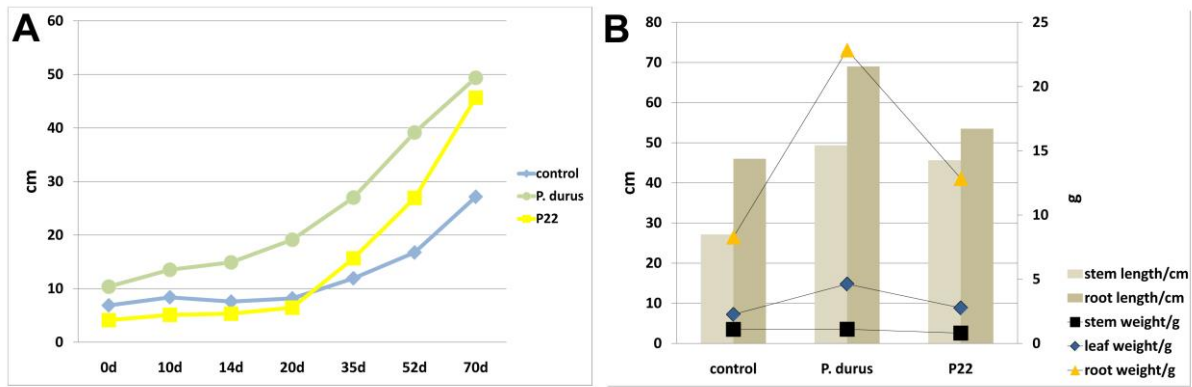


Figure 34: Schemata of different data of AF2. (A) Gain of stem length 70 days after IO for e.g. between control and inoculation with *Paenibacillus* sp. P22 $p \leq 0.00551081$ and between control and *P. durus* inoculated plants $p \leq 0.0079541$. (B) All data in overview.

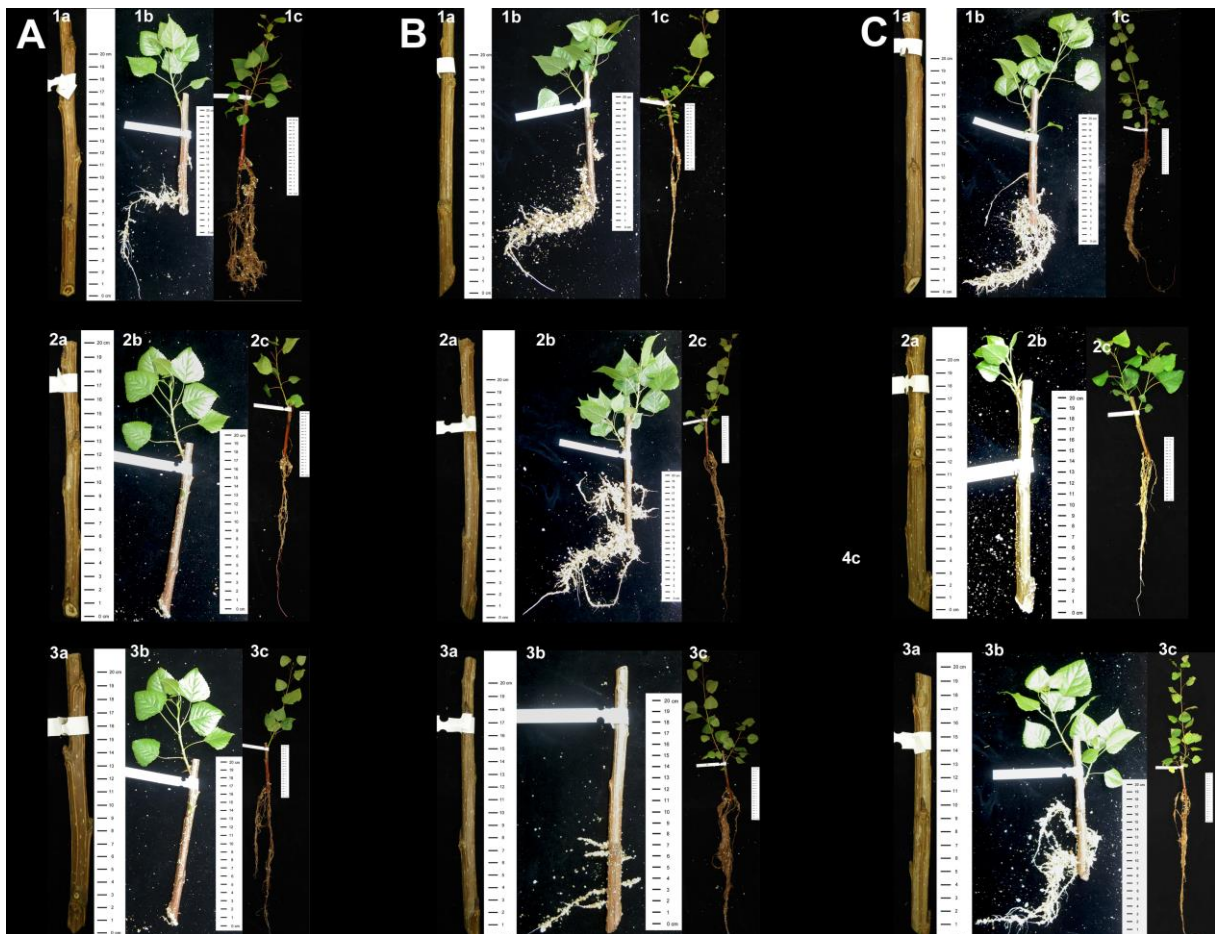


Figure 35: Harvest of poplar hybrid AF2 70 days after IO. (A) Control (1-3: number of replica, a: day 0, b: day of inoculation, c: day 70 after IO). (B) IO with *Paenibacillus* sp. P22 (1-3: number of replica, a: day 0, b: day of inoculation, c: day 70 after IO). (C) IO with *Paenibacillus durus* 1-3: number of replica, a: day 0, b: day of inoculation, c: day 70 after IO).

3.2.2.2 POPLAR HYBRID MONVISO

Monviso has a minimal significance in biomass. There are no significances in the data 10 days (Fig. 36 and 37) and 28 days (Fig. 38 and 39) after inoculation with *Paenibacillus* sp. P22 and *Paenibacillus durus*. In figure 40 differences in biomass 70 days after inoculation with the 2 different bacterial strains are shown. Significances in the area leaf index can be registered (Fig. 41) between the control and the inoculated explants.



Figure 36: Harvest of Monviso 10 days after IO with *Paenibacillus* sp. P22 and *Paenibacillus durus*. (A) Control (1-3: number of replica, a: day 0, b: day of inoculation, c: day 10 after IO). (B) IO with *Paenibacillus* sp. P22 (1-3: number of replica, a: day 0, b: day of inoculation, c: day 10 after IO). (C) IO with *Paenibacillus durus* (1-3: number of replica, a: day 0, b: day of inoculation, c: day 10 after IO).

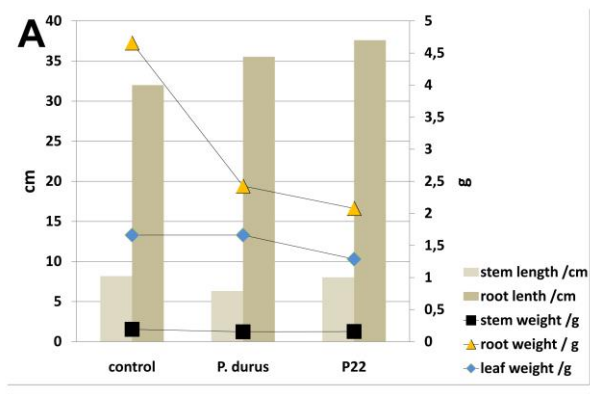


Figure 37: Schemata of all measured data of Monviso. (A) Harvest 10 days after IO.

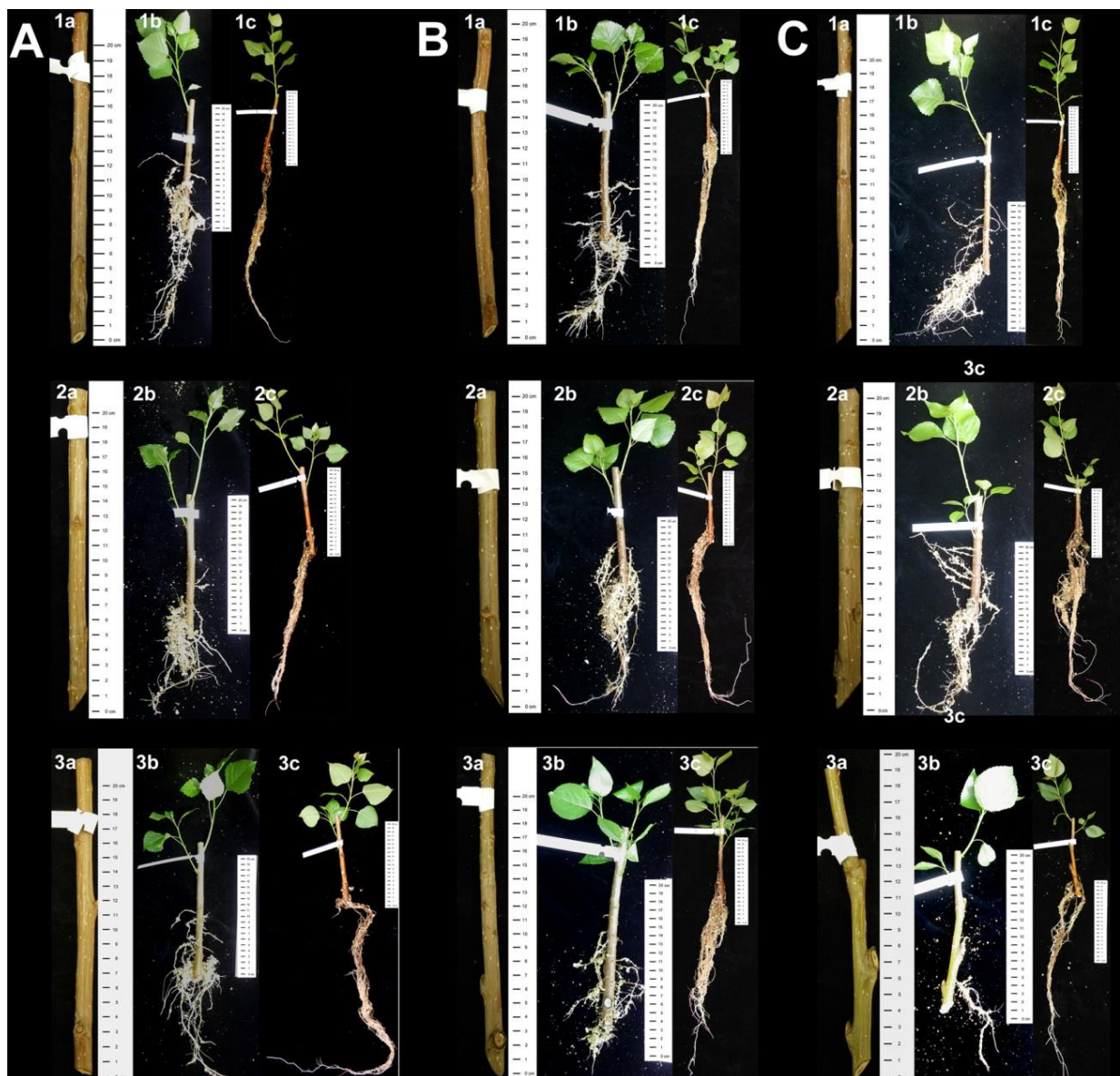


Figure 38: Harvest of poplar hybrid Monviso 28 days after IO. (A) Control 1-3: number of replica, a: day 0, b: day of inoculation, c: day 28 after IO). (B) IO with *Paenibacillus* sp. P22 (1-3: number of replica, a: day 0, b: day of inoculation, c: day 28 after IO). (C) IO with *Paenibacillus durus* ((1-3: number of replica, a: day 0, b: day of inoculation, c: day 28 after IO).

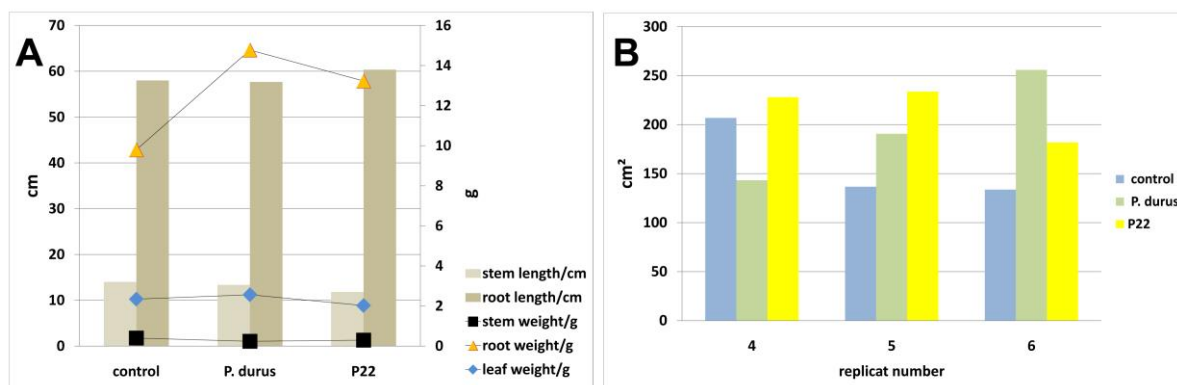


Figure 39: Schemata of all measured data of Monviso. (A) Harvest 28 days after IO. (B) Area leaf index 28 days after IO.

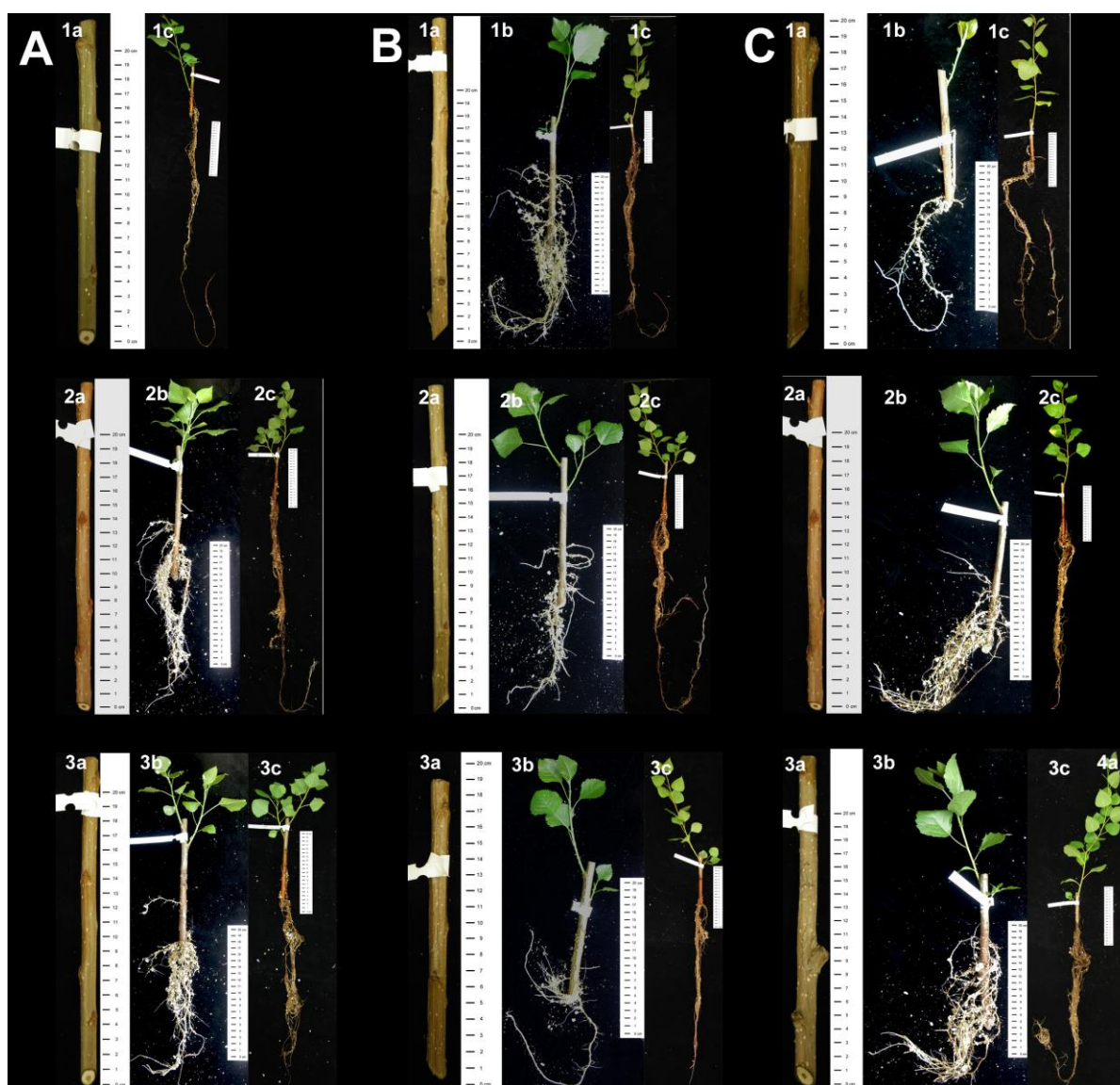


Figure 40: Harvest of poplar hybrid Monviso 70 days after IO. (A) Control (1-3: number of replica, a: day 0, b: day of inoculation, c: day 70 after IO). (B) IO with *Paenibacillus* sp. P22 (1-3: number of replica, a: day 0, b: day of inoculation, c: day 70 after IO). (C) IO with *Paenibacillus durus* (1-3: number of replica, a: day 0, b: day of inoculation, c: day 70 after IO).

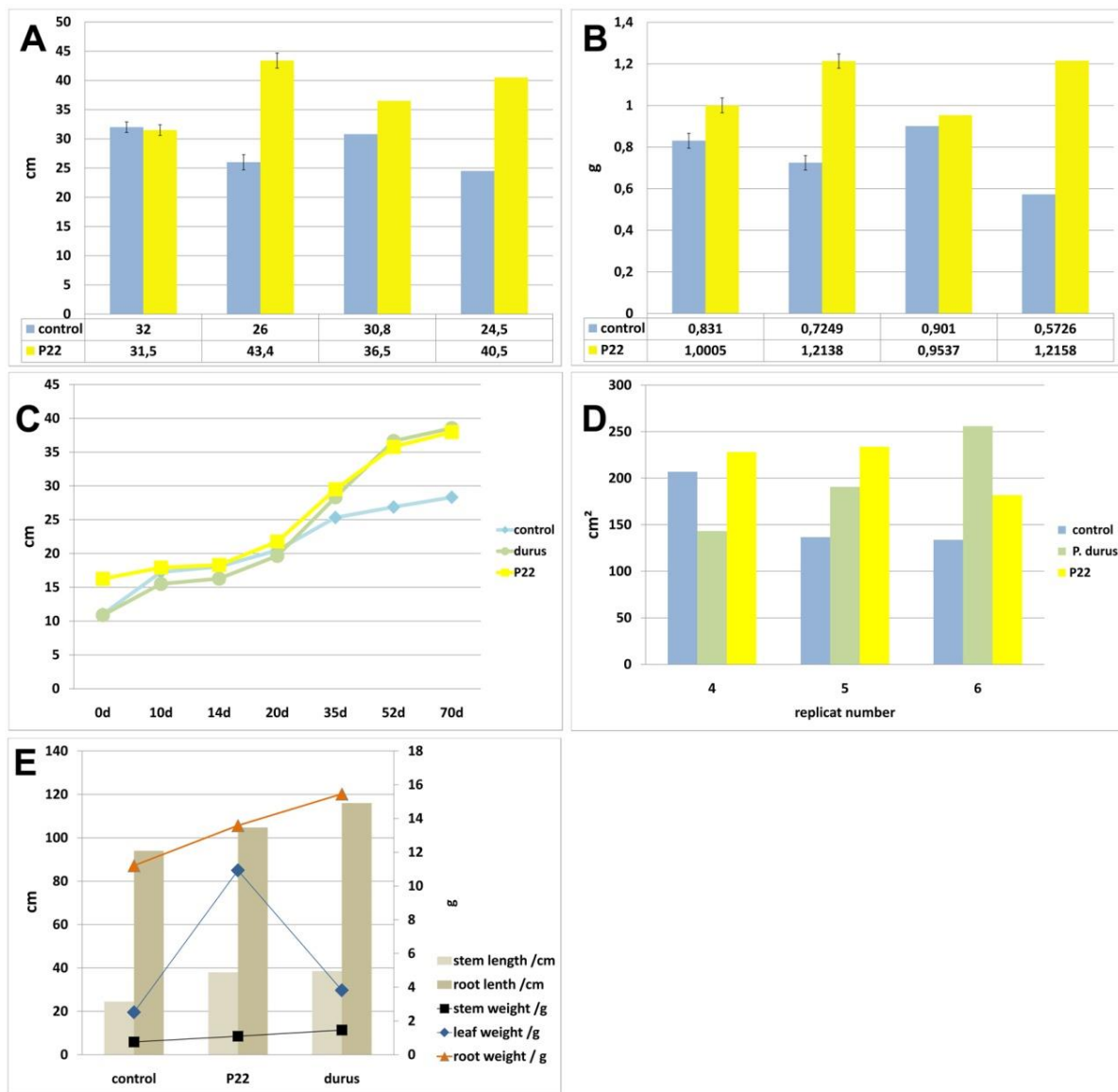


Figure 41: Schemata of all measured data of Monviso. (A) Stem length 70 days after IO; $p \leq 0.02819775$ between control and inoculated with *Paenibacillus* sp. P22. (B) Stem weight 70 days after IO; $p \leq 0.01445703$ between control and inoculated with *Paenibacillus* sp. P22. (C) Gain of stem length 70 days of IO. (D) Area leaf index 70 days after IO; the significance in area leaf index could be calculated with $p \leq 0.04723383$. (E) Harvest 70 days after inoculation.

3.2.2.3 POPLAR HYBRID AF8

Minor significances between the control and the inoculated shoot cuttings can be distinguished 10 days and 28 days after inoculation (Fig. 42, 43 and 44). Poplar hybrid AF8 shows significances in biomass 70 days after inoculation with *Paenibacillus* sp. P22 and *Paenibacillus durus* in the root length and the root weight compared to the control plants (Fig. 45 and 46).

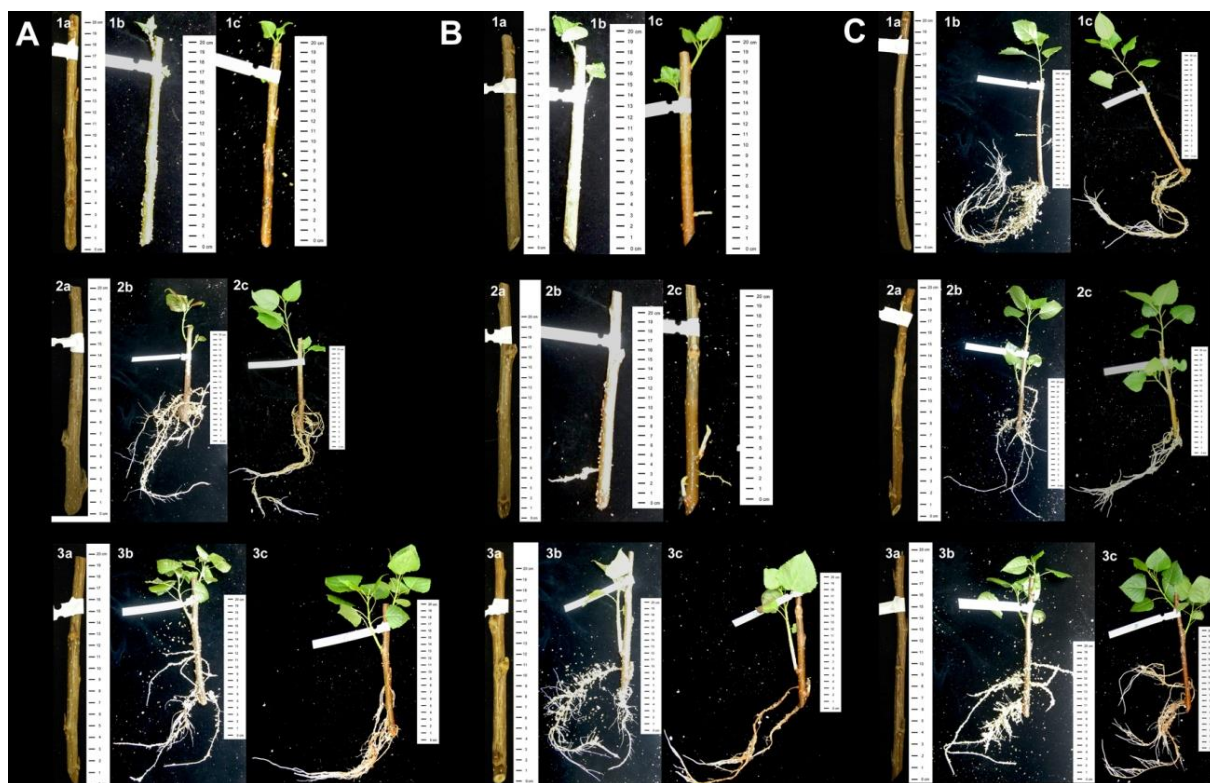


Figure 42: Harvest of AF8 10 days after IO with *Paenibacillus* sp. P22 and *Paenibacillus durus*. (A) Control (1-3: number of replica, a: day 0, b: day of inoculation, c: day 10 after IO). (B) IO with *Paenibacillus* sp. P22 (1-3: number of replica, a: day 0, b: day of inoculation, c: day 10 after IO). (C) IO with *Paenibacillus durus* (1-3: number of replica, a: day 0, b: day of inoculation, c: day 10 after IO).

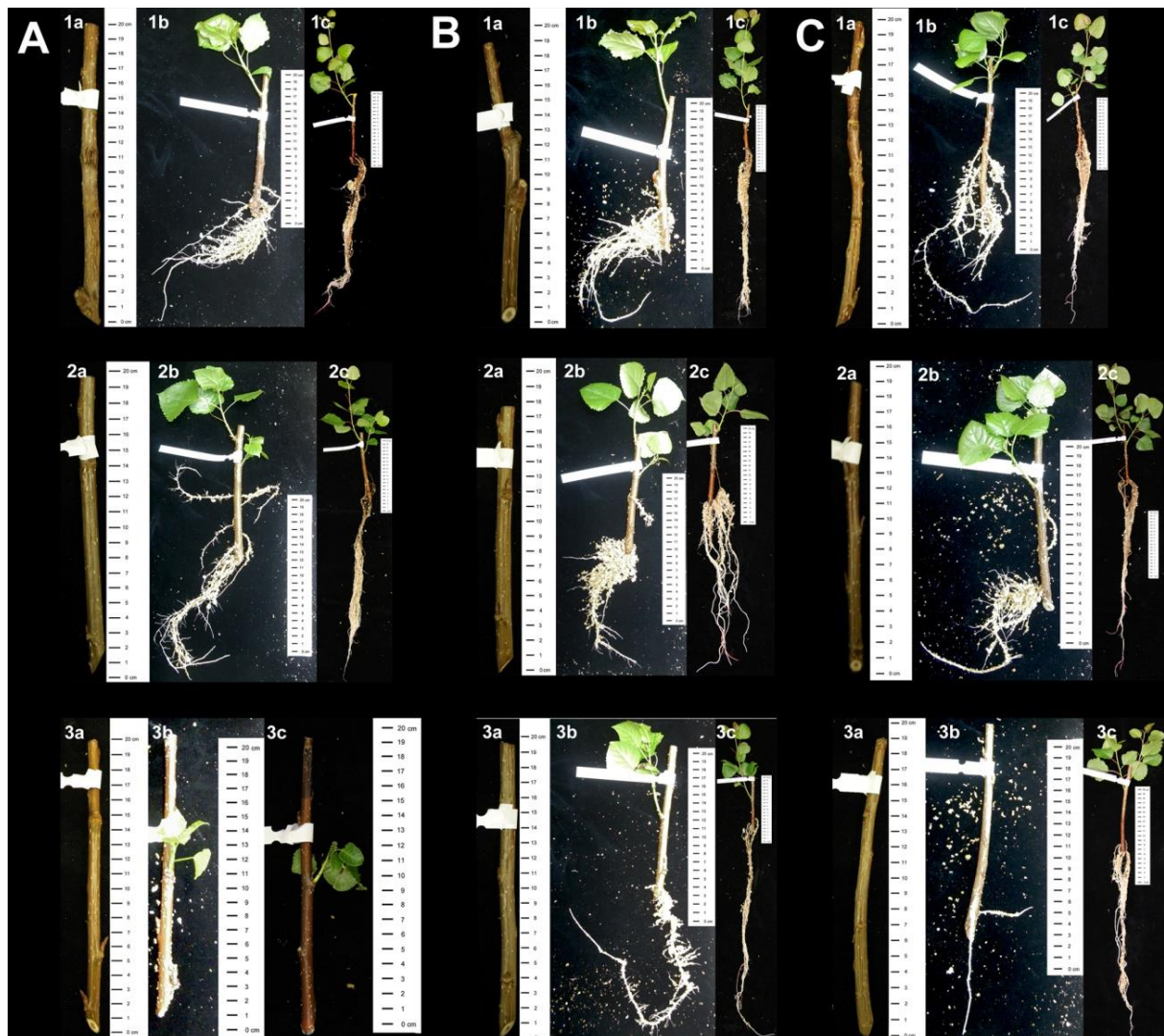


Figure 43: Harvest of poplar hybrid AF8 28 days after IO. (A) Control (1-3: number of replica, a: day 0, b: day of inoculation, c: day 28 after IO). (B) IO with *Paenibacillus* sp. P22 (1-3: number of replica, a: day 0, b: day of inoculation, c: day 28 after IO). (C) IO with *Paenibacillus durus* (1-3: number of replica, a: day 0, b: day of inoculation, c: day 28 after IO).

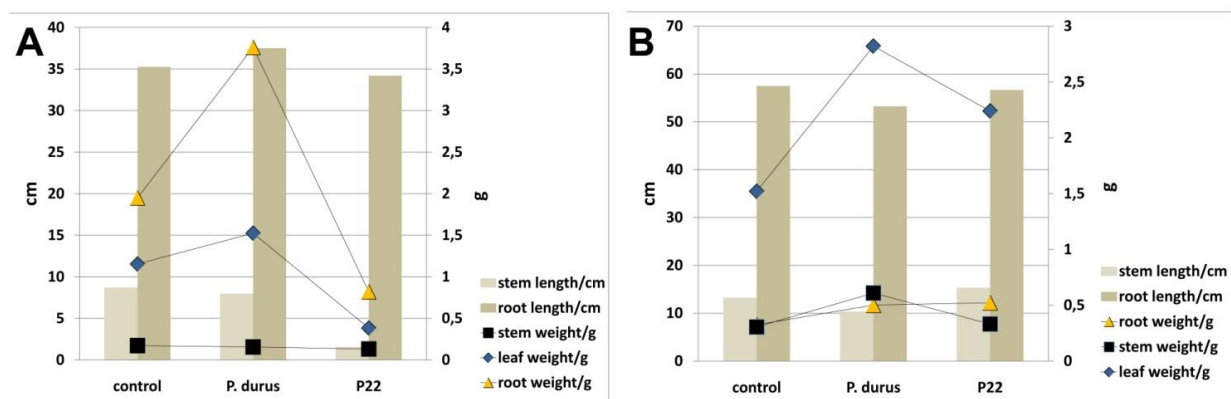


Figure 44: Schemata of all measured data of poplar hybrid AF8. (A) Harvest 10 days after IO. Minor significances in root weight between the control and shoots inoculated with *Paenibacillus durus* can be distinguished. (B) Harvest 28 days after inoculation. High difference in leaf weight between control and the inoculated shoot explants.

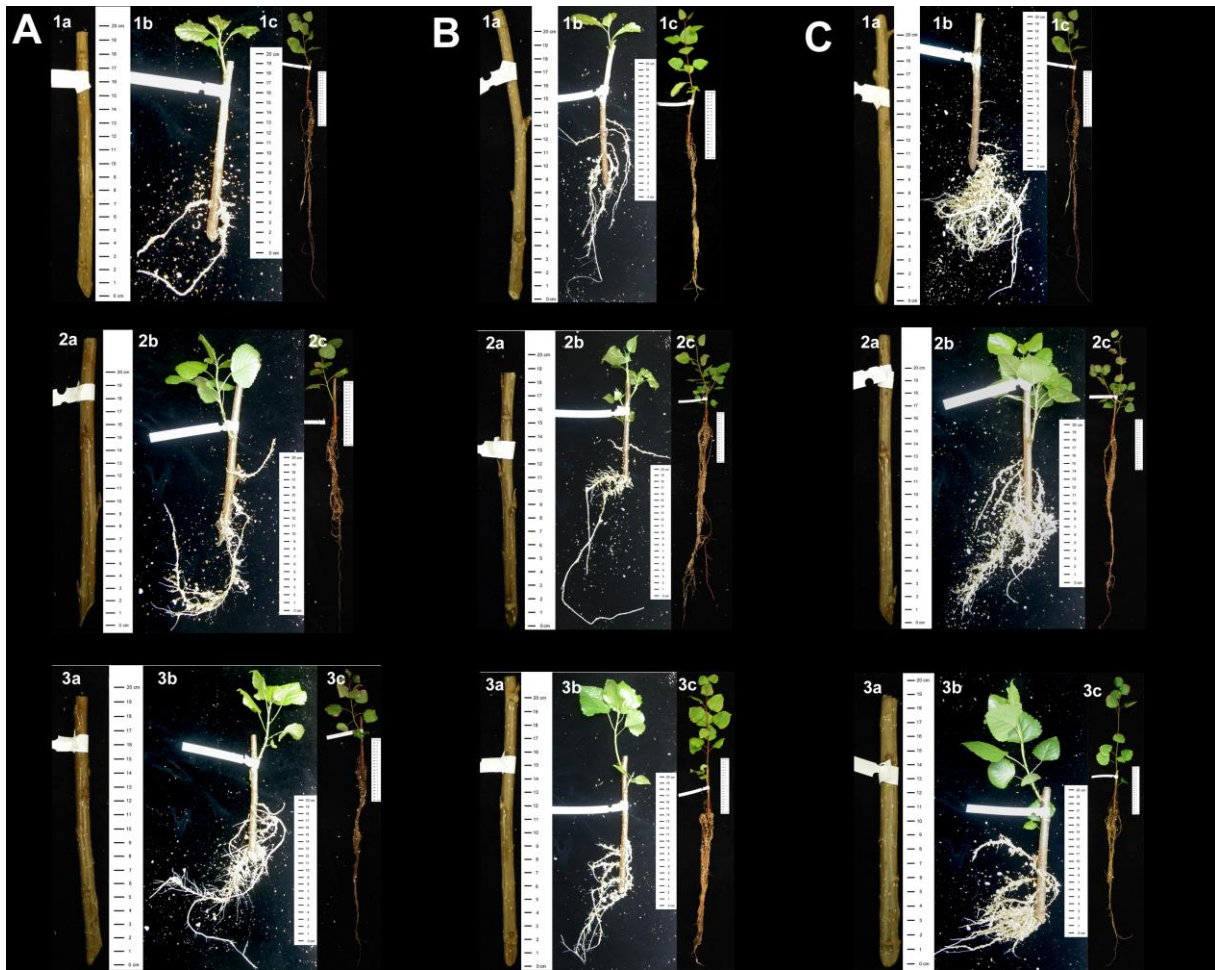


Figure 45 Harvest of poplar hybrid AF8 70 days after IO. (A) Control (1-3: number of replica, a: day 0, b: day of inoculation, c: day 70 after IO). (B) IO with *Paenibacillus* sp. P22 (1-3: number of replica, a: day 0, b: day of inoculation, c: day 70 after IO). (C) IO with *Paenibacillus durus* (1-3: number of replica, a: day 0, b: day of inoculation, c: day 70 after IO).

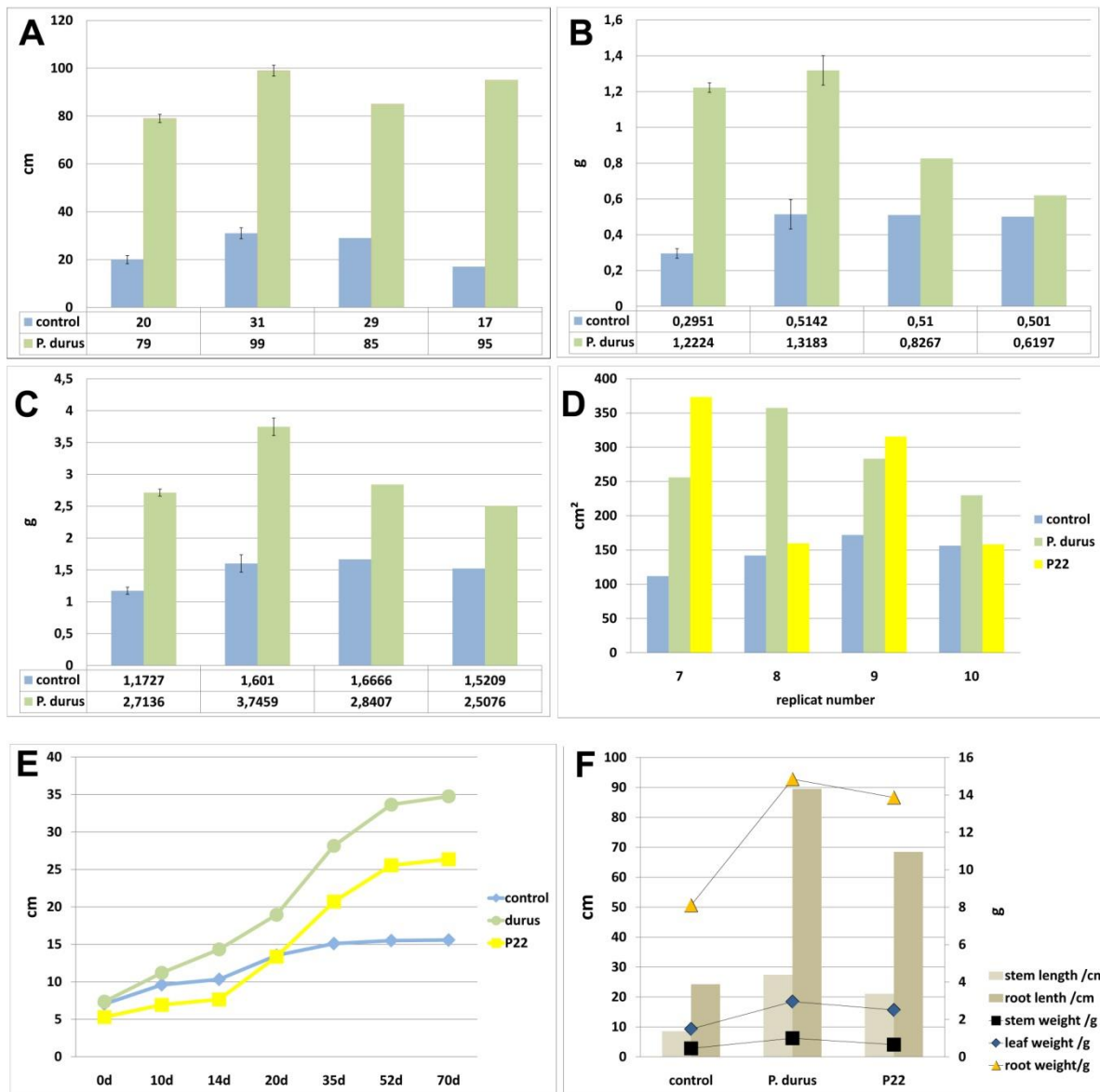


Figure 46: Schemata of measured data of AF8. (A) Root length 70 days after IO; p-value of control to *P. durus* $p \leq 2.6643E^{-05}$ and control to P22 $p \leq 0.00770669$. (B) Stem weight 70 days after IO $p \leq 0.03521231$, stem gain control to *P. durus* $p \leq 0.00027471$ stem gain control / P22 $p \leq 0.00312697$. (C) Leaf weight 70 days after IO; between the control and *P. durus* is $p \leq 0.00760181$ and the area leaf index $p \leq 0.0109157$. (D) Area leaf index 70 days after IO. (E) Gain of stem length after IO. (F) All data in overview.

3.2.3 VERMICULITE / PERLITE CULTURE WITH DIRECT INOCULATION

3.2.3.1 POPLAR HYBRID AF2

AF2 shows significances in stem weight after 28 days of inoculation with *Paenibacillus* sp. P22 (Fig. 47 and 48).

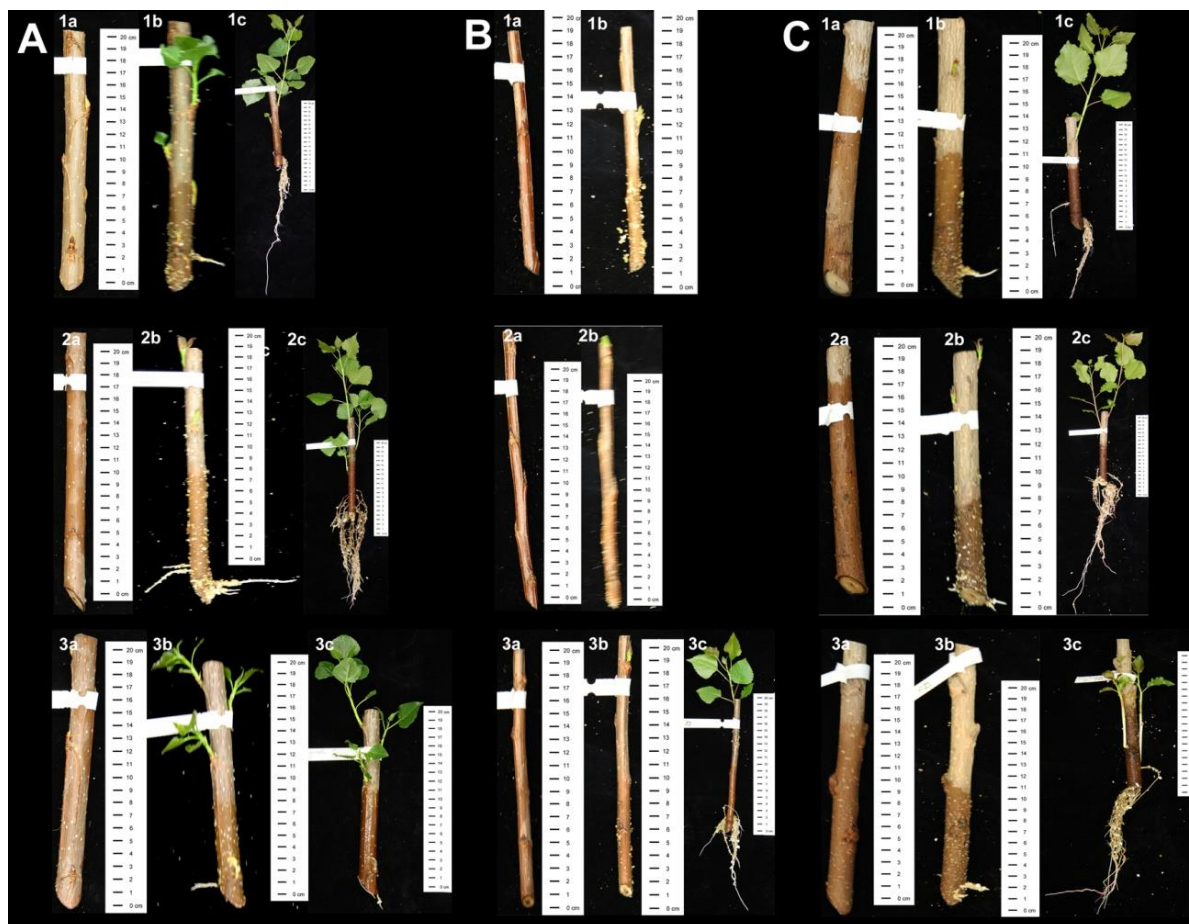


Figure 47: Harvest of poplar hybrid AF2 28 days after IO. (A) Control (1-3: number of replica, a: day 0, b: day of inoculation, c: day 28 after IO). (B) IO with *Paenibacillus* sp. P22 (1-3: number of replica, a: day 0, b: day of inoculation, c: day 28 after IO). (C) IO with *Paenibacillus durus* (1-3: number of replica, a: day 0, b: day of inoculation, c: day 28 after IO).

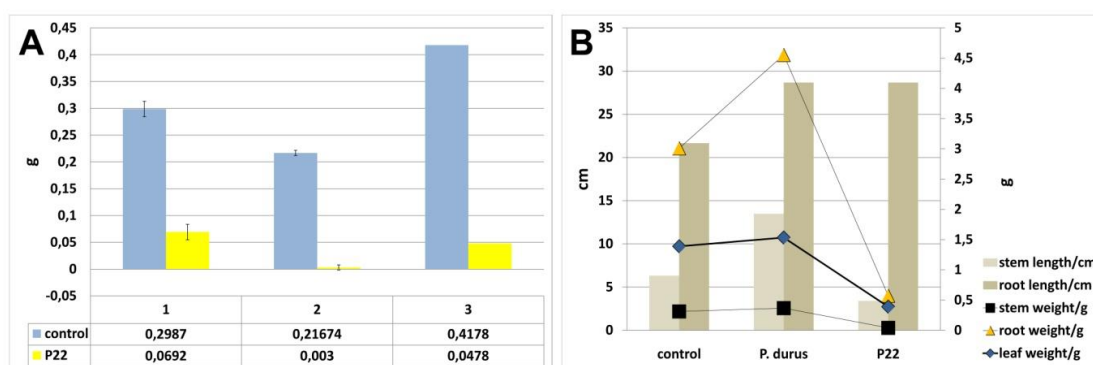


Figure 48: Schemata of measured data of AF2. (A) Stem weight 28 days after IO. (B) Harvest 28 days after inoculation; AF2 shows significances in stem weight 28 days after of inoculation with *Paenibacillus* sp. P22; $p \leq 0.0478707$.

3.2.3.2 POPLAR HYBRID MONVISO

Only the stem inoculated with *Paenibacillus* sp. P22 shows a significance in weight compared to the control, 28 days after inoculation (Fig. 49 and 50).



Figure 49: Harvest of poplar hybrid Monviso 28 days after IO. (A) Control (1-3: number of replica, a: day 0, b: day of inoculation, c: day 28 after IO). (B) IO with *Paenibacillus* sp. P22 (1-3: number of replica, a: day 0, b: day of inoculation, c: day 28 after IO). (C) IO with *Paenibacillus durus* (1-3: number of replica, a: day 0, b: day of inoculation, c: day 28 after IO).

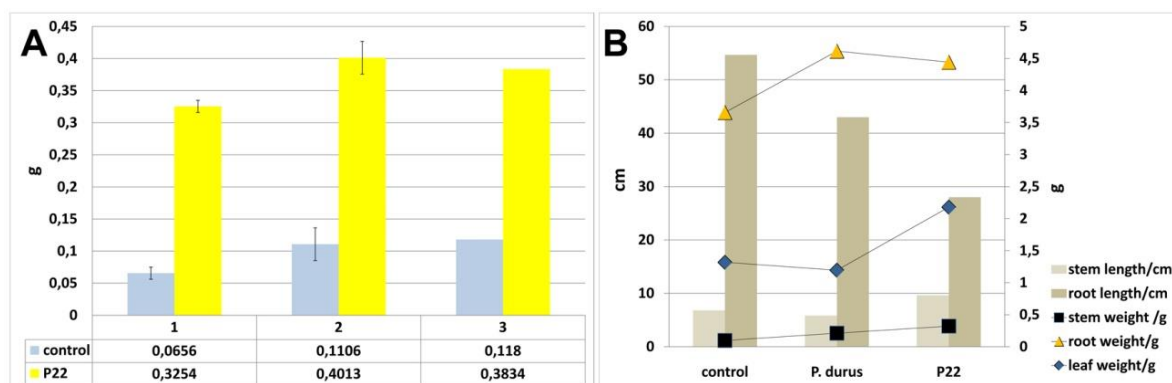


Figure 50: Schemata of measured data of Monviso. (A) Stem weight 28 days after inoculation, for e.g. p-value is about $p \leq 0.01407893$. (B) Harvest 28 days after IO. Difference in leaf weight between control and shoot cutting inoculated with *Paenibacillus* sp. P22.

3.2.3.3 POPLAR HYBRID AF8

28 days after inoculation with *Paenibacillus* sp. P22 or *Paenibacillus durus* shoot cuttings of poplar hybrid AF8 shows minimal differences in biomass (Fig. 51 and 52). The leaf weight and the root weight do not show any significant differences in the t-test.

Neither in poplar hybrid AF8 nor in poplar hybrid AF2 any significance in biomass could be investigated 70 days after inoculation with *Paenibacillus* sp. P22 and *Paenibacillus durus* (Fig. 53 and 55). In figure 55 some of the leaf dysfunctions can be seen including the supposed fungi *Venturia* sp. (D).

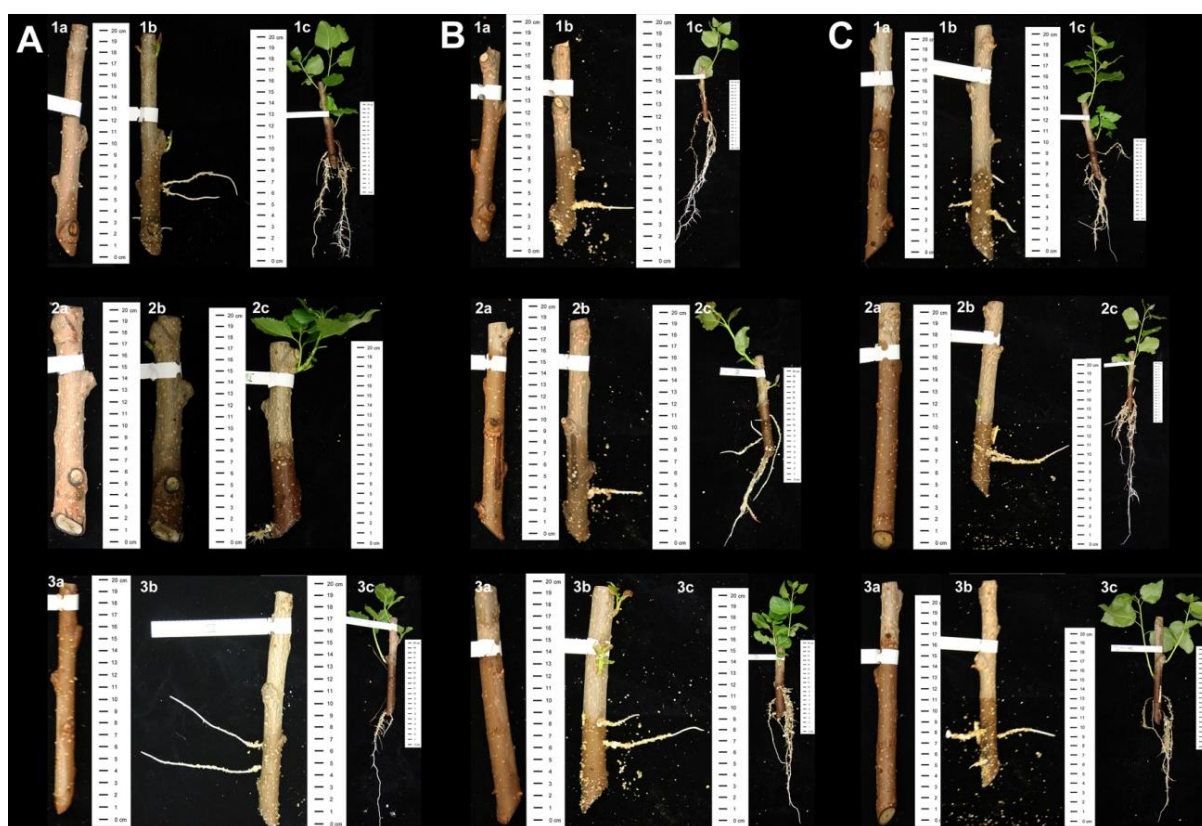


Figure 51: Harvest of poplar hybrid AF8, 28 days after IO. (A) Control (1-3: number of replica, a: day 0, b: day of inoculation, c: day 28 after IO). (B) IO with *Paenibacillus* sp. P22 (1-3: number of replica, a: day 0, b: day of inoculation, c: day 28 after IO). (C) IO with *Paenibacillus durus* (1-3: number of replica, a: day 0, b: day of inoculation, c: day 28 after IO).

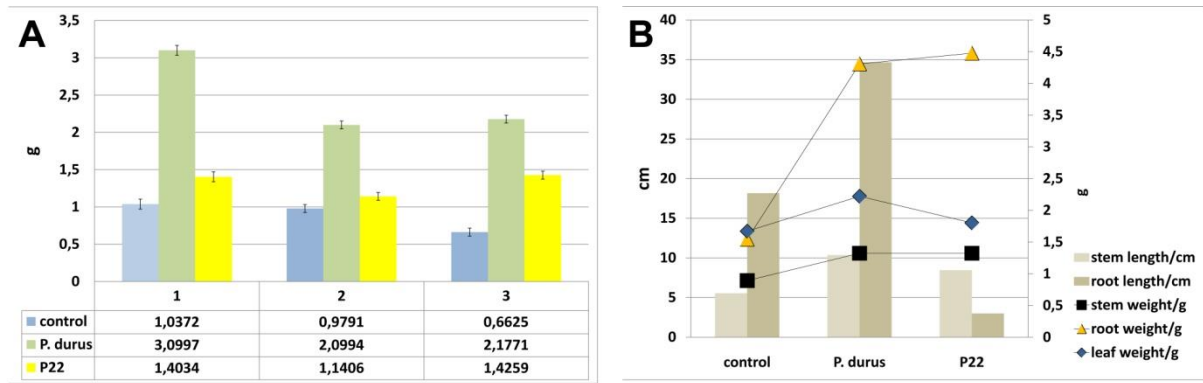


Figure 52: Schemata of measured data of AF8. (A) Stem weight 28 days after IO, the main difference is visible between the control and *P. durus* IO. (B) Harvest 28 days after inoculation; p-value between control and *P. durus* of the stem weight was $p \leq 0.01951573$ and between control and P22 $p \leq 0.04388488$.



Figure 53: (A, B, C) Harvest of poplar hybrid AF2 70 days after IO (1-6: numbers of replica, a: day 0, b: day 70 after IO). (D, E, F) Harvest of poplar hybrid AF8 70 days after IO (1-6: numbers of replica, a: day 0, b: day 70 after IO). (G, H, I) Harvest of poplar hybrid Monviso 70 days after IO (1-6: numbers of replica, a: day 0, b: day 70 after IO).

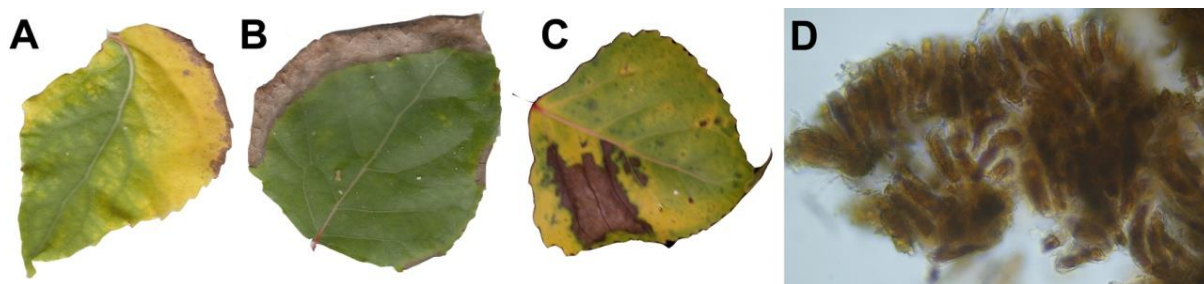


Figure 54: (A) Leaf of poplar hybrid AF8 with signs of nutrient deficits. (B) Poplar hybrid Monviso with signs of infected tissue. (C) Poplar hybrid AF2 with signs of nutrient deficits and infected tissue. (D) Light microscopy image of *Venturia* sp..

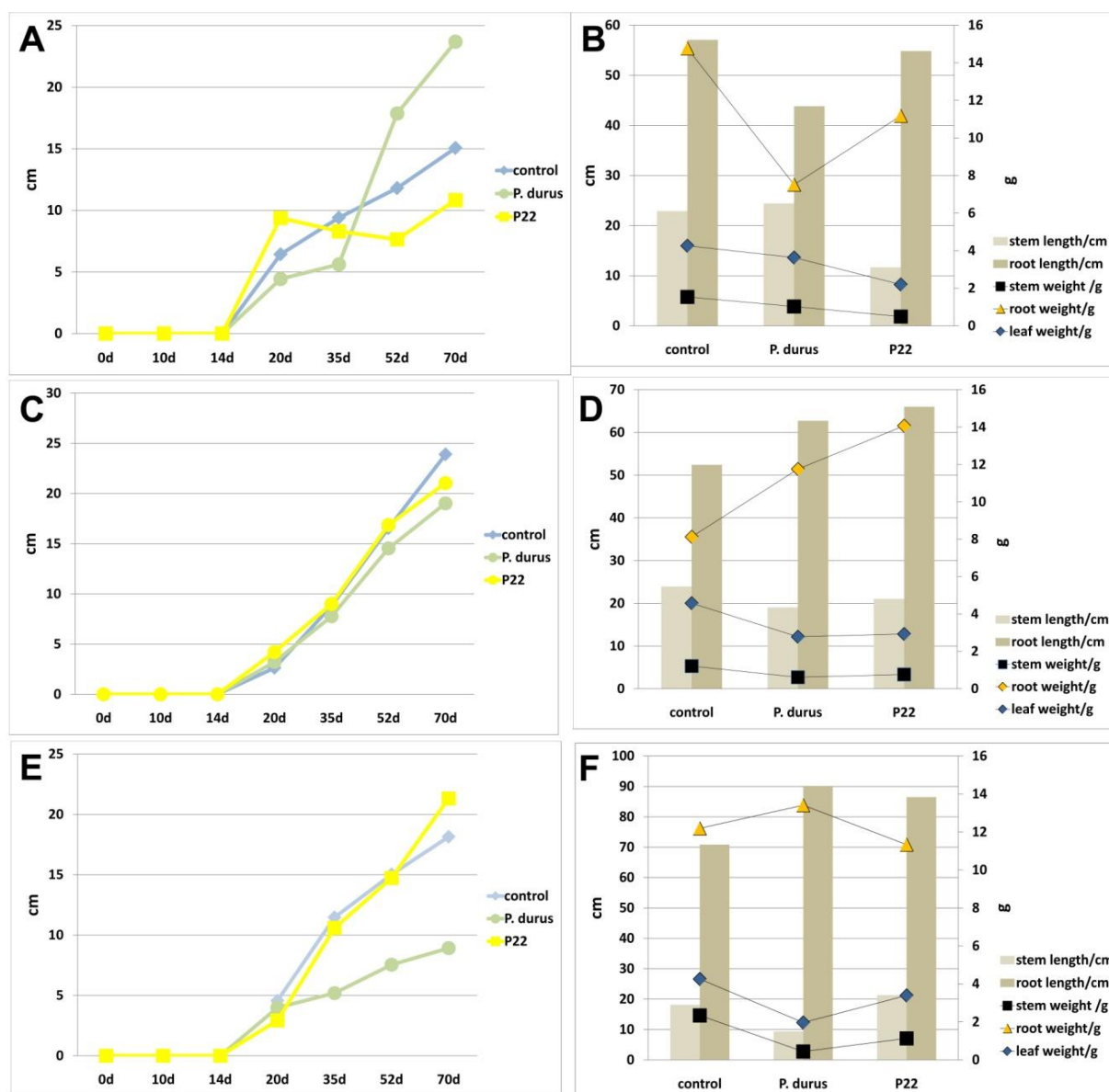


Figure 55: Schemata of measured data of AF2, AF8 and Monviso. (A) Gain of stem length of AF2 70 days after IO. (B) Harvest of AF2 70 days after IO. (C) Gain of stem length of AF8 70 days after IO. (D) Harvest of AF8 70 days after IO. (E) Gain of stem length of Monviso 70 days after IO. (F) Gain of stem length of Monviso 70 days after IO; for e.g. poplar hybrid Monviso showed 70 days after inoculation the p-value between control and inoculation with *Paenibacillus durus* in the leaf weight $p \leq 0.00132173$.

3.3 DIFFERENT EXPERIMENTS IN *IN-VITRO* CULTURED POPLAR HYBRIDS

3.3.1 GROWTH PROMOTING EFFECTS OF *PAENIBACILLUS* SP. P22 INOCULATED IN POPLAR HYBRID 741 IN *IN-VITRO* CULTURE

As already mentioned poplar hybrid 741 grown in *in-vitro* cultures showed significant changes in growth while inoculated with *Paenibacillus* sp. P22 (188). For this experiment the shoot cuttings were inoculated with two different methods. Figure 56 and figure 58 show the results of the inoculation with the endophyte *Paenibacillus* sp. P22 direct at the stem cutting and the growth rate of the plant inoculated after rooting. In fig. 57 and 59 the control of both inoculation experiments are shown. It is clearly visible that the bacterial inoculation directly on the stem cutting produces more biomass compared to the control plants (Fig. 56, 57). The control plants show an elongated growth of the stem and a minor amount of new leaves compared to the inoculated plants which have more leaves and a thicker stem. The root growth of inoculated (Fig. 56) and non-inoculated (Fig. 57) explants are very common. Figure 58 shows in comparison to the control (Fig. 59) a faster growth of the poplar shoot cuttings and a higher root growth rate.

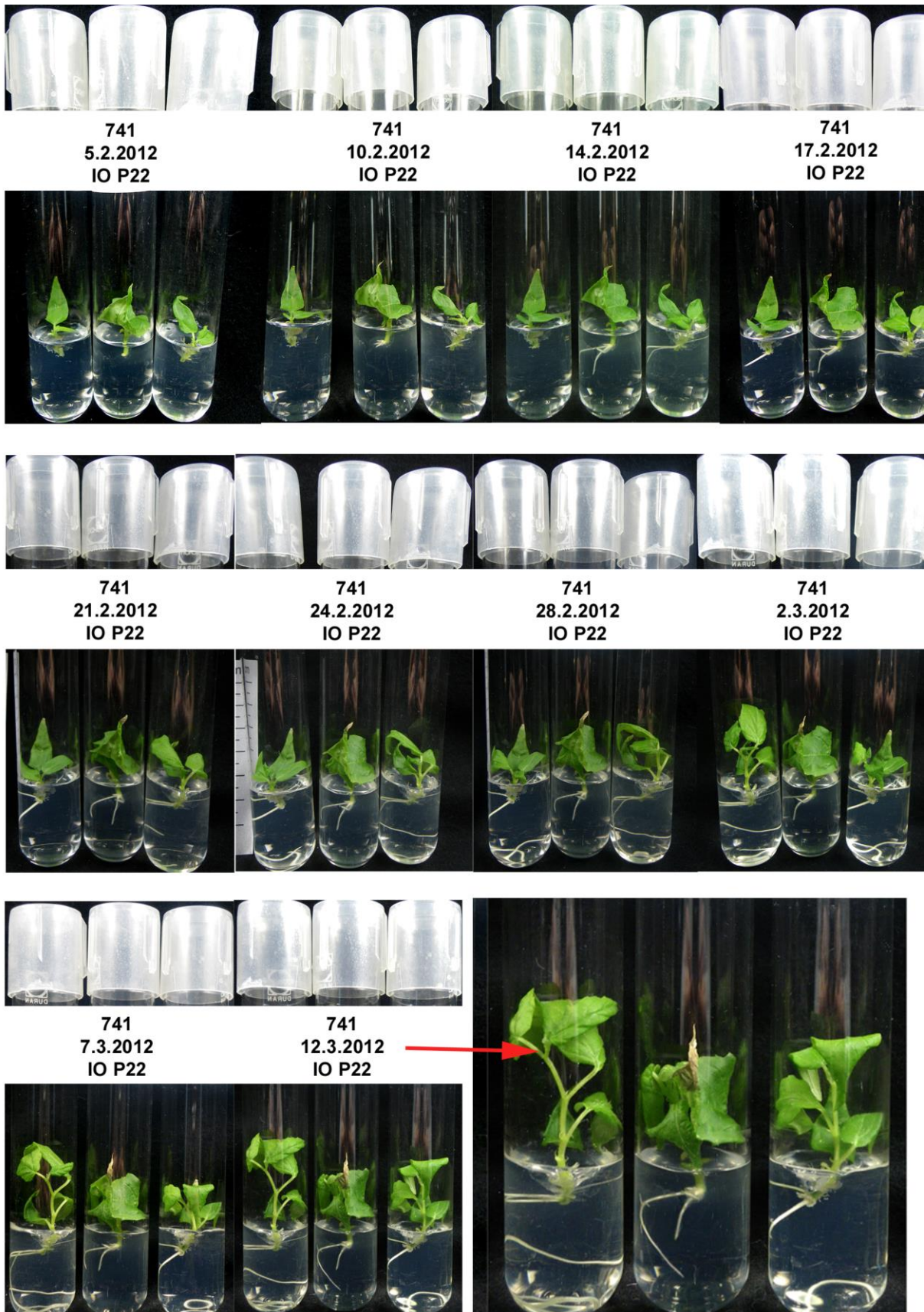


Figure 56: Growth experiment of *in-vitro* growing shoots of poplar hybrid 741, inoculated with *Paenibacillus* sp. P22 investigated over a period of 6 weeks. Method of experiment explained in chapter 2.3.1.

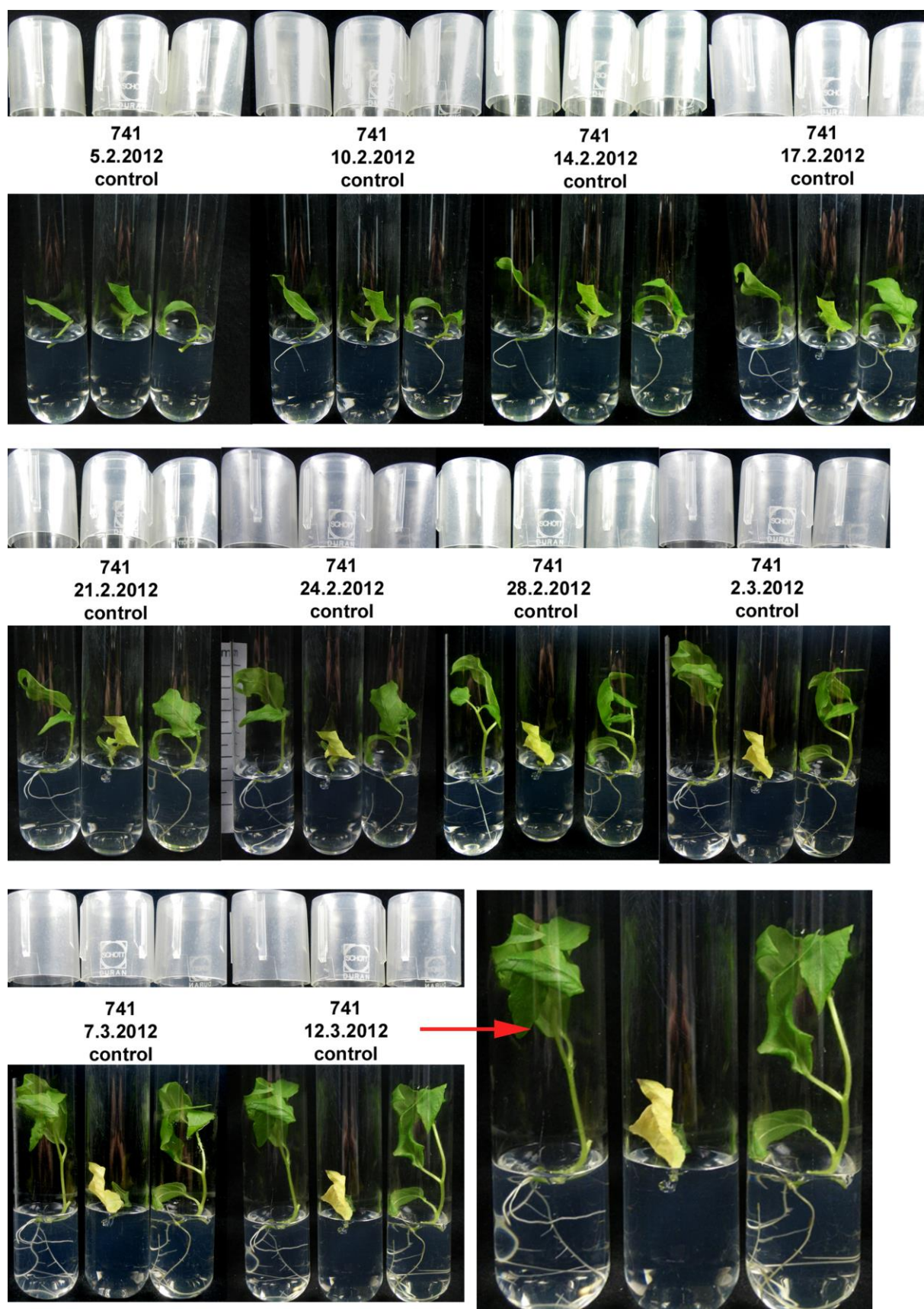


Figure 57: Control plants to growth experiment in figure 56. Method of experiment explained in chapter 2.3.1.

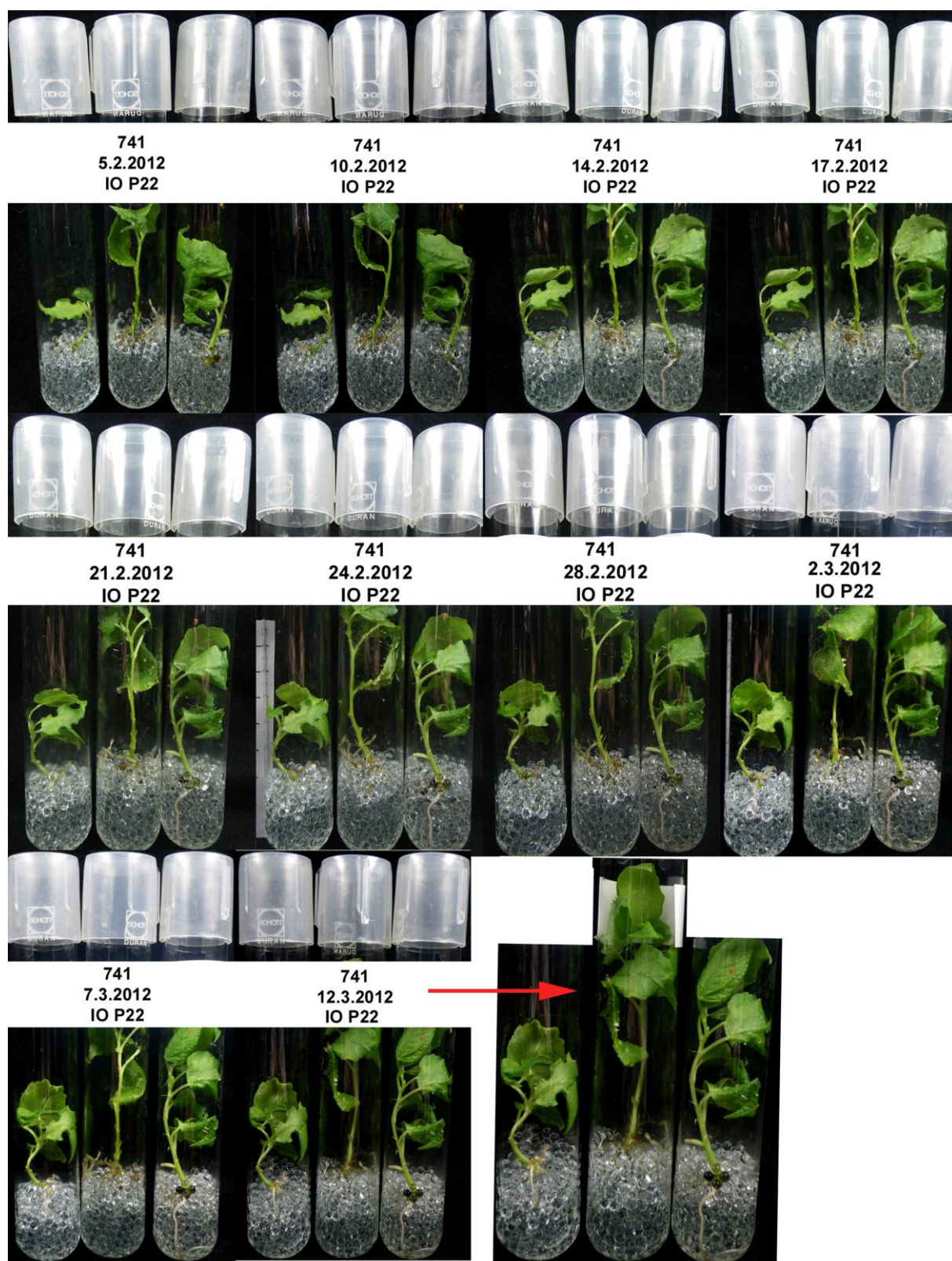


Figure 58: Growth experiment of root inoculated explants of *in-vitro* growing poplar hybrid 741 investigated over a period of 6 weeks. Method of experiment explained in chapter 2.3.1.

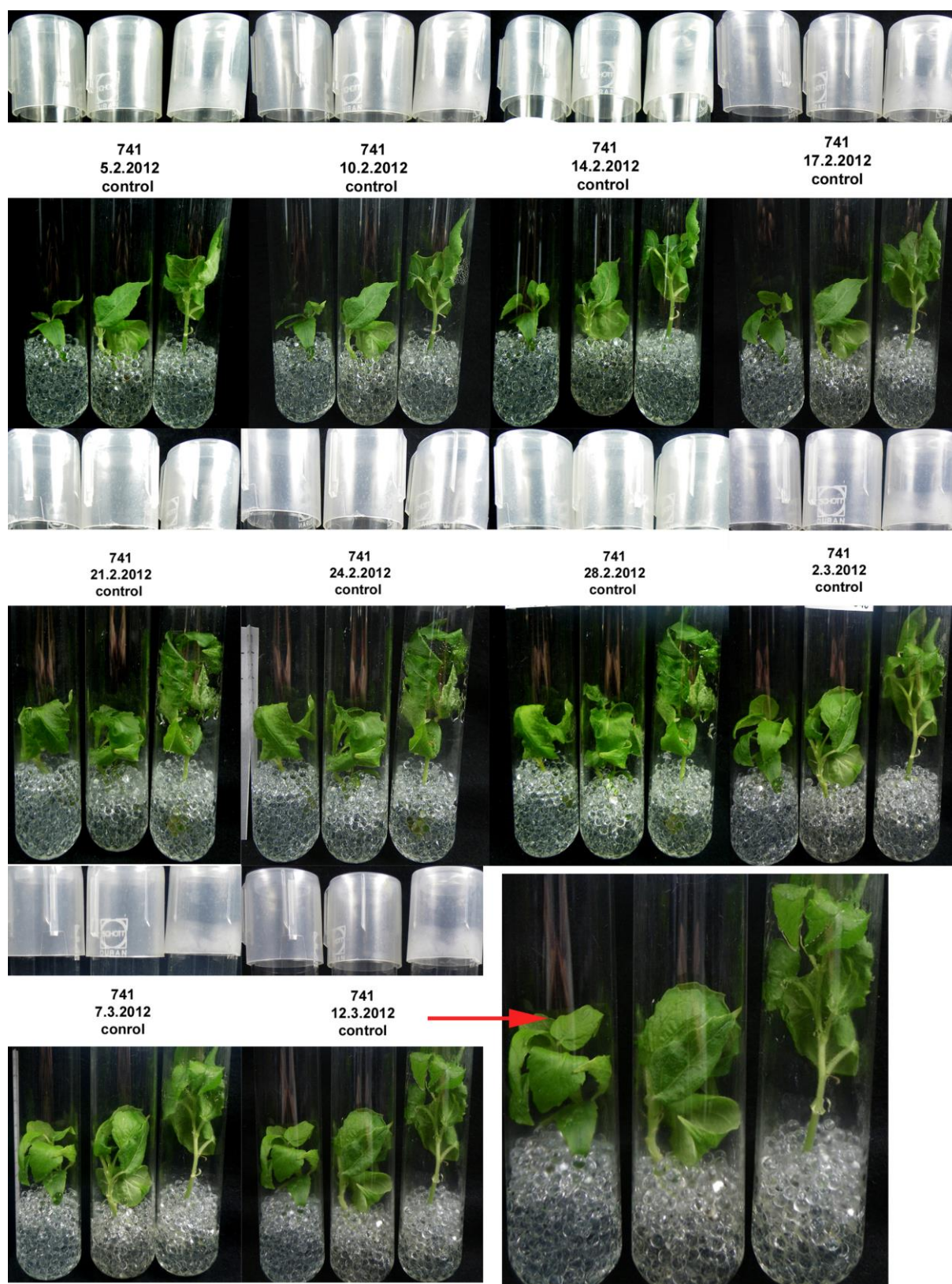


Figure 59: Control plants to growth experiment in figure 58. Method of experiment explained in chapter 2.3.1.

3.3.2 ALLOCATION OF BACTERIA IN *IN-VITRO* POPLAR HYBRID 741

In figure 60 the longitudinal sections of the xylematic tissue from *in-vitro* poplar 741 shows the trachea cells and tracheids. The trachea cells (te) and the tracheids (tr) show the typical significances with the bordered pits (bp) in the wood vessels and the small, nearly not visible pits in the tracheids. It is highly visible that the bacteria can be located in the trachea cells (red circle) close to the pits. Picture (a) shows three bacteria located in one cell close to the wood vessels. The size of the bacteria can be distinguished with about 1-3 μm .

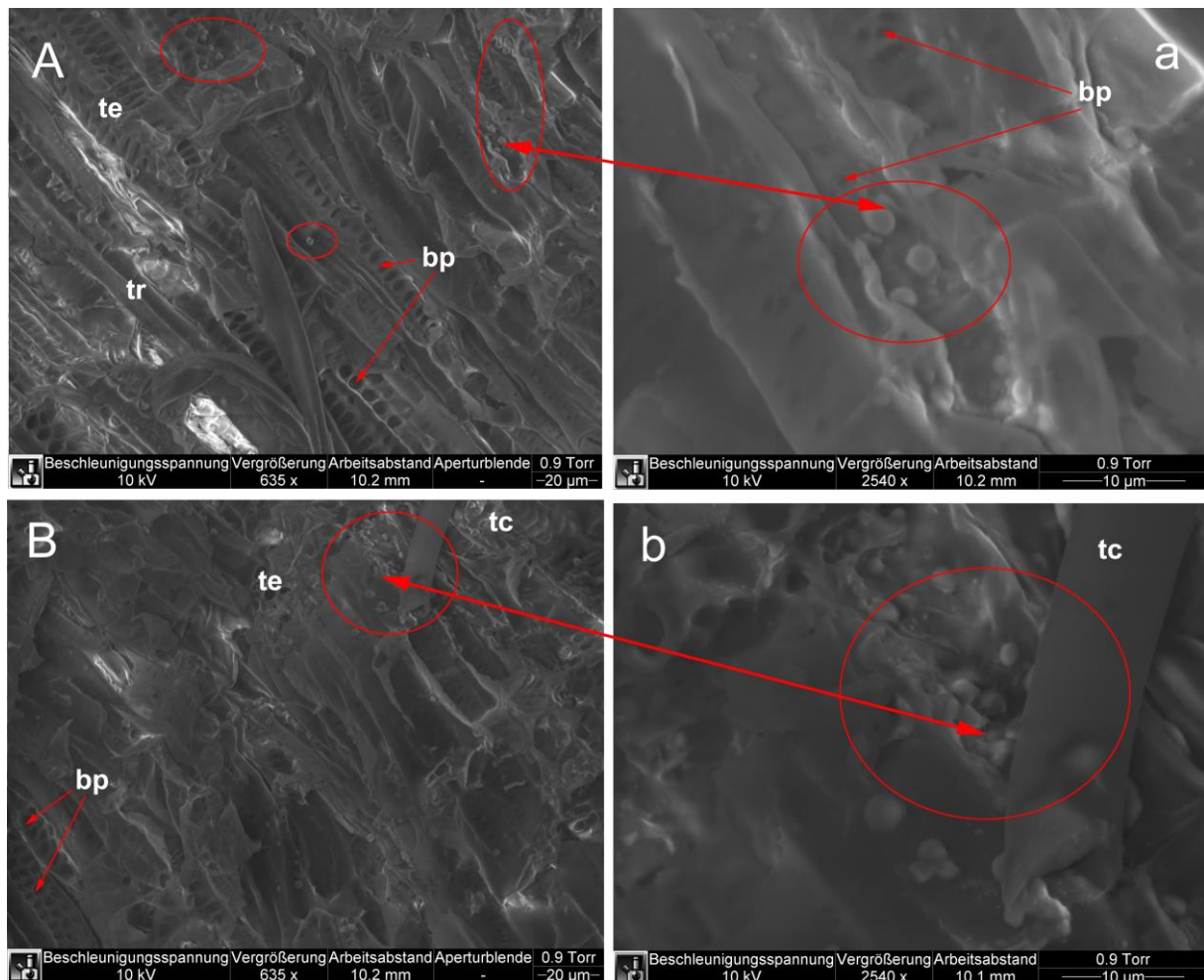


Figure 60: A-B longitudinal sections taken from the *in-vitro* poplar 741 with the ESEM. (A) Section of the xylem (te trachea, tr tracheid, bp bordered pits) with bacteria (red circles). (a) Higher resolution of the bacteria (red circle) from image A (red arrow). (B) Section of xylem (te trachea, tc trichome, bp bordered pits). (b) Higher resolution of the bacteria (red circle) from shot B (red arrow) localized in one cell.

Another longitudinal section in figure 61 (A) shows the bacteria (red circle) residing in the xylematic tissue. In picture (a) the bacteria from shot (A) are shown in a higher resolution conducted with the ESEM. In image (B) the red circle shows the bacteria altogether in one cell and in the cell aside which both are located close the wood vessels. Image (C) shows the bacteria (red circle) directly in the wood vessel and the tracheid. The bacteria of the trachea cells are located very close to the bordered pits.

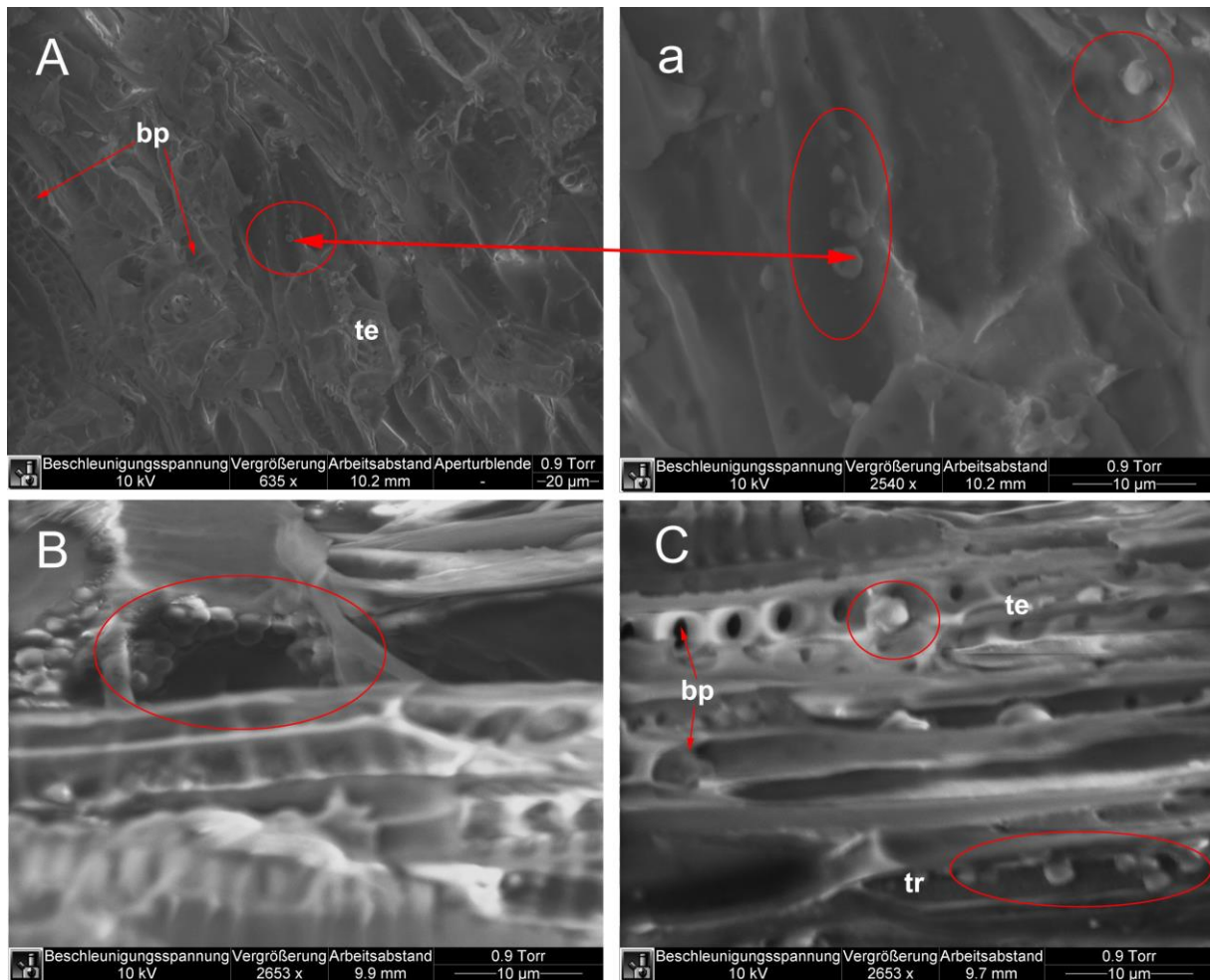


Figure 61: A-C longitudinal sections taken from the *in-vitro* poplar 741 with ESEM. (A) Section of the xylem with the trachea cells (te, bp bordered pits) and the hosted bacteria (red circle). (a) Bacteria taken with a higher resolution. (B) High resolution picture of the bacteria in one to two cells. (C) Bacteria (red circle) localized in the trachea cells (te) and tracheids (tr).

3.3.3 MEDIA SCREENING ON DIFFERENT POPLAR CLONES

Depending on the kind of experiment which wants to be conducted it is important to choose the right growth medium for tissue culture explants before starting the final experiment. For shoot propagation it is important to use a medium which includes growth promoting substances. Doležel et al. investigated karyological changes in *in-vitro* cultivated leaf explants of *Allium sativum* L. ($2n = 16$). The growth medium included KIN, NAA and 2,4-dichlorophenoxyacetic acid for inducing callus formation. The callus induction was conducted by an increase in the ploidy level (48).

Sree Ramulu et al. showed that during *in-vitro* growth of calli and cell suspensions of potato (*Solanum tuberosum*) that polyploidization and aneuploidy can occur during the initial stages of callus induction (207).

As seen in figure 62 the explants of the tetraploid poplar clone L447 show already 4 weeks after micropropagation visible differences in growth while growing on different media. Only the $\frac{1}{2}$ -strength L&S-medium with GPH shows root growth after 3 weeks compared to (A) and (C). Explants growing on $\frac{1}{2}$ -strength L&S-medium without GPH show an earlier leaf gain than growing on full-strength L&S-medium with GPH but not as good as in (B), the $\frac{1}{2}$ -strength L&S-medium, including GPH.

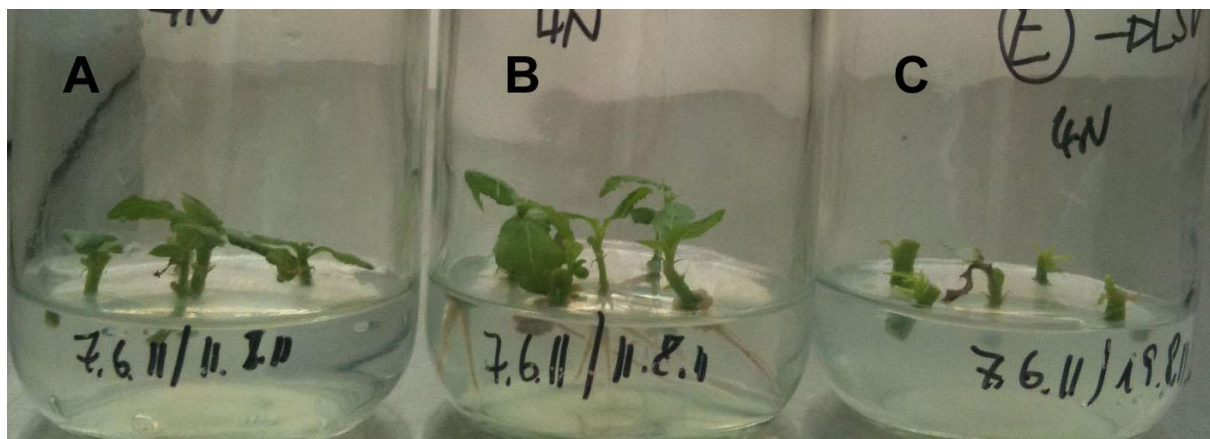


Figure 62: Media screening of tetraploid poplar hybrid L447. (A) Half-strength L&S-medium without growth promoting hormones. (B) Half-strength L&S-medium with growth promoting hormones. (C) Full-strength L&S-medium with growth promoting hormones.

The diploid poplar hybrid L447 shows differences in growth between the media with and without GPH seen in figure 63. Growing on the $\frac{1}{2}$ -strength medium without GPH the root growth started already 2 weeks after micropropagating compared to the full-strength medium included GPH which started root growth after 5-6 weeks. The amount of leaves is higher in the full-strength medium with GPH then in the $\frac{1}{2}$ -strength medium without GPH.



Figure 63: Media screening of diploid poplar hybrid L447. (A) Half-strength L&S-medium without growth promoting hormones. (B) Full strength L&S-medium with growth promoting hormones.

The mixoploid explants (Fig. 64) of poplar hybrid L 447 also show differences in growth if placing on different growth media. Like 2N and 4N the mixoploid shoots have a faster growth on $\frac{1}{2}$ -strength L&S-medium without GPH. The root growth started after 3 weeks and the leave growth was definitively higher than in the full-strength L&S-medium with GPH.

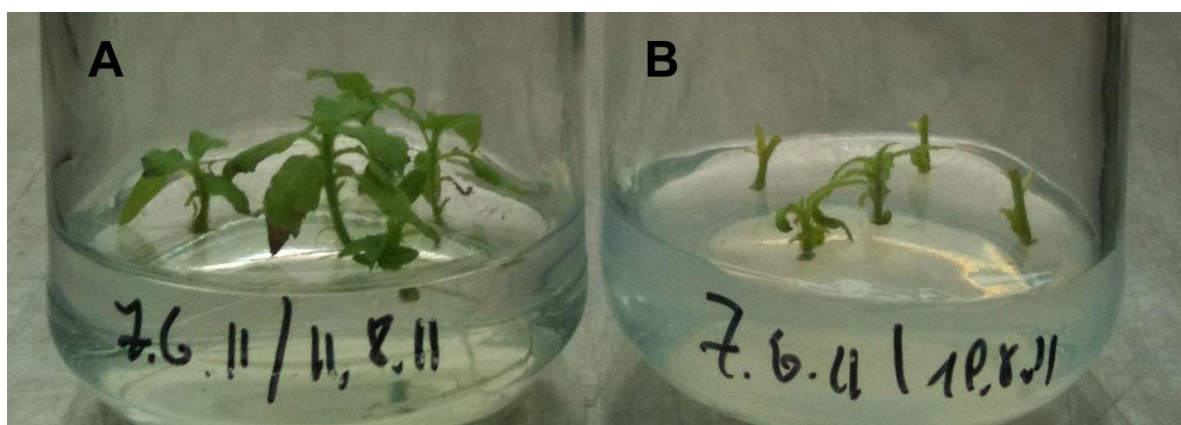


Figure 64: Media screening of mixoploid poplar hybrid L447. (A) Half-strength L&S-medium without growth promoting hormones. (B) Full-strength L&S-medium with growth promoting hormones.

Poplar clone 741 is growing very well in ½-strength L&S-medium without growth promoting hormones (Fig. 65). On the other hand from 4 placed shoot cuttings only two of them were growing very well. Placed on a full-strength M&S-medium 3 out of 5 plants grew successfully.



Figure 65: Media screening of poplar hybrid 741 with endophytes. (A) Half-strength L&S-medium without growth promoting hormones. (B) Full-strength L&S-medium with growth promoting hormones.

Explants of poplar clone 741 inoculated with *Paenibacillus* sp. P22 (Fig. 66) show the same signs as the explants without cultivable endophytes. The growth is very good without any growth promoting hormones and also shows some curious habits growing on full-strength medium including growth promoting hormones. The small pictures in (B) show the different forms of growth of poplar 741 cuttings while growing on a full-strength medium.



Figure 66: Media screening of poplar hybrid 741 without cultivable endophytes. (A) Half-strength L&S-medium without growth promoting hormones. (B) Full-strength L&S-medium including growth promoting hormones.

3.4 *IN-VITRO* GROWTH OF POPLAR CLONE AF2, AF8 AND MONVISO

Nearly the most sophisticated applications of biotechnology with woody plants have been done with poplar (89, 163, 182) which is already established as a model system for forest tree studies. Clones within specific sections of the genus *Populus*, and individual clones, have been studied *in vitro* and as callus cultures (194). After surface sterilization shoot cuttings of poplar clone AF2, A8 and Monviso were grown on full-strength L&S-medium (Fig. 67). Based on the non-satisfying growth of the explants in this medium it was replaced into ½-strength L&S-medium without GPH. The results are showing that the shoot cuttings of poplar hybrid AF2 had a better development in *in-vitro* culture than the poplar hybrids AF8 and Monviso.



Figure 67: Poplar clone AF2, AF8, Monviso in greenhouse cultured on vermiculite / perlite and *in-vitro* cultures of all three clones growing on half-strength L&S-medium without growth promoting hormones. (A) AF2: *Populus x canadensis*. (B) AF8: (*Populus generosa*) x *Populus trichocarpa*. (C) Monviso: *Populus x generosa* x *Populus nigra*.

3.5 ACCLIMATIZATION OF DIFFERENT POPLAR HYBRIDS

The acclimatization was done due to the fact of having acclimatized poplar plants in field grown conditions for new experimental setups for example proteomic measurements. About 60% of the cultures which had been acclimatized were successfully grown. As shown in the figures 68 to 72 explants from poplar hybrid 741, Esch 5 diploid, Esch 5 tetraploid and Brauna 11 were acclimatized from tissue culture except the hybrid Esch mixoploid.

The starting size of the acclimatized *in-vitro* shoots was the prescribed 1-3 cm, including short roots. 38 days of growth in the climate chamber the gain of the plantlets was about 4 - 5 cm in height this is a growth of about 60 - 80%. Approximately 7 months after the acclimatization had started the poplar plantlets had a 35 fold increase of growth, which was about 69 – 75 cm. At this time the plants could already be used for further experiments. All of the acclimatized poplar trees are kept in the greenhouse under natural conditions.

In special detail figure 68 shows the diploid poplar hybrid L447 and figure 64 the tetraploid poplar hybrid L447. All the polyploid explants show the typical signs like serrate leaves with dense trichomes on it. The acclimatization of poplar hybrid 741 inoculated with *Paenibacillus* sp. P22 (Fig. 70) arose to a 50% satisfied final result. Poplar hybrid 741 inoculated with *Paenibacillus durus* (Fig. 71) shows in difference to 741 inoculated with P22 a compressed growth of the shoot and much bigger leaves. There are more branches in the *P. durus* inoculated plants then in the P22 inoculated ones. The acclimatization of poplar clone Brauna 11 (Fig. 71) had a 100% success. The stem is very long and the grade of lignification is less than those of the polyploidy explants.



Figure 68: Poplar hybrid L447 diploid. (a/b) Day 0 of acclimatization placed in the acclimatization chamber. (A/B) Day 38 of acclimatization placed in the greenhouse. (AA/BB) Day 194 of acclimatization placed in the greenhouse outdoor.

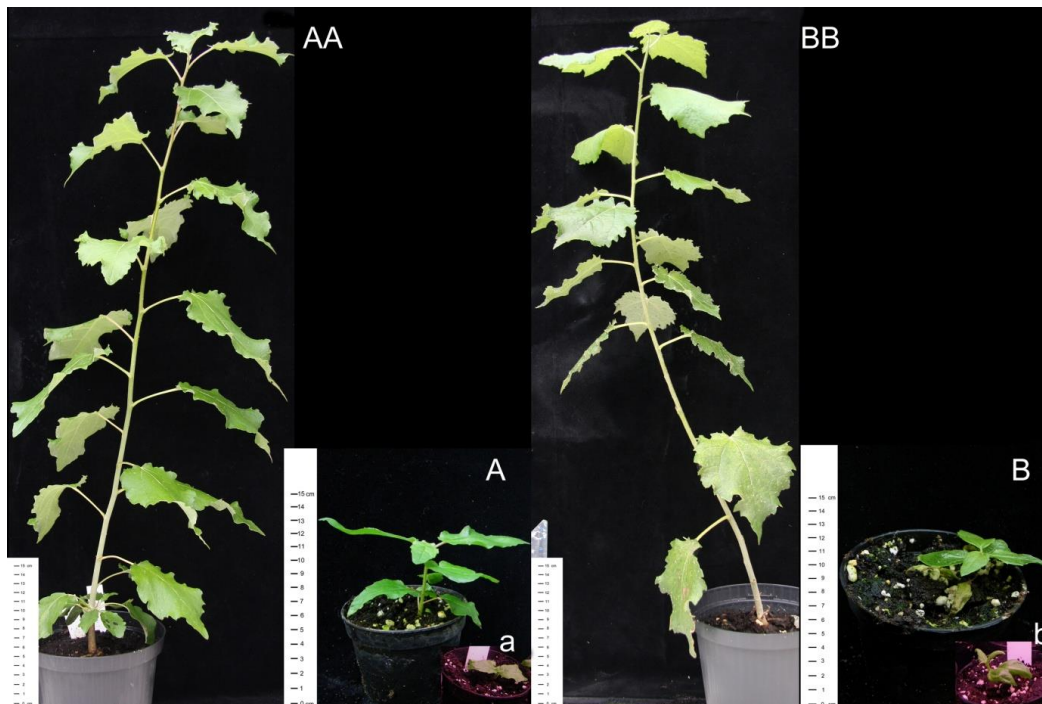


Figure 69: Poplar hybrid L447 tetraploid. (a/b) Day 0 of acclimatization placed in the acclimatization chamber. (A/B) Day 38 of acclimatization placed in the greenhouse. (AA/BB) Day 194 of acclimatization placed in the greenhouse outdoor.



Figure 70: Poplar hybrid 741 inoculated with *Paenibacillus* sp. P22. (a/b) Day 0 of acclimatization placed in the acclimatization chamber. (A/B) Day 38 of acclimatization placed in the greenhouse. (AA/BB) Day 194 of acclimatization placed in the greenhouse outdoor.

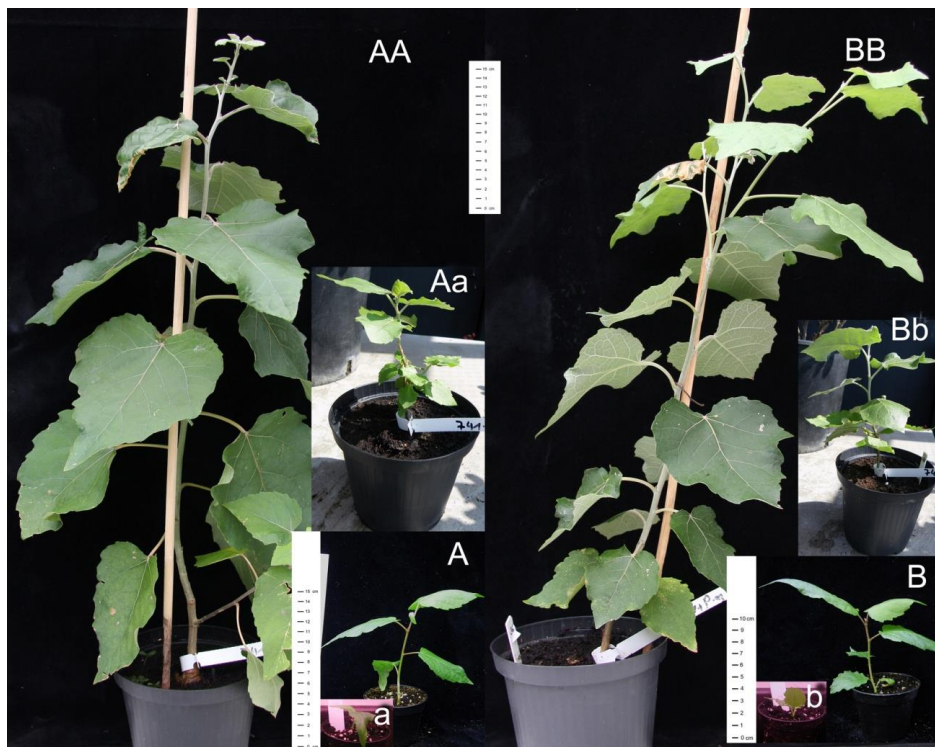


Figure 71: Poplar hybrid 741 inoculated with *Paenibacillus durus*. (a/b) Day 0 of acclimatization placed in the acclimatization chamber. (A/B) Day 38 of acclimatization placed in the greenhouse. (Aa/Bb) Day 156 of acclimatization placed in the greenhouse. (AA/BB) Day 194 of acclimatization placed in the greenhouse outdoor.



Figure 72: Poplar hybrid Brauna 11. (a/b) Day 0 of acclimatization placed in the acclimatization chamber. (A/B) Day 38 of acclimatization placed in the greenhouse. (AA/BB) Day 194 of acclimatization placed in the greenhouse outdoor.

3.6 MICROSCOPIC, FLOW CYTOMETRIC AND PROTEOMIC MEASUREMENTS ON FIELD GROWN 2N, 4N AND 2N4N POPLAR HYBRIDS

3.6.1 FLOW CYTOMETRIC MEASUREMENT

Figure 73 shows the results of two year old diploid, tetraploid and mixoploid poplar plants described as Esch 5 (A, B and C) and the respective flow cytometric measurements (a, b and c) to each clone. The 2D scatter plot in A, B and C shows the nuclei for the prepared solution in time. The peak for the 2N samples is shown at channel 100 (red) and the 4N lies at channel 200 (green). The mixoploid flow cytometric measurement shows both peaks but the peak at 200 is much lower which is typical for this kind of measurement.

There are about 3100 counts on nuclei (orange) for the spectra in the tetraploid explants and about 6500 counts for the diploid. The mixoploid samples show a count of 4700 for the diploid nuclei and a count of 550 for the triploid nuclei. The DNA content of the nuclei correlates with the ploidy level.

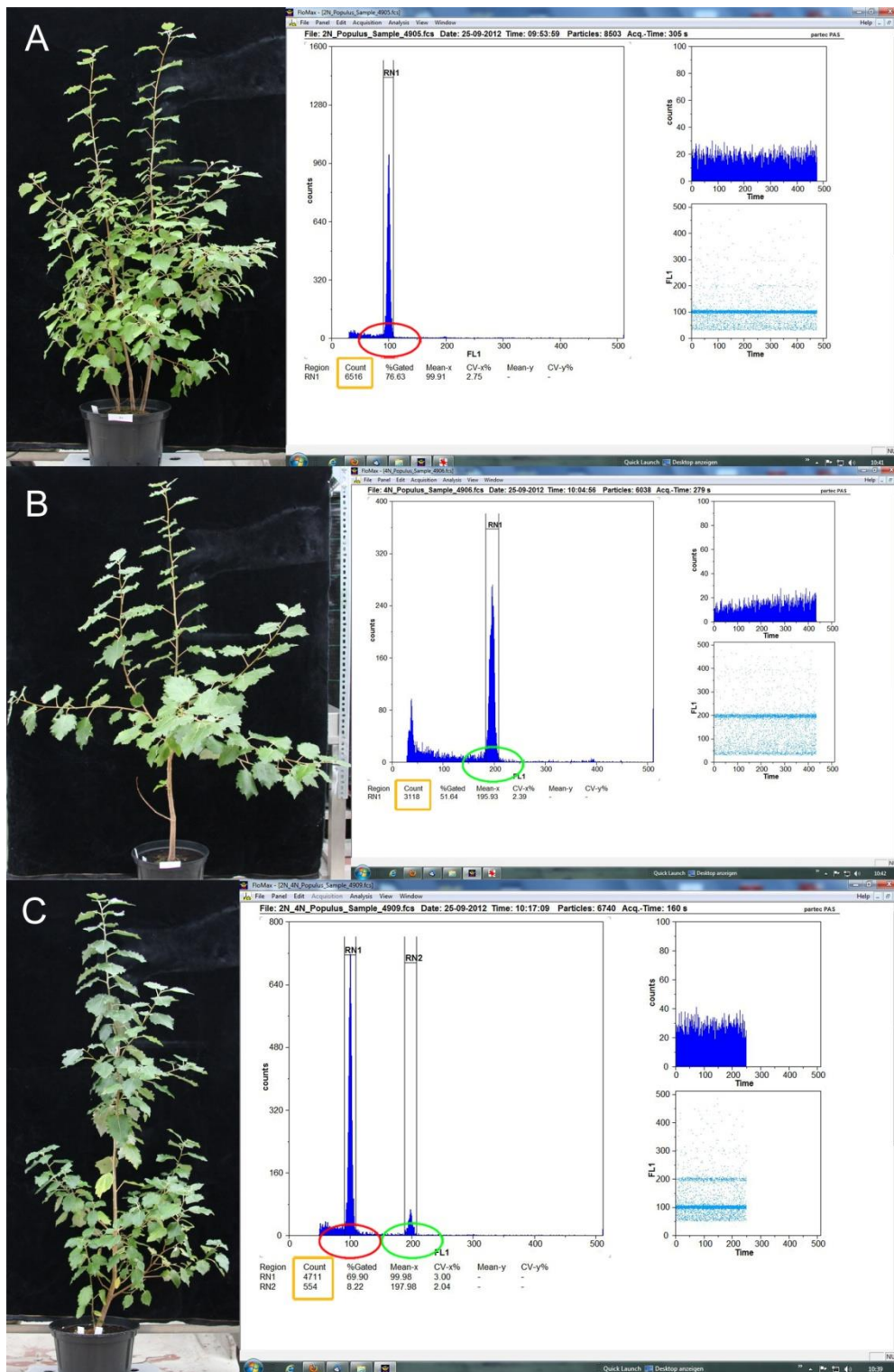


Figure 73: (A) 2 year old diploid poplar hybrid Esch 5 grown under greenhouse conditions and flow cytometric histogram, peak at channel 100 (red) with a nuclei number of 6500 counts (orange). (B) Tetraploid polar hybrid Esch 5, flow cytometric histogram peak at channel 200 (green), with a nuclei number of 3100 counts (orange). (C) Mixoploid poplar hybrid Esch 5, flow cytometric histogram, peak at channel 100 (for 2N) and at channel 200 (for 4N) with a nuclei number of 4700 and 500 (orange).

3.6.2 ANATOMIC STUDIES

Figures 74 to 76 show different anatomical leaf sections of diploid, tetraploid and mixoploid poplar hybrid Esch 5. Due to the fact that guard cells are often much larger in polyploids than in diploids, Masterson (138) compared leaf guard cells size in fossil and extant taxa from a few angiosperm families to estimate polyploidy occurrence through time. He estimated that about 70% of all angiosperms had one or more episodes of polyploidy in their ancestry.

In figure 74 different leaf sections of diploid poplar Esch 5 are shown. Picture A shows a cross section of the leaf in the area of the upper epidermis including two layers of palisade parenchyma while in (B) an overview of the upper epidermis can be seen. In picture C a cross section in the area of the lower epidermis, including the stomata cells (white arrow) surrounded by the guard cells is shown compared to (D) which is the overview of the lower epidermis. (E) and (F) show the same picture of a single stomata cell with its containing chloroplast (white arrow) in taken with light microscopy and fluorescence microscopy.

Figure 75 shows anatomical leaf sections of the tetraploid poplar hybrid Esch 5. The cross section of the upper leaf section (A) shows that the first layer of palisade parenchyma is bigger as in the diploid poplar leaf. In (B) an overview of the upper epidermic cell layer is shown. Picture (C) shows a cross section of stomata cells (white arrow), guard cells and epidermic cells of the lower epidermis. (E) and (F) show a stomata cell including the chloroplasts under light- and fluorescence microscopy. The chloroplasts are marked with the white arrow. Already here the difference between the 2N and 4N poplar plants is visible relating to the amount and size of chloroplast in the stomata cells.

Leaf sections of the mixoploid poplar hybrid Esch 5 are shown in figure 76. The first layer of palisade parenchyma (A) of the leaf is bigger than in the diploid poplar hybrid. The white arrows in (C) and (D) show the square section and the overview of stomata cells of the lower epidermis. In (E) the chloroplast of the stomata cells are marked with a white arrow like in (F) investigated with fluorescence microscopy. The amount of chloroplast is relative high and compared to the diploid and tetraploid explants the chloroplasts are bigger in size.

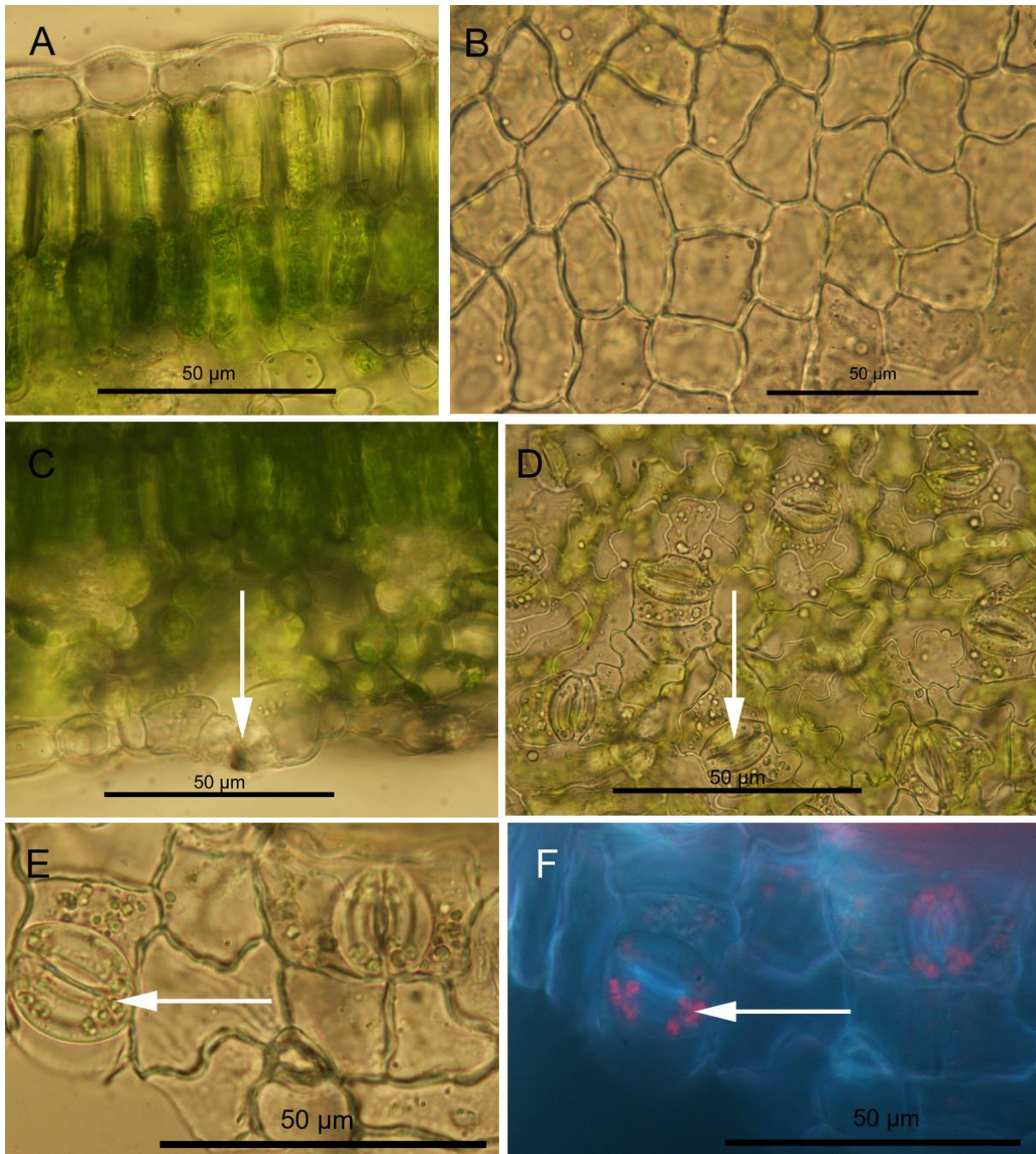


Figure 74: Leaf square section of diploid poplar Esch 5. (A) Cross section of upper epidermis. (B) Upper epidermis square section. (C) Lower epidermis cross section with stomata (white arrow). (D) Lower epidermis square section with stomata (white arrow). (E) Lower epidermis square section stomata with guard cells and chloroplasts (white arrow). (F) Section E with chloroplast marked with white arrow under epifluorescence view.

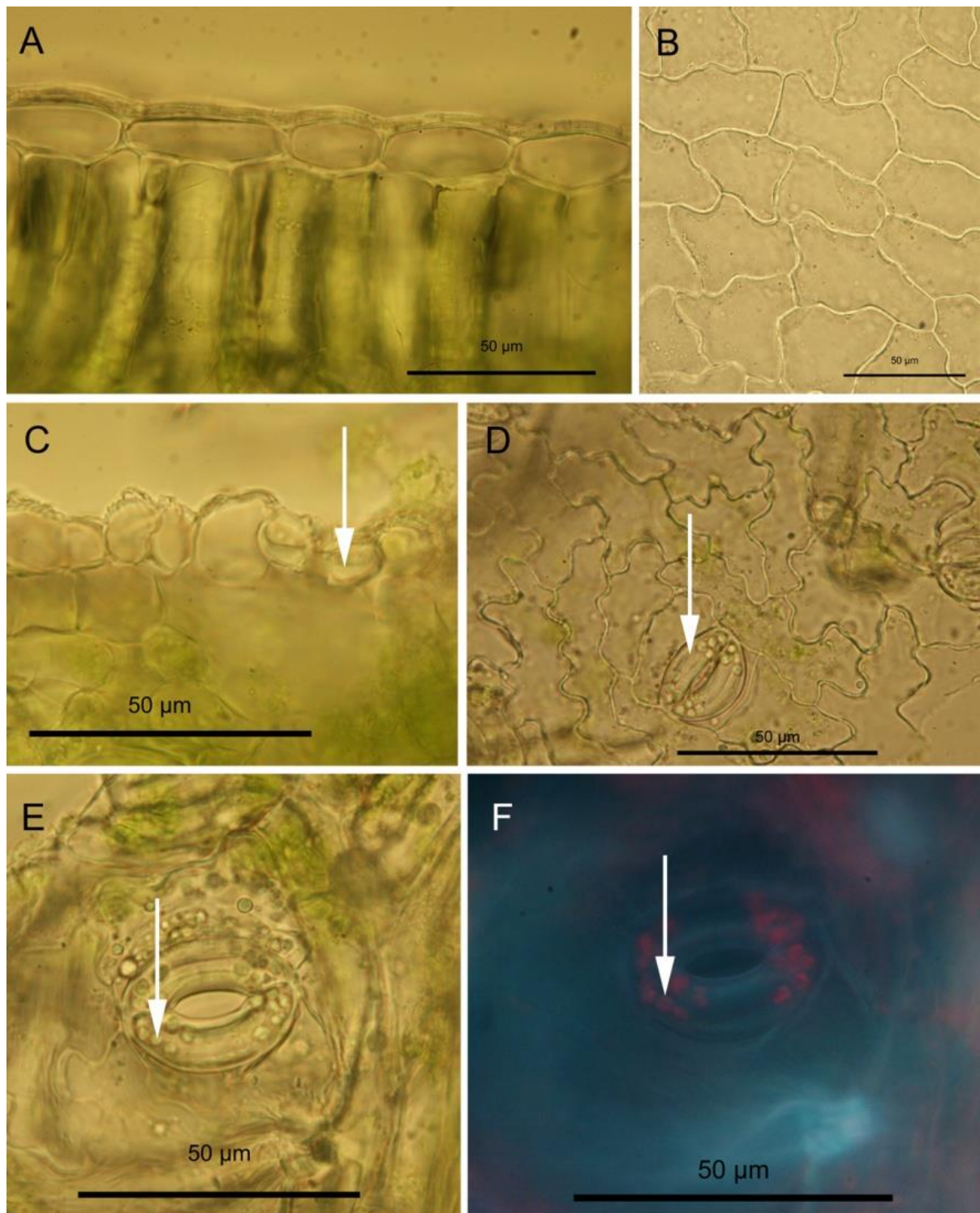


Figure 75: Leaf square section tetraploid poplar Esch 5. (A) Cross section of upper epidermis. (B) Upper epidermis square section. (C) Lower epidermis cross section with stomata (white arrow). (D) Lower epidermis square section with stomata (white arrow). (E) Lower epidermis square section stomata with guard cells and chloroplasts (white arrow). (F) Section E with chloroplast marked with white arrow under epifluorescence view.

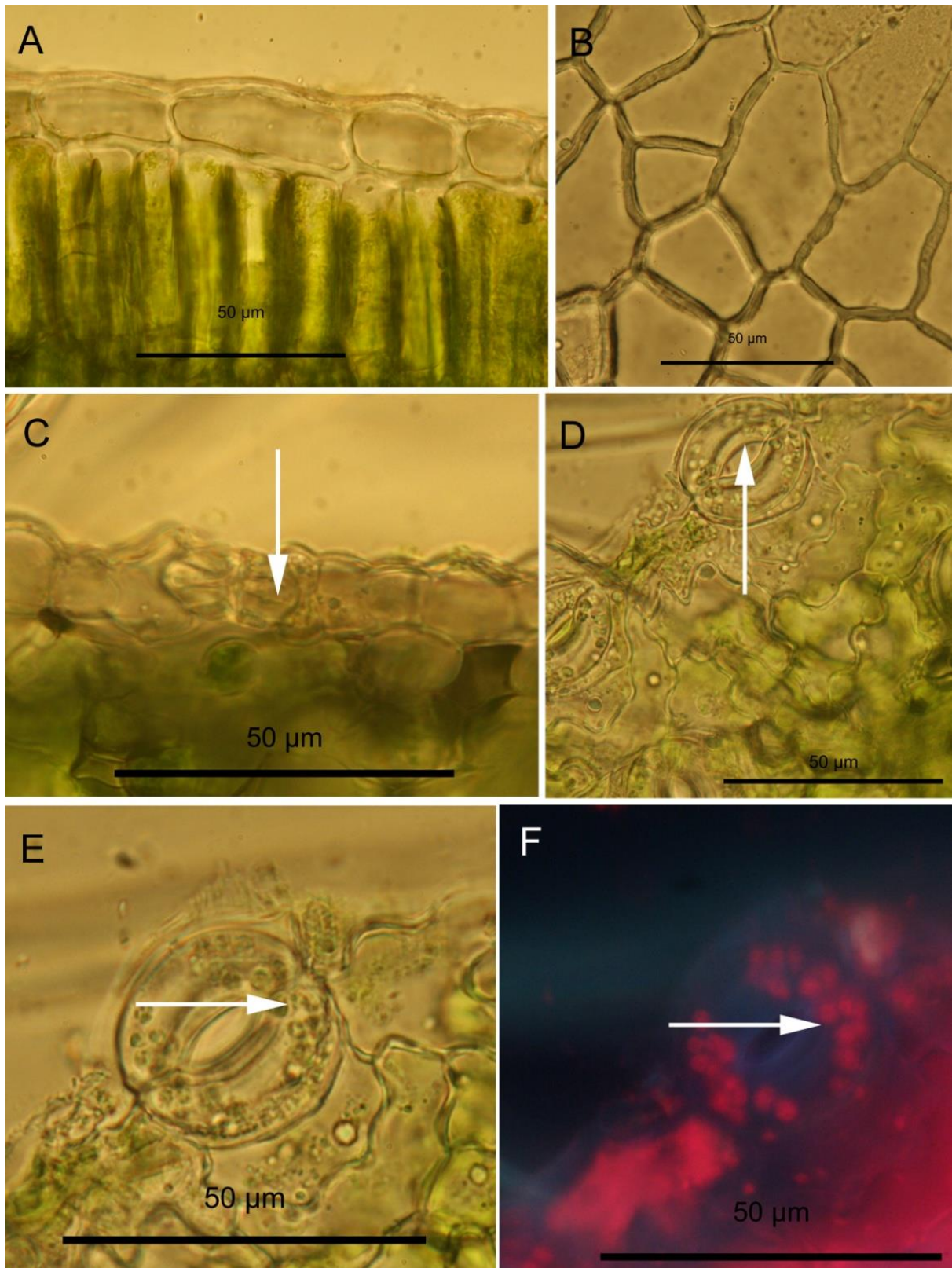


Figure 76: Leaf square section of mixoploid poplar Esch 5. (A) Cross section of upper epidermis. (B) Upper epidermis square section. (C) Lower epidermis cross section with stomata (white arrow). (D) Lower epidermis square section with stomata (white arrow). (E) Lower epidermis stomata with guard cells and chloroplasts (white arrow). (F) Section E with chloroplast marked with white arrow under epifluorescence view.

3.6.3 CHLOROPLAST COUNTS IN STOMATA CELLS

In Figure 77 leaf samples from *in-vitro* cultures of diploid and tetraploid poplar hybrid L447 has been analyzed. Image (A) shows the difference in the amount of chloroplast in the stomata cells between the diploid and tetraploid poplar plants. The t-test was set with two variances with a p-value ≤ 0.05 . The t-tests show high significances between the single ploidy levels. The size and the frequency of chloroplast in the stomata of the diploid leaf samples differ to the tetraploid explants. In the diploid explants the chloroplasts are bigger but less compared to the tetraploid samples where they are smaller but higher in number. Former experiments from Ewald et al. (61) have shown that the amount of chloroplast in the stomata cells of 2N is about 7 - 9 and in 4N about 12 - 16.

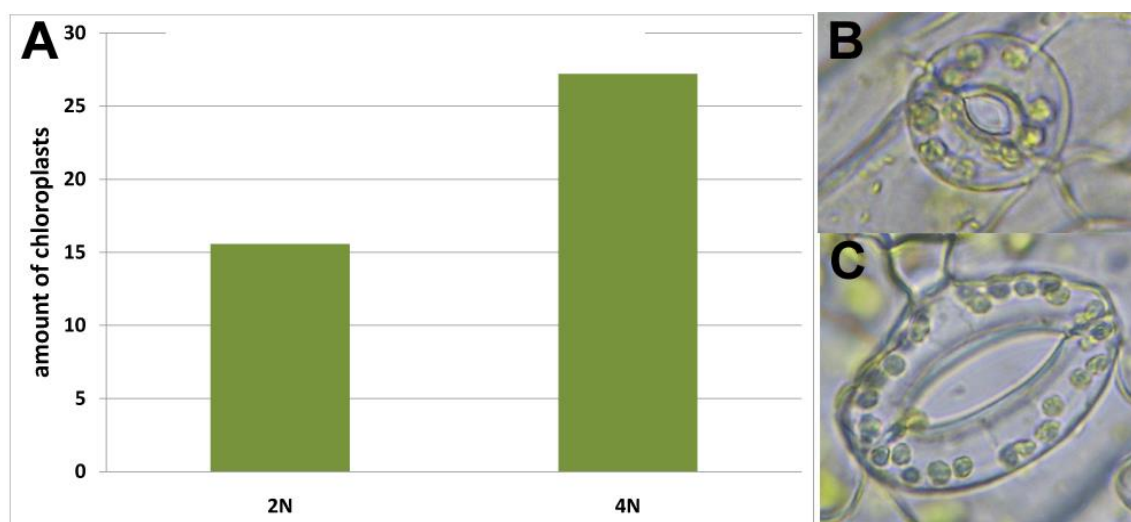


Figure 77: (A) Comparison of amount of chloroplast in stomata cells of diploid poplar hybrid L447 with an amount of ~ 15 chloroplasts per stomata and tetraploid with an amount of about 27 chloroplasts per stomata in *in-vitro* culture samples; there is a significance of $p \leq 5.0133E^{-13}$ which leads to a high difference in the number of chloroplast between diploid and tetraploid explants. (B) Stomata of diploid poplar hybrid L447 shows few but big sized chloroplasts. (C) Stomata of tetraploid poplar hybrid L447 shows smaller but in amount more chloroplast than in 2N.

The diagrams of figure 78 show the significance of leaf area in the upper epidermis area in old leaves between the diploid and tetraploid poplar explants. A p-value of $\leq 8.87E^{-07}$ between 2N and 4N and between diploid and mixoploid a p-value of ≤ 0.0004592 could be distinguished. There is no significance between tetraploid and mixoploid plants in the upper epidermis area. The younger leaves show a high significance between 2N and 4N ($p \leq 0.013$) and between 2N and 2N4N ($p \leq 0.000035$). As well as in the older leaves the younger leaves do not show any significance between tetraploid and mixoploid explants.

The lower epidermis area of older leaves shows higher differences between 2N, 4N and 2N4N poplar hybrid as the upper epidermis. The significance between 2N and 4N is $p \leq 3.37E^{-10}$ and between 2N and 2N4N the p-value shows a significance of ≤ 0.002 . In the lower epidermis there is significance between 4N and 2N4N of $p \leq 0.002$ in the older leaves and $p \leq 0.17$ in the younger leaves. There is no significance in the epidermic cell area between 2N and 4N plants but between 2N and 2N4N ($p \leq 0.17$). The size of stomata cells in old leaves have a significance between diploid and tetraploid explants ($p \leq 0.001$) and between 2N and 2N4N ($p \leq 0.00010$). Again there is no significance between 4N and 2N4N in older leaves. In young leaves there is a significance between 2N and 4N poplar leaves $p \leq 0.0000067$ and between 2N and 2N4N $p \leq 1.46796E^{-08}$. The younger leaves show a difference between 4N and 2N4N $p \leq 0.01119$. In older leaves the guard cells which surround the stomata have a p-value of $p \leq 0.00350$ and between 2N and 2N4N ($p \leq 0.000070$). Again there is no significance between 4N and 2N4N in older leaves. The younger leaves show a significance in 2N and 4N ($p \leq 4.32364E^{-08}$) and 2N and 2N4N ($p \leq 0.00332$). Between 4N and 2N4N there is a significance of $p \leq 0.01581$.

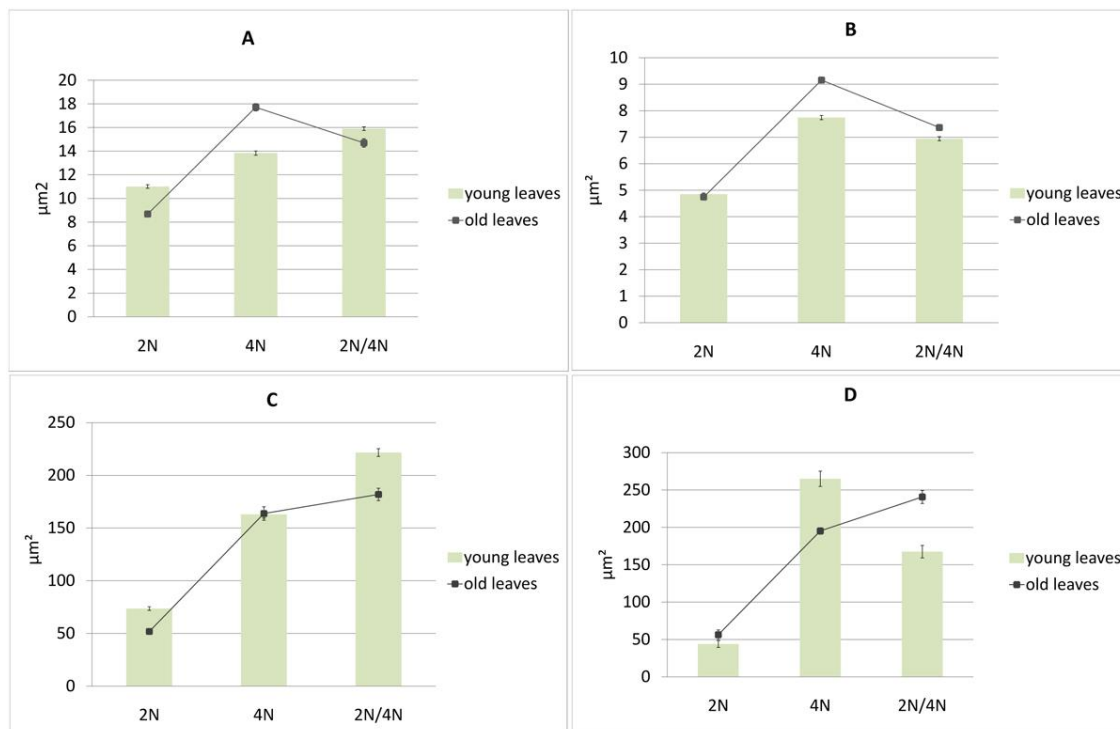


Figure 78: Schemata of the cell area of upper and lower epidermis and stomata size. (A) Upper epidermis cell area. (B) Lower epidermis cell area. (C) Size of stomata cells of the lower leaf side. (D) Size of guard cell of the lower leaf side.

3.6.4 PROTEOME ANALYSIS OF LEAF SAMPLES

After leaf protein extraction the fractions were analyzed via liquid chromatography coupled to tandem-mass spectrometry. The MS/MS spectra were compared to the predicted spectra of the six-frame translated *Populus trichocarpa* Gene Index, release 10.0 genomic database using the SEQUEST algorithm (59). Stringent quality criteria were used, high-confidence and at least two different peptides per protein, so that at least 248 proteins could be identified.

Agenda: 1 + 2: poplar 2N: (1) young leaf, (2) old leaf

3 + 4: poplar 4N: (3) young leaf, (4) old leaf

3.6.4.1 PCA AND ICA USING LOG¹⁰- AND Z-TRANSFORMATION

All 248 identified proteins were used for PCA and ICA analyses without using any selection of significances.

In figure 79 the principal component analysis of the log¹⁰- and z-transformed data reveals a clear separation of the diploid, tetraploid and the mixoploid poplar leaves. The PC1, the component of the highest variance, allows the discrimination of the young diploid leaf samples. The PC2 shows the similarities of the old leaf samples of the single ploidy gradients compared to the young leaves. Also in the ICA plot a clear separation can be distinguished. The variances of the PCA plot and the Kurtosis of the ICA plot show a good measuring of the samples.

Figure 80 shows the PCA and the ICA of log¹⁰-transformed data. The PCA plot shows a nice separation of the single experimental setups but mirror inverted to figure 83. The highest difference can be recognized between the old and young leaves of the diploid sample. But still a difference between diploid, tetraploid and mixoploid can be distinguished. The ICA also shows a separation between the single ploidy levels but not so clearly within a group as in the PCA plot.

The z-transformed data (Fig. 81) can only be shown as a PCA plot because the ICA plot could not separate any of the single samples. Again the PCA plot shows an absolute clear separation of the single polyploidy levels as well as between the young and old leaves.

Table 1 shows all significant identified proteins with different transformation methods. Interestingly only the loadings of the z-transformed data show the protein with the acc. Nr. D0QTN3 which is coding for the Ribulose-1.5-bisphosphat carboxylase/oxygenase an absolutely important factor in the Calvin-cycle.

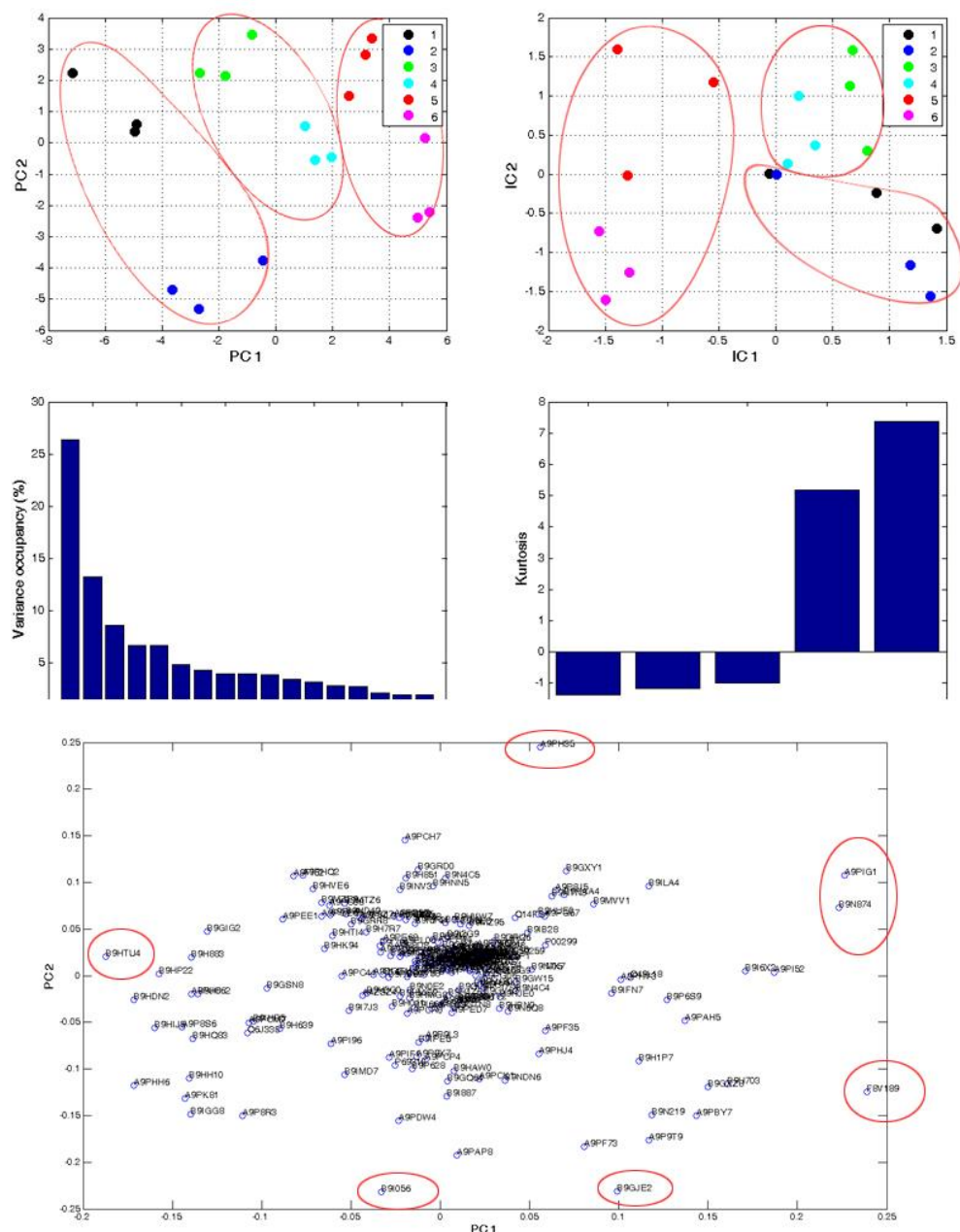


Figure 79: PCA of \log_{10} - and z-transformed. PC1 explains 26.38% and PC2 13.22% of the total variance in the data set (3 biological replicates of 6 different setups), and ICA.

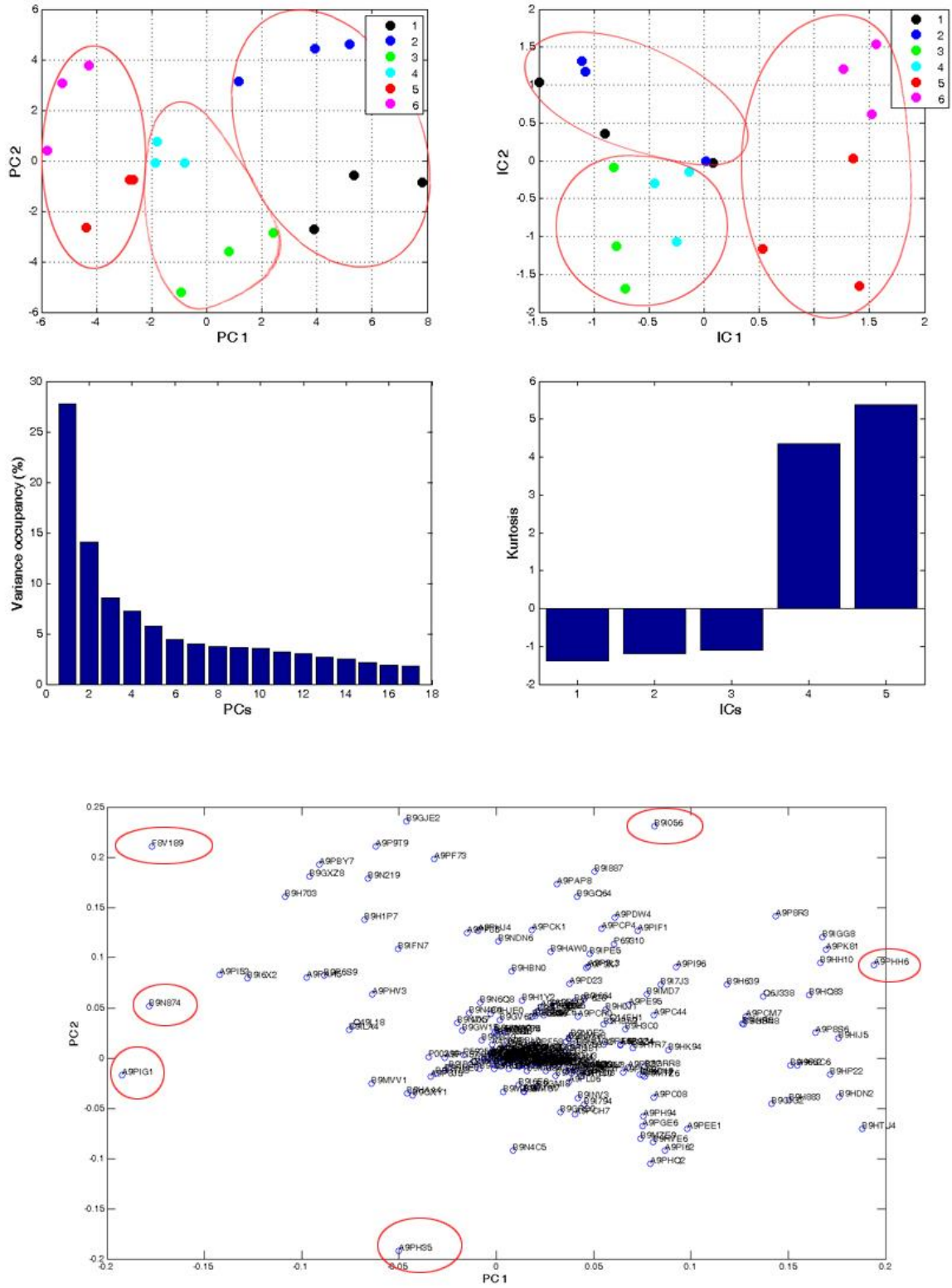


Figure 80: PCA of \log^{10} -transformed data. PC1 explains 27.78% and PC2 14.98% of the total variance in the data set (3 biological replicates, of 6 different setups) and ICA.

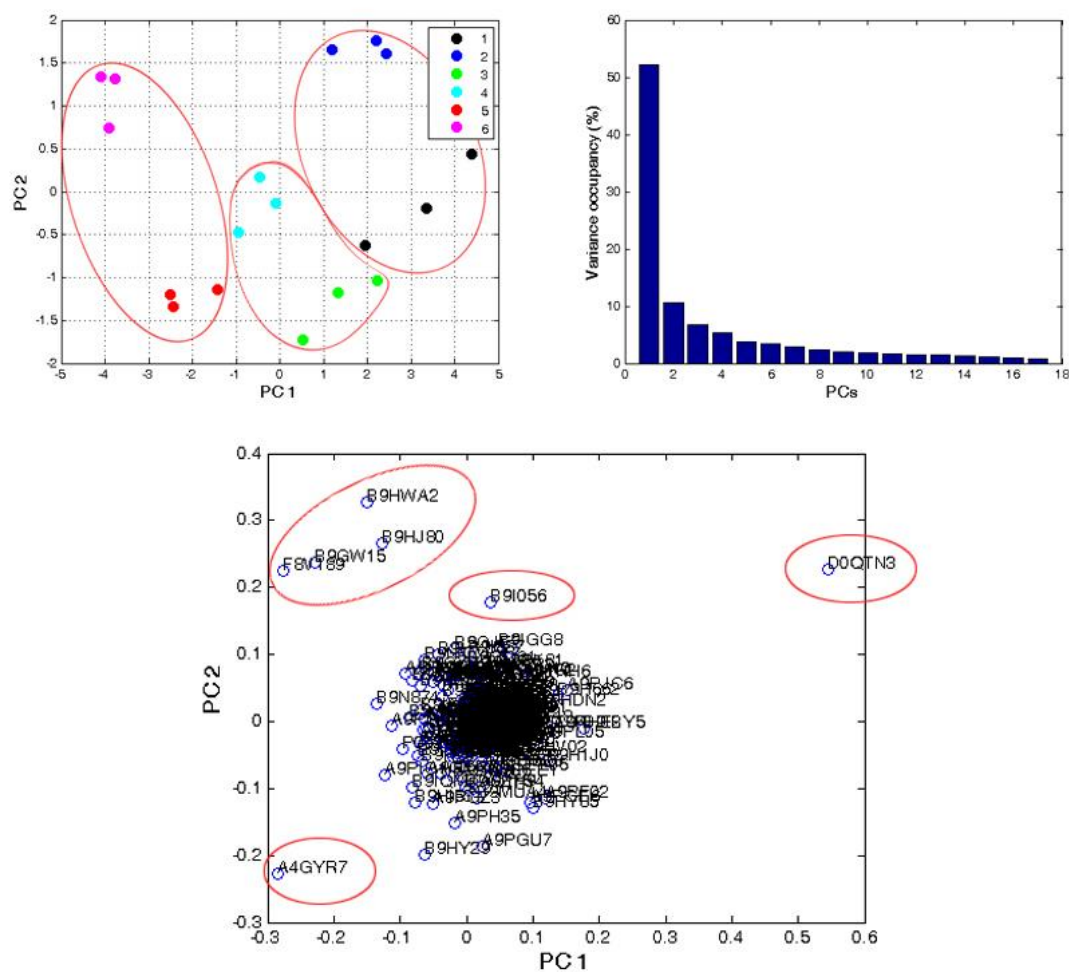


Figure 81: PCA of z-transformed. PC1 explains 774.19% explains and PC2 405.39% of the total variance in the data set (3 biological replicates of 6 different setups).

Table 1: Data sheet of identified proteins with different transformation calculation with covain tool. Explanation: 10: \log^{10} -transformation, z: z-transformation, 10z: \log^{10} - together with z-transformation.

acc. N°	description					
	"uncharacterized" proteins	10	z	10z	PC1	PC2
A9PH35	68%, B9VQ34, Class IV chitinase, <i>Pyrus pyrifolia</i> (Chinese pear) (<i>Pyrus serotina</i>), e= 1.0×10^{-137}	▲		▲	0.056	0.244
A9PI52	81%, G7KIR6, Serine-type peptidase, <i>Medicago truncatula</i> (Barrel medic) (<i>Medicago tribuloides</i>), e= 0.0		▲		-0.046	0.009

	predicted proteins	10	z	10z	PC1	PC2
B9GJE2	86%, B9SVA7, Aspartic proteinase, putative, <i>Ricinus communis</i> (Castor bean), e= 0.0	▲			-0.046	0.235
B9HTU4	89%, Q45RS3, AlaT1, <i>Vitis vinifera</i> (Grape), e= 0.0			▲	-0.187	0.020
B9I056	92%, Minor allergen Alt a, putative, <i>Ricinus communis</i> (Castor bean), e= 1.0×10^{-137}	▲	▲	▲	0.081	0.231
	secondary cell wall	10	z	10z	PC1	PC2
F8V189	Polyphenol oxidase n=2 Tax= <i>Populus trichocarpa</i> RepID=F8V189_POPTR	▲	▲	▲	0.238	- 0.124
	mitochondria electron transport	10	z	10z	PC1	PC2
A4GYR7	ATP synthase subunit beta, chloroplastic n=1 Tax= <i>Populus trichocarpa</i> RepID=ATPB_POPTR			▲	0.014	0.014
B9HJ80	ATP synthase subunit beta n=1 Tax= <i>Populus trichocarpa</i> RepID=B9HJ80_POPTR			▲	0.056	0.244
B9HWA2	ATP synthase subunit beta n=2 Tax= <i>Populus trichocarpa</i> RepID=B9HWA2_POPTR			▲	0.024	- 0.012
	redox	10	z	10z	z	10z
B9N874	Superoxide dismutase [Cu-Zn] n=1 Tax= <i>Populus trichocarpa</i> RepID=B9N874_POPTR	▲		▲	-0.178	0.051
A9PHH6	Phi class glutathione transferase GSTF1 n=1 Tax= <i>Populus trichocarpa</i> RepID=A9PHH6_POPTR	▲			0.194	0.092

	photosystem	10	z	10z	PC1	PC2
A9PIG1	86%, B9RJ42, Photosystem II 22 kDa protein, chloroplast, <i>Ricinus communis</i> (Castor bean), e = 2.0×10^{-163}	▲		▲	0.226	0.107
	calvin-cycle	10	z	10z	PC1	PC2
D0QTN3	Ribulose-1.5-bisphosphat carboxylase/oxygenase large subunit (Fragment) n=3 Tax= <i>Salicaceae</i> RepID=D0QTN3_9ROSI		▲		0.544	0.226

3.6.4.2 DATA ANALYSIS USING PROTMAX

Only \log^{10} -transformed data yield to good results as shown in figure 82. The most significant separation can be seen in the ICA plot which shows the separation between the young and old leaves of the diploid leaf sample.

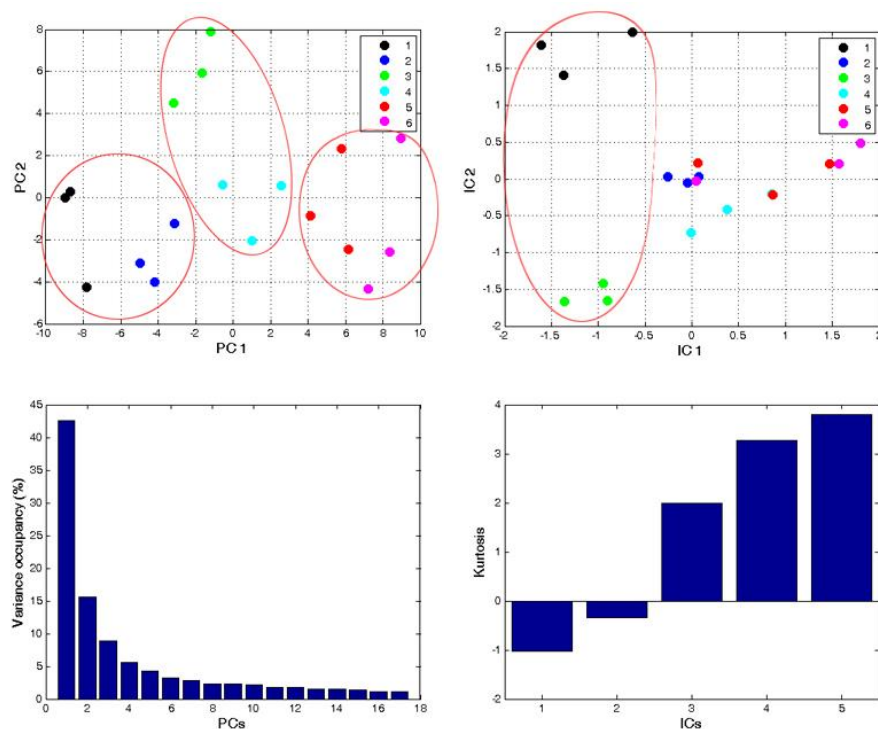


Figure 82: PCA plot conducted with \log^{10} -transformed data from ProtMAX show a separation between the three ploidy levels.

3.6.4.3 DATA ANALYSIS USING UNIPROT

The resulted proteins can be grouped in functional groups (Table 2): photosynthesis related, tricarboxylic acid (TCA) cycle, metal handling, N-metabolism, cellular development and organization. The function of some of them will be described as followed.

Photosystem (1) Light-harvesting complex I protein and the light-harvesting complex II protein have main functions in the photosynthesis reaction. Fructose-bisphosphate aldolase and fructose-1,6-bisphosphate with aldolase are catalyzing the last reaction. In glycolysis fructose-1,6-bisphosphate is oxidized to PEP with aldolase catalyzing the first reaction. The aldolase used in gluconeogenesis and glycolysis is a cytoplasmic protein. **TCA-cycle (2)** Carbonic anhydrase catalyses the reaction $\text{H}_2\text{CO}_3 = \text{CO}_2 + \text{H}_2\text{O}$. **Metal handling (3)** Ferritin is a multimeric protein and a key iron-storage protein which synthesis is developmentally and environmentally controlled. **N-Metabolism (4)** No difference between the cytosolic or chloroplastic glutamine synthetase could be investigated in the leaf samples. The GS is the major assimilatory enzyme for ammonia produced from N-fixation, and nitrate or ammonia nutrition. It re-assimilates ammonia released as a result of photorespiration and the breakdown of proteins and nitrogen transport compounds. **Gluconeogenesis (5)** The malate dehydrogenase catalyzes a reversible NAD(+)-dependent-dehydrogenase reaction involved in redox homeostasis between organelle compartments and central metabolism. **Nucleus (6)** Two different coding proteins were detected. The histone core component of nucleosome is a protein that codes for nucleosomes wrap and compact DNA into chromatin. Histones thereby play a central role in transcription regulation, DNA replication, DNA repair and chromosomal stability. **Secondary cell wall (7)** Polyphenol oxidase can be found in several different plants (68). It is a tetramer that contains four atoms of copper per molecule, and binding sites for two aromatic compounds and oxygen. The enzyme catalyzes different phenols and also the oxidation of phenols which causes the coloring of plant layer after for ex. damage. **Methylation (8)** Protein coding N° B9HV02 a precursor of transferase serine hydroxymethyltransferase was detected in the poplar samples. **Mitochondria electron transport (9)** Protein with the acc. N° G7J108 coding for the ATP synthase subunit alpha and beta was detected in the leaf samples as well. **Amino acid metabolism (10)** Aminomethyltransferase (G7JJ96) is a part of the glycine cleavage

system which catalysis the degradation of glycine and is located in the cytoplasm (50). **One carbon metabolism (11)** A protein coding for the mitochondrial serine hydroxymethyltransferase catalytic pathway 5.10-methylenetetrahydrofolate + glycine + H₂O = tetrahydrofolate + L-serine. **Calvin cycle (12)** Phosphoribulokinase is one unique enzyme to the reductive pentose phosphate pathway of CO₂ assimilation. It exhibits distinctive contrasting properties when the proteins from eukaryotic and prokaryotic sources are compared (152). **Redox (13)** Peroxiredoxins are abundant low-efficiency peroxidases and located in distinct cell compartments including the chloroplast and mitochondria (44).

Table 2: Data sheet of identified groups using UniProt.

acc. N°	description	appearance in leaves		
(1)	photosystem	2N	4N	2N4N
B9N4C4	Light-harvesting complex I protein Lhca4 n=1 Tax= <i>Populus trichocarpa</i> RepID=B9N4C4_POPTR	▲	▲	
A9PEE1	Fructose-bisphosphate aldolase n=1 Tax= <i>Populus trichocarpa</i> RepID=A9PEE1_POPTR	▲		
B9I013	Light-harvesting complex II protein Lhcb3 n=2 Tax= <i>Populus</i> RepID=B9I013_POPTR			▲

(2)	TCA cycle	2N	4N	2N4N
B9GHR1	Carbonic anhydrase n=1 Tax= <i>Populus trichocarpa</i> RepID=B9GHR1_POPTR		▲	▲

(3)	metal handling	2N	4N	2N4N
B9IGG8	Ferritin n=2 Tax= <i>Populus trichocarpa</i> RepID=B9IGG8_POPTR	▲		

(4)	N-metabolism	2N	4N	2N4N
B9HY85	Glutamine synthetase n=1 Tax= <i>Populus trichocarpa</i> RepID=B9HY85_POPTR	▲	▲	
A9PF02	Glutamine synthetase n=1 Tax= <i>Populus trichocarpa</i> RepID=A9PF02_POPTR		▲	

(5)	gluconeogenesis	2N	4N	2N4N
A9PGE6	Malate dehydrogenase n=1 Tax= <i>Populus trichocarpa</i> RepID=A9PGE6_POPTR	▲	▲	▲

(6)	nucleus	2N	4N	2N4N
P59259	Histone H4 n=59 Tax=Embryophyta RepID=H4_ARATH	▲		
A9PDX1	Histone H2A n=2 Tax= <i>Populus trichocarpa</i> RepID=A9PDX1_POPTR			▲

(7)	secondary cell wall	2N	4N	2N4N
F8V189	Polyphenol oxidase n=2 Tax= <i>Populus trichocarpa</i> RepID=F8V189_POPTR	▲	▲	▲
B9GXZ8	Pectinesterase n=1 Tax= <i>Populus trichocarpa</i> RepID=B9GXZ8_POPTR		▲	

(8)	methylation	2N	4N	2N4N
B9HV02	Precursor of transferase serine hydroxymethyltransferase 7 n=1 Tax= <i>Populus trichocarpa</i> RepID=B9HV02_POPTR	▲		
9)	mitochondria electron transport	2N	4N	2N4N

A4GYR7	ATP synthase subunit beta, chloroplastic n=1 Tax= <i>Populus trichocarpa</i> RepID=ATPB_POPTR	▲		
B9HJ80	ATP synthase subunit beta n=1 Tax= <i>Populus trichocarpa</i> RepID=B9HJ80_POPTR	▲		
B9HWA2	ATP synthase subunit beta n=2 Tax= <i>Populus trichocarpa</i> RepID=B9HWA2_POPTR	▲		

(10)	amino acid metabolism	2N	4N	2N4N
B9HZ70	Aminomethyltransferase n=1 Tax= <i>Populus trichocarpa</i> RepID=B9HZ70_POPTR	▲		

(11)	one- carbon metabolism	2N	4N	2N4N
A9PL05	Mitochondrial serine hydroxymethyltransferase n=2 Tax= <i>Populus</i> RepID=A9PL05_POPTM	▲		

(12)	calvin-cycle	2N	4N	2N4N
B9MUA4	Phosphoribulokinase n=1 Tax= <i>Populus trichocarpa</i> RepID=B9MUA4_POPTR			▲

(13)	redox	2N	4N	2N4N
B9MT31	Peroxioredoxin n=1 Tax= <i>Populus trichocarpa</i> RepID=B9MT31_POPTR	▲		▲

3.6.4.4 DIPLOID POPLAR HYBRID L447

As shown in table 3 some of the uncharacterized proteins could be detected in both leaves or only in young or only in the old leaf samples.

For examples both uncharacterized proteins with the acc. N°s A9PHQ2 and A9PGZ8 which are similar to an ATP-dependent protease and NAD-dependent epimerase/dehydratase could be determined in old and young diploid poplar leaves. The uncharacterized protein identified with the acc. N° A9PDW4 shows a similarity of 94% to the Minor allergen, could only be identified in old leaf samples as well as the Rhicadhesin receptor which is a bacterial attachment protein. Both are highly present in the old leaf sample.

Table 3: Data sheet of proteins which are present only in young or only in old or even in both leaf samples of diploid poplar hybrid L447. The \log^2 -transformation was performed simply to obtain symmetric values around zero instead of asymmetric values (< 0.5 and > 2). Explanation: yl: young leaves, ol: old leaves, y/o: young and old leaves.

acc. N°	description	yl	ol	y/o	\log^2
	putative "uncharacterized" proteins				
A9PHQ2	96%, B9RA77, ATP-dependent clp protease, putative, <i>Ricinus communis</i> (Castor bean), e= 0.0			▲	2.321
A9PGZ8	92%, B9RFM2, NAD dependent epimerase/dehydratase, putative, <i>Ricinus communis</i> (Castor bean), e= 0.0			▲	0.642
A9PAH5	71%, Q5QJA3, Harpin binding protein 1, <i>Vitis</i> sp. NL-2003, e= 2.0×10^{-136}			▲	-3.254
A9PDW4	94%, B9T876, Minor allergen Alt a, putative, <i>Ricinus communis</i> (Castor bean), e= 2.0×10^{-136}		▲		5.321
A9PF73	83%, B9RFS5, Rhicadhesin receptor, putative, <i>Ricinus communis</i> (Castor bean), e= 2.0×10^{-120}		▲		4.544
	predicted proteins	yl	ol	y/o	\log^2
A9PI62	73%, B9SCL1, 50S ribosomal protein L9, putative, <i>Ricinus communis</i> (Castor bean), e= 3.0×10^{-95}	▲			4.906

A9P9T9	99%, Q9XEW4, 14-3-3 protein, <i>Populus canescens</i> (Grey poplar) (<i>Populus tremula</i> x <i>Populus alba</i>), e= 3.0×10^{-179}		▲		5.321
A9PBY7	52%, Os04g05, 13000 protein, <i>Oryza sativa subsp. japonica</i> (Rice), e= 9.0×10^{-26}		▲		5.196
B9GJE2	86%, B9SVA7, Aspartic proteinase, putative, <i>Ricinus communis</i> (Castor bean), e= 0.0		▲		5.736
B9N219	98%, Q9LKL0, 14-3-3 protein, <i>Populus canescens</i> (Grey poplar) (<i>Populus tremula</i> x <i>Populus alba</i>), e= 1.0×10^{-177}		▲		5.437
A9PFI8	93%, H2D5S6, Glycolate oxidase, <i>Gossypium hirsutum</i> (Upland cotton) (<i>Gossypium mexicanum</i>), e= 0.0			▲	0.635
B9GXY0	93%, B9SBN5, Rubisco subunit binding-protein beta subunit, rubb, putative, <i>Ricinus communis</i> (Castor bean), e= 0.0			▲	0.463
B9H1J0	95%, B9T0F2, Hydroxypyruvate reductase, putative, <i>Ricinus communis</i> (Castor bean), e= 0.0			▲	0.378
B9MZE9	83%, B9REQ4, Ribose-5-phosphate isomerase, putative, <i>Ricinus communis</i> (Castor bean), e= 2.0×10^{-161}			▲	0.369
B9HY29	96%, A9PIR4, Phosphoglycerate kinase, <i>Populus trichocarpa</i> x <i>Populus deltoides</i> , e= 0.0 / 96%, O82160, <i>Populus nigra</i> (Lombardy poplar), e= 0.0			▲	0.305
B9I5E5	83%, B9REQ4, Ribose-5-phosphate isomerase, putative, <i>Ricinus communis</i> (Castor bean), e= 2.0×10^{-161}			▲	0.229

B9IQM7	62%, G7JLC6, ATP synthase, <i>Medicago truncatula</i> (Barrel medic) (<i>Medicago tribuloides</i>), e= 1.0×10^{-92}			▲	0.152
B9GW15	77%, B9S5Q9, Auxin-binding protein ABP19a, putative, <i>Ricinus communis</i> (Castor bean), e= 1.0×10^{-108}			▲	-0.477
B9I056	92%, B9T876, Minor allergen Alt a, putative, <i>Ricinus communis</i> (Castor bean), e= 2.0×10^{-134}			▲	-2.736

3.6.4.5 TETRAPLOID POPLAR HYBRID L447

In tetraploid poplar leaves only some putative and predicted proteins could be determined in the young or only in the old samples (Table 4). The uncharacterized protein which had a 68% similarity with a Chitinase could only be identified in young leaves. A Serine-type peptidase similarity of 81% was detected only in old samples as well as the 86% similarity of Asparatic proteinase. The most proteins were identified in young and old leaf samples like Phosphoglycerate kinase and the 96% similar Heat shock protein from *Ricinus communis*.

Table 4: Data sheet of proteins which are present only in young or only in old or even in both leaf samples of tetraploid poplar hybrid L447. The \log^2 -transformation was performed simply to obtain symmetric values around zero instead of asymmetric values (< 0.5 and > 2). Explanation: yl: young leaves, ol: old leaves, y/o: young and old leaves.

Acc. N°	description	yl	ol	y/o	\log^2
	putative "uncharacterized" proteins				
A9PH35	68%, B9VQ34, Class IV chitinase, <i>Pyrus pyrifolia</i> (Chinese pear) (<i>Pyrus serotina</i>), e= 1.0×10^{-137}	▲			5.544
A9PI52	81%, G7KIR6, Serine-type peptidase, <i>Medicago truncatula</i> (Barrel medic) (<i>Medicago tribuloides</i>), e= 0.0		▲		5.321
A9PAH5	71%, Q5QJA3, Harpin binding protein 1, <i>Vitis sp.</i> NL-2003, e= 2.0×10^{-136}			▲	- 0.807
	predicted proteins	yl	ol	y/o	\log^2

B9GJE2	86%, B9SVA7, Aspartic proteinase, putative, <i>Ricinus communis</i> (Castor bean), e= 0.0		▲		5.058
B9HTU4	89%, Q45RS3, AlaT1, <i>Vitis vinifera</i> (Grape), e= 0.0			▲	2.321
B9H1J0	95%, B9T0F2, Hydroxypyruvate reductase, putative, <i>Ricinus communis</i> (Castor bean),e= 0.0			▲	0.648
B9HI53	99%, A9PIR4, Phosphoglycerate kinase, <i>Populus trichocarpa</i> x <i>Populus deltoides</i> , e= 0.0			▲	0.242
B9HMG8	96%, B9T228, Heat shock protein, putative, <i>Ricinus communis</i> (Castor bean), e= 0.0			▲	- 0.387
A9PG06	91%, G3FGV1, Glyceraldehyde-3-phosphate dehydrogenase C, <i>Scoparia dulcis</i> (Sweet broom) (<i>Capraria dulcis</i>), e= 0.0			▲	- 0.584
B9HX68	99%, Q9AR79, Stable protein 1, <i>Populus tremula</i> (European aspen), e= 9.0×10^{-71}			▲	- 0.782

3.6.4.6 MIXOPLOID POPLAR HYBRID L447

The comparison between the young and old leaves of the mixoploid poplar hybrid samples showed that the most uncharacterized proteins could be identified both leaf ages (Table 5). Like in the 4N sample the uncharacterized protein with the acc. N°

A9PH35 which has a similarity of 68% to Class IV chitinase in *Pyrus pyrifolia* could be detected in the mixoploid but not in the diploid sample. In both samples a DHAR class of Gluthathione transferase was identified. Only in the old leaf samples the Chitinase 1 could be detected.

Table 5: Data sheet of proteins which are present only in young or only in old or even in both leaf samples of mixoploid poplar hybrid L447. The \log^2 -transformation was performed simply to obtain symmetric values around zero instead of asymmetric values (< 0.5 and > 2). Explanation: yl: young leaves, ol: old leaves, y/o: young and old leaves.

acc. N°	description	yl	ol	y/o	\log^2
	putative "uncharacterized" proteins				
A9PH35	68.0% ,B9VQ34, Class IV chitinase, <i>Pyrus pyrifolia</i> (Chinese pear) (<i>Pyrus serotina</i>), $e= 1.0 \times 10^{-137}$	▲			5.906
A9PF73	83.0%, B9RFS5, Rhicadhesin receptor, putative, <i>Ricinus communis</i> (Castor bean), $e= 2.0 \times 10^{-120}$		▲		5.058
A9PH94	87%, B9SVD3, Photosystem II 10 kDa polypeptide, chloroplast, putative, <i>Ricinus communis</i> (Castor bean), $e= 5.0 \times 10^{-80}$			▲	2.491
A9PHA9	92%, I0B7J4, Chloroplast PsbO4, <i>Nicotiana benthamiana</i> , $e= 1.569$			▲	0.317
A9PGU7	88%, B9SDY7, Ribulose bisphosphate carboxylase/oxygenase activase 1, chloroplast, putative, <i>Ricinus communis</i> (Castor bean), $e= 0.0$			▲	0.283
A9PGS6	91%, I0B7J4, Chloroplast PsbO4, <i>Nicotiana benthamiana</i> , $e= 1,552$			▲	0.268
A9PFE9	69%, D7MA68, ATP synthase family, <i>Arabidopsis lyrata</i> subsp. <i>lyrata</i> (Lyre-leaved rock-cress), $e= 2.0 \times 10^{-89}$			▲	-0.447
	predicted proteins	yl	ol	y/o	\log^2

B9H851	71%, B9RG39, Photosystem II 11 kDa protein, putative, <i>Ricinus communis</i> (Castor bean), $e= 5.0 \times 10^{-74}$	▲			5.544
B9P6S9	92%, E9N6T8, 1,3-beta-D-glucanase GH17_39, <i>Populus tremula</i> x <i>Populus tremuloides</i> , $e= 0.0$		▲		5.321
B9H1P7	88%, H6WS85, Chitinase 1, <i>Populus canadensis</i> (Canadian poplar) (<i>Populus deltoides</i> x <i>Populus nigra</i>), $e= 0.0$		▲		5.736
B9GJE2	86%, B9SVA7, Aspartic proteinase, putative, <i>Ricinus communis</i> (Castor bean), $e= 0.0$		▲		5.196
B9H1J0	95%, B9T0F2, Hydroxypyruvate reductase, putative, <i>Ricinus communis</i> (Castor bean), $e= 0.0$			▲	0.750
B9GW15	77%, B9S5Q9, Auxin-binding protein ABP19a, putative, <i>Ricinus communis</i> (Castor bean), $e= 1.0 \times 10^{-108}$			▲	-0.620
B9GV62	99%, D2WL73, DHAR class glutathione transferase DHAR1, <i>Populus trichocarpa</i> (Western balsam poplar) (<i>Populus balsamifera</i> subsp. <i>trichocarpa</i>), $e= 1.0 \times 10^{-158}$			▲	-1.247

3.6.4.7 PCA, HEAT MAP AND ANOVA ANALYSIS OF SELECTED PROTEINS I

Only data with significances between young and old leaf samples were measured with the t-test that was set to $p \leq 0.05$. Together with the t-test and the p-value a \log^2 -

transformation with 0.3 and 1.6 for a two-fold change (Fig. 83) was used for these analyses.

The 102 identified proteins show a clear separation between young and old leaves. The leaf samples of the diploid poplar hybrid have the highest separation in the PCA compared to the tetraploid and mixoploid leaf samples.

The heat-map (Fig. 84) shows the identified proteins from figure 78. The red colored bars shows an up-regulation and the green colored bars a down-regulation of the identified proteins. The bars placed at the -1 level represent no identified proteins.

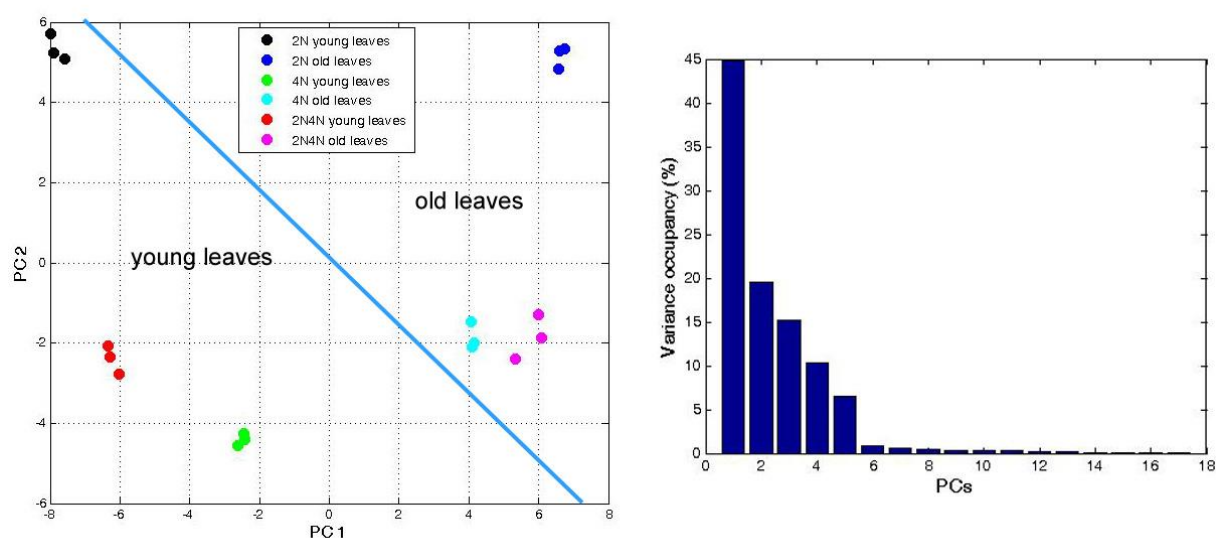


Figure 83: PCA plot conducted with \log^{10} -transformed data. PC1 explains 44.87% and PC2 0.02% of the total variance in the data set (3 biological replicates, of 6 different setups).

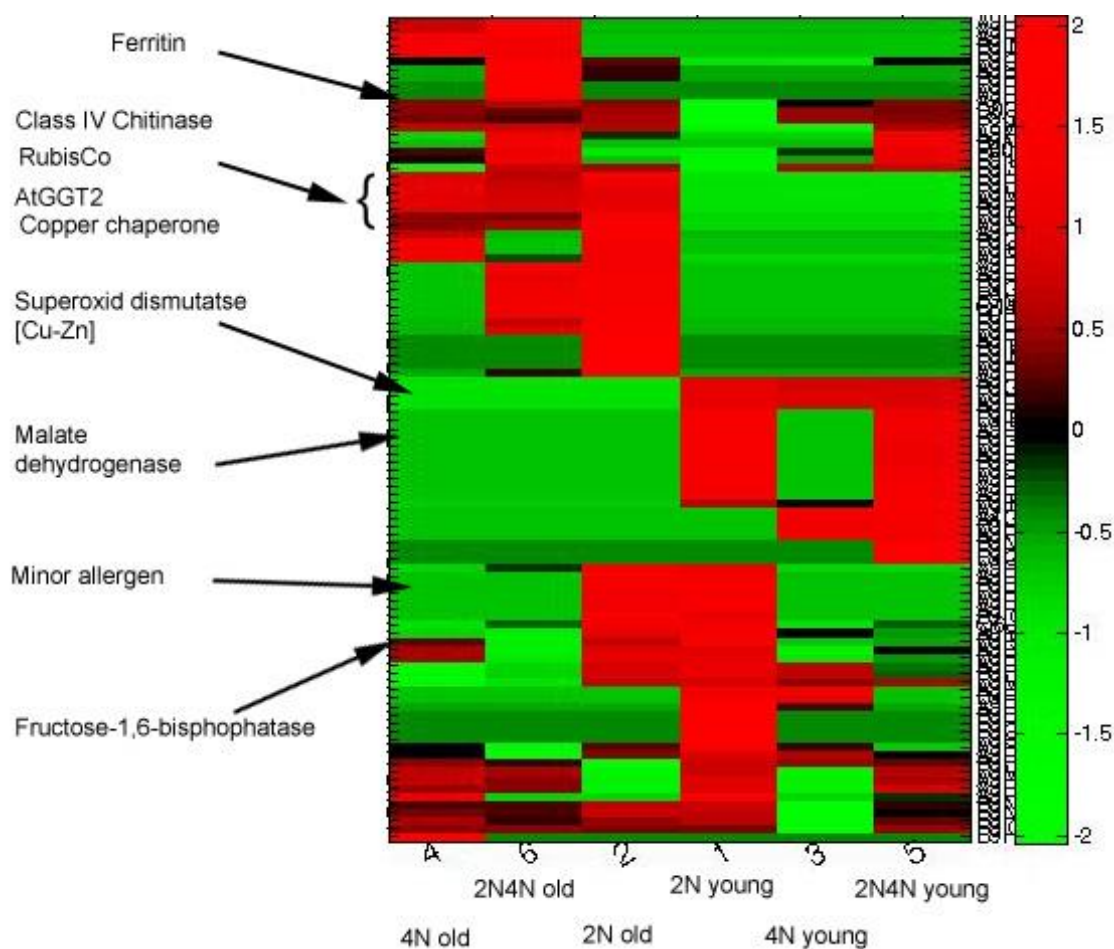


Figure 84: Heat-map of PCA of figure 83 shows different important proteins and enzymes listed (red up-regulation, green down-regulation); the rate -1 shows not identified proteins.

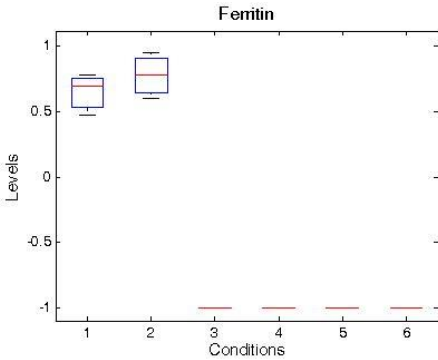
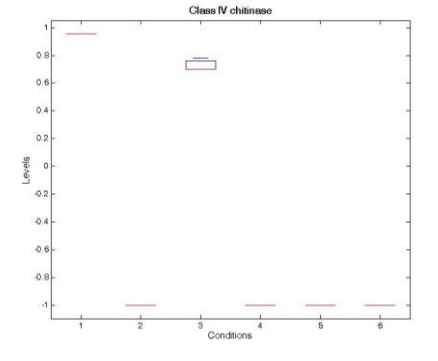
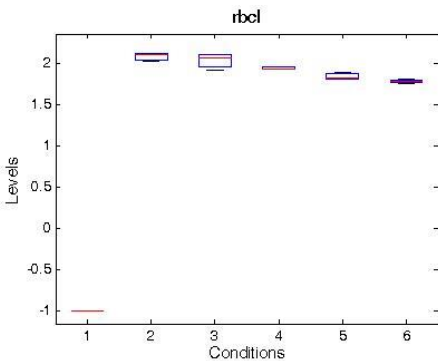
Figure 85 a-j shows almost all identified proteins of figure 84 analyzed with the Anova statistics program. The p-value was set to < 0.01.

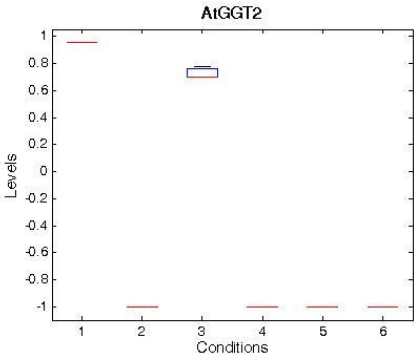
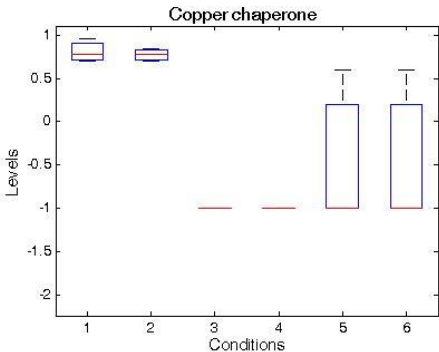
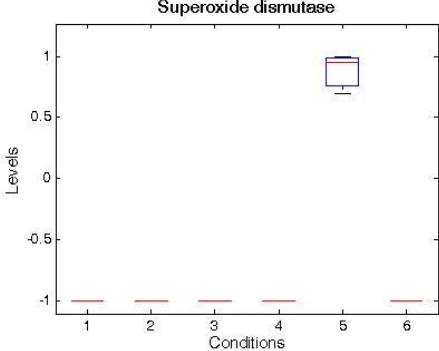
As seen in figure 84 the identified protein Ferritin (a) with the acc. N° A9PK81 was identified only in the diploid leaf samples.

The putative uncharacterized protein (b) with the acc. N° A9PH35 and identified to Class IV chitinase could only be detected in young leaves of the diploid and tetraploid sample.

The identified protein with the acc. N° D0QTN3 RubisCo (c) was detected in all leaf samples except in the young samples of the diploid poplar hybrid. The predicted protein (d) with the acc. N° B9HTU4 and a similarity of 88% to Glutamate-glyoxylate aminotransferase could be detected in old diploid and tetraploid leaf samples. The Copper chaperone (e) with the acc. N° Q6J338 was only detected in the leaf samples of the diploid poplar hybrid. The enzyme Superoxide dismutase [Cu-Zn] (f) with the

acc. N° B9N874 was only significant in the young leaves of the mixoploid poplar sample. The acc. N° A9P8R3 coding for Malate dehydrogenase (g) was identified only in diploid leaf samples. The protein coding for the Minor allergen (h) with the acc. N° B9I056 was detected in all old leaf samples. The predicted protein (i) with the acc. N° A9PGB1 with an 81% similarity to Fructose-1.6-bisphosphate was identified in young diploid and mixoploid leaf samples.

<p>(a)</p>  <p>Ferritin</p> <p>Levels</p> <p>Conditions</p>	<p>A9PK81 <i>Ferritin</i></p> <p>Ferritin is an iron-storage protein and plays a preliminary pool for the building up of Fe containing proteins in leaves. It also plays a role in stress response (24)</p>
<p>(b)</p>  <p>Class IV chitinase</p> <p>Levels</p> <p>Conditions</p>	<p>A9PH35 putative uncharacterized protein 68% similarity of B9VQ34 <i>Class IV chitinase</i> of <i>Pyrus pyrifolia</i></p> <p>The chitinase produces proteins which are involved in the hydrolyzation of glycosidic bonds in chitin (175)</p>
<p>(c)</p>  <p>rbcL</p> <p>Levels</p> <p>Conditions</p>	<p>D0QTN3 <i>Ribulose-1,5-bisphosphate carboxylase/oxygenase large subunit</i></p> <p>RuBisCO is responsible for the CO₂ uptake in plants and bacteria.</p>

<p>(d)</p>  <p>AtGGT2</p>	<p>B9HTU4 predicted protein 88% similarity to Q9S7E9 <i>Glutamate-glyoxylate aminotransferase of Arabidopsis thaliana</i></p> <p>The GGA adjust the amino acid content in photorespiration (98).</p>
<p>(e)</p>  <p>Copper chaperone</p>	<p>Q6J338 <i>Copper chaperone</i></p> <p>It is known that the CCH to be upregulated during senescence and to mobilize metal ions in leaves (119).</p>
<p>(f)</p>  <p>Superoxide dismutase</p>	<p>B9N874 <i>Superoxid dismutase [Cu-Zn]</i></p> <p>SOD's are metalloproteins that catalyze the dismutation of superoxide to protect organisms from oxidative damage.</p>

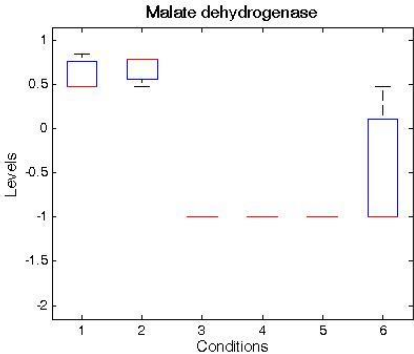
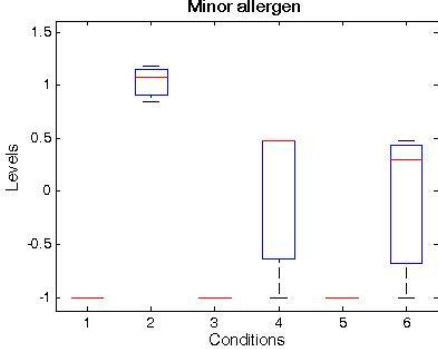
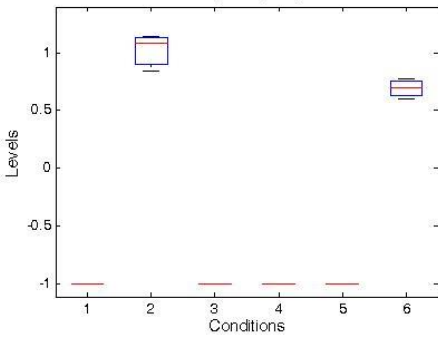
<p>(g)</p>  <p>Malate dehydrogenase</p> <p>Levels</p> <p>Conditions</p>	<p>A9P8R3 <i>Malate dehydrogenase</i></p> <p>Malate is an intermediate of the TCA-cycle as well as a regulator for turgor processes in stomata guard cells (67).</p>
<p>(h)</p>  <p>Minor allergen</p> <p>Levels</p> <p>Conditions</p>	<p>B9I056 <i>Minor allergen</i></p>
<p>(i)</p>  <p>Fructose-1,6-bisphosphatase</p> <p>Levels</p> <p>Conditions</p>	<p>A9PGB1 predicted protein 81% similarity to P46275 <i>Fructose-1,6-bisphosphatase, chloroplastic of Pisum sativum</i></p> <p>This enzyme catalyzes the reaction fructose-6-phosphat to fructose-1,6-bisphosphat.</p>

Figure 85: Significant identified proteins analyzed with Anova statistics. Conditions of the x-axis as followed: 1: 2N young, 2: 2N old, 3: 4N young, 4: 4N old, 5: 2N4N young, 6: 2N4N old. Y-axis shows the scale of the measured levels.

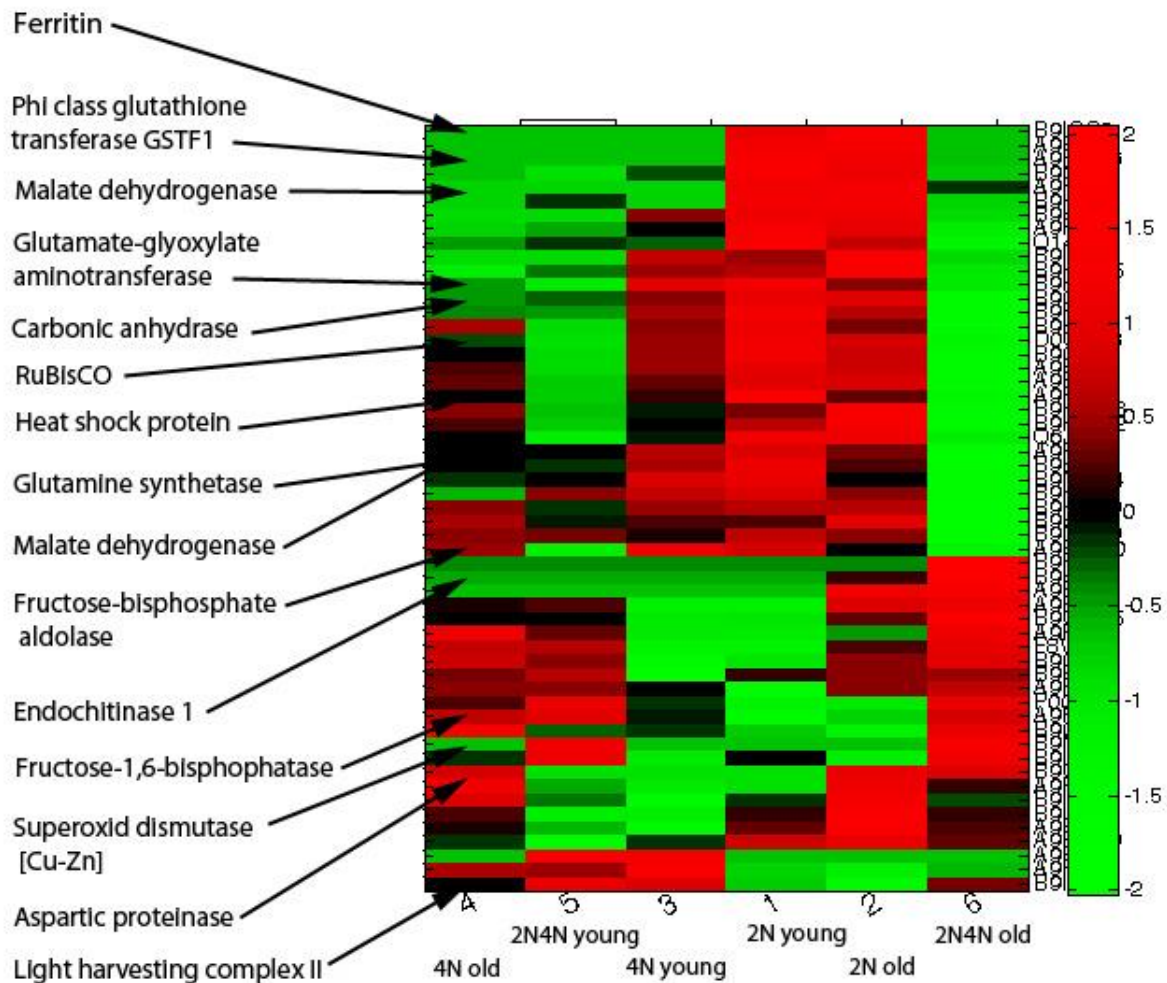


Figure 87: Heat-map of PCA in figure 85, different important proteins and enzymes listed (red up-regulation, green down-regulation); the rate -1 shows not detected proteins.

The Anova data research can estimate different up- and down-regulating proteins in the young and old leaves of diploid, tetraploid and mixoploid samples. The p-value was set to < 0.01 and only protein data which were analyzed with the t-test $p < 0.05$ were shown in the following results (Figures 88-97).

Figures 88-97 show the acc. N° of the up-regulated proteins together with their protein name.

Figure 88 shows proteins that only were identified in the diploid young and old leaf samples.

The identified protein with the acc. N° B9HH10 (a) has a 96% similarity to the B9RI35 Eukaryotic translation elongation factor of *Ricinus communis* is similar regulated in young and old leaves.

The iron storage protein Ferritin, acc. N° B9IGG8 (b) and A9PK81 (c), shows an up-regulation in the old and young leaf samples. Additionally it is visible that the old leaf sample is slightly higher regulated than the young leaf samples.

The enzyme Malate dehydrogenase A9P8R3 (d) is similarly regulated in the young and old leaves while the Phi class glutathione transferase GSTF1 (e) with the acc. N° A9PHH6 was a slightly higher up-regulated in the old leaf samples than in the young leaf samples.

Figure 89 (a) shows the predicted protein B9H1P7 with a similarity of 76% to the Endochitinase 1 with the acc. N° Q41596. It was only detected in the old leaf sample of the mixoploid poplar hybrid.

In all diploid, tetraploid and mixoploid old leaf samples (Figure 90 a) the predicted protein with the acc. N° B9GJE2 with an 86% similarity to the Aspartic proteinase B9GJE2 has been detected. The maximum up-regulation can be exhibited in the diploid leaf sample followed by the tetraploid sample and mixoploid sample.

In figure 91 (a) the enzyme Superoxide dismutase [Cu-Zn] with the acc. N° B9N874 was detected only in the mixoploid leaf samples. No big difference in the regulation can be seen between young and old leaves.

Figure 92 (a) shows the predicted protein B9HTU4 with a similarity of 88% to Glutamate-glyoxylate aminotransferase that was measured in the diploid young and old leaves and only young leaf in the tetraploid samples.

The Copper chaperone with the acc. N° Q6J338 has been identified in the diploid and tetraploid leaf samples. In (b) it is visible that this protein is up-regulated in the young as well as in the old leaves with no severe difference in their mean value.

The putative uncharacterized protein with the acc. N° A9PIG1 (Figure 93) has a similarity of 79% with the Photosystem II 22KDa protein Q02060 and is only detected in the tetraploid and mixoploid leaf samples.

Only detectable in the old leaves of the diploid and mixoploid leaf sample is the putative uncharacterized protein with the acc. N° A9PF73 with a similarity of 83% to the Rhicadhesin receptor B9RFS5 (Figure 94 a).

The Class IV chitinase with the acc. N° A9PH35 could only be detected in young tetraploid and mixoploid leaf samples with no big difference in their mean value (Figure 95 a).

Figure 96 a-x shows proteins and enzymes that have been identified in all leaf samples with different regulation levels.

The Aminomethyltransferase with the acc. N° B9HZ70 (a) is up-regulated in the young leaf samples of the diploid and mixoploid samples while the tetraploid young and old leaves do not show a big difference in their mean value.

The predicted protein with the acc. N° B9HVE6 has a similarity of 79% to the Amino acid binding protein of *Ricinus communis* is constant regulated between all samples while the old leaf sample of the mixoploid poplar hybrid do not show any regulated protein.

The predicted protein with the acc. N° B9GW15 (c) shows a 67% similarity to the Q9ZRA4 Auxin-binding protein and was identified in all leaf samples. A severe up-regulation can be seen in the mixoploid old leaf samples compared to the diploid and tetraploid samples. All young leaf samples have a lower regulation level than the old leaf samples.

The chloroplastic ATP synthase subunit alpha with the acc. N° Q14FH2 (d) is up-regulated in all young leaf samples. The highest value can be identified in the diploid leaf samples. Just as the ATP synthase the Carbonic anhydrase (e) with the acc. N° B9GHR1 is up-regulated in the young leaf samples with the highest value in the diploid leaf samples.

The predicted protein acc. N° B9GSZ2 (f) which is 88% similar to the Chlorophyll a-b binding protein 3C is up-regulated in the young diploid leaf sample while in the tetraploid and mixoploid only the old leaf samples were up-regulated.

Another predicted protein B9GZ04 (g) with an 87% similarity to the Ferredoxin-NADP reductase is up-regulated in the old leaf samples of all ploidy levels and the highest mean can be seen in the diploid leaf sample.

The predicted protein A9PGB1 (h) with an 81% similarity to the Fructose-1,6-bisphosphatase is up-regulated in the old leaf samples of the diploid poplar hybrid. In comparison to the Fructose-1,6-bisphosphatase the Fructose-bisphosphate aldolase A9PGW0 (i) shows the opposite regulation to the diploid leaf sample. Here the young leaf sample is up-regulated and the old leaf sample down-regulated. In all young leaf samples the Glycerate dehydrogenase HPR (j) with the acc. N° B9H1J0 is higher regulated compared to the old leaf samples.

The Glyceraldehyde-3-phosphat dehydrogenase (k) with the acc. N° A9PG06 shows a higher regulation in the old leaf samples compared to the young leaf samples.

The Glutamine synthetase (l) with the acc. N° B9HY85 does not show any severe differences between the ploidy levels but a difference between young and old leaf samples.

The predicted protein with the acc. N° B9HMG8 (m) and a 96% similarity to B9HMG7 Heat shock protein shows a higher regulation in the diploid leaf samples compared to the tetraploid and mixoploid samples. The diploid and tetraploid samples show a higher regulation in the old leaf samples compared to the young samples.

The predicted protein coding B9HMG2 (n) with a 97% similarity to D2D322 Heat shock protein 70 shows a similar graph. A third Stromal heat shock related protein (o) with the acc. N° Q02028 shows much higher regulations in diploid leaf samples than in tetraploid and mixoploid samples.

The Light harvesting complex II (p) with the acc. N° A9PGZ3 shows a higher regulation in all young leaf samples than the old leaf samples.

The protein coding for the Malate dehydrogenase (q) with the acc. N° A9PGE6 is up-regulated in all leaf samples.

The Mitochondrial serine hydroxymethyltransferase (r) with the acc. N° A9PL05 shows the highest regulation in young leaf samples. Interestingly the highest up-regulation can be found in the young leaf of the diploid samples.

The protein with the acc. N° B9MUA4 coding for the Phosphoribulokinase (s) is higher regulated in all young leaf samples and shows the lowest regulation in the old leaf samples of the mixoploid poplar hybrid.

The putative uncharacterized protein (t) with the acc. N° A9P828 has a similarity of 91% to the Phosphoglycerate kinase Q42962 and it shows the highest regulation in all young leaf samples. It shows the highest value in the diploid poplar hybrid.

The Ribulose-1.5-bisphosphate carboxylase/oxygenase large subunit (u) with the acc. N° D0QTN3 was higher regulated in all young leaf samples. The highest regulation can be detected in the diploid leaf samples.

Compared to RubisCo the predicted protein (w) with the acc. N° B9HQD5 which has an 87% similarity to RubisCo large subunit-binding protein subunit alpha P08926 (w), the young leaf samples of the tetraploid and mixoploid poplar hybrid are higher regulated while the young leaf of the diploid sample shows a less regulation.

Similar to the RubisCo the Ribose-5-phosphate isomerase (v) with the acc. N° B9MZE9 is higher regulated in the young leaf samples of the diploid poplar samples. The tetraploid leaf samples shows a higher regulation of the old leaf samples while only in the young leaves of the mixoploid samples the Ribose-5-phosphate isomerase could be detected.

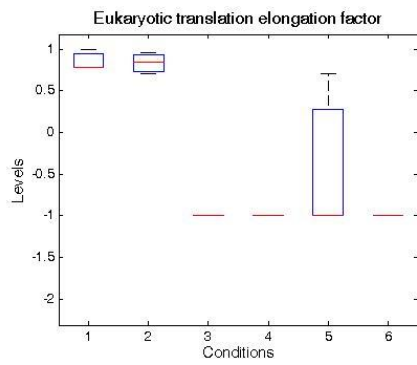
The predicted protein (x) with the acc. N° B9HX69 has a 99% similarity to Q9AR79 Stable protein 1 shows an higher regulation in the old leaf samples of the diploid and tetraploid poplar. The mixoploid leaf samples show a more stable result.

In figure 97 following proteins were detected in the different polyploidy levels. The predicted protein (a) with the acc. N° B9IHR5 with a similarity of 86% to the 2 Isoform of Ferredoxin-dependent glutamate synthase was detected in the diploid young and old leaves and the tetraploid young leaves. It is higher regulated in the old leaves of the diploid samples while the young leaves of the diploid and tetraploid samples show the same level.

The Pectinesterase (b) with the acc. N° B9GXZ had been detected in all three ploidy levels. Only in the old leaf sample of the diploid poplar hybrid the appearance of this protein can be determined. The same is shown in the tetraploid leaf sample. Only the mixoploid leaf samples show an incidence of Pectinesterase in the young and old leaf samples.

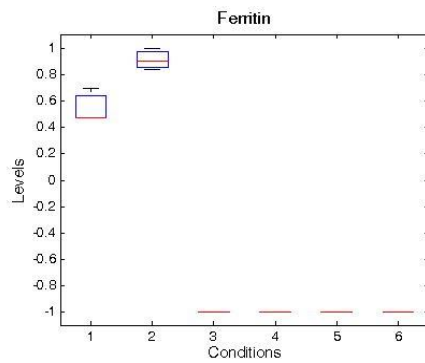
The Polyphenol oxidase (c) with the acc. N° F8V189 was detected in all ploidy levels. The detected amount is very similar to the Pectinesterase. Only in the old leaf samples of the diploid and tetraploid poplar hybrid this protein can be seen. While in the mixoploid poplar hybrid in the young as well as in the old leaf samples the Polyphenol oxidase is shown.

(a)



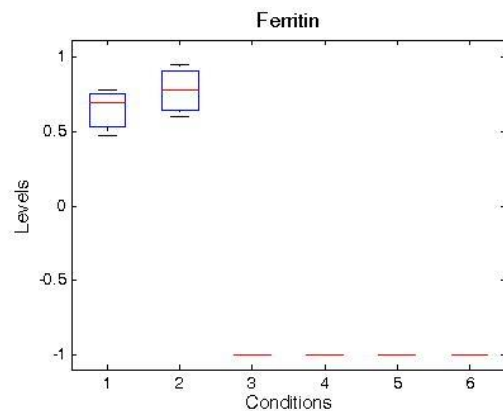
B9HH10 predicted protein 96% similarity to B9RI35 *Eukaryotic translation elongation factor, putative of Ricinus communis*

(b)



B9IGG8 *Ferritin*

(c)



A9PK81 *Ferritin*

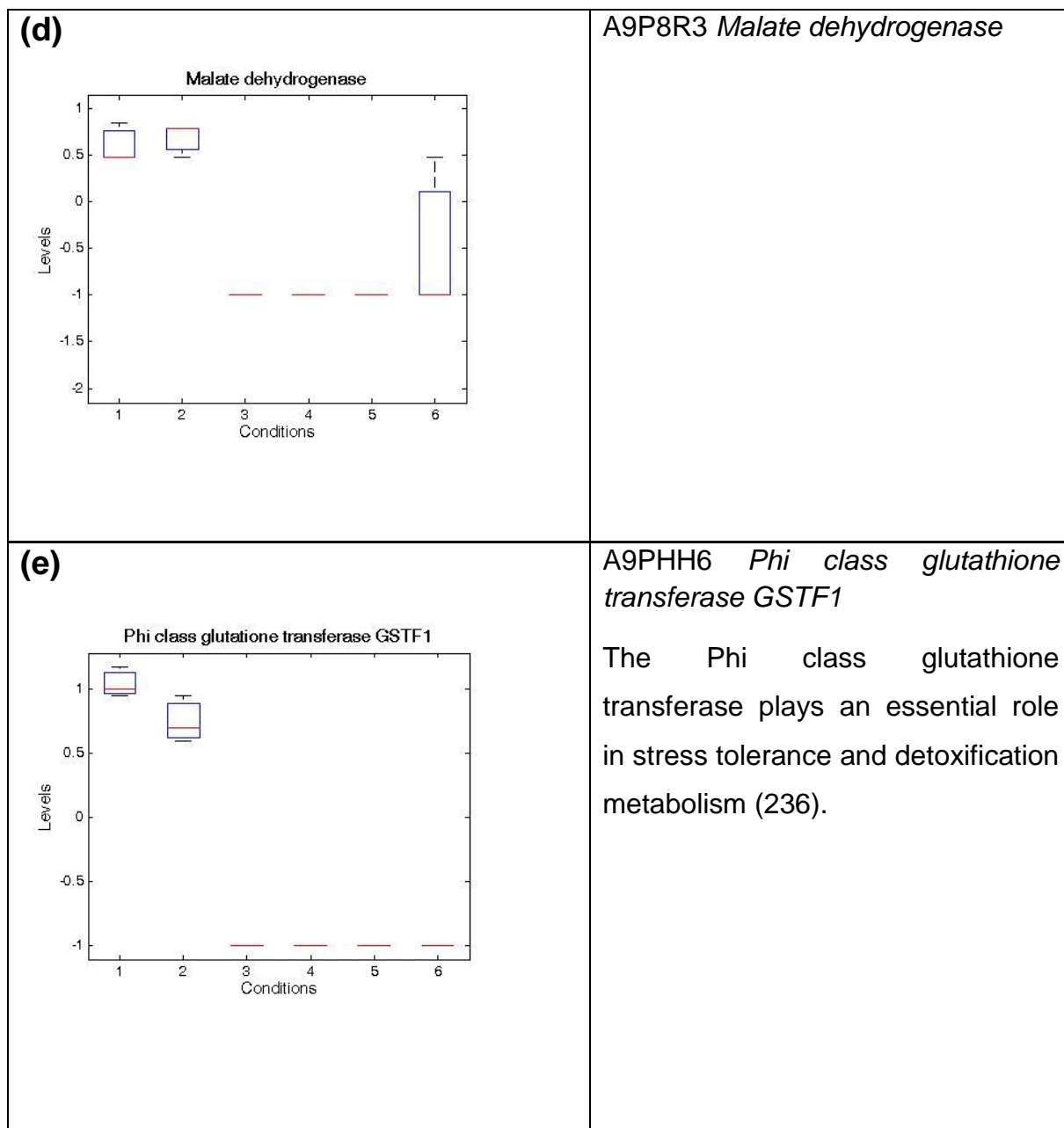


Figure 88: Anova statistics of all identified proteins from young and leaves of the diploid poplar hybrid analyzed with Anova statistics. Conditions of the x-axis as followed: 1: 2N young, 2: 2N old, 3: 4N young, 4: 4N old, 5: 2N4N young, 6: 2N4N old. Y-axis shows the scale of the measured levels.

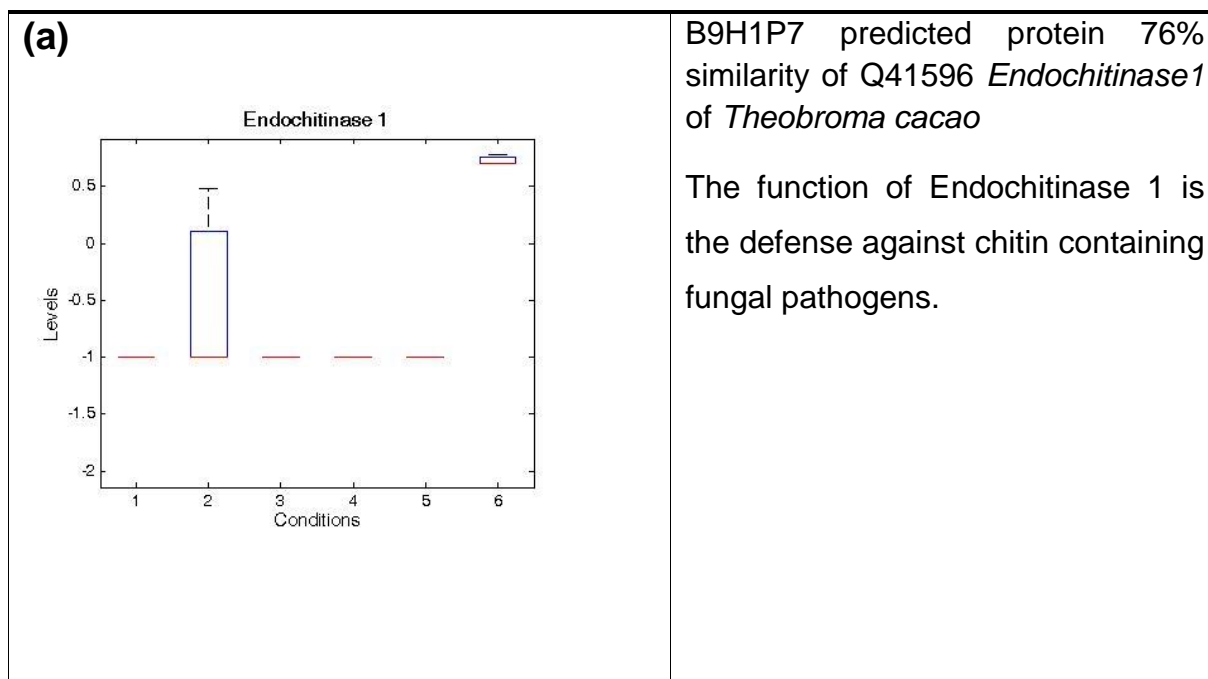


Figure 89: Some of the identified proteins from the old leaf samples of the mixoploid poplar hybrid analyzed with Anova statistics. Conditions of the x-axis as followed: 1: 2N young, 2: 2N old, 3: 4N young, 4: 4N old, 5: 2N4N young, 6: 2N4N old. Y-axis shows the scale of the measured levels.

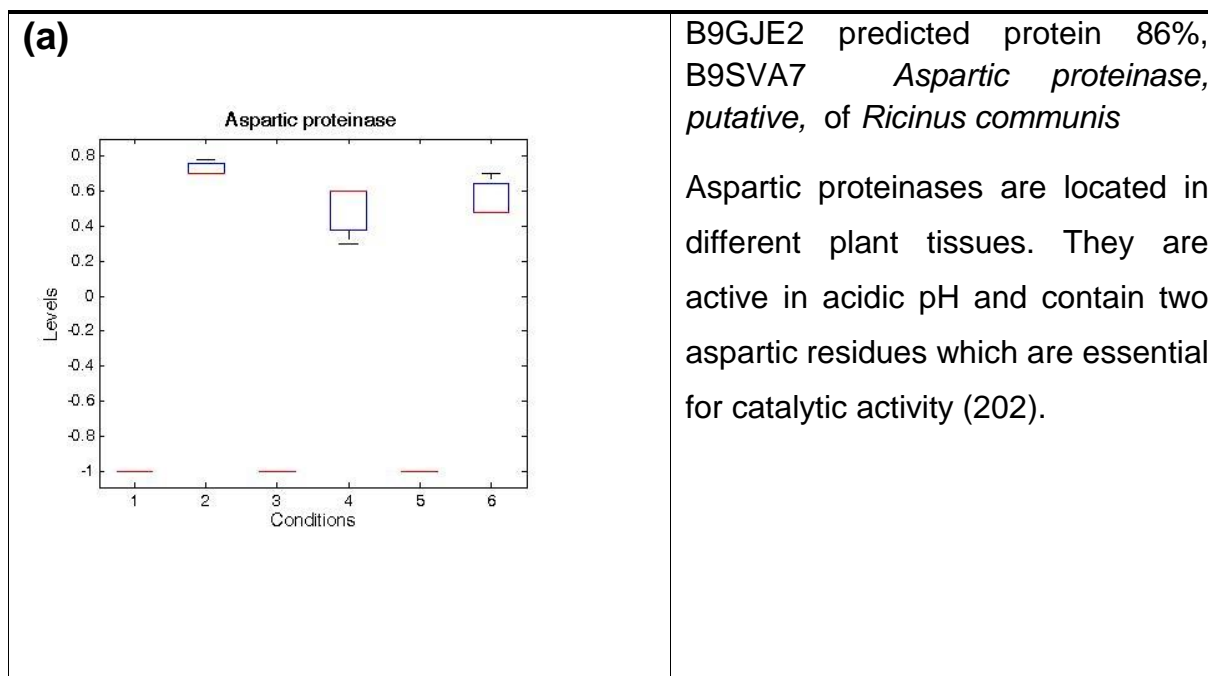
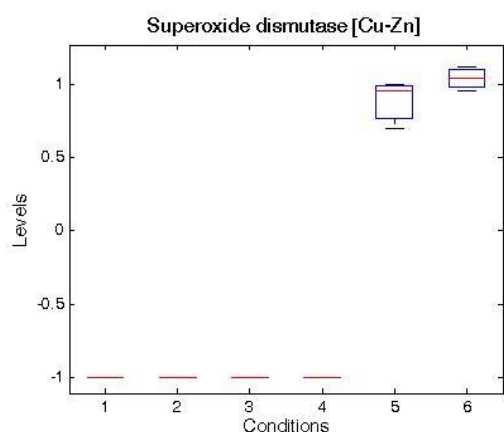


Figure 90: Identified protein in the old leaf sample of the diploid, tetraploid and mixoploid poplar hybrid analyzed with Anova statistics. Conditions of the x-axis as followed: 1: 2N young, 2: 2N old, 3: 4N young, 4: 4N old, 5: 2N4N young, 6: 2N4N old. Y-axis shows the scale of the measured levels.

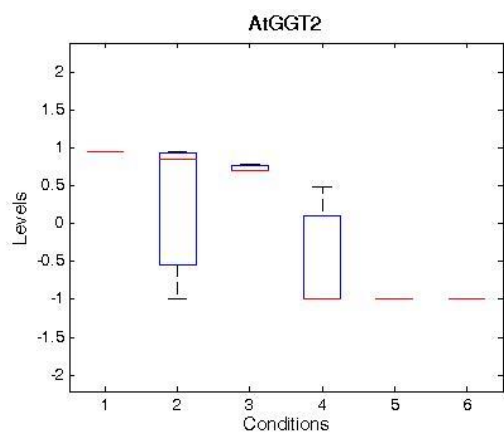
(a)



B9N874 *Superoxide dismutase [Cu-Zn]*

Figure 91: Identified protein in young and old leaf samples of the mixoploid poplar hybrid analyzed with Anova statistics. Conditions of the x-axis as followed: 1: 2N young, 2: 2N old, 3: 4N young, 4: 4N old, 5: 2N4N young, 6: 2N4N old. Y-axis shows the scale of the measured levels.

(a)



B9HTU4 predicted protein 88% similarity to Q9S7E9 *Glutamate-glyoxylate aminotransferase* of *Arabidopsis thaliana*

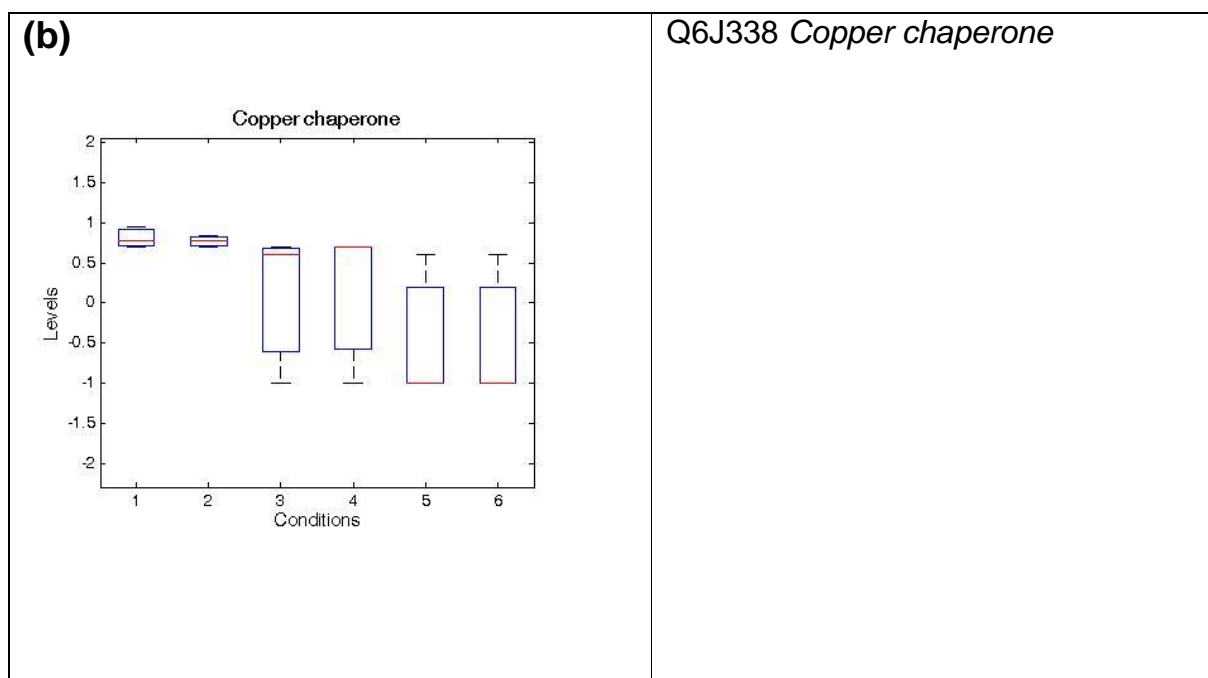


Figure 92: Some identified proteins of mixoploid young and old leaf samples analyzed with Anova statistics. Conditions of the x-axis as followed: 1: 2N young, 2: 2N old, 3: 4N young, 4: 4N old, 5: 2N4N young, 6: 2N4N old. Y-axis shows the scale of the measured levels.

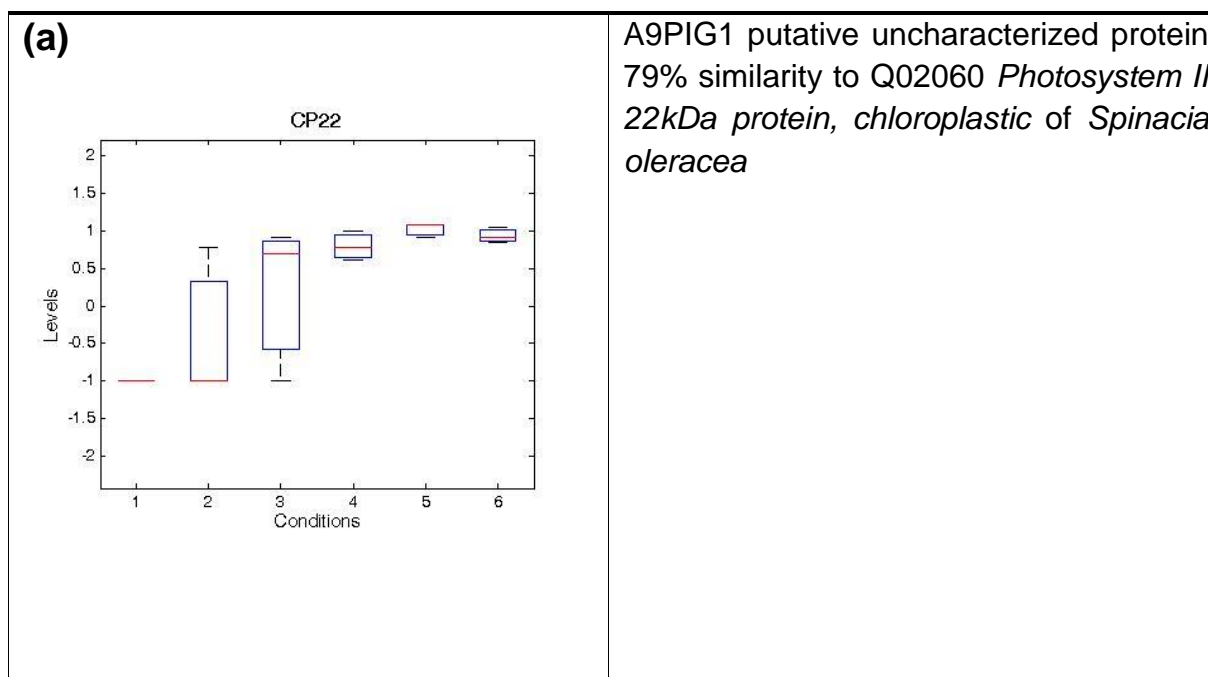


Figure 93: Identified protein in old leaf samples of tetraploid and mixoploid poplar hybrid analyzed with Anova statistics. Conditions of the x-axis as followed: 1: 2N young, 2: 2N old, 3: 4N young, 4: 4N old, 5: 2N4N young, 6: 2N4N old. Y-axis shows the scale of the measured levels.

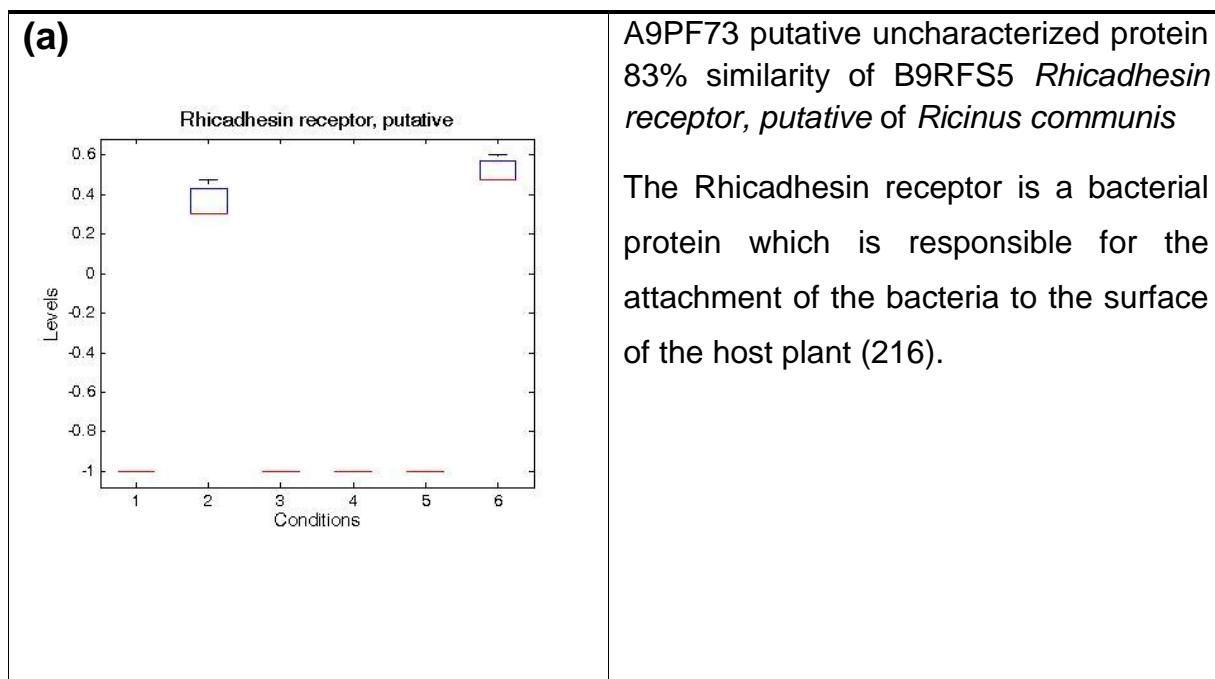


Figure 94: Identified protein in old leaf samples of all ploidy levels analyzed with Anova statistics. Conditions of the x-axis as followed: 1: 2N young, 2: 2N old, 3: 4N young, 4: 4N old, 5: 2N4N young, 6: 2N4N old. Y-axis shows the scale of the measured levels.

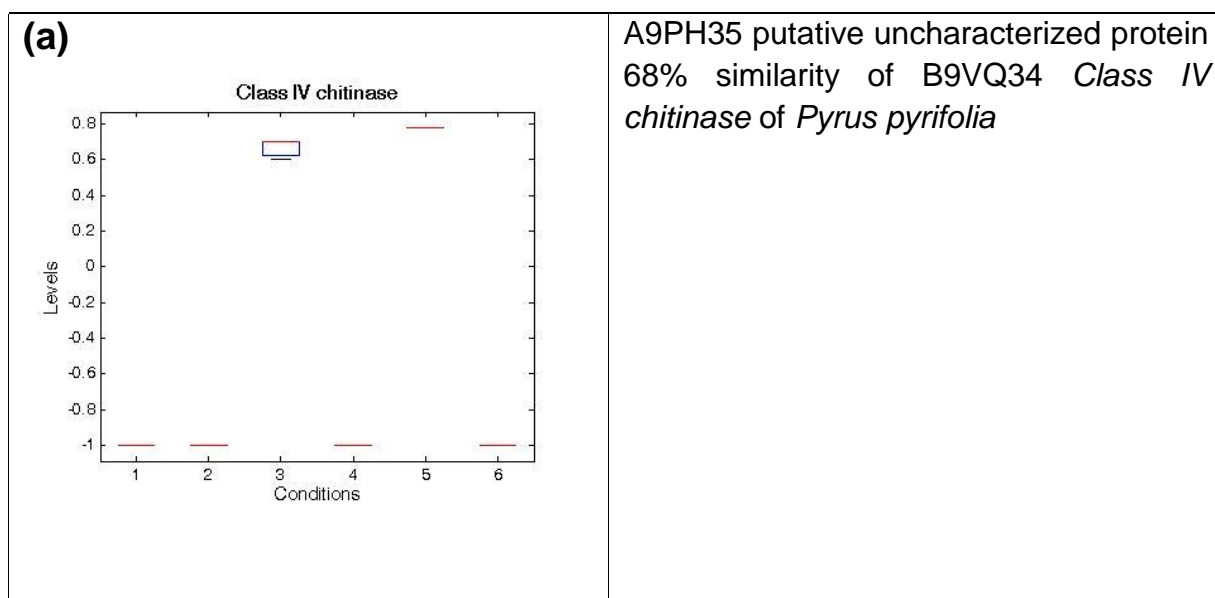
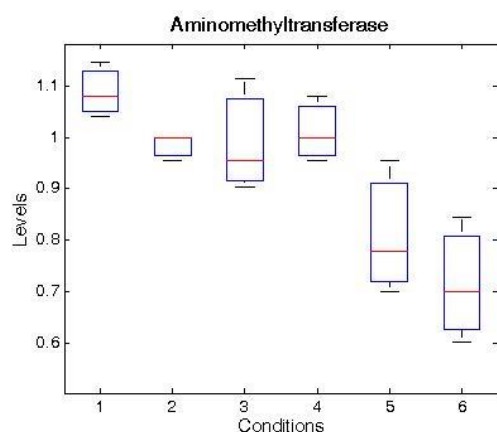


Figure 95: Identified protein in young leaf samples of tetraploid and mixoploid poplar hybrid analyzed with Anova statistics. Conditions of the x-axis as followed: 1: 2N young, 2: 2N old, 3: 4N young, 4: 4N old, 5: 2N4N young, 6: 2N4N old. Y-axis shows the scale of the measured levels.

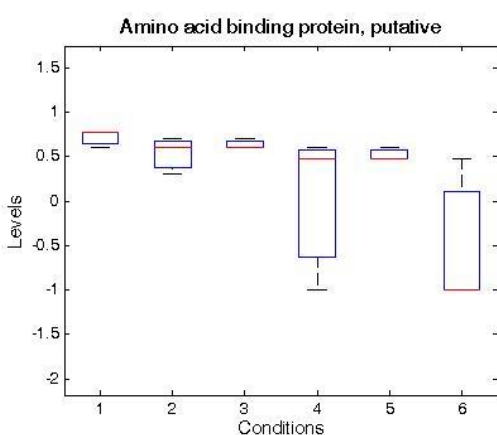
(a)



B9HZ70 *Aminomethyltransferase*

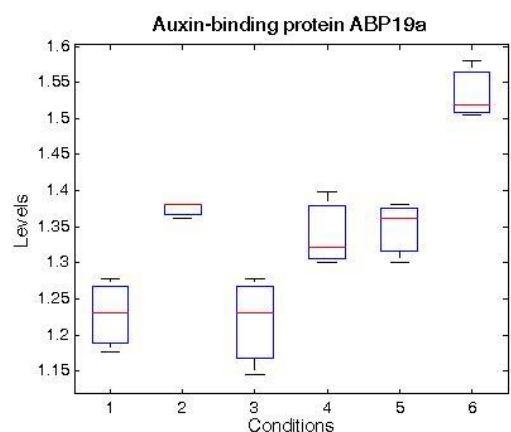
The *Aminomethyltransferase* is a component of the glycine decarboxylase complex.

(b)



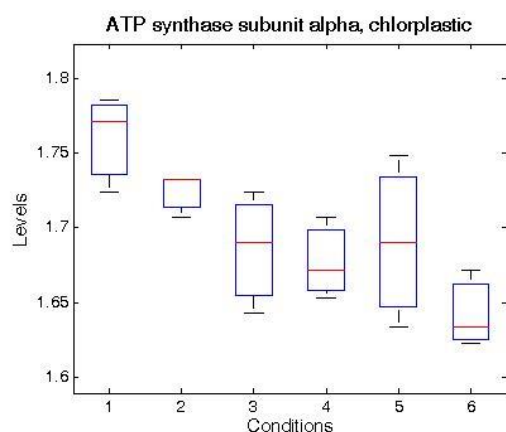
B9HVE6 predicted protein 79% similarity to B9SAK5 *Amino acid binding protein, putative* of *Ricinus communis*

(c)



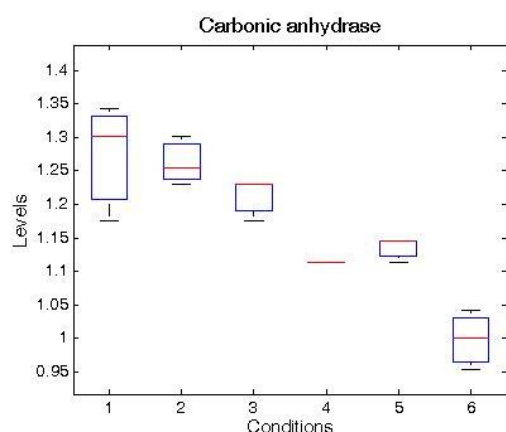
B9GW15 predicted protein 67% similar to Q9ZRA4 *Auxin-binding protein ABP19a* of *Prunus persica*

(d)



Q14FH2 *ATP synthase subunit alpha, chloroplastic*

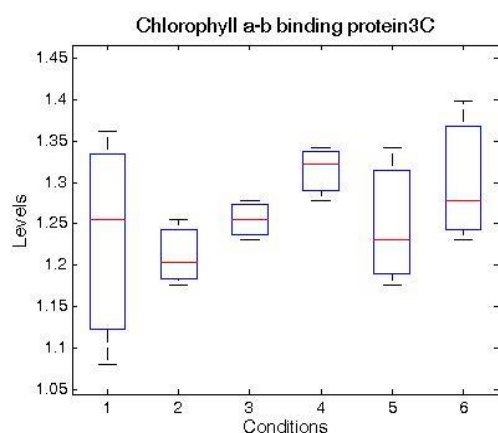
(e)



B9GHR1 *Carbonic anhydrase*

The carbonic anhydrase is an important factor in the photosynthesis.

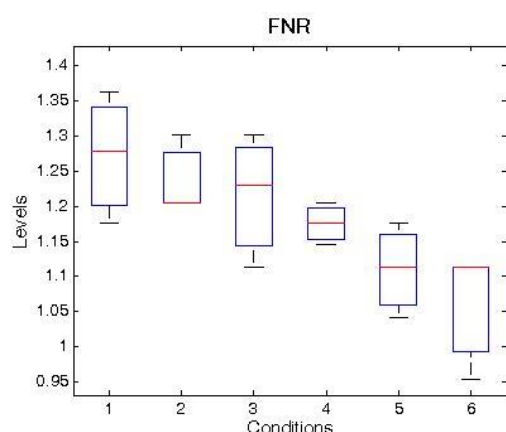
(f)



B9GSZ2 predicted protein 88% similartiy to P07369 *Chlorophyll a-b binding protein 3C, chloroplastic* of *Solanum lycopersicum*

They belong to the membrane proteins of plant cells. Connected to the other light harvesting-factors they are responsible for stomatal movement and further on to drought-stress in plants.

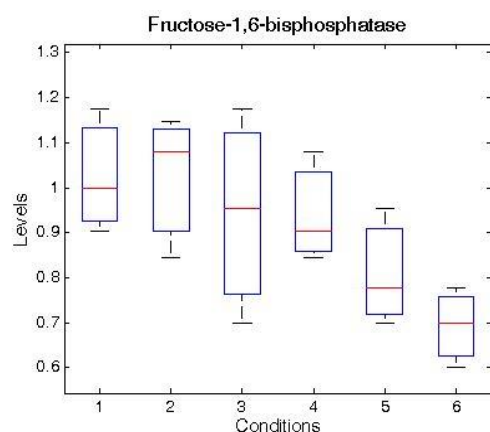
(g)



B9GZ04 predicted protein 87% similarity to P10933 *Ferredoxin--NADP reductase, leaf isozyme, chloroplastic of Pisum sativum*

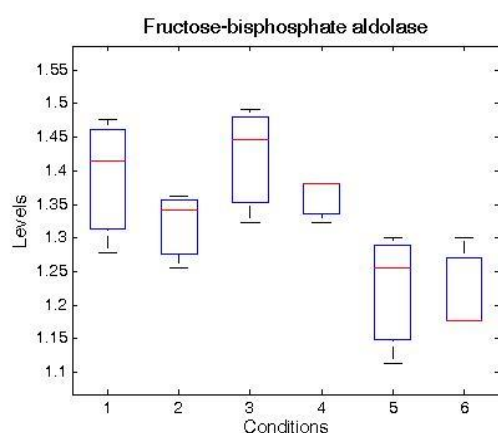
As a part of the photosynthesis it catalyze the reaction: 2 reduced ferredoxin + NADP^+ + H^+ \rightleftharpoons 2 oxidized ferredoxin + NADPH with an addition of iron-sulfur proteins as electron donors and NAD^+ or NADP^+ as electron acceptors.

(h)



A9PGB1 predicted protein 81% similarity to P46275 *Fructose-1,6-bisphosphatase, chloroplastic of Pisum sativum*

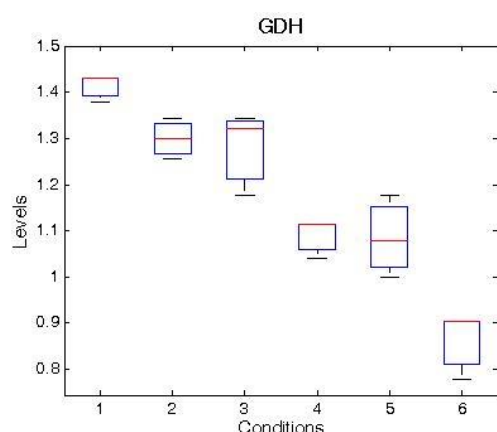
(i)



A9PGW0 *Fructose-bisphosphate aldolase*

This enzyme catalyze following substances: D-fructose 1,6-bisphosphate = glycerone phosphate + D-glyceraldehyde 3-phosphate.

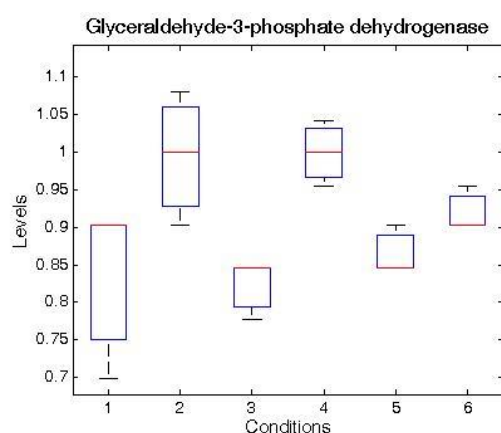
(j)



B9H1J0 predicted protein 89% similarity to Q9C9W5 *Glycerate dehydrogenase HPR, peroxisomal of Arabidopsis thaliana*

The glycerate dehydrogenase catalyze the reaction: D-glycerate + NAD⁺ \rightleftharpoons hydroxypyruvate + NADH + H⁺.

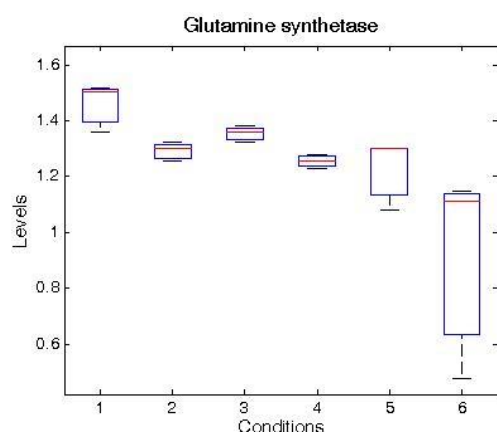
(k)



A9PG06 predicted protein 90% similarity to Q7FAH2 *Glyceraldehyde-3-phosphate dehydrogenase 2, cytosolic of Oryza sativa*

The Glyceraldehydes-3-phosphate dehydrogenase catalyzes the reaction Glyceraldehyde 3-phosphate to d-Glycerate-1.3-bisphosphate.

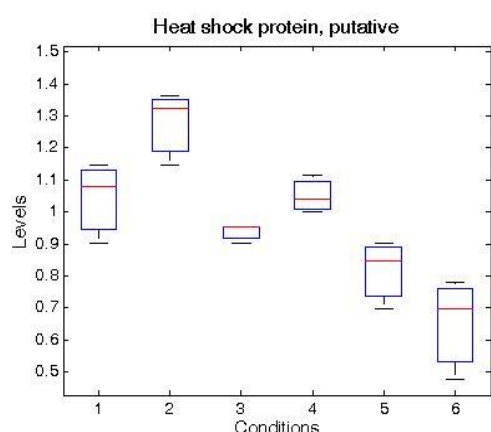
(l)



B9HY85 *Glutamine synthetase*

The function of GS lies as a major assimilatory enzyme for ammonia produced from N fixation and ammonia or nitrate nutrition. The GS also reassimilated ammonia which was released as a result of photorespiration (147).

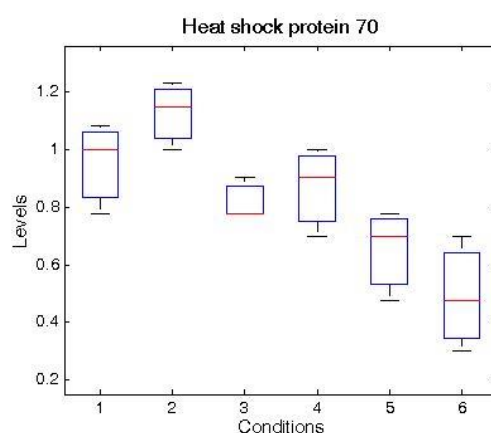
(m)



B9HMG8 predicted protein 96% similarity to B9HMG7 *Heat shock protein, putative of Ricinus communis*

These proteins are induced by heat shock. The expression of these proteins is increased when cells are exposed to high temperature or other stress situations.

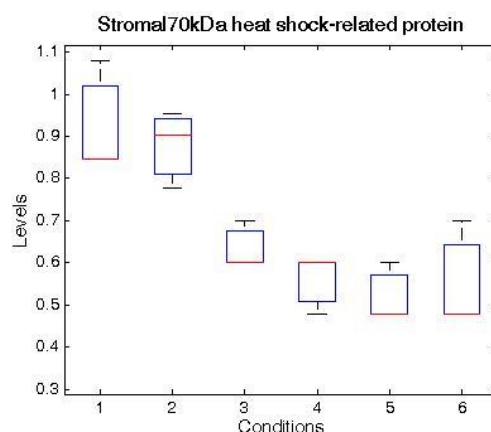
(n)



B9HMG2 predicted protein 97% similarity to D2D322 *Heat shock protein 70 of Gossypium hirsutum*

The Heat shock protein 70 is located in different cellular compartments. Their functions has a wide range like the prevention of protein aggregation and as well as the assistance in protein folding (199).

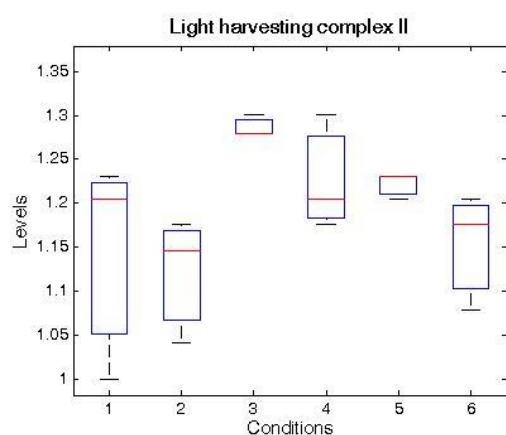
(o)



B9N758 predicted protein 88% similarity to Q02028 *Stromal 70 kDa heat shock-related protein, chloroplastic of Pisum sativum*

The molecular chaperones of the stromal Heat shock-related protein are involved in protein folding and protein transport processes as well as stress related conditions (117).

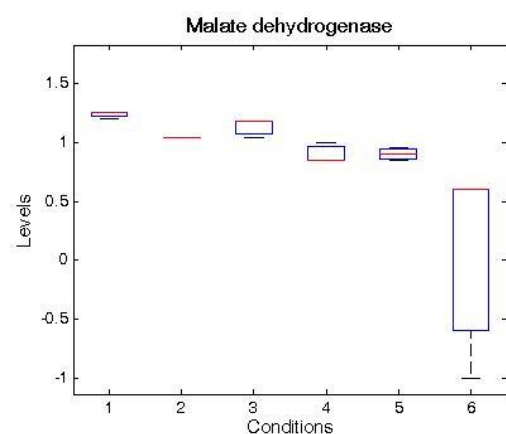
(p)



A9PGZ3 *Light-harvesting complex II protein Lhcb5*

This complex is a large part of the photosystem complex. It is surrounding the reaction center to funnel absorbed energy to the special energy transfer.

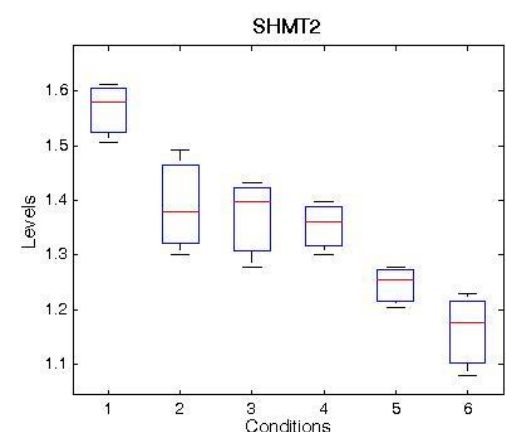
(q)



A9PGE6 *Malate dehydrogenase*

Malate has multiple functions in plant metabolism and homeostasis specially in the TCA-cycle (67).

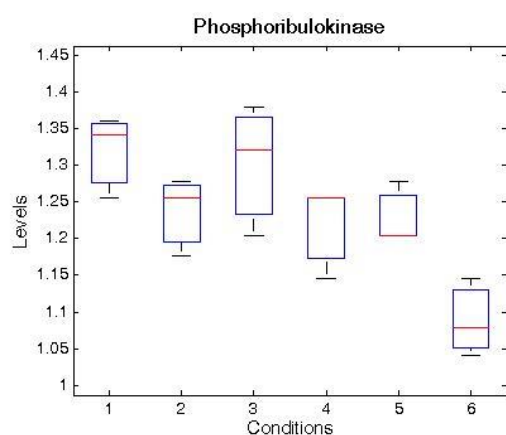
(r)



A9PL05 *Mitochondrial serine hydroxymethyltransferase*

The SHMT is an enzyme which is a main key in cellular one-carbon pathway. It is catalyzing the conversion of L-serine to glycine.

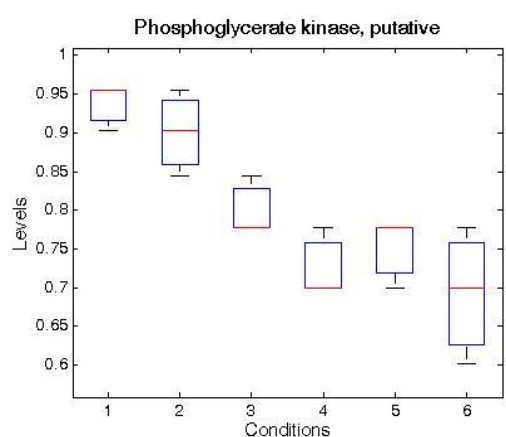
(s)



B9MUA4 *Phosphoribulokinase*

The Phosphoribulokinase is an important factor in the Calvin-cycle function.

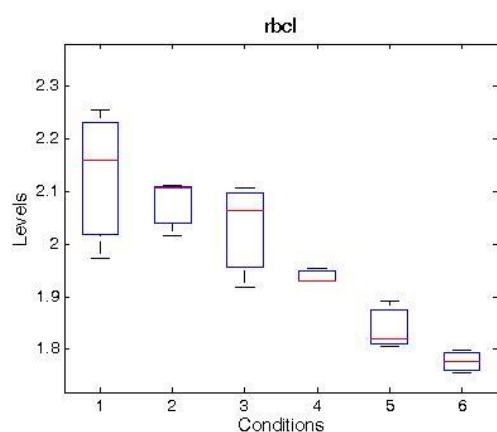
(t)



A9P828 putative uncharacterized protein 91% similarity to Q42962 *Phosphoglycerate kinase, cytosolic of Nicotiana tabacum*

This enzyme catalyze the reversible transfer of 1,3-bisphosphoglycerate to 3-phosphoglycerate.

(u)



D0QTN3 *Ribulose-1,5-bisphosphate carboxylase/oxygenase large subunit*

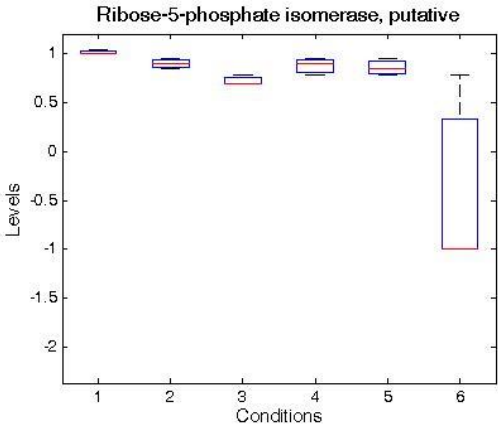
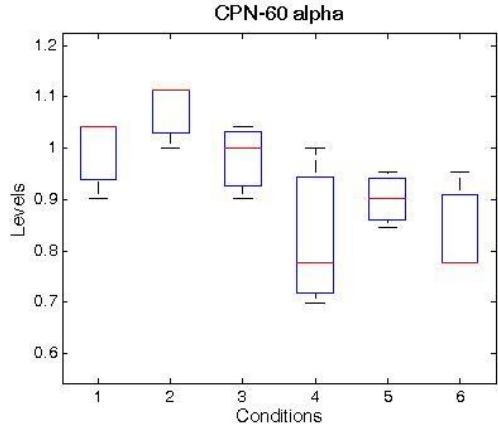
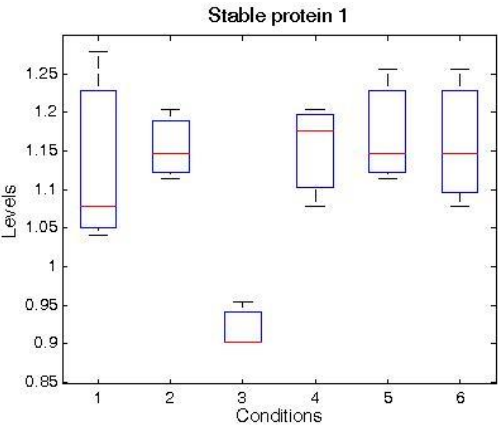
<p>(v)</p>  <p>Ribose-5-phosphate isomerase, putative</p>	<p>B9MZE9 predicted protein 83% similarity to B9REQ4 <i>Ribose-5-phosphate isomerase, putative</i> of <i>Ricinus communis</i></p> <p>Rpi is a enzyme of the Calvin-cycle and catalyzes the conversion between Ribose-5-phosphate and Ribulose-5-phosphate.</p>
<p>(w)</p>  <p>CPN-60 alpha</p>	<p>B9HQD5 predicted protein 87% similarity to P08926 <i>RuBisCo large subunit-binding protein subunit alpha</i> of <i>Pisum sativum</i></p>
<p>(x)</p>  <p>Stable protein 1</p>	<p>B9HX69 predicted protein 99% similarity to Q9AR79 <i>Stable protein 1</i> of <i>Populus tremula</i></p> <p>The stable protein 1 (SP1) is a stress related protein (43).</p>

Figure 96: Identified proteins in all poplar samples analyzed with Anova statistics. Conditions of the x-axis as followed: 1: 2N young, 2: 2N old, 3: 4N young, 4: 4N old, 5: 2N4N young, 6: 2N4N old. Y-axis shows the scale of the measured levels.

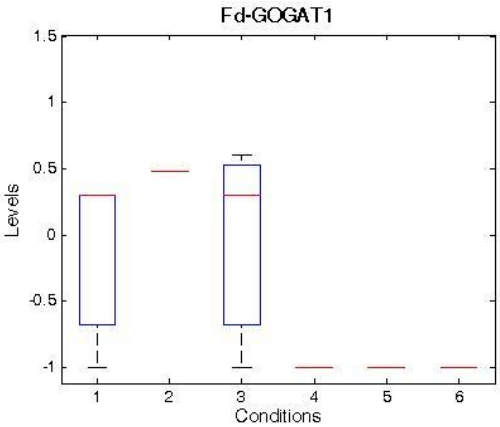
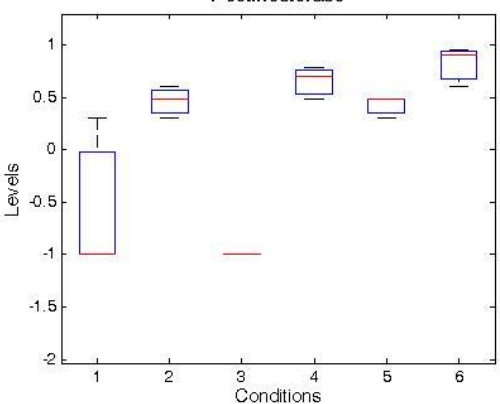
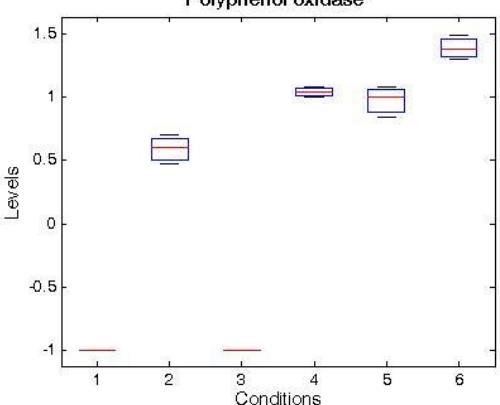
<p>(a)</p>  <p>Fd-GOGAT1</p>	<p>B9IHR5 predicted protein 86% similarity to Q9ZNZ7-2 <i>Isoform 2 of Ferredoxin-depquent glutamate synthase, chloroplastic/mitochondrial of Arabidopsis thaliana</i></p>
<p>(b)</p>  <p>Pectinesterase</p>	<p>B9GXZ <i>Pectinesterase</i></p> <p>The Pectinesterase is an enzyme which is responsible for the demethylation of galacturonyl that residues in high-molecular-weight pectin.</p>
<p>(c)</p>  <p>Polyphenol oxidase</p>	<p>F8V189 <i>Polyphenol oxidase</i></p> <p>The Polyphenol oxidase is assumed to be an antiherbivore enzyme (233).</p>

Figure 97: Identified proteins in different leaf samples analyzed with Anova statistics. Conditions of the x-axis as followed: 1: 2N young, 2: 2N old, 3: 4N young, 4: 4N old, 5: 2N4N young, 6: 2N4N old. Y-axis shows the scale of the measured levels.

3.7 SYNCHRONIZATION OF *CHLAMYDOMONAS REINHARDTII* CC 503 M⁺

When a circadian light/dark system is applied to *Chlamydomonas reinhardtii*, cell division takes place during the dark period and a release of daughter cells is phased round the dark/light change. Also a chloroplast division occurs successively, and zoospores are liberated at the end of the dark period (54).

In this experiment *Chlamydomonas reinhardtii* cells were synchronized over a 24 h cycle and examined every 3rd hour with the light microscope. While light phase, shown in figure 98, which is 5 hours of light, the cells show the typical morphology for the algae *Chlamydomonas reinhardtii* CC 503 m⁺. The cells are different in size but the pyrenoid (py), the nucleus (nu) and the chloroplast (cl) were very good visible. In (b) there can be seen two single cells hanging together with their flagella (fl). These flagellae are going to be lost during mitosis and rebuilt after dark phase. Over a period of 12 h a homogenous course could be obtained. In image (c) the beginning of the mitoses can already be observed even it was already the 8th of the dark phase. Outmost perfect visible are the two daughter cells (dc) surrounded by the cell wall (mc) of the mother cell. In one cycle about 4 to 16 daughter cells can be developed which results from 2 - 4 cleavages. Even 11 h after starting the dark phase (d), mitosis of some *Chlamydomonas reinhardtii* cells can be seen. It is possible that there are more 3 or more daughter cells which cannot be completely investigated.

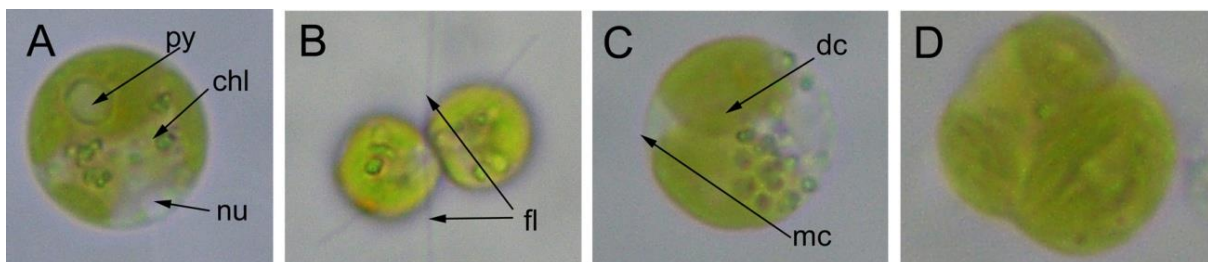


Figure 98: Synchronization of *Chlamydomonas reinhardtii*. (A) Image taken after 5 h of exposure to light. (B) Image taken after 5 h of exposure to light. (C) Image taken 8 h after dark period, already starting of mitosis. (D) Image taken 11 h after dark period, end of dark phase still mitosis visible.

3.7.1 LIPID EXPERIMENTS OF *CHLAMYDOMONAS REINHARDTII*

In figure 99 Aa-Ff *Chlamydomonas reinhardtii* has been treated for 6 days and more in different liquid media including/excluding nitrogen and acetate. Image (A) was taken with light microscopy compared to (a) with fluorescence microscopy. Both were sampled 2 days after a treatment of a medium including nitrogen and acetate. The lipid bodies can already be distinguished. Four days after growing in this liquid medium the lipid bodies kept on growing and are better visible. After 6 days of treatment the lipid bodies are not visible anymore.

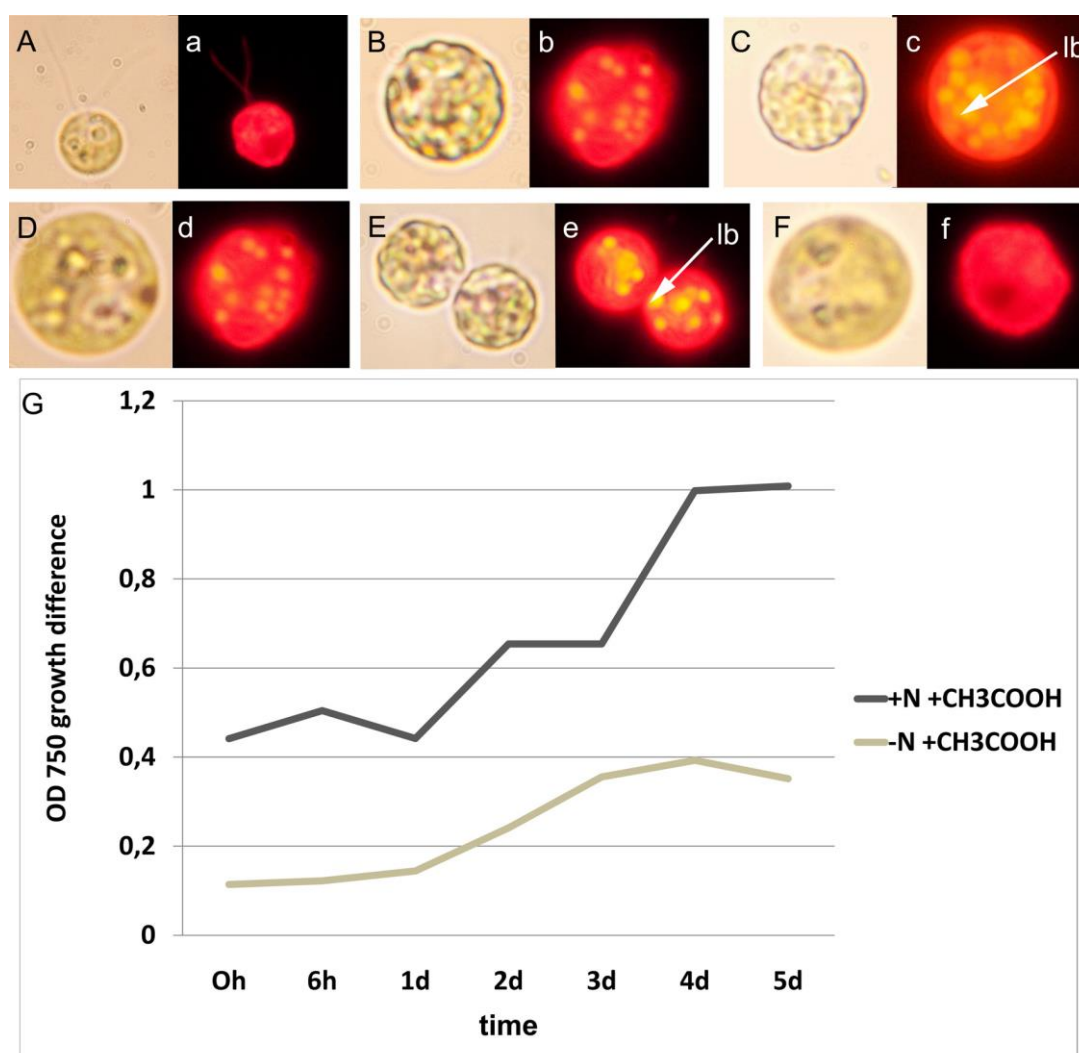


Figure 99: *Chlamydomonas reinhardtii* CC503. (A) 2 days growing in liquid medium +N +acetate taken with light microscope (a) 2 days of growing in liquid medium +N +acetate taken with fluorescence microscope. (B) 4 days of growing in liquid medium +N +acetate taken with light microscope (b) 4 days of growing in liquid medium +N +acetate taken with fluorescence microscope. (C) 6 days of growing in +N +acetate taken with light microscope (lp) lipid bodies (c) 6 days of growing in +N +acetate taken with fluorescence microscope. (D) 2 days of growing on liquid medium -N +acetate taken with light microscope (d) 2 days growing in liquid medium -N +acetate taken with fluorescence microscope. (E) 4 days growing in liquid medium -N +acetate taken with light microscope (e) 4 days growing in liquid medium -N +acetate taken with fluorescence microscope (lp) lipid bodies. (F) 6 days growing in liquid medium -N +acetate taken with light microscope (f) 6 days growing in liquid medium -N +acetate taken with fluorescence microscope. (G) Growth curve of *C. reinhardtii* with data from the previous experiment.

Figure 100 shows complete opposite results. *Chlamydomonas reinhardtii* was grown on nitrogen free medium and/or including nitrogen and excluding acetate. A nitrogen starvation leads to the development of lipid drops in *C. reinhardtii*. Two days after growing in this medium no lipid bodies are visible. After four days (A) of treatment lipid bodies occurred, better visible in the fluorescence image (B). After six days of nitrogen starvation (B) the amount of lipid bodies increased. Samples for this growth curve (C) was taken for a period over 5 days and measured with an OD of 750 nm. It shows that both experimental setups have a similar growth curve in the first 2 days. *C. reinhardtii* growing on nitrogen free medium start dying after 3 days while the setup including nitrogen was still growing until day 3 to 4 and then had a continuous phase of dying off.

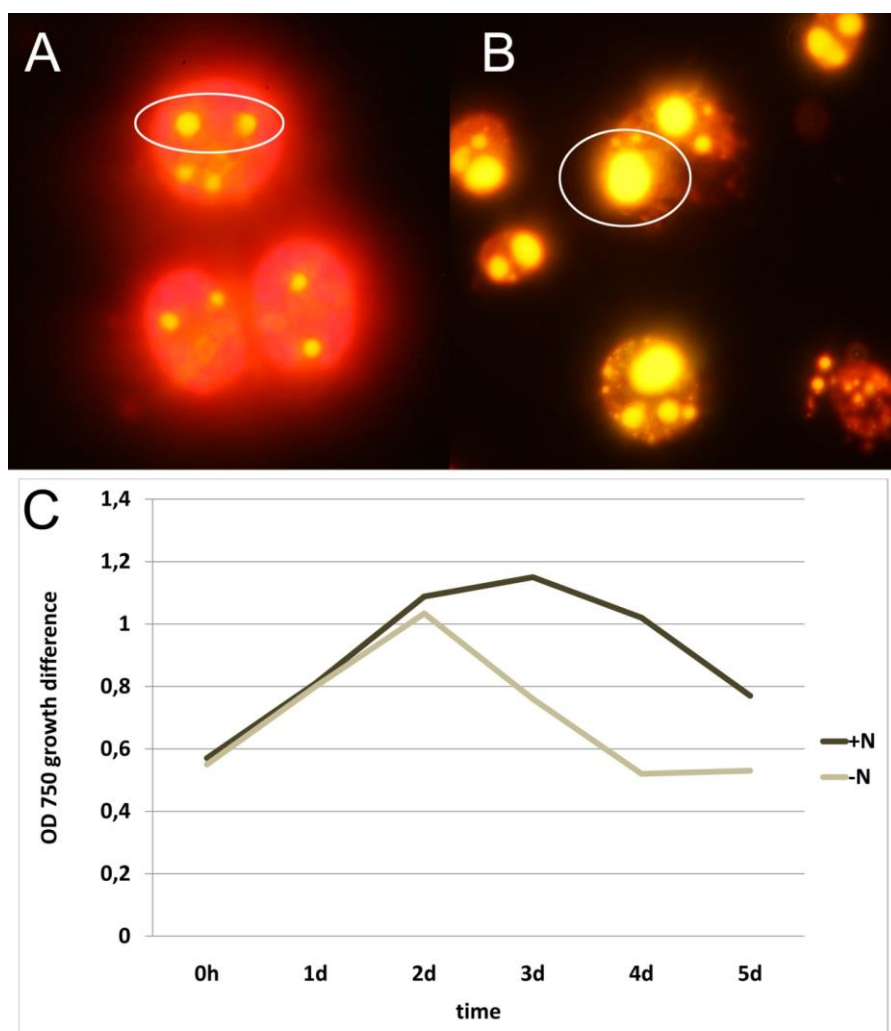


Figure 100: (A) *Chlamydomonas reinhardtii* 4 weeks after growth in liquid media with nitrogen lipid bodies (white circles). (B) *C. reinhardtii* 4 weeks after growth in liquid media with nitrogen and without nitrogen, lipid bodies (white circles). (C) Growth curve of *C. reinhardtii* grown under nitrogen starvation (grey) and including nitrogen (black).

3.8 *MEDICAGO TRUNCATULA* 'JEMALONG A17'

Productivity and growth of plants are greatly affected by drought and salinity (125). In Legumes, nitrogen availability seems to play a crucial role during abiotic stress response. A reduction in the rates of nitrogen can be caused by drought (75). *Medicago truncatula* with root nodulation features additional anatomical differences in contrast to nitrogen assimilating plants.

3.8.1 MORPHOLOGY AND STOMATA IMPRINT

Comparison between nitrogen fixing and assimilating plants show differences in phenotype such as in leaf size and color.

After exposure to high salt concentrations (50 mM), nitrogen assimilating plants show inhibition in growth. Surprisingly, first experiments show that in contrast to nitrogen assimilating plants, nodulated plants show faster growth rates after salt treatment. Figure 101 (a) shows 1 day salt treated *Medicago truncatula*, (b) day 1 of rewatering and (c) the 3rd day of rewatered nitrogen fixing plants. In (d) nitrogen assimilating plants at the first day of salt-stress are shown. In image (e) and (f) the first and the 3rd day of rewatering of *M. truncatula* are shown. Differences in growth and regeneration of the plants are clearly visible between the nitrogen fixing and the nitrogen assimilating plants. Another interesting difference could be observed in leaf color. Explants inoculated with *Sinorhizobium meliloti* show a darker leaf color while non-inoculated explants of *Medicago truncatula* stay nearly the same.

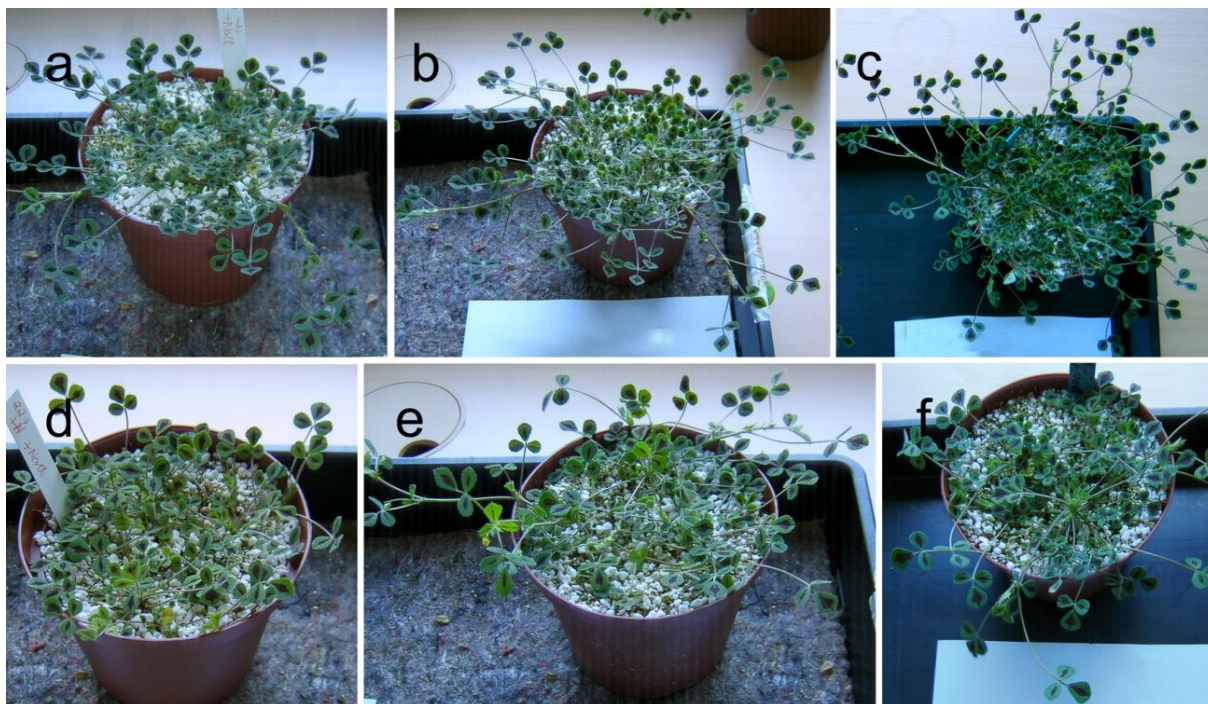


Figure 101: *Medicago truncatula* under salt-stress. (a) First day of salt-stress of nitrogen fixing *M. truncatula*. (b) First day of rewatering of nitrogen fixing *M. truncatula*. (c) Third day of rewatering of nitrogen fixing *M. truncatula*. (d) First day of salt-stress nitrogen assimilating *M. truncatula*. (e) First day of rewatering of nitrogen assimilating *M. truncatula*. (f) Third day of rewatering of nitrogen assimilating *M. truncatula*.

Figure 102 shows the same experimental setup like in figure 101 with the change of salt-stress instead of drought-stress. Figure 102 A-C shows the control plant of nitrogen assimilating *Medicago truncatula*. Nitrogen assimilating plants show a closure of the leaves while being under drought-stress. Three days after rewatering of these plants this closure cannot be observed anymore. The nitrogen fixing plants do not show this closure of the leaves while drought-stress compared to the nitrogen assimilating explants (Fig. 102 J-L). Another difference between nodulated and non-nodulated plants could be investigated in leaf color. *Medicago truncatula* inoculated with *Sinorhizobium meliloti* did not show any differences in color while those which were not inoculated started to get a light green color and the anthocyanin square got smaller.

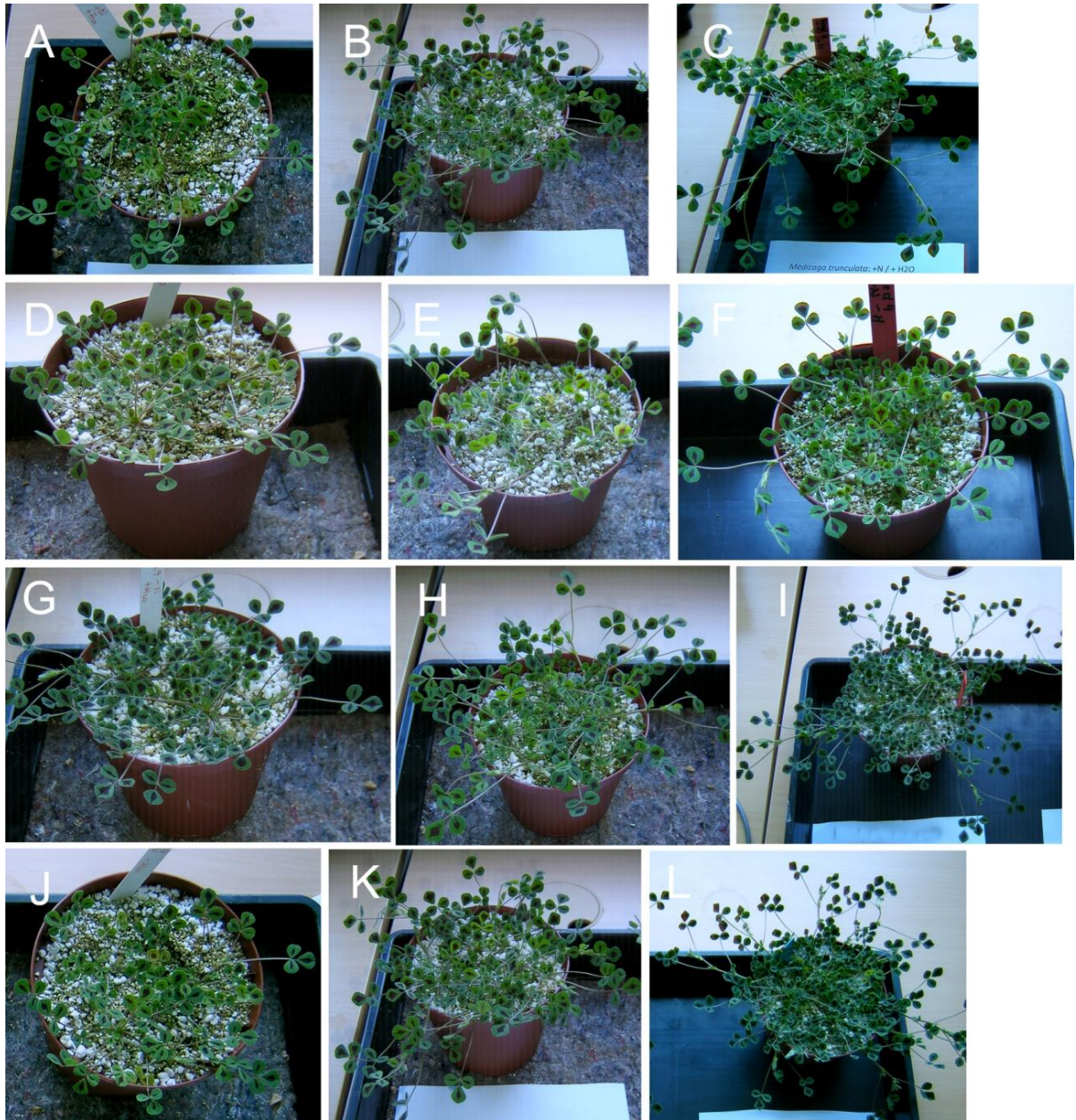


Figure 102: *Medicago truncatula* under drought-stress. (A) Control of first day of drought-stress of nitrogen assimilating *M. truncatula*. (B) Control 1 day of rewatering of nitrogen assimilating. (C) Control of nitrogen assimilating *M. truncatula* 2 days after rewatering. (D) 1 day of drought-stress of nitrogen assimilation. (E) 1 day of rewatering of nitrogen assimilating *M. truncatula*. (F) Second day of rewatering of nitrogen assimilating *M. truncatula*. (G) Control first day of drought-stress of nitrogen fixing *Medicago truncatula*. (H) First day of rewatering control of nitrogen fixing *M. truncatula*. (I) Control second day of rewatering of nitrogen fixing. (J) First day of drought-stress of nitrogen fixing *M. truncatula*. (K) First day of rewatering of nitrogen fixing *M. truncatula*. (L) Second day rewatering of nitrogen fixing *Medicago truncatula*.

For counting the amount of stomata cells and epidermic cells an imprint of the leaves was prepared which can be seen in figure 103 (A) and (B). *Medicago truncatula* has amphistomatic leaves with an anomocytic position of the guard cells surrounding the stomata cells. Image (A) shows the upper leaf epidermis of a stomata imprint of nitrogen fixing *M. truncatula* leaf compared to image (B) that pictures the lower epidermis. Interestingly shows image (D), which is the lower epidermis of nitrogen assimilating *M. truncatula* leaf, the typically morphology of epidermic structure of lower epidermic cells compared to the nitrogen fixing leaf. Another interesting aspect is the number of stomata in the leaves of *Medicago truncatula* exposed to drought-stress which can be distinguished in figure 104.

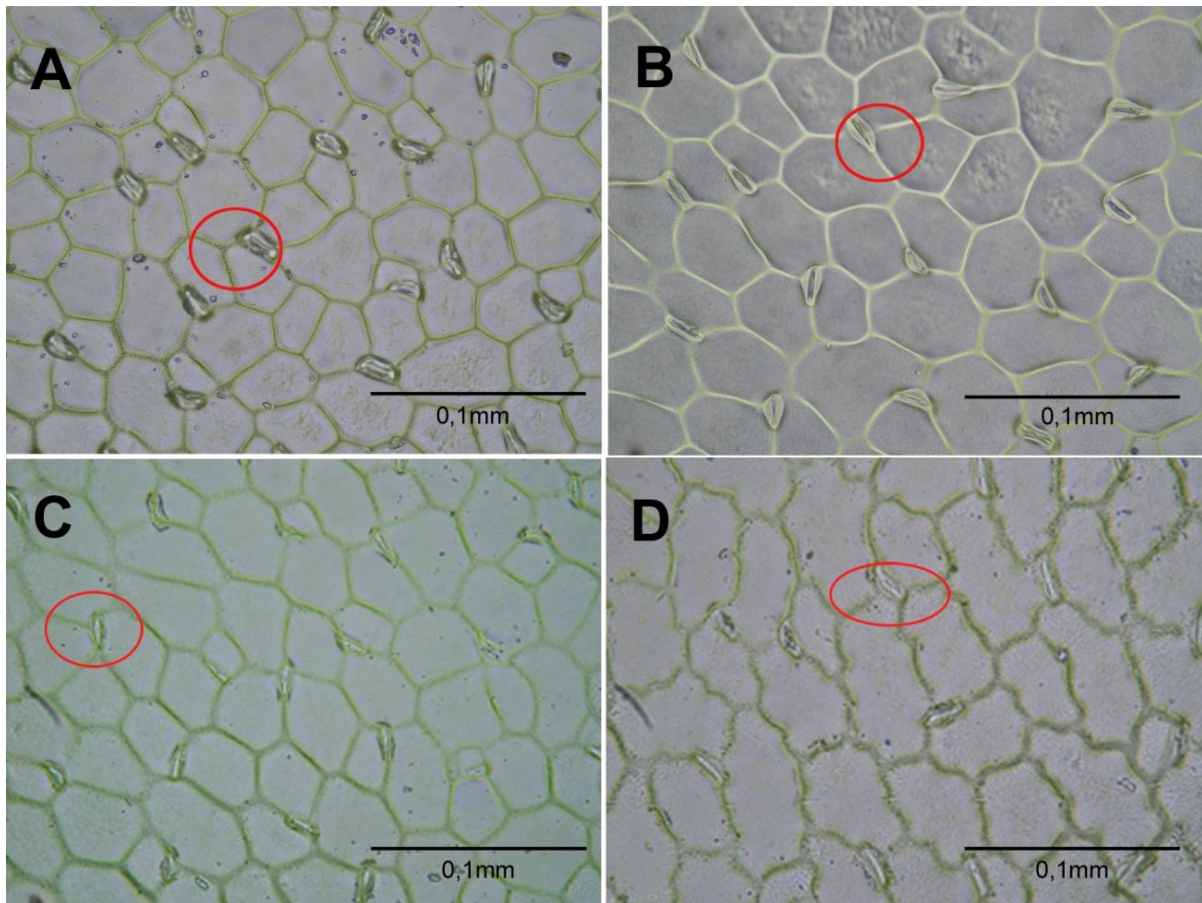


Figure 103: Stomata imprint of *Medicago truncatula*. (A) Nitrogen fixing *M. truncatula*, upper leaf epidermis, stomata (red rectangle). (B) Nitrogen fixing *M. truncatula*, lower leaf epidermis, stomata (red rectangle). (C) Nitrogen assimilating *M. truncatula*, upper leaf epidermis, stomata (red rectangle). (D) Nitrogen assimilating *M. truncatula*, lower leaf epidermis, stomata (red rectangle).

Nitrogen assimilating plants show a higher number of stomata in the upper (max. 900) and lower (max. 750) leaf epidermis (Fig. 104 a/b) which in general causes higher transpiration rates and therefore a faster wilt of assimilating organs during drought-stress.

The maximum of the amount of stomata in nitrogen fixing plants is about 650 stomata in the upper leaf epidermis and 600 stomata in the lower epidermis. The amount of epidermic cells in the upper leaf side (c) is max. 3500 cells in non-nodulated plants and max. 2500 cells in nodulated plants. The lower leaf side shows completely different results, shown in (d). Here the difference is not that high, both experimental setups reach the maximum at about 3000 cells.

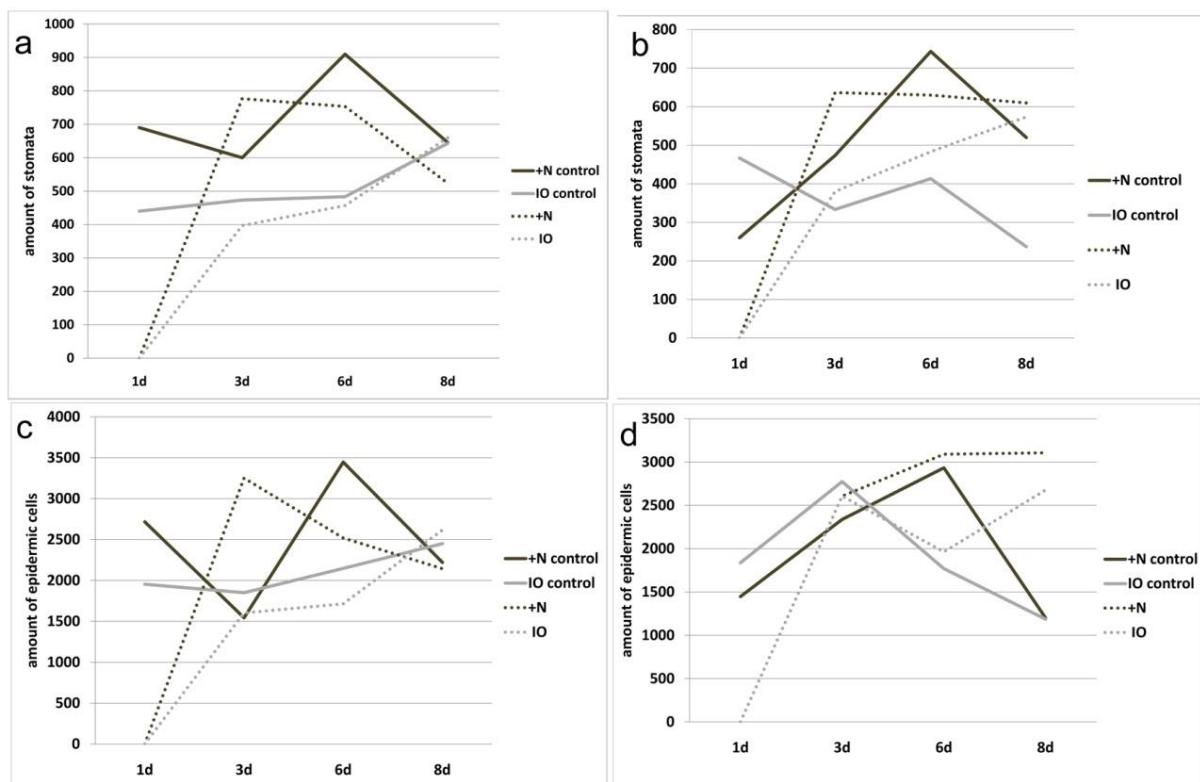


Figure 104: (a) Amount of stomata on the upper leaf side. (b) Amount of stomata on the lower leaf side. (c) Amount of epidermic cells on the upper leaf side. (d) Amount of epidermic cells on the lower leaf side.

3.8.2 ANATOMIC ANALYSES OF VEGETATIVE ORGANS OF *MEDICAGO TRUNCATULA*

The leaves of the control plants show in their spongy parenchyma (sp) a lot of intercellular spaces (isp) in contrast to the plants which were exposed to drought- and salt-stress (Fig. 105 A, B). A different development of the palisade parenchyma (pp) cannot be distinguished. No difference concerning the volume of the lower and upper epidermis cells can be investigated at this time (ue, le). As already mentioned stomata cells (st) can be seen in the upper and the lower epidermis of the leaves.

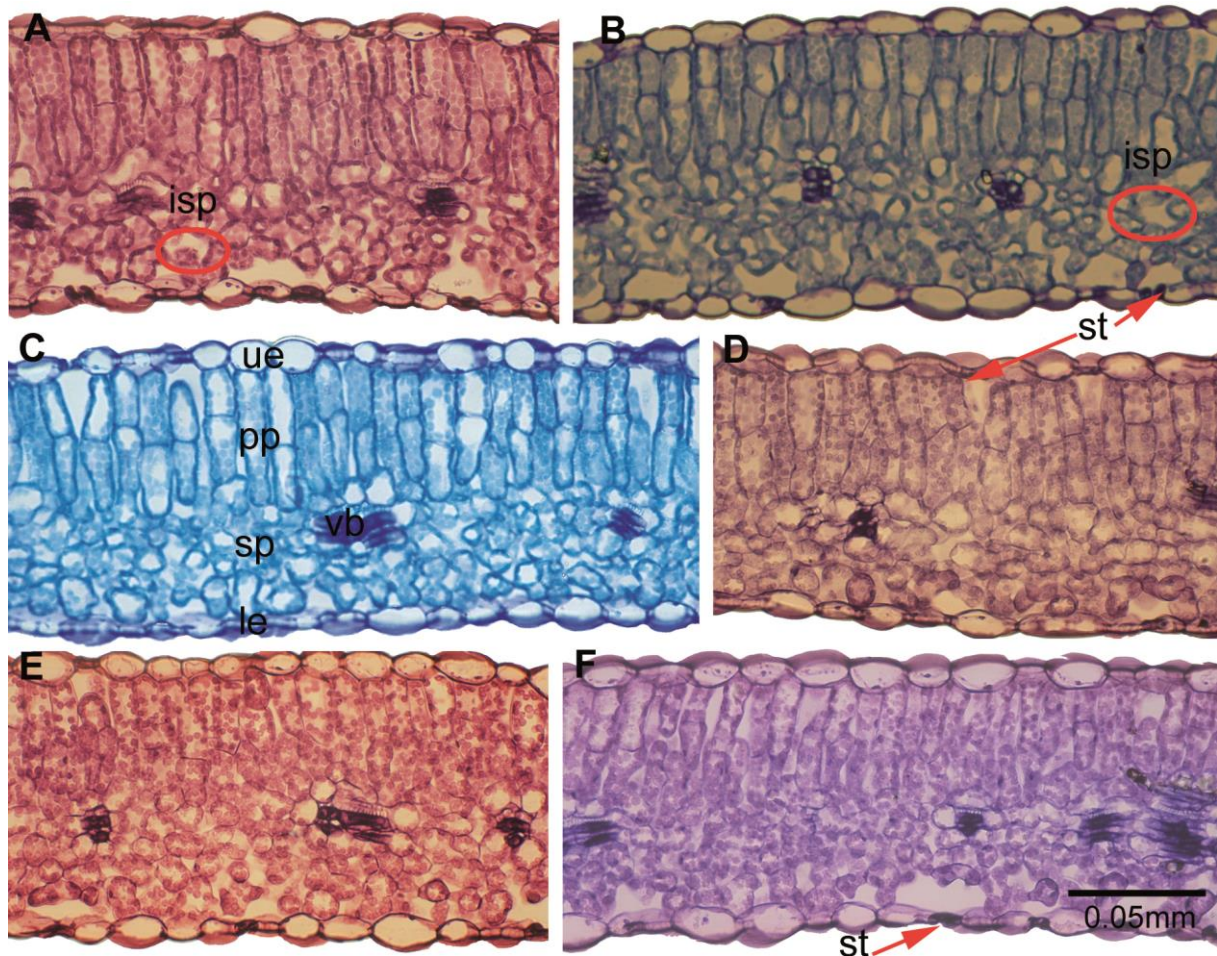


Figure 105: Leaf square sections of *Medicago truncatula*. (A) Control of nitrogen fixing, isp intercellular space. (B) Control of nitrogen assimilating, st stomata. (C) Salt-stress nitrogen assimilating, ue upper epidermis, pp palisade parenchyma, sp spongy parenchyma, le lower epidermis, vb vascular bundle. (D) Salt-stress nitrogen fixing. (E) Drought-stress nitrogen assimilating. (F) Drought-stress nitrogen fixing.

Sections of the stem show that the lignification rate in the xylematic tissue was much faster in the nitrogen fixing than in nitrogen assimilating plants. Figure 106 (A) shows a square section of the control from nitrogen assimilating plant and (B) a section of a nitrogen fixing *Medicago truncatula*. In image (C) an inoculated explant under salt-stress is shown in contrast to the non-inoculated ones shown in (D). No differences between the inoculated and the non-inoculated explants during salt-stress can be observed. The difference between the explants of nitrogen fixing and nitrogen assimilating *Medicago truncatula* under drought-stress is shown in (E) and (F). In both experimental setups the parenchymatic cells decrease in cell size.

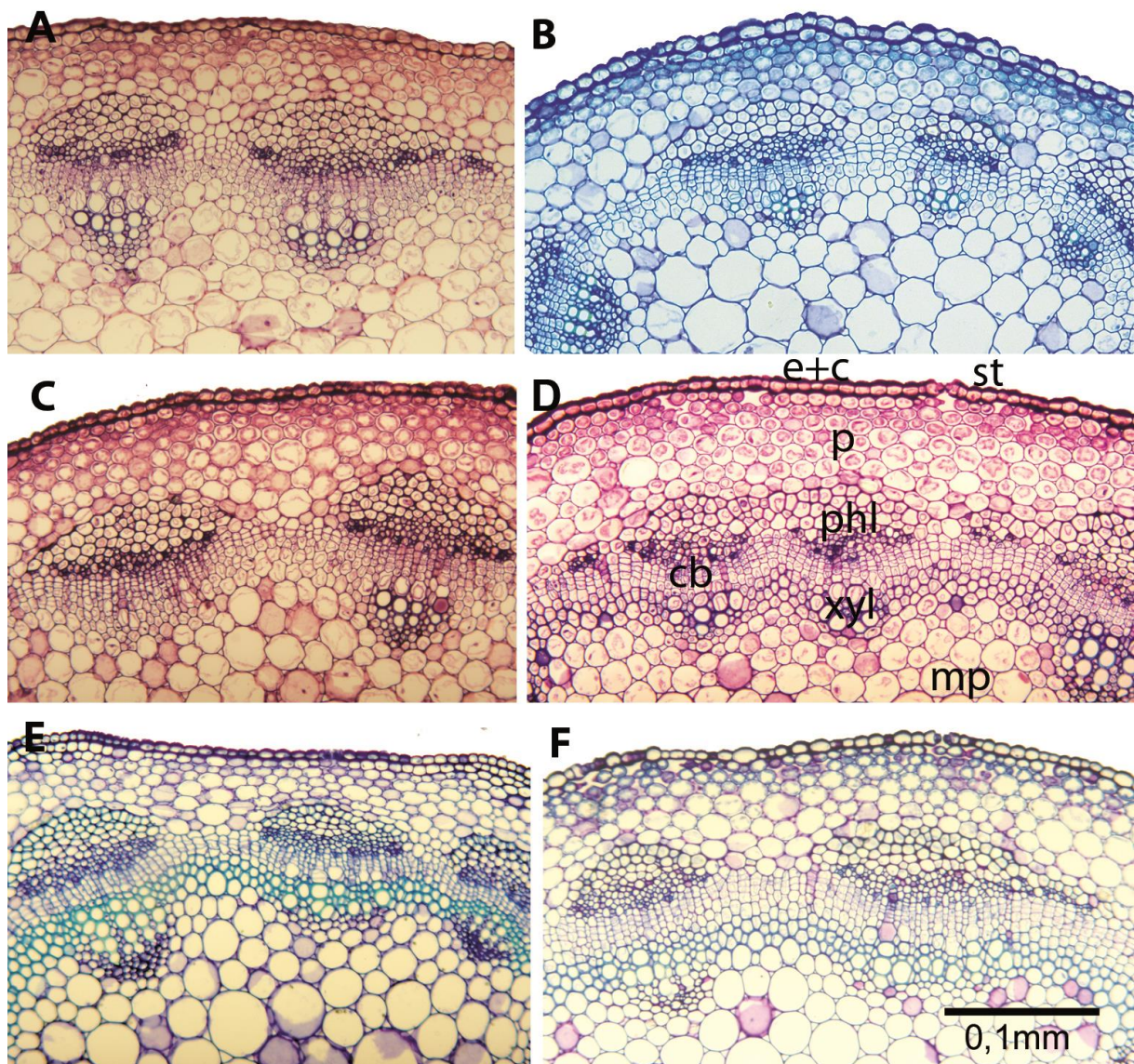


Figure 106: Stem square sections of *Medicago truncatula*. (D) Control of nitrogen assimilating *M. truncatula*. (B) Control nitrogen fixing. (C) Salt-stress nitrogen assimilating. (D) Salt-stress nitrogen fixing, e + c epidermis and cuticula, st stomata, p parenchyma of the cortex, phl phloematic tissue, cb cambium, xyl xylematic tissue, mp marc parenchyma. (E) Drought-stress nitrogen assimilating. (F) Drought-stress nitrogen fixing.

In figure 107 A-F square sections of the secondary root of *Medicago truncatula* are shown. No anatomic differences can be investigated in plants grown under salt- or drought-stress. Image (A) shows a square section of the root of the control nitrogen assimilating *Medicago truncatula* compared to image (B) which is the control of the nitrogen fixing plant. It shows the root epidermis (rh) the subjacent cortex consisting of parenchymatic cells (p). The vascular system is composed of the phloem (phl), the meristematic zone (cb) and the xylem (xyl). (C) and (D) show the secondary root of nodulated (D) and non-nodulated (C) *Medicago truncatula* under stress where no anatomical differences can be investigated. The images (E) and (F) show square sections of drought-stressed explants of nitrogen fixing (F) and nitrogen assimilating (E) plants.

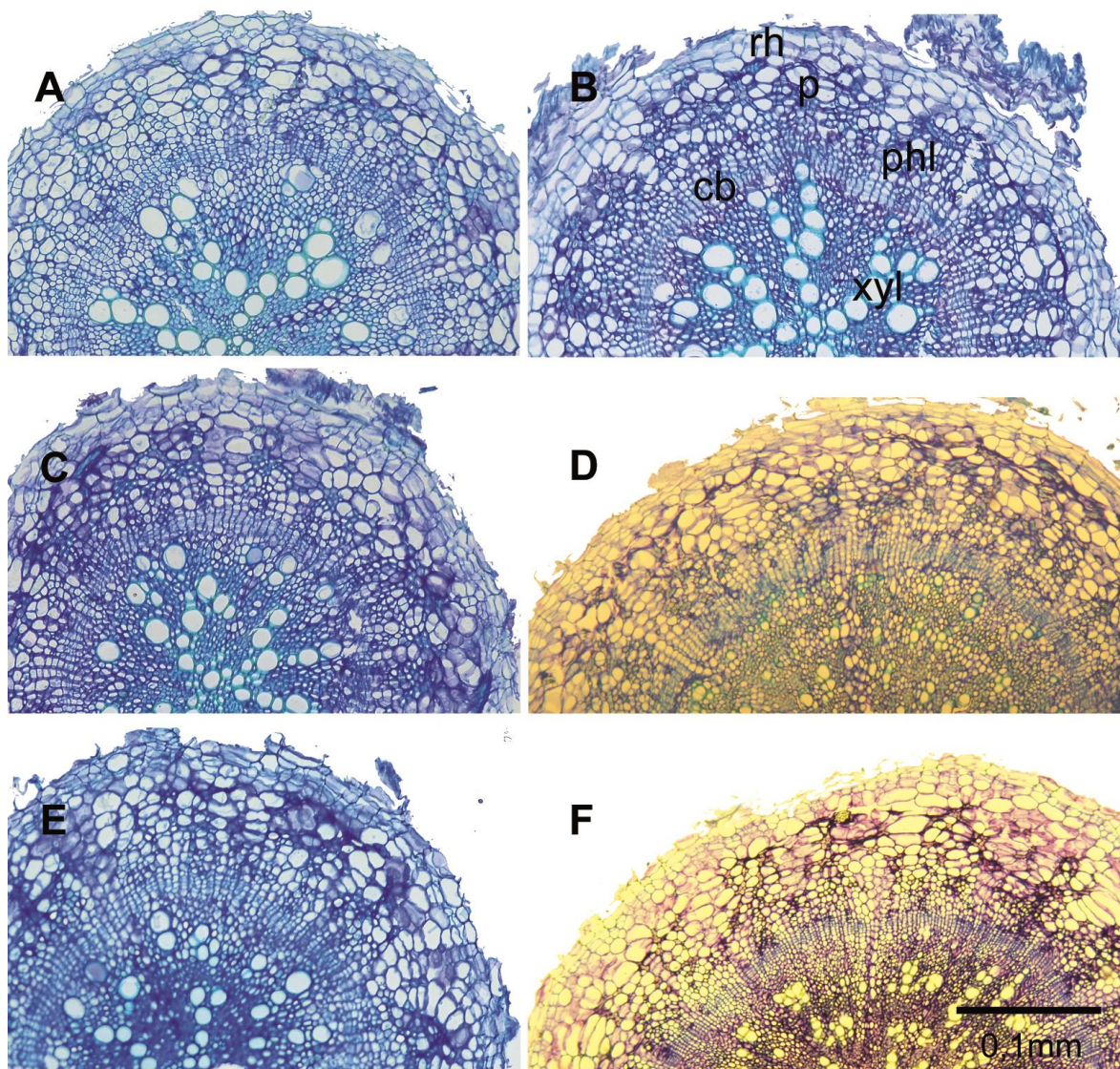


Figure 107: Root square section of *Medicago truncatula*. (A) Control of nitrogen assimilating. (B) Control of nitrogen fixing plant, rh root epidermis, p parenchyma, phl phloematic tissue, cb cambium, xyl xylematic tissue. (C) Salt-stress nitrogen assimilating. (D) Salt-stress nitrogen fixing. (E) Nitrogen assimilating drought-stress. (F) Nitrogen fixing drought-stress.

In figure 108 (A) a square section of the root nodule of *Medicago truncatula* grown under normal conditions without any stress influences is shown. Added to image (A) in image (B) a 100 fold magnification with bacteria residing the cells can be seen (red circle). In image (C) a nodule exposed to salt-stress over 6 days with a significant cell shrinking (F) compared to the control (A) is shown. No difference in size and in amount of nodules between drought- and salt-stressed plants could be distinguished.

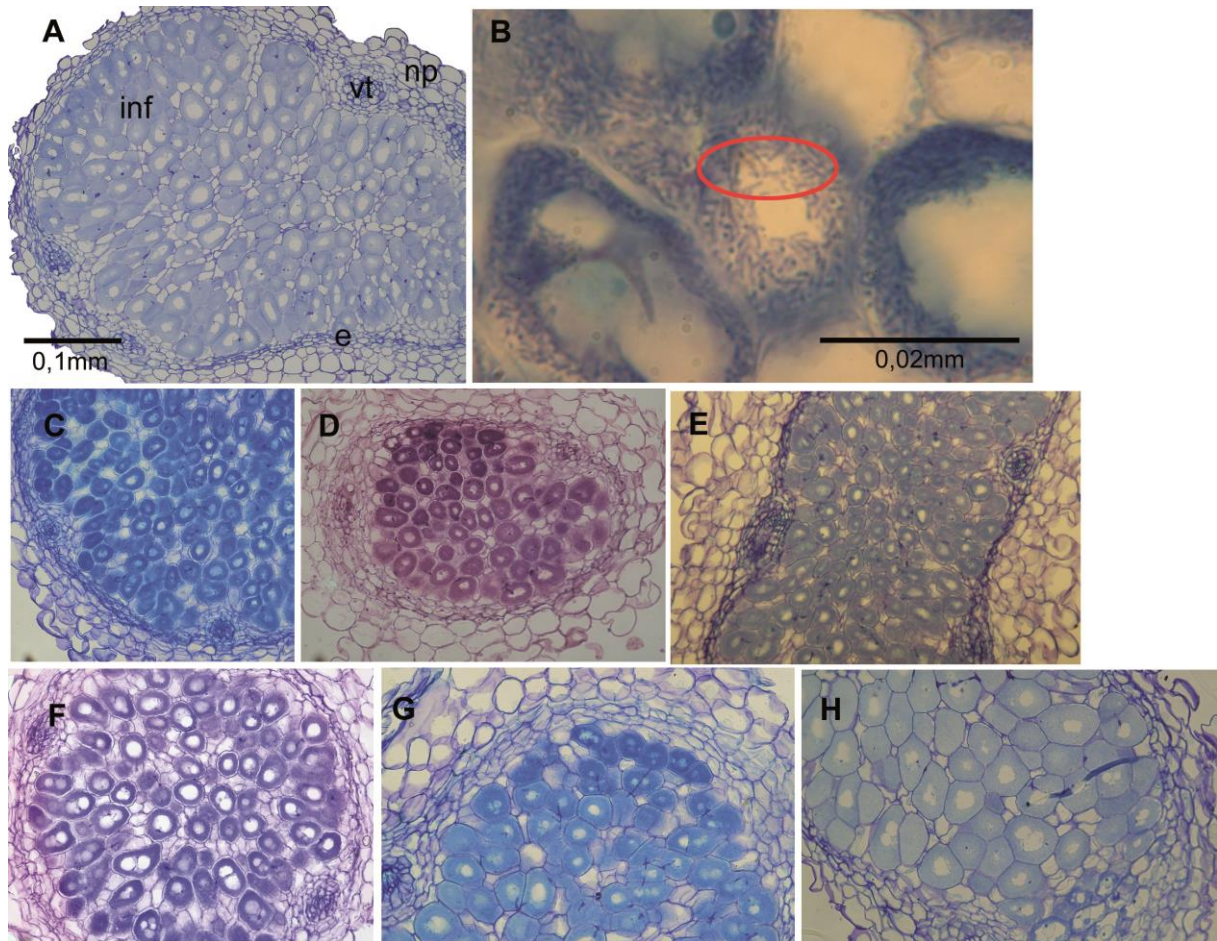


Figure 108: Nodule square section of *Medicago truncatula*. (A) Control, np nodule parenchyma, vt vascular tissue, e endodermis, inf infected tissue. (B) Single cells of the nodule with bacteria inside (red circle). (D) Nodule in salt-stress. (D) Salt-stress rewatering day 2. (E) Salt-stress rewatering day 4. (F) Nodule in drought stress. (G) Drought-stress rewatering day 2. (H) Drought-stress rewatering day 5.

4 DISCUSSION

4.1 COMPARISON OF *PAENIBACILLUS* SP. P22 AND *PAENIBACILLUS*

DURUS

In the growth experiments of these two different *Paenibacillus* strains both media contained nitrogen, thus inhibiting nitrogen fixation processes. The only limiting factors were glucose and sodium-chloride. Since *Paenibacillus* sp. P22 uses glucose as energy supply, the bacteria in the glucose limited medium started to grow later, than those cultivated in the medium with no limitation. Conversely, *Paenibacillus durus* did not show this difference in growth indicating not identified differences in heterotrophic growth between these two strains. Differences in the color of the liquid media between *Paenibacillus* sp. P22 and *Paenibacillus durus* were assumed to be caused by acid production due to sugar digestion. However, pH testing could not confirm this theory. In the first stage of growth sugar is used until no more glucose is available. After this stage lactose is utilized for further bacterial growth. If no glucose and other nutrients are left in the medium the bacteria will die. Sung et al. state that it is possible that cells within a culture of *Bacillus subtilis* differentiate, with respect to the development of sporulation. Hence different colors and amounts of cells within a culture can be a response of the bacteria's regulatory networks involved in the control of a variety of functions and processes (214).

The storage stock solution including 25% glycerol showed an earlier growth (1 day) of *Paenibacillus* sp. P22 than the 50% glycerol stock solution 30 days after freezing. No severe cause could be determined.

Another test of *Paenibacillus* sp. P22 growth ability was the transfer of P22 from a nitrogen free medium to a medium with normal nitrogen levels compared to the starting medium. The difference in growth could be seen in the optical density of bacteria in liquid medium which was much lower for those grown on a nitrogen free medium beforehand than for those grown on a nitrogen medium.

4.2 BIOMASS OF AF2, AF8 AND MONVISO

Soilless is a method used for plant cultivation in nutrient solutions with or without the use of an organic medium (102). Hydroponics are used in many fields of plant biology research such as screening for abiotic stress, root function, root anatomy and many others (104).

All hydroponic plants exhibited yellow-colored leaves after a couple of weeks, which indicates a nutrient deficiency. This nutrient deficiency could be caused by two important factors. On the one hand it is possible that the limited space in the 500 ml beakers and on the other hand the absence of continuous aeration of the solution. This is causing a decreased uptake of nutrients. Even though the water was changed every 3rd day the hydroponic developed roots were not able to provide the plant with enough nutrients. In order to minimize the damage to the plant, the concentration of the Hoagland solution was decreased from ½- to a ¾-strength solution. A full concentrated Hoagland solution would have „branded“ the leaves, because the concentration of Mg, N, and Ca would have been too high. Another possible reason for a limited nutrient uptake is the anatomical structure of hydroponic grown roots. Altogether the best hydroponic growth was found in clone AF8 which has already been announced by the Alasia Institute.

As already mentioned in the results of the soil experiment with the inoculated plants, 8 weeks after the start of the experiment, signs of a fungi infection were observed in AF8 and Monviso. Microscopic analyses showed that it might have been the fungi *Venturia populina* which is a typical infection for the species *Populus* (160). All significances differed a lot within the same group which was most likely due to the minimal amount of replicates.

The experimental setup with the direct inoculation of the fresh planted shoot cuttings did not show any good growth. This might be due to the fact that the shoot cuttings were not vital anymore and could not take up the endophytic solution, even when the cuttings have been placed in this solution for three days. Another option is given by the endophytic solution itself which could have been too high concentrated.

The minimal growth of AF8, AF2 and Monviso *in-vitro*, growing on a full-strength L&S-medium, can be explained by the plant hormones of the field grown plants which do not tolerate the simulated conditions that are used in *in-vitro* trials.

4.3 LOCALIZATION OF *PAENIBACILLUS* SP. P22 IN *IN-VITRO* GROWN

POPLAR HYBRID 741

The challenge in investigating the allocation of bacteria in the plant xylem is due to the turgor pressure that flushes the bacteria out when the cells get damaged. The fixation with different methods like low melting agarose gives the opportunity to let the bacteria stay in their place. Another problem that has to be solved is that it is never known in which section of the stem the endophytes are located. For microscopically methods only small pieces of the plants are investigated each at the time which minimizes the chance of locating the endophytes in the plant. To investigate the bacteria with confocal microscopic methods, again another severe problem occurs because of the size of samples which can be investigated. Only small parts of stems or leaves are possible to prepare. Germaine et al. (74) documented the bacteria with gfp labeling residing in the xylematic tissue located in one or more cells.

To refer to the *in-vitro* poplar 741 sample it is important to know that the endophyte free sample was freshly inoculated with *Paenibacillus* sp. P22. Figure 61 (B) shows that the bacteria are concentrated in one or two cells of these xylematic tissue. In case of fig. 60 and 61 the already mentioned bacteria flush can be confirmed. After cutting the stem the bacteria were located in a lot of tracheids and wood vessels. This can falsify the results but for knowing if there are bacteria inside the plant it is a very good method.

4.4 MEDIA-SCREENING

The *in-vitro* experiments with different poplar hybrids growing on different media have shown that all hybrids, except the mixoploid plant, grew best in a ½-strength L&S-medium without any GPH. Former experiments have demonstrated that an increase of agar strength inhibits organogenesis and shoot growth. It also reduces the water availability to the cultures (215). Conversely a low concentration of agar provides a poorly gelled medium. This facilitates contact between the plant tissue and the medium, as well as a better diffusion of medium constituents which results in a better growth and rooting (28). Therefore the polysaccharide “gelrite” was used as an agar supplement. It was reported that this polysaccharide yields better results in regeneration and shoot multiplication (232). In fact, two of the added GPH are

cytokinin derivatives which are important for cell division, and are probably needed for growth.

4.5 ANATOMIC SECTIONS OF 2N, 4N AND 2N4N LEAVES

The photosynthesis potential is higher in polyploid plants than in diploid plants (212) which was confirmed by the results of the anatomical sections of the mixoploid plants which exhibited the highest contents of palisade parenchyma.

4.6 CHLOROPLAST COUNTS IN STOMATA CELLS

The amount of chloroplasts in the stomata of leaves of 2N and 4N poplar plants differed from the data shown in the results from Ewald et al. (62). This can be due to the fact that the samples tested in this experiment were from an *in-vitro* cultures, those used by Ewald et al. were field cultured plants.

Concerning the acclimatization of the poplar hybrids, Tich et al. discovered a decrease of stomata during acclimatization of tobacco plants. This decrease was compensated by an increase in stomata size and form (221).

As the amount of stomata is higher in mixoploid plants, it is possible that the adaption to the natural conditions was not possible for those explants and the reason for their death.

4.7 PROTEOME PROFILING OF POPLAR HYBRID L447

The analysis of variances shows on the one hand that the highest amount of proteins could be scored between the young and old leaf samples or only between the polyploidy levels. On the other hand the considerably separation of the single leaf samples (young, old, 2N, 4N, 2N4N) could only be reached by identifying a smaller amount of proteins.

Due to the identification of three Heat shock related proteins (Figure 96 m, n and o) in all leaf samples it is possible that the climatic situation e.g. lightning conditions, location in the greenhouse, or the age of the leaves, were responsible for the appearance of these stress related proteins. Also the detected Stable protein 1 (Figure 96 x) in all leaf samples should provide an indication of stress in the leaf samples. Another protein which leads to this assumption is the Pectinesterase (Figure 97 b) and the Polyphenol oxidase (Figure 97 c) which were detected in the

old leaf samples of the diploid and tetraploid plants and the young and old leaf samples of the mixoploid poplar plants. The Pectinesterase as a cell-wall associated enzyme would be a sign for aging of the leaves while the Polyphenole oxidase was identified in the all old leaf samples which would also be a sign for aging.

Figure 96 (u and w) the enzymes Ribulose-1.5-bisphosphate carboxylase/oxygenase large subunit D0QTN3 and P08926 were much higher regulated in the diploid and also higher regulated in the tetraploid leaf samples then in the mixoploid samples. This up-regulation of these enzymes can be an allusion that the diploid and tetraploid plants were exposed to strong light and so higher temperature compared to the mixoploid plants.

Endochitinase 1 (Figure 89 a) was only identified in the old leaf samples of mixoploid poplar hybrid L447. Its function as a defense against chitin containing fungal pathogens can be a sign for an already existing infection with fungi of this plant. This can be proved by the detection of the Rhicadhesin receptor (Figure 90 a) that has been detected in the old mixoploid leaf samples. Additionally to the Endochitinase 1 and the Rhicadesin receptor, the Superoxide dismutase [Cu-Zn] was identified in the old leaf samples. These three results lead to the assumption that there were some fungal pathogens on the mixoploid leaves (142).

The appearance of the Aspartic proteinase (Figure 90 a) only in all old leaf samples can be a hint to a high metabolic activity in the leaves.

Figure 84 (a) and figure 88 (b and c) show the identification of the iron-storage protein Ferritin only in the diploid leaf samples. In all three figures it is evident that the old leaf samples are minimal higher regulated then the young leaf samples. Beside the function of building Fe containing proteins, Ferritin is also a factor in stress response. Beside the already mentioned stress related proteins the identification of Ferritin will suggest that in this case its function lies in stress response. Also the Copper chaperone that was found in both diploid leaf samples can be connected to the Ferritin. The incidence of the enzyme Glutamate-glyoxylate-aminotransferase (Figure 84 d) in all diploid leaves and only in the young tetraploid leaf sample can be explained by the age of these leaves.

The Fructose-1.6-bisphosphatase together with the Fructose-bisphosphate-aldolase (Fig. 96 h and i) catalyzes severe processes in the glycolysis. The up-regulation of all old leaf samples in all three polyploidy leaf samples can be explained by the fact that the mechanism of auxin is both, division and expansion of plant cells (31).

4.8 ANALYSIS OF *CHLAMYDOMONAS REINHARDTII*

During the synchronization of *Chlamydomonas reinhardtii* not all of the daughter cells could be investigated. It is possible that there are 3 or more daughter cells which could not be completely investigated because the possibility of overlapping was given.

4.9 STRESS-RELATED EXPERIMENTS ON *MEDICAGO TRUNCATULA*

Growing leaves are characterized by the simultaneous development of function and structure. The functional development are for example developing stomata for the active water- and CO₂ exchange control and growth processes like these ratios between tissue layers (193). It is suggested that alfalfa plants inoculated with engineered *S. meliloti* may maintain water content more effectively than the control plants under drought-stress conditions (240).

The plant anatomic aspects showed that the leaves of *Medicago truncatula* had a different amount of intercellular spaces between control plants and plants set under stress. This leads to the assumption that shrinking of the surrounding cells during drought- and salt-stress minimizes these intercellular spaces.

In square sections of the stem the parenchymatic cells decreased in cell size during drought- and salt-stress in the nitrogen fixing plants as well as in the nitrogen assimilating plants. The earlier development of xylem in the nitrogen fixing plants can be seen as a result of the plant-bacteria-interaction (*Sinorhizobium meliloti*) based on the controlled nitrogen uptake.

Similar to the leaves, the shrinking of nodule cells during drought- and salt-stress may be due to osmotic effects causing uptake of water from the cell into the vacuole.

5 List of Abbreviations

SRF	short rotation forest
%	percent
°C	Celsius degree
NUE	nitrogen use efficiency
N	nitrogen
C	carbon
NO_3^-	nitrate
NH_4^+	nitrite
G_w	grain per unit of available nitrogen in the soil
N_s	including the N present in soil and the fertilizers
N_{av}	plant available nitrogen
GNACE	grain nitrogen accumulation efficiency
N_g	nitrogen in the grain
N_t	total plant nitrogen
NUE	nitrogen use efficiency
HI	harvest index
μm	micrometer
cm	centimeter
et al.	et alteres
mg	milligramm
l	liter

conc.	concentration
y	year
h	hour
d	day
TISH	tissue in-situ hybridization
ESEM	environmental scanning electron microscopy
GPH	growth promoting hormones
FA	formic acid
ACN	acetonitrile
TEM	transmission electron microscope
CLSM	confocal laser scan microscope
KIN	kinetin
IAA	indole-acetic-acid
IO	inoculation
e.g.	exempli gratia

6 Literature

1. , posting date. Probstdorfer Saatzucht. Probstdorfer Saatzucht. [Online.]
2. **Aarts, M. G., and M. W. Fiers.** 2003. What drives plant stress genes? Trends Plant Sci **8**:99-102.
3. **Abbott, R. J., and A. J. Lowe.** 2004. Origins, establishment and evolution of new polyploid species: *Senecio cambrensis* and *S. eboracensis* in the British Isles. Biol J Linn Soc **82**:467-474.
4. **Adams, K. L.** 2007. Evolution of duplicate gene expression in polyploid and hybrid plants. J Hered **98**:136-141.
5. **Adams, K. L., and J. F. Wendel.** 2005. Polyploidy and genome evolution in plants. Curr Opin Plant Biol **8**:135-141.
6. **Aguilera, M., M. Monteoliva-Sanchez, A. Suarez, V. Guerra, C. Lizama, A. Bennasar, and A. Ramos-Cormenzana.** 2001. *Paenibacillus jamilae* sp. nov., an exopolysaccharide-producing bacterium able to grow in olive-mill wastewater. Int J Syst Evol Microbiol **51**:1687-1692.
7. **Alasia, F. V.,** posting date. Alasia New Clones. [Online.]
8. **Araujo, W. L., J. Marcon, W. Maccheroni, Jr., J. D. Van Elsas, J. W. Van Vuurde, and J. L. Azevedo.** 2002. Diversity of endophytic bacterial populations and their interaction with *Xylella fastidiosa* in citrus plants. Appl Environ Microbiol **68**:4906-4914.
9. **Arshad, M., and W. T. Frankenberger, Jr.** 1991. Microbial production of plant hormones. Plant and Soil **133**:1-8.
10. **Asghar, H. N., Z. A. Zahir, and M. Arshad.** 2004. Screening rhizobacteria for improving the growth, yield, and oil content of canola (*Brassica napus* L.). Aust J Agr Res **55**:187-194.
11. **Ash, C., F. G. Priest, and M. D. Collins.** 1993. Molecular identification of rRNA group 3 bacilli (Ash, Farrow, Wallbanks and Collins) using a PCR probe test. Proposal for the creation of a new genus *Paenibacillus*. Antonie Van Leeuwenhoek **64**:253-260.
12. **Atkinson, N. J., and P. E. Urwin.** 2012. The interaction of plant biotic and abiotic stresses: from genes to the field. J Exp Bot.

13. **Bacon, C., and D. Hinton.** 2006. Bacterial endophytes: The endophytic niche, its occupants, and its utility, p. 155-194. *In* S. Gnanamanickam (ed.), *Plant - Associated Bacteria*. Springer Netherlands.
14. **Badger, J. H., and G. J. Olsen.** 1999. CRITICA: coding region identification tool invoking comparative analysis. *Molecular Biology and Evolution* **16**:512-524.
15. **Barka, E. A., A. Belarbi, C. Hachet, J. Nowak, and J. C. Audran.** 2000. Enhancement of in vitro growth and resistance to gray mould of *Vitis vinifera* co-cultured with plant growth-promoting rhizobacteria. *FEMS Microbiol Lett* **186**:91-95.
16. **Bell, C. D., D. E. Soltis, and P. S. Soltis.** 2005. The age of the angiosperms: A molecular timescale without a clock. *Evolution* **59**:1245-1258.
17. **Benedito, V. A., I. Torres-Jerez, J. D. Murray, A. Andriankaja, S. Allen, K. Kakar, M. Wandrey, J. Verdier, H. Zuber, T. Ott, S. Moreau, A. Niebel, T. Frickey, G. Weiller, J. He, X. Dai, P. X. Zhao, Y. Tang, and M. K. Udvardi.** 2008. A gene expression atlas of the model legume *Medicago truncatula*. *Plant J* **55**:504-513.
18. **Bent, E., and C. P. Chanway.** 2002. Potential for misidentification of a spore-forming *Paenibacillus polymyxa* isolate as an endophyte by using culture-based methods. *Appl Environ Microbiol* **68**:4650-4652.
19. **Bent, E., S. Tuzun, C. P. Chanway, and S. Enebak.** 2001. Alterations in plant growth and in root hormone levels of lodgepole pines inoculated with rhizobacteria. *Can J Microbiol* **47**:793-800.
20. **Berge, O., M. H. Guinebretiere, W. Achouak, P. Normand, and T. Heulin.** 2002. *Paenibacillus graminis* sp nov and *Paenibacillus odorifer* sp nov., isolated from plant roots, soil and food. *International Journal of Systematic and Evolutionary Microbiology* **52**:607-616.
21. **Boddey, R. M., S. Urquiaga, B. J. R. Alves, and V. Reis.** 2003. Endophytic nitrogen fixation in sugarcane: present knowledge and future applications. *Plant and Soil* **252**:139-149.
22. **Boeckmann, B., A. Bairoch, R. Apweiler, M.-C. Blatter, A. Estreicher, E. Gasteiger, M. J. Martin, K. Michoud, C. O'Donovan, I. Phan, S. Pilbout, and M.**

- Schneider.** 2003. The SWISS-PROT protein knowledgebase and its supplement TrEMBL in 2003. *Nucleic acids research* **31**:365-370.
23. **Bowers, J. E., B. A. Chapman, J. Rong, and A. H. Paterson.** 2003. Unravelling angiosperm genome evolution by phylogenetic analysis of chromosomal duplication events. *Nature* **422**:433-438.
24. **Briat, J. F.** 1996. Roles of ferritin in plants. *Journal of Plant Nutrition* **19**:1331-1342.
25. **Burger, M., and L. Jackson.** 2005. Plant and microbial nitrogen use and turnover: Rapid conversion of nitrate to ammonium in soil with roots. *Plant and Soil* **266**:289-301.
26. **Cankar, K., H. Kraigher, M. Ravnikar, and M. Rupnik.** 2005. Bacterial endophytes from seeds of Norway spruce (*Picea abies* L. Karst). *FEMS Microbiology Letters* **244**:341-345.
27. **Carr, G. D.** 1998 Chromosome evolution and speciation in Hawaiian flowering plants, p. 5-48. *In* T. F. Stuessy (ed.), *Evolution and Speciation of Island Plants*, vol. 1. Cambridge University Press UK.
28. **Casanova, E., L. Moysset, and M. I. Trillas.** 2008. Effects of agar concentration and vessel closure on the organogenesis and hyperhydricity of adventitious carnation shoots. *Biol Plantarum* **52**:1-8.
29. **Chandra, S., R. Bandopadhyay, V. Kumar, and R. Chandra.** 2010. Acclimatization of tissue cultured plantlets: from laboratory to land. *Biotechnol Lett* **32**:1199-1205.
30. **Chanway, C. P., M. Shishido, J. Nairn, S. Jungwirth, J. Markham, G. Xiao, and F. B. Holl.** 2000. Endophytic colonization and field responses of hybrid spruce seedlings after inoculation with plant growth-promoting rhizobacteria. *Forest Ecology and Management* **133**:81-88.
31. **Chen, J. G., S. Shimomura, F. Sitbon, G. Sandberg, and A. M. Jones.** 2001. The role of auxin-binding protein 1 in the expansion of tobacco leaf cells. *Plant J* **28**:607-617.
32. **Chen, Z. J.** 2007. Genetic and epigenetic mechanisms for gene expression and phenotypic variation in plant polyploids. *Annu Rev Plant Biol* **58**:377-406.
33. **Chen, Z. J., M. Ha, and D. Soltis.** 2007. Polyploidy: genome obesity and its consequences. *New Phytologist* **174**:717-720.

34. **Chevreux, B., T. Wetter, and S. Suhai.** 1999. Presented at the Computer Science and Biology: Proceedings of the German Conference on Bioinformatics (GCB).
35. **Chisti, Y.** 2008. Biodiesel from microalgae beats bioethanol. *Trends Biotechnol* **26**:126-131.
36. **Choo, Q. C., M. R. Samian, and N. Najimudin.** 2003. Phylogeny and Characterization of Three *nifH*-Homologous Genes from *Paenibacillus azotofixans*. *Applied and Environmental Microbiology* **69**:3658-3662.
37. **Cooke, J. E. K., and M. Weih.** 2005. Nitrogen storage and seasonal nitrogen cycling in *Populus*: bridging molecular physiology and ecophysiology. *New Phytologist* **167**:19-30.
38. **Cseke, L., S. Cseke, and G. Podila.** 2007. High efficiency poplar transformation. *Plant Cell Reports* **26**:1529-1538.
39. **Dalton, D. A., S. Kramer, N. Azios, S. Fusaro, E. Cahill, and C. Kennedy.** 2004. Endophytic nitrogen fixation in dune grasses (*Ammophila arenaria* and *Elymus mollis*) from Oregon. *FEMS Microbiology Ecology* **49**:469-479.
40. **Dawson, J. C., D. R. Huggins, and S. S. Jones.** 2008. Characterizing nitrogen use efficiency in natural and agricultural ecosystems to improve the performance of cereal crops in low-input and organic agricultural systems. *Field Crop Res* **107**:89-101.
41. **Delcher, A. L., K. A. Bratke, E. C. Powers, and S. L. Salzberg.** 2007. Identifying bacterial genes and endosymbiont DNA with Glimmer. *Bioinformatics (Oxford, England)* **23**:673-679.
42. **Desbrosses, Guilhem J., and J. Stougaard.** 2011. Root Nodulation: A Paradigm for How Plant-Microbe Symbiosis Influences Host Developmental Pathways. *Cell Host & Microbe* **10**:348-358.
43. **Dgany, O., A. Gonzalez, O. Sofer, W. Wang, G. Zolotnitsky, A. Wolf, Y. Shoham, A. Altman, S. G. Wolf, O. Shoseyov, and O. Almog.** 2004. The structural basis of the thermostability of SP1, a novel plant (*Populus tremula*) boiling stable protein. *Journal of Biological Chemistry* **279**:51516-51523.
44. **Dietz, K. J.** 2003. Plant peroxiredoxins. *Annu Rev Plant Biol* **54**:93-107.

45. **Dluzniewska, P., A. Gessler, H. Dietrich, J. P. Schnitzler, M. Teuber, and H. Rennenberg.** 2007. Nitrogen uptake and metabolism in *Populus × canescens* affected by salinity. *New Phytologist* **173**:279-293.
46. **Dobereiner, J., S. Urquiaga, and R. Boddey.** 1995. Alternatives for nitrogen nutrition of crops in tropical agriculture. *Fertilizer Research* **42**:339-346.
47. **Dolezel, J., J. Greilhuber, and J. Suda.** 2007. Estimation of nuclear DNA content in plants using flow cytometry. *Nature Protocols* **2**:2233-2244.
48. **Doležel, J., and F. J. Novák.** 1985. Karyological and Cytophotometric Study of Callus Induction in *Allium sativum* L. *Journal of Plant Physiology* **118**:421-429.
49. **Doty, S. L., B. Oakley, G. Xin, J. W. Kang, G. L. Singleton, Z. Khan, A. Vajzovic, and J. T. Staley.** 2009. Diazotrophic endophytes of native black cottonwood and willow. *Symbiosis* **47**:23-33.
50. **Douce, R., J. Bourguignon, M. Neuburger, and F. Rebeille.** 2001. The glycine decarboxylase system: a fascinating complex. *Trends Plant Sci* **6**:167-176.
51. **Durrett, T. P., C. Benning, and J. Ohlrogge.** 2008. Plant triacylglycerols as feedstocks for the production of biofuels. *Plant J* **54**:593-607.
52. **Eckenwalder, J. E.** 1996. Systematics and evolution of *Populus*, p. 7-30. *In* R. F. Stettler, Jr, P. E. Heilman, and T. M. Hinckley (ed.), *Biology of Populus*. NRC Research Press.
53. **Egelhofer, V., W. Hoehenwarter, D. Lyon, W. Weckwerth, and S. Wienkoop.** 2013. Using ProtMAX to create high-mass-accuracy precursor alignments from label-free quantitative mass spectrometry data generated in shotgun proteomics experiments. *Nat Protoc* **8**:595-601.
54. **Ehara, T., T. Osafune, and E. Hase.** 1995. Behavior of mitochondria in synchronized cells of *Chlamydomonas reinhardtii* (Chlorophyta). *J Cell Sci* **108 (Pt 2)**: 499-507.
55. **Ehlting, B., P. Dluzniewska, H. Dietrich, A. Selle, M. Teuber, R. HÄNsch, U. Nehls, A. Polle, J. P. Schnitzler, H. Rennenberg, and A. Gessler.** 2007. Interaction of nitrogen nutrition and salinity in Grey poplar (*Populus tremula* × *alba*). *Plant, Cell & Environment* **30**:796-811.
56. **Elbeltagy, A., K. Nishioka, T. Sato, H. Suzuki, B. Ye, T. Hamada, T. Isawa, H. Mitsui, and K. Minamisawa.** 2001. Endophytic colonization and in planta

- nitrogen fixation by a *Herbaspirillum* sp isolated from wild rice species. *Applied and Environmental Microbiology* **67**:5285-5293.
57. **Elbeltagy, A., K. Nishioka, T. Sato, H. Suzuki, B. Ye, T. Hamada, T. Isawa, H. Mitsui, and K. Minamisawa.** 2001. Endophytic colonization and in planta nitrogen fixation by a *Herbaspirillum* sp. isolated from wild rice species. *Appl Environ Microbiol* **67**:5285-5293.
 58. **Ellwood, S., J. Lichtenzweig, T. Pfaff, L. Kamphuis, and R. Oliver.** 2007. The *Medicago truncatula* Handbook, p. 1-6. *In* E.-P. Journet (ed.), U Mathesius. The Samuel Roberts Nobel Foundation, Ardmore.
 59. **Eng, J. K., A. L. McCormack, and J. R. Yates lii.** 1994. An approach to correlate tandem mass spectral data of peptides with amino acid sequences in a protein database. *Journal of the American Society for Mass Spectrometry* **5**:976-989.
 60. **Evans, H. J.** 1981. Symbiotic nitrogen fixation in legume nodules, p. 294-310. *In* T. C. Moore (ed.), *Research Experiences in Plant Physiology*. Springer-Verlag, New York.
 61. **Ewald, D., K. Ulrich, G. Naujoks, and M. B. Schroder.** 2009. Induction of tetraploid poplar and black locust plants using colchicine: chloroplast number as an early marker for selecting polyploids in vitro. *Plant Cell Tissue Organ Cult.* **99**:353-357.
 62. **Ewald, D., K. Ulrich, G. Naujoks, and M. B. Schröder.** 2009. Induction of tetraploid poplar and black locust plants using colchicine: chloroplast number as an early marker for selecting polyploids in vitro. *Plant Cell, Tissue and Organ Culture* **99**:353-357.
 63. **Felix, E.** 2008. Biomass production of hybrid poplar (*Populus* sp.) grown on deep-trenched municipal biosolids. *Ecological Engineering* **33**:8-14.
 64. **Fiez, T. E., W. L. Pan, and B. C. Miller.** 1995. Nitrogen Use Efficiency of Winter-Wheat among Landscape Positions. *Soil Sci Soc Am J* **59**:1666-1671.
 65. **Fila, G., J. Ghashghaie, J. Hoarau, and G. Cornic.** 1998. Photosynthesis, leaf conductance and water relations of in vitro cultured grapevine rootstock in relation to acclimatisation. *Physiol Plantarum* **102**:411-418.
 66. **Filat, M.** 2010. First year development of poplar clones in biomass short rotation coppiced experimental cultures. *Annals of Forest Research* **53**.

67. **Finkemeier, I., and L. J. Sweetlove.** 2009. The role of malate in plant homeostasis. *F1000 Biol Rep* 1:47.
68. **Flurkey, W. H.** 1986. Polyphenoloxidase in higher plants: immunological detection and analysis of in vitro translation products. *Plant Physiol* 81:614-618.
69. **Fransz, P., J. H. de Jong, M. Lysak, M. R. Castiglione, and I. Schubert.** 2002. Interphase chromosomes in *Arabidopsis* are organized as well defined chromocenters from which euchromatin loops emanate. *Proceedings of the National Academy of Sciences* 99:14584-14589.
70. **Frommel, M. I., J. Nowak, and G. Lazarovits.** 1991. Growth Enhancement and Developmental Modifications of in Vitro Grown Potato (*Solanum tuberosum* spp. *tuberosum*) as Affected by a Nonfluorescent *Pseudomonas* sp. *Plant Physiol* 96:928-936.
71. **Gagné, S., C. Richard, H. Rousseau, and H. Antoun.** 1987. Xylem-residing bacteria in alfalfa roots. *Canadian Journal of Microbiology* 33:996-1000.
72. **Garcia de Salamone, I. E., R. K. Hynes, and L. M. Nelson.** 2001. Cytokinin production by plant growth promoting rhizobacteria and selected mutants. *Can J Microbiol* 47:404-411.
73. **Gardner, J. M., A. W. Feldman, and R. M. Zablotowicz.** 1982. Identity and behavior of xylem-residing bacteria in rough lemon roots of Florida citrus trees. *Appl Environ Microbiol* 43:1335-1342.
74. **Germaine, K., E. Keogh, G. Garcia-Cabellos, B. Borremans, D. van der Lelie, T. Barac, L. Oeyen, J. Vangronsveld, F. P. Moore, E. R. B. Moore, C. D. Campbell, D. Ryan, and D. N. Dowling.** 2004. Colonisation of poplar trees by gfp expressing bacterial endophytes. *FEMS Microbiology Ecology* 48:109-118.
75. **Gil-Quintana, E., E. Larrainzar, C. Arrese-Igor, and E. M. González.** 2012. Is N-feedback involved in the inhibition of nitrogen fixation in drought-stressed *Medicago truncatula*? *J Exp Bot*.
76. **Giles, J.** 2005. Nitrogen study fertilizes fears of pollution. *Nature* 433:791-791.
77. **Gimeno, V., J. P. Syvertsen, M. Nieves, I. Simón, V. Martínez, and F. García-Sánchez.** 2009. Additional nitrogen fertilization affects salt tolerance of lemon trees on different rootstocks. *Scientia Horticulturae* 121:298-305.

78. **Glass, A. D. M., D. T. Britto, B. N. Kaiser, J. R. Kinghorn, H. J. Kronzucker, A. Kumar, M. Okamoto, S. Rawat, M. Y. Siddiqi, S. E. Unkles, and J. J. Vidmar.** 2002. The regulation of nitrate and ammonium transport systems in plants. *J Exp Bot* **53**:855-864.
79. **Glick, B.** 1995. The enhancement of plant growth by free-living bacteria. *Canadian Journal of Microbiology* **41**:109-117.
80. **Glick, B. R., D. M. Penrose, and J. Li.** 1998. A Model For the Lowering of Plant Ethylene Concentrations by Plant Growth-promoting Bacteria. *Journal of Theoretical Biology* **190**:63-68.
81. **Griffiths-Jones, S., S. Moxon, M. Marshall, A. Khanna, S. R. Eddy, and A. Bateman.** 2005. Rfam: annotating non-coding RNAs in complete genomes. *Nucleic acids research* **33**:D121-124.
82. **Gupta, A., M. Gopal, and K. V. Tilak.** 2000. Mechanism of plant growth promotion by rhizobacteria. *Indian J Exp Biol* **38**:856-862.
83. **Hallmann, J., A. Quadt-Hallmann, W. F. Mahaffee, and J. W. Kloepper.** 1997. Bacterial endophytes in agricultural crops. *Canadian Journal of Microbiology* **43**:895-914.
84. **Hasegawa, P. M., R. A. Bressan, J. K. Zhu, and H. J. Bohnert.** 2000. PLANT CELLULAR AND MOLECULAR RESPONSES TO HIGH SALINITY. *Annu Rev Plant Physiol Plant Mol Biol* **51**:463-499.
85. **Heilman, P.** 1999. Planted forests: poplars. *New For.* **17**:89-93.
86. **Hirel, B., J. Le Gouis, B. Ney, and A. Gallais.** 2007. The challenge of improving nitrogen use efficiency in crop plants: towards a more central role for genetic variability and quantitative genetics within integrated approaches. *J Exp Bot* **58**:2369-2387.
87. **Hirel, C., L. Li, P. Brough, K. Vostrikova, J. Pecaut, B. Mehdaoui, M. Bernard, P. Turek, and P. Rey.** 2007. New spin-transition-like copper(II) -nitroxide species. *Inorg Chem* **46**:7545-7552.
88. **Hirsch, A. M.** 2004. Plant-microbe symbioses: A continuum from commensalism to parasitism. *Symbiosis* **37**:345-363.
89. **Ho, R. H., and Y. Raj.** 1985. Haploid plant production through anther culture in poplars. *Forest Ecol Manag* **13**:133-142.

90. **Hoagland, D., and D. Arnon (ed.).** 1950. The Water-Culture Method for Growing Plants without Soil, vol. 3. California Agricultural Experiment Station, Berkeley.
91. **Hoehenwarter, W., J. T. van Dongen, S. Wienkoop, M. Steinfath, J. Hummel, A. Erban, R. Sulpice, B. Regierer, J. Kopka, P. Geigenberger, and W. Weckwerth.** 2008. A rapid approach for phenotype-screening and database independent detection of cSNP/protein polymorphism using mass accuracy precursor alignment. *Proteomics* **8**:4214-4225.
92. **Hong, Y. Y., Y. C. Ma, Y. G. Zhou, F. Gao, H. C. Liu, and S. F. Chen.** 2009. *Paenibacillus sonchi* sp. nov., a nitrogen-fixing species isolated from the rhizosphere of *Sonchus oleraceus*. *International Journal of Systematic and Evolutionary Microbiology* **59**:2656-2661.
93. **Huggins, D. R., and W. L. Pan.** 2003. Key Indicators for Assessing Nitrogen Use Efficiency in Cereal-Based Agroecosystems. *Journal of Crop Production* **8**:157-185.
94. **Hunter, S., P. Jones, A. Mitchell, R. Apweiler, T. K. Attwood, A. Bateman, T. Bernard, D. Binns, P. Bork, S. Burge, E. de Castro, P. Coggill, M. Corbett, U. Das, L. Daugherty, L. Duquenne, R. D. Finn, M. Fraser, J. Gough, D. Haft, N. Hulo, D. Kahn, E. Kelly, I. Letunic, D. Lonsdale, R. Lopez, M. Madera, J. Maslen, C. McAnulla, J. McDowall, C. McMenamin, H. Mi, P. Mutowo-Muellenet, N. Mulder, D. Natale, C. Orengo, S. Pesseat, M. Punta, A. F. Quinn, C. Rivoire, A. Sangrador-Vegas, J. D. Selengut, C. J. Sigrist, M. Scheremetjew, J. Tate, M. Thimmajananathan, P. D. Thomas, C. H. Wu, C. Yeats, and S. Y. Yong.** 2012. InterPro in 2011: new developments in the family and domain prediction database. *Nucleic Acids Research* **40**:D306-312.
95. **Hurek, T., B. Reinhold-Hurek, M. Van Montagu, and E. Kellenberger.** 1994. Root colonization and systemic spreading of *Azoarcus* sp. strain BH72 in grasses. *J Bacteriol* **176**:1913-1923.
96. **Hussain, S. S., M. A. Kayani, and M. Amjad.** 2011. Transcription factors as tools to engineer enhanced drought stress tolerance in plants. *Biotechnol Prog* **27**:297-306.

97. **Hyatt, D., G.-L. Chen, P. F. Locascio, M. L. Land, F. W. Larimer, and L. J. Hauser.** 2010. Prodigal: prokaryotic gene recognition and translation initiation site identification. *BMC bioinformatics* **11**:119.
98. **Igarashi, D., H. Tsuchida, M. Miyao, and C. Ohsumi.** 2006. Glutamate:Glyoxylate Aminotransferase Modulates Amino Acid Content during Photorespiration. *Plant Physiol* **142**:901-910.
99. **James, E. K., F. Olivares, aacute, and L. bio.** 1998. Infection and Colonization of Sugar Cane and Other Graminaceous Plants by Endophytic Diazotrophs. *Critical Reviews in Plant Sciences* **17**:77-119.
100. **James, E. K., V. M. Reis, F. L. Olivares, J. I. Baldani, and J. Döbereiner.** 1994. Infection of sugar cane by the nitrogen-fixing bacterium *Acetobacter diazotrophicus*. *J Exp Bot* **45**:757-766.
101. **Jansson, S., and C. J. Douglas.** 2007. *Populus*: A Model System for Plant Biology. *Annual Review of Plant Biology* **58**:435-458.
102. **Jensen, M. H.** 1999. Hydroponics Worldwide, p. 719-730, vol. 2. *Acta Horticulturae*.
103. **Jimenez-Salgado, T., L. E. Fuentes-Ramirez, A. Tapia-Hernandez, M. A. Mascarua-Esparza, E. Martinez-Romero, and J. Caballero-Mellado.** 1997. *Coffea arabica* L., a new host plant for *Acetobacter diazotrophicus*, and isolation of other nitrogen-fixing acetobacteria. *Appl Environ Microbiol* **63**:3676-3683.
104. **Jones, J. B.** 1982. Hydroponics: Its history and use in plant nutrition studies. *Journal of Plant Nutrition* **5**:1003-1030.
105. **Kanehisa, M., S. Goto, Y. Sato, M. Furumichi, and M. Tanabe.** 2012. KEGG for integration and interpretation of large-scale molecular data sets. *Nucleic Acids Res* **40**:D109-114.
106. **Kefford, N., J. Brockwell, and J. Zwar.** 1960. The Symbiotic Synthesis of Auxin by Legumes and Nodule Bacteria and its Eole in Nodule Development. *Australian Journal of Biological Sciences* **13**:456-467.
107. **Khan, Z., and S. L. Doty.** 2009. Characterization of bacterial endophytes of sweet potato plants. *Plant and Soil* **322**:197-207.
108. **Khattab, S.** 2011. Effect of Different Media and Growth Regulators on the in vitro Shoot Proliferation of Aspen, Hybrid Aspen and White Poplar Male Tree

- and Molecular Analysis of Variants in Micropropagated Plants. *Life Sci J* **8**:177-184.
109. **Kloepper, J. W., M. N. Schroth, and T. D. Miller.** 1980. Effects of rhizosphere colonization by plant growth-promoting Rhizobacteria on potato plant development and yield. *Phytopathology* **70**:1078-1082.
 110. **Kozai, T.** 1991. Photoautotrophic micropropagation. *In Vitro Cell Dev Biol - Plant* **27**:47-51.
 111. **Kozlowksi, T. T. (ed.).** 1971. Growth and Development of Trees, vol. Volume 1. Academic Press Wisconsin.
 112. **Kuklinsky-Sobral, J., W. L. Araujo, R. Mendes, I. O. Geraldi, A. A. Pizzirani-Kleiner, and J. L. Azevedo.** 2004. Isolation and characterization of soybean-associated bacteria and their potential for plant growth promotion. *Environ Microbiol* **6**:1244-1251.
 113. **Lagesen, K., P. Hallin, E. A. Rødland, H.-H. Staerfeldt, T. Rognes, and D. W. Ussery.** 2007. RNAmmer: consistent and rapid annotation of ribosomal RNA genes. *Nucleic acids research* **35**:3100-3108.
 114. **Lamb, T. G., D. W. Tonkyn, and D. A. Kluepfel.** 1996. Movement of *Pseudomonas aureofaciens* from the rhizosphere to aerial plant tissue. *Canadian Journal of Microbiology* **42**:1112-1120.
 115. **Lambert, B., and H. Joos.** 1989. Fundamental aspects of rhizobacterial plant growth promotion research. *Trends in Biotechnology* **7**:215-219.
 116. **Laroche, J., P. Li, and J. Bousquet.** 1995. Mitochondrial DNA and Monocot-Dicot Divergence Time. *Molecular Biology and Evolution* **12**:1151.
 117. **Latijnhouwers, M., X. M. Xu, and S. G. Moller.** 2010. Arabidopsis stromal 70-kDa heat shock proteins are essential for chloroplast development. *Planta* **232**:567-578.
 118. **Lattanzi, F. A., H. Schnyder, and B. Thornton.** 2005. The Sources of Carbon and Nitrogen Supplying Leaf Growth. Assessment of the Role of Stores with Compartmental Models. *Plant Physiol* **137**:383-395.
 119. **Lee, H., J. S. Lee, E. K. Bae, Y. I. Choi, and E. W. Noh.** 2005. Differential expression of a poplar copper chaperone gene in response to various abiotic stresses. *Tree Physiol* **25**:395-401.

120. **Leitch, A. R., and I. J. Leitch.** 2008. Genomic plasticity and the diversity of polyploid plants. *Science* **320**:481-483.
121. **Li, Y. H., X. Y. Kang, S. D. Wang, Z. H. Zhang, and H. W. Chen.** 2008. Triploid Induction in *Populus alba* x *P. glandulosa* by Chromosome Doubling of Female Gametes. *Silvae Genet* **57**:37-40
122. **Lian, B., D. L. Smith, and P. Fu.** 2000. Application and mechanism of silicate bacteria in agriculture and industry. *Guizhou Science* **18**:43-53.
123. **Lieseback, H., G. Naujoks, and D. Ewald.** 2011. Successful hybridisation of normally incompatible hybrid aspen (*Populus tremula* x *P. tremuloides*) and eastern cottonwood (*P. deltoides*) . *Sex Plant Reprod* **24**:189-198.
124. **Lilley, A. K., J. C. Fry, M. J. Bailey, and M. J. Day.** 1996. Comparison of aerobic heterotrophic taxa isolated from four root domains of mature sugar beet (*Beta vulgaris*). *FEMS Microbiology Ecology* **21**:231-242.
125. **Lim, K. Y., R. Matyasek, A. Kovarik, and A. R. Leitch.** 2004. Genome evolution in allotetraploid *Nicotiana*. *Biol J Linn Soc* **82**:599-606.
126. **Lin, S.-Z., Z.-Y. Zhang, Q. Zhang, and Y.-Z. Lin.** 2006. Progress in the Study of Molecular Genetic Improvements of Poplar in China. *Journal of Integrative Plant Biology* **48**:1001-1007.
127. **Linsmaie, E. M., and F. Skoog.** 1965. Organic Growth Factor Requirements of Tobacco Tissue Cultures. *Physiol Plantarum* **18**:100-&.
128. **Ljung, K., A. Hull, M. Kowalczyk, A. Marchant, J. Celenza, J. Cohen, and G. Sandberg.** 2002. Biosynthesis, conjugation, catabolism and homeostasis of indole-3-acetic acid in *Arabidopsis thaliana*. *Plant Molecular Biology* **49**:249-272.
129. **Lodewyckx, C., J. Vangronsveld, F. Porteous, E. R. B. Moore, S. Taghavi, M. Mezgeay, and D. v. der Lelie.** 2002. Endophytic Bacteria and Their Potential Applications. *Critical Reviews in Plant Sciences* **21**:583-606.
130. **Löve, Á.** 1949. The geobotanical significance of polyploidy. 1. Polyploidy and latitude, Lisbon.
131. **Lowe, T. M., and S. R. Eddy.** 1997. tRNAscan-SE: a program for improved detection of transfer RNA genes in genomic sequence. *Nucleic acids research* **25**:955-964.

132. **Lteif, A., J. K. Whalen, R. L. Bradley, and C. Camiré.** 2010. Nitrogen transformations revealed by isotope dilution in an organically fertilized hybrid poplar plantation. *Plant and Soil* **333**:105-116.
133. **Lukashin, A. V., and M. Borodovsky.** 1998. GeneMark.hmm: new solutions for gene finding. *Nucleic Acids Res* **26**:1107-1115.
134. **Ma, Y., Z. Xia, X. Liu, and S. Chen.** 2007. *Paenibacillus sabinae* sp. nov., a nitrogen-fixing species isolated from the rhizosphere soils of shrubs. *International Journal of Systematic and Evolutionary Microbiology* **57**:6-11.
135. **Marilley, L., and M. Aragno.** 1999. Phylogenetic diversity of bacterial communities differing in degree of proximity of *Lolium perenne* and *Trifolium repens* roots. *Applied Soil Ecology* **13**:127-136.
136. **Mart, iacute, L. nez, J. Caballero-Mellado, J. Orozco, and E. nez-Romero.** 2003. Diazotrophic bacteria associated with banana (*Musa* spp.). *Plant and Soil* **257**:35-47.
137. **Masclaux, C., I. QuillerÉ, A. Gallais, and B. Hirel.** 2001. The challenge of remobilisation in plant nitrogen economy. A survey of physio-agronomic and molecular approaches. *Annals of Applied Biology* **138**:69-81.
138. **Masterson, J.** 1994. Stomatal size in fossil plants: evidence for polyploidy in majority of angiosperms. *Science* **264**:421-424.
139. **Mastretta, C., T. Barac, J. Vangronsveld, L. Newman, S. Taghavi, and D. Van der Lelie.** 2006. Endophytic bacteria and their potential application to improve the phytoremediation of contaminated environments. *Biotechnol Genet Eng Rev* **23**:175-207.
140. **Mathesius, U.** 2008. Goldacre paper: Auxin: at the root of nodule development? *Functional Plant Biology* **35**:651-668.
141. **Mccown, B. H., and G. Lloyd.** 1981. Woody Plant Medium (Wpm) - a Mineral Nutrient Formulation for Microculture of Woody Plant-Species. *Hortscience* **16**:453-453.
142. **Mehdy, M. C.** 1994. Active Oxygen Species in Plant Defense against Pathogens. *Plant Physiol* **105**:467-472.
143. **Meister, M. H., and H. R. Bolhàr Nordenkamp.** 2003. Stomata Imprints: A New and Quick Method to Count Stomata and Epidermis Cells, p. 235-250. *In*

- M. Reigosa Roger (ed.), Handbook of Plant Ecophysiology Techniques. Springer Netherlands.
144. **Melaragno, J. E., B. Mehrotra, and A. W. Coleman.** 1993. Relationship between Endopolyploidy and Cell Size in Epidermal Tissue of Arabidopsis. *Plant Cell* **5**:1661-1668.
 145. **Merchant, S. S., S. E. Prochnik, O. Vallon, E. H. Harris, S. J. Karpowicz, G. B. Witman, A. Terry, A. Salamov, L. K. Fritz-Laylin, L. Marechal-Drouard, W. F. Marshall, L. H. Qu, D. R. Nelson, A. A. Sanderfoot, M. H. Spalding, V. V. Kapitonov, Q. Ren, P. Ferris, E. Lindquist, H. Shapiro, S. M. Lucas, J. Grimwood, J. Schmutz, P. Cardol, H. Cerutti, G. Chanfreau, C. L. Chen, V. Cognat, M. T. Croft, R. Dent, S. Dutcher, E. Fernandez, H. Fukuzawa, D. Gonzalez-Ballester, D. Gonzalez-Halphen, A. Hallmann, M. Hanikenne, M. Hippler, W. Inwood, K. Jabbari, M. Kalanon, R. Kuras, P. A. Lefebvre, S. D. Lemaire, A. V. Lobanov, M. Lohr, A. Manuell, I. Meier, L. Mets, M. Mittag, T. Mittelmeier, J. V. Moroney, J. Moseley, C. Napoli, A. M. Nedelcu, K. Niyogi, S. V. Novoselov, I. T. Paulsen, G. Pazour, S. Purton, J. P. Ral, D. M. Riano-Pachon, W. Riekhof, L. Rymarquis, M. Schroda, D. Stern, J. Umen, R. Willows, N. Wilson, S. L. Zimmer, J. Allmer, J. Balk, K. Bisova, C. J. Chen, M. Elias, K. Gendler, C. Hauser, M. R. Lamb, H. Ledford, J. C. Long, J. Minagawa, M. D. Page, J. Pan, W. Pootakham, S. Roje, A. Rose, E. Stahlberg, A. M. Terauchi, P. Yang, S. Ball, C. Bowler, C. L. Dieckmann, V. N. Gladyshev, P. Green, R. Jorgensen, S. Mayfield, B. Mueller-Roeber, S. Rajamani, R. T. Sayre, P. Brokstein, et al.** 2007. The *Chlamydomonas* genome reveals the evolution of key animal and plant functions. *Science* **318**:245-250.
 146. **Michael Beman, J., K. R. Arrigo, and P. A. Matson.** 2005. Agricultural runoff fuels large phytoplankton blooms in vulnerable areas of the ocean. *Nature* **434**:211-214.
 147. **Mifflin, B. J., and D. Z. Habash.** 2002. The role of glutamine synthetase and glutamate dehydrogenase in nitrogen assimilation and possibilities for improvement in the nitrogen utilization of crops. *J Exp Bot* **53**:979-987.
 148. **Millard, P.** 1996. Ecophysiology of the internal cycling of nitrogen for tree growth. *Zeitschrift für Pflanzenernährung und Bodenkunde* **159**:1-10.

149. **Minocha, R., and S. M. Jain.** 2000. Tissue culture of woody plants and its relevance to molecular biology. *Molecular biology of woody plants* 315-340.
150. **Misaghi, I. J., and C. R. Donndelinger.** 1990. Endophytic bacteria in symptom-free cotton plants. *Phytopathology* **80**:808-811.
151. **Misko, A. L., and J. J. Germida.** 2002. Taxonomic and functional diversity of pseudomonads isolated from the roots of field-grown canola. *FEMS Microbiol Ecol* **42**:399-407.
152. **Miziorko, H. M.** 2000. Phosphoribulokinase: current perspectives on the structure/function basis for regulation and catalysis. *Adv Enzymol Relat Areas Mol Biol* **74**:95-127.
153. **Mocali, S., E. Bertelli, F. Di Cello, A. Mengoni, A. Sfalanga, F. Viliari, A. Caciotti, S. Tegli, G. Surico, and R. Fani.** 2003. Fluctuation of bacteria isolated from elm tissues during different seasons and from different plant organs. *Res Microbiol* **154**:105-114.
154. **Moellering, E. R., and C. Benning.** 2010. RNA Interference Silencing of a Major Lipid Droplet Protein Affects Lipid Droplet Size in *Chlamydomonas reinhardtii*. *Eukaryotic Cell* **9**:97-106.
155. **Moll, R. H., E. J. Kamprath, and W. A. Jackson.** 1982. Analysis and Interpretation of Factors Which Contribute to Efficiency of Nitrogen Utilization¹. *Agron. J.* **74**:562-564.
156. **Moore, F. P., T. Barac, B. Borremans, L. Oeyen, J. Vangronsveld, D. van der Lelie, C. D. Campbell, and E. R. Moore.** 2006. Endophytic bacterial diversity in poplar trees growing on a BTEX-contaminated site: the characterisation of isolates with potential to enhance phytoremediation. *Syst Appl Microbiol* **29**:539-556.
157. **Müntzing, A.** 1936. The Chromosomes of a Giant *Populus Tremula*. *Hereditas* **21**:383-393.
158. **Murashige, T., and F. Skoog.** 1962. A Revised Medium for Rapid Growth and Bio Assays with Tobacco Tissue Cultures. *Physiol Plantarum* **15**:473-497.
159. **Näsholm, T., K. Kielland, and U. Ganeteg.** 2009. Uptake of organic nitrogen by plants. *New Phytologist* **182**:31-48.

160. **Newcombe, G., and C. van Oosten.** 1997. Variation in resistance to *Venturia populina*, the cause of poplar leaf and shoot blight in the Pacific Northwest. *Canadian Journal of Forest Research* **27**:883-889.
161. **Nilsson-Ehle, H.** 1936. Über Eine in der Natur Gefundene Gigasform von *Populus Tremula*. *Hereditas* **21**:379-382.
162. **Novitskaya, L., S. J. Trevanion, S. Driscoll, C. H. Foyer, and G. Noctor.** 2002. How does photorespiration modulate leaf amino acid contents? A dual approach through modelling and metabolite analysis. *Plant, Cell & Environment* **25**:821-835.
163. **Ostry, M. E., and D. D. Skilling.** 1988. Somatic variation in resistance of *Populus* to *Septoria musiva*. *Plant Dis* **72**:724-727.
164. **Parida, A. K., and A. B. Das.** 2005. Salt tolerance and salinity effects on plants: a review. *Ecotoxicol Environ Saf* **60**:324-349.
165. **Paris, P., L. Mareschi, M. Sabatti, A. Pisanelli, A. Ecosse, F. Nardin, and G. Scarascia-Mugnozza.** 2011. Comparing hybrid *Populus* clones for SRF across northern Italy after two biennial rotations: Survival, growth and yield. *Biomass Bioenerg* **35**:1524-1532.
166. **Park, S., S. Oh, and K.-H. Han.** 2004. Large-scale computational analysis of poplar ESTs reveals the repertoire and unique features of expressed genes in the poplar genome. *Molecular Breeding* **14**:429-440.
167. **Perry, C. H., R. C. Miller, and K. N. Brooks.** 2001. Impacts of short-rotation hybrid poplar plantations on regional water yield. *Forest Ecol Manag* **143**:143-151.
168. **Popova, O. V., K. J. Dietz, and D. Gollack.** 2003. Salt-dependent expression of a nitrate transporter and two amino acid transporter genes in *Mesembryanthemum crystallinum*. *Plant Mol Biol* **52**:569-578.
169. **Pospíšilová, J., I. Tichá, P. Kadleček, D. Haisel, and Š. Plizáková.** 1999. Acclimatization of Micropropagated Plants to Ex Vitro Conditions. *Biologia Plantarum* **42**:481-497.
170. **Proschold, T., E. H. Harris, and A. W. Coleman.** 2005. Portrait of a species: *Chlamydomonas reinhardtii*. *Genetics* **170**:1601-1610.
171. **QUADT-HALLMANN, #160, A., KLOEPPER, and J. W.** 1996. Immunological detection and localization of the cotton endophyte *Enterobacter asburiae*

- JM22 in different plant species, vol. 42. National Research Council of Canada, Ottawa, ON, CANADA.
172. **Quadt-Hallmann, A., J. W. Kloepper, and N. Benhamou.** 1997. Bacterial endophytes in cotton: mechanisms of entering the plant. *Canadian Journal of Microbiology* **43**:577-582.
 173. **Ramshaw, J. A. M., D. L. Richardson, B. T. Meatyard, R. H. Brown, M. Richardson, E. W. Thompson, and D. Boulter.** 1972. THE TIME OF ORIGIN OF THE FLOWERING PLANTS DETERMINED BY USING AMINO ACID SEQUENCE DATA OF CYTOCHROME C. *New Phytologist* **71**:773-779.
 174. **Rennenberg, H., H. Wildhagen, and B. Ehrling.** 2010. Nitrogen nutrition of poplar trees. *Plant Biology* **12**:275-291.
 175. **Renner, T., and C. D. Specht.** 2012. Molecular and functional evolution of class I chitinases for plant carnivory in the caryophyllales. *Mol Biol Evol* **29**:2971-2985.
 176. **Rhodes, D., and A. Nadolska-Orczyk.** 2001. *Plant Stress Physiology*, eLS. John Wiley & Sons, Ltd.
 177. **Rodolfi, L., G. Chini Zittelli, N. Bassi, G. Padovani, N. Biondi, G. Bonini, and M. R. Tredici.** 2009. Microalgae for oil: strain selection, induction of lipid synthesis and outdoor mass cultivation in a low-cost photobioreactor. *Biotechnol Bioeng* **102**:100-112.
 178. **Rogers, A., K. McDonald, M. F. Muehlbauer, A. Hoffman, K. Koenig, L. Newman, S. Taghavi, and D. van der Lelie.** 2011. Inoculation of hybrid poplar with the endophytic bacterium *Enterobacter* sp. 638 increases biomass but does not impact leaf level physiology. *GCB Bioenergy*:n/a-n/a.
 179. **Roos, I. M. M., and M. J. Hattingh.** 1983. Scanning Electron-Microscopy of *Pseudomonas-Syringae* Pv *Morsprunorum* on Sweet Cherry Leaves. *Phytopathol Z* **108**:18-25.
 180. **Rosado, A. S., F. S. de Azevedo, D. W. da Cruz, J. D. van Elsas, and L. Seldin.** 1998. Phenotypic and genetic diversity of *Paenibacillus azotofixans* strains isolated from the rhizoplane or rhizosphere soil of different grasses. *Journal of Applied Microbiology* **84**:216-226.

181. **Rosenblueth, M., and E. Martínez-Romero.** 2006. Bacterial Endophytes and Their Interactions with Hosts. *Molecular Plant-Microbe Interactions* **19**:827-837.
182. **Russell, J. A., and B. H. McCown.** 1986. Culture and regeneration of *Populus* leaf protoplasts isolated from non-seedling tissue. *Plant Science* **46**:133-142.
183. **Ryan, R. P., K. Germaine, A. Franks, D. J. Ryan, and D. N. Dowling.** 2008. Bacterial endophytes: recent developments and applications. *FEMS Microbiology Letters* **278**:1-9.
184. **Ryu, C. M., M. A. Farag, C. H. Hu, M. S. Reddy, H. X. Wei, P. W. Pare, and J. W. Kloepper.** 2003. Bacterial volatiles promote growth in *Arabidopsis*. *Proc Natl Acad Sci U S A* **100**:4927-4932.
185. **Sahay, N. S., and A. Varma.** 1999. *Piriformospora indica*: a new biological hardening tool for micropropagated plants. *FEMS Microbiology Letters* **181**:297-302.
186. **Sayers, E. W., T. Barrett, D. A. Benson, S. H. Bryant, K. Canese, V. Chetvernin, D. M. Church, M. DiCuccio, R. Edgar, S. Federhen, M. Feolo, L. Y. Geer, W. Helmberg, Y. Kapustin, D. Landsman, D. J. Lipman, T. L. Madden, D. R. Maglott, V. Miller, I. Mizrachi, J. Ostell, K. D. Pruitt, G. D. Schuler, E. Sequeira, S. T. Sherry, M. Shumway, K. Sirotkin, A. Souvorov, G. Starchenko, T. A. Tatusova, L. Wagner, E. Yaschenko, and J. Ye.** 2009. Database resources of the National Center for Biotechnology Information. *Nucleic acids research* **37**:D5-15.
187. **Schenk, R. U., and Hildebra.Ac.** 1972. MEDIUM AND TECHNIQUES FOR INDUCTION AND GROWTH OF MONOCOTYLEDONOUS AND DICOTYLEDONOUS PLANT-CELL CULTURES. *Canadian Journal of Botany* **50**:199-&.
188. **Scherling, C., K. Ulrich, D. Ewald, and W. Weckwerth.** 2009. A metabolic signature of the beneficial interaction of the endophyte *paenibacillus* sp. isolate and in vitro-grown poplar plants revealed by metabolomics. *Mol Plant Microbe Interact* **22**:1032-1037.
189. **Scherling, C., K. Ulrich, D. Ewald, and W. Weckwerth.** 2009. A Metabolic Signature of the Beneficial Interaction of the Endophyte *Paenibacillus* sp.

- Isolate and In Vitro - Grown Poplar Plants Revealed by Metabolomics. *Molecular Plant-Microbe Interactions* **22**:1032-1037.
190. **Schmadel-Hageböling, H. E., C. Engel, V. Schmitt, and A. Wild.** 1998. The combined effects of CO₂, ozone and drought on rubisco and nitrogen metabolism of young oak trees (*Quercus petraea*) A phytotron study. *Chemosphere* **36**:789-794.
 191. **Scholz, M.** 2006. Approaches to analyse and interpret biological profile data.
 192. **SCHULTEN, #160, H.-R., SCHNITZER, and M.** 1998. The chemistry of soil organic nitrogen : a review, vol. 26. Springer, Berlin, ALLEMAGNE.
 193. **Schurr, U., U. Heckenberger, K. Herdel, A. Walter, and R. Feil.** 2000. Leaf development in *Ricinus communis* during drought stress: dynamics of growth processes, of cellular structure and of sink-source transition. *J Exp Bot* **51**:1515-1529.
 194. **Sellmer, J. C., B. H. McCown, and B. E. Haissig.** 1989. Shoot culture dynamics of six *Populus* clones. *Tree Physiol* **5**:219-227.
 195. **Sessitsch, A., P. Hardoim, J. Doring, A. Weilharter, A. Krause, T. Woyke, B. Mitter, L. Hauberg-Lotte, F. Friedrich, M. Rahalkar, T. Hurek, A. Sarkar, L. Bodrossy, L. van Overbeek, D. Brar, J. D. van Elsas, and B. Reinhold-Hurek.** 2012. Functional Characteristics of an Endophyte Community Colonizing Rice Roots as Revealed by Metagenomic Analysis. *Mol Plant Microbe In* **25**:28-36.
 196. **Sessitsch, A., B. Reiter, U. Pfeifer, and E. Wilhelm.** 2002. Cultivation-independent population analysis of bacterial endophytes in three potato varieties based on eubacterial and Actinomycetes-specific PCR of 16S rRNA genes. *FEMS Microbiol. Ecol.* **39**:23-32.
 197. **Sessitsch, A., B. Reiter, U. Pfeifer, and E. Wilhelm.** 2002. Cultivation-independent population analysis of bacterial endophytes in three potato varieties based on eubacterial and Actinomycetes-specific PCR of 16S rRNA genes. *FEMS Microbiol Ecol* **39**:23-32.
 198. **Sevilla, M., R. H. Burris, N. Gunapala, and C. Kennedy.** 2001. Comparison of Benefit to Sugarcane Plant Growth and ¹⁵N₂ Incorporation Following Inoculation of Sterile Plants with *Acetobacter diazotrophicus* Wild-Type and Nif⁻ Mutant Strains. *Molecular Plant-Microbe Interactions* **14**:358-366.

199. **Shi, L. X., and S. M. Theg.** 2010. A stromal heat shock protein 70 system functions in protein import into chloroplasts in the moss *Physcomitrella patens*. *Plant Cell* **22**:205-220.
200. **Shishido, M., C. Breuil, and C. P. Chanway.** 1999. Endophytic colonization of spruce by plant growth-promoting rhizobacteria. *FEMS Microbiology Ecology* **29**:191-196.
201. **Silla, F., and A. Escudero.** 2003. Uptake, demand and internal cycling of nitrogen in saplings of Mediterranean *Quercus* species. *Oecologia* **136**:28-36.
202. **Simoes, I., and C. Faro.** 2004. Structure and function of plant aspartic proteinases. *European Journal of Biochemistry* **271**:2067-2075.
203. **Sims, R., A. Hastings, B. Schlamadinger, G. Taylor, and P. Smith.** 2006. Energy crops: current status and future prospects. *Global Change Biology* **12**:2054-2076.
204. **Soltis, D. E., V. A. Albert, J. Leebens-Mack, C. D. Bell, A. H. Paterson, C. F. Zheng, D. Sankoff, C. W. dePamphilis, P. K. Wall, and P. S. Soltis.** 2009. Polyploidy and Angiosperm Diversification. *Am J Bot* **96**:336-348.
205. **Spaepen, S., J. Vanderleyden, and R. Remans.** 2007. Indole-3-acetic acid in microbial and microorganism-plant signaling. *Fems Microbiol Rev* **31**:425-448.
206. **Sprent, J. I., and S. M. Faria.** 1988. Mechanisms of infection of plants by nitrogen fixing organisms. *Plant and Soil* **110**:157-165.
207. **Sree Ramulu, K., P. Dijkhuis, C. H. Hanisch Ten Cate, and B. De Groot.** 1985. Patterns of DNA and chromosome variation during in vitro growth in various genotypes of potato. *Plant Science* **41**:69-78.
208. **Sterck, L., S. Rombauts, S. Jansson, F. Sterky, P. Rouzé, and Y. Van de Peer.** 2005. EST data suggest that poplar is an ancient polyploid. *New Phytologist* **167**:165-170.
209. **Strobel, G., B. Daisy, U. Castillo, and J. Harper.** 2004. Natural products from endophytic microorganisms. *J Nat Prod* **67**:257-268.
210. **Sturz, A. V., and B. R. Christie.** 1996. Endophytic bacteria of red clover as agents of allelopathic clover-maize syndromes. *Soil Biology and Biochemistry* **28**:583-588.
211. **Su, X.** 2003. Advances in Tree Genetic Engineering in China, World Forestry Congress XII, Québec, Canada.

212. **SUGIYAMA, S.-I.** 2005. Polyploidy and Cellular Mechanisms Changing Leaf Size: Comparison of Diploid and Autotetraploid Populations in Two Species of *Lolium*. *Annals of Botany* **96**:931-938.
213. **Sun, X., and W. Weckwerth.** 2012. COVAIN: a toolbox for uni- and multivariate statistics, time-series and correlation network analysis and inverse estimation of the differential Jacobian from metabolomics covariance data. *Metabolomics* **8**:81-93.
214. **Sung, H. M., and R. E. Yasbin.** 2000. Transient growth requirement in *Bacillus subtilis* following the cessation of exponential growth. *Appl Environ Microbiol* **66**:1220-1222.
215. **Suthar, R. K., N. Habibi, and S. D. Purohit.** 2011. Influence of agar concentrataion and liquid medium on *in vitro* propagation of *Boswellia serrata* Roxb., p. 224-227, 2011 ed. NISCAIR-CSIR, India.
216. **Swart, S., T. J. Logman, G. Smit, B. J. Lugtenberg, and J. W. Kijne.** 1994. Purification and partial characterization of a glycoprotein from pea (*Pisum sativum*) with rece ptor activity for rhicadhesin, an attachment protein of Rhizobiaceae. *Plant Mol Biol* **24**:171-183.
217. **Taghavi, S., C. Garafola, S. Monchy, L. Newman, A. Hoffman, N. Weyens, T. Barac, J. Vangronsveld, and D. van der Lelie.** 2009. Genome Survey and Characterization of Endophytic Bacteria Exhibiting a Beneficial Effect on Growth and Development of Poplar Trees. *Appl. Environ. Microbiol.* **75**:748-757.
218. **Taghavi, S., D. van der Lelie, A. Hoffman, Y. B. Zhang, M. D. Walla, J. Vangronsveld, L. Newman, and S. Monchy.** 2010. Genome Sequence of the Plant Growth Promoting Endophytic Bacterium *Enterobacter* sp 638. *PLoS Genetics* **6**.
219. **Tapia-Hernandez, A., M. R. Bustillos-Cristales, T. Jimenez-Salgado, J. Caballero-Mellado, and L. E. Fuentes-Ramirez.** 2000. Natural Endophytic Occurrence of *Acetobacter diazotrophicus* in Pineapple Plants. *Microb Ecol* **39**:49-55.
220. **Thomas, J. C., E. F. McElwain, and H. J. Bohnert.** 1992. Convergent Induction of Osmotic Stress-Responses : Absciscic Acid, Cytokinin, and the Effects of NaCl. *Plant Physiol* **100**:416-423.

221. Tich, aacute, I, Radochov, B, and P. Kadleek. 1999. Stomatal Morphology during Acclimatization of Tobacco Plantlets to ex vitro Conditions. *Biol Plantarum* **42**:469-474.
222. Trevaskis, B., G. Colebatch, G. Desbrosses, M. Wandrey, S. Wienkoop, G. Saalbach, and M. Udvardi. 2002. Differentiation of plant cells during symbiotic nitrogen fixation. *Comparative and functional genomics* **3**:151-157.
223. Triplett, E. 1996. Diazotrophic endophytes: progress and prospects for nitrogen fixation in monocots. *Plant and Soil* **186**:29-38.
224. Tuck, G., M. Glendining, P. Smith, J. House, and M. Wattenbach. 2006. The potential distribution of bioenergy crops in Europe under present and future climate. *Biomass and Bioenergy* **30**:183-197.
225. Ulrich, K., T. Stauber, and D. Ewald. 2008. *Paenibacillus* | a predominant endophytic bacterium colonising tissue cultures of woody plants. *Plant Cell, Tissue and Organ Culture* **93**:347-351.
226. Ulrich, K., A. Ulrich, and D. Ewald. 2008. Diversity of endophytic bacterial communities in poplar grown under field conditions. *FEMS Microbiology Ecology* **63**:169-180.
227. Van Aken, B., C. M. Peres, S. L. Doty, J. M. Yoon, and J. L. Schnoor. 2004. *Methylobacterium populi* sp. nov., a novel aerobic, pink-pigmented, facultatively methylotrophic, methane-utilizing bacterium isolated from poplar trees (*Populus deltoides* x *nigra* DN34). *Int J Syst Evol Microbiol* **54**:1191-1196.
228. Van de Peer, Y., and A. Mayer. 2005. Large-scale gene and ancient genome duplication, p. 330-363. *In* T. R. Gregory (ed.), *The Evolution of the Genome*, San Diego, Elsevier.
229. van der Lelie, D., S. Taghavi, S. Monchy, J. Schwender, L. Miller, R. Ferrieri, A. Rogers, X. Wu, W. Zhu, N. Weyens, J. Vangronsveld, and L. Newman. 2009. Poplar and its Bacterial Endophytes: Coexistence and Harmony. *Critical Reviews in Plant Sciences* **28**:346 - 358.
230. Vaz-Moreira, I., C. Faria, M. F. Nobre, P. Schumann, O. C. Nunes, and C. M. Manaia. 2007. *Paenibacillus humicus* sp. nov., isolated from poultry litter compost. *International Journal of Systematic and Evolutionary Microbiology* **57**:2267-2271.

231. **Vega, F. E., M. Pava-Ripoll, F. Posada, and J. S. Buyer.** 2005. Endophytic bacteria in *Coffea arabica* L. *J Basic Microbiol* **45**:371-380.
232. **Veramendi, J., M. J. Villafranca, V. Sota, and A. M. Mingo-Castel.** 1997. Gelrite as an alternative to agar for micropropagation and microtuberization of *Solanum tuberosum* L. cv. Baraka. *In Vitro Cell Dev Biol - Plant* **33**:195-199.
233. **Wang, J., and C. P. Constabel.** 2004. Polyphenol oxidase overexpression in transgenic *Populus* enhances resistance to herbivory by forest tent caterpillar (*Malacosoma disstria*). *Planta* **220**:87-96.
234. **Wang, P.** 2008. Insect-resistance selectivity of transgenic hybrid poplar 741. *Scientia Silvae Sinicae* **44**:67-71.
235. **Weckwerth, W.** 2011. Green systems biology - From single genomes, proteomes and metabolomes to ecosystems research and biotechnology. *J Proteomics* **75**:284-305.
236. **Wei, T., C.-L. Wang, H.-N. Kao, H.-L. Yang, X.-R. Wang, and Q.-Y. Zeng.** 2012. Molecular and catalytic characterization of a phi class glutathione transferase from *Cathaya argyrophylla*. *Biochemical Systematics and Ecology* **40**:75-85.
237. **Wienkoop, S., J. Weiss, P. May, S. Kempa, S. Irgang, L. Recuenco-Munoz, M. Pietzke, T. Schwemmer, J. Rupprecht, V. Egelhofer, and W. Weckwerth.** 2010. Targeted proteomics for *Chlamydomonas reinhardtii* combined with rapid subcellular protein fractionation, metabolomics and metabolic flux analyses. *Mol Biosyst* **6**:1018-1031.
238. **Wu, M., and A. J. Scott.** 2012. Phylogenomic analysis of bacterial and archaeal sequences with AMPHORA2. *Bioinformatics* **28**:1033-1034.
239. **Xin, G., G. Zhang, J. W. Kang, J. T. Staley, and S. L. Doty.** 2009. A diazotrophic, indole-3-acetic acid-producing endophyte from wild cottonwood. *Biology and Fertility of Soils* **45**:669-674.
240. **Xu, J., X. L. Li, and L. Luo.** 2012. Effects of engineered *Sinorhizobium meliloti* on cytokinin synthesis and tolerance of alfalfa to extreme drought stress. *Appl Environ Microbiol* **78**:8056-8061.
241. **Zhu, J. K.** 2001. Plant salt tolerance. *Trends Plant Sci* **6**:66-71.

7 Acknowledgements

An dieser Stelle möchte ich mich bei allen bedanken, die mich während meiner Doktorarbeit unterstützt haben und mir auch in der ein oder anderen schwierigen Situation zur Seite standen.

Allen voran danke ich meinem Doktorvater Prof. Dr. Wolfram Weckwerth für die Bereitschaft meine Promotion zu betreuen und mir die Möglichkeit zu geben, auf diesem Fachgebiet in seiner Abteilung zu arbeiten.

Bei Herrn Dr. Markus Teige möchte ich mich für die Bereitschaft zur Begutachtung dieser Arbeit bedanken. Ebenso bei Frau Doz. DI Dr. Angela Sessitsch bedanke ich mich, dass sie sich als Begutachterin meiner Arbeit bereit erklärt hat.

Ein großer Dank geht auch an Gärtnermeister Thomas Joch und Andreas Schröfl die sich mit großer Hingabe um meine Pflanzen gekümmert haben.

Ebenso bedanke ich mich sehr bei meinen ganzen Kolleginnen und Kollegen die mich über die Jahre hinweg begleitet haben, mit mir gelacht, manchmal auch über mich gelacht, sich mit mir geärgert aber auch mit mir über die verschiedensten Dinge gegrübelt haben. Auch intensive Gespräche über Unsinniges und Wichtiges will ich nicht missen!

DANKE!!!

Ein besonders großer Dank geht an **meine Eltern** und an **meine kleine Familie**, die mir mein Studium und damit die Durchführung dieser Arbeit ermöglichen haben. Für ihre uneingeschränkte Unterstützung zu jeder Zeit in jeglicher Beziehung möchte ich ihnen sehr danken!

8 Appendix

8.1 ZUSAMMENFASSUNG

Untersuchungen der Pappel-Endophyten-Interaktion mit Pflanzenwachstumsfördernden Effekten

Derzeit ist die Pappel eine der wichtigsten Energiepflanzen und einer der meist untersuchten Modelorganismen im Bereich der Dendrologie. Ferner wird die Pappel für Untersuchungen bezüglich Wirt-Endophyten-Interaktionen verwendet, um die Mechanismen der Pflanzenwachstumsförderung durch Bakterien zu verstehen. Endophytische Bakterien besiedeln das interne Gewebe der Wirtspflanze und können in Leguminosen Wurzelknöllchen bilden. Endophyten wurden bisher sowohl in freiwachsenden Pflanzen als auch in *in-vitro* Kulturen entdeckt, ohne Anzeichen einer Infektion oder Kontamination. Die Funktionen und Effekte von Endophyten in ihrer Wirtspflanze sind vielfältig und schließen wachstumsfördernde Prozesse, Möglichkeiten der Pathogenabwehr und erhöhte Stressresistenz mit ein.

In dieser Arbeit wurde der Mechanismus einer hoch-spezifischen wachstumsfördernden Pappel-Endophyten-Interaktion anhand eines erst kürzlich aus *in-vitro* Pappelpflanzen isolierten Endophyten, *Paenibacillus* sp. P22, untersucht. *Paenibacillus* sp. P22 ist ein gram-positiv, fakultativ anaerobes Endosporen - bildendes Bakterium, das aus der Pappel Hybride 741 ($\text{♀}[\textit{Populus alba} \times (\textit{P. davidiana} + \textit{P. simonii}) \times \textit{P. tomentosa}]$) isoliert wurde. Die Sequenzierung des Genoms dieses Endophyten erfolgte mittels Ion Torrent® und 454® Sequenzierungstechnologie. Die bisherige Annotation des Genoms von *Paenibacillus* sp. P22 umfasst ca. 5.224 codierende Gene, 65 tRNA Gene und 1 16S rRNA Gen. Aufgrund der Präsenz von allen tRNA Genen der 20 essentiellen Aminosäuren und 31 von 34 phylogenetischen Markerproteinen, kann man die Vollständigkeit des Genoms auf ca. 99% schätzen. Eine Rekonstruktion des Metabolismus von *Paenibacillus* sp. P22 zeigten putative Mechanismen für Pflanzenwachstumsförderung. Ein Gen konnte für die Nitrogenase [EC 1.19.6.1], welche der Stickstofffixierung dient, identifiziert werden. Dies stimmt mit zwei Untersuchungsergebnissen überein: (i) *Paenibacillus* sp. P22 besitzt die Fähigkeit

auf stickstofffreiem Medium zu wachsen (ii) das Metabolitprofil von Pappelpflanzen, die mit diesem Endophyten inokuliert wurden, zeigten einen stark unterschiedlichen C/N Gehalt, die in direkter Verbindung mit der Besiedelung der Endophyten steht. Weitere Gene der Nitrataassimilation in *Paenibacillus* sp. P22 wurden gefunden wie z.B. die große Subeinheit der Nitrat Reduktase [NAD(P)H] [EC:1.7.1.4]. Darüber hinaus wurden Gene entdeckt, die dem Auxin-Stoffwechsel angehören, z.B. die Tryptophansynthase beta Kette [EC 4.2.1.20]. Daraus lässt sich schließen, dass die Pappel-Endophyten spezifische Wachstumsförderung auch durch die Sekretion von Phytohormonen durch das Bakterium gesteuert werden kann. Interessanterweise wurde in einer Gaschromatographie-massenspektrometrischen Metabolitanalyse des *Paenibacillus* sp. P22 Isolats auch Auxin detektiert.

Die Pappel-Endophyten-spezifische Wachstumsförderung wurde auch in der Stecklingsvermehrung von verschiedenen schnell-wachsenden Pappelkultivaren untersucht. Im Glashaus kultivierte Stecklinge, welche durch unterschiedlichste Methoden mit *Paenibacillus* sp. P22 inokuliert wurden, zeigten verschiedene Ergebnisse. Die Inokulierung mit *Paenibacillus* sp. P22 an bereits bewurzelten Holzstecklingen zeigte in frühen Stadien ein signifikant erhöhtes Wurzelwachstum aber kein signifikant erhöhtes Stecklingswachstum. Dieser Effekt setzte erst in einer späteren Phase nach 70 Tagen Wachstum ein, bei der inokulierte Pappelstecklinge eine signifikant höhere Biomasse bzw. Längenwachstum im Vergleich zu nicht inokulierten Pappelstecklingen aufwiesen. Diese Ergebnisse sind von großer Bedeutung für die Anwendung der Pappel als Energiepflanze in Kurzumtriebkultivierungen, die von diesem schnellen Wachstum abhängig sind.

In einer weiteren Studie wurde der Einfluss der Polyploidie auf das Proteom von Pappelhybriden untersucht. Die Resultate zeigten signifikante Unterschiede, sowohl zwischen jungen und alten Blättern, als auch zwischen den einzelnen Ploidiegraden der Pappelhybride.

8.2 ABSTRACT

Studies on Poplar-Endophyte-Interactions with Plant-Growth-Promoting Effects

Poplar is an important energy crop and currently one of the most investigated model systems for tree biology. Furthermore, poplar plants have been used as a model system for tree-endophyte-interaction studies with the purpose to understand mechanisms of bacterial plant-growth-promotion. Endophytic bacteria colonize the internal tissue of their host plants and are able to build root nodules in some legumes. They have been detected in nearly all plants studied under field conditions as well as in many tissue cultures without showing any signs of pathogen infection. The function and effects of endophytes on host plants are manifold, including plant growth promoting effects, capacity of controlling pathogens and increased stress resistance. The mechanism of poplar-endophyte-interaction was investigated by studying a recently isolated poplar-specific endophyte, *Paenibacillus* sp. P22. P22 is a gram-positive facultative anaerobic endospore-forming bacterium isolated from a poplar hybrid 741 ($\text{♀}[\textit{Populus alba} \times (\textit{P. davidiana} + \textit{P. simonii}) \times \textit{P. tomentosa}]$). Application of the 454[®] sequencing technology resulted in 561.213 reads and 61.143.112 nucleotides. In an Ion Torrent[™] PGM sequencing approach 1.978.332 reads and 343.311.791 nucleotides were gathered. Consensus assembly using MIRA (34) yielded in 5.443.257 bp in 297 contigs (< 300 bp) with an overall GC content of 58%. The genome of *Paenibacillus* sp. P22 contains 5.224 protein-coding genes, 65 tRNAs and 1 16S rRNA. Presence of tRNAs for all 20 proteinogenic amino acids as well as 31 out of 31 phylogenetic marker proteins, identified with the Software AMPHORA2 (238), that are essential in prokaryotes indicate an estimated completeness of the genome of about 99%.

Further investigation of the metabolic capabilities of *Paenibacillus* sp. P22 yielded two particularly interesting elucidations. We found a gene encoding a nitrogenase [EC:1.19.6.1] for nitrogen fixation. This coincides with the observation that *Paenibacillus* sp. P22 is able to grow without nitrogen in the medium (189). Furthermore the metabolite profiles of the poplar plants which were inoculated with *Paenibacillus* sp. P22 showed a strongly altered C/N homeostasis directly pointing to a changed nitrogen assimilation pathway as a result of the endophyte-plant

interaction. Further investigation of the metabolic capabilities of *Paenibacillus* sp. P22 revealed putative mechanism of plant-growth promotion. First, a gene encoding a nitrogenase [EC 1.19.6.1] for nitrogen fixation was detected. This coincides with two observations: (i) *Paenibacillus* sp. P22 is able to grow without nitrogen in the medium and (ii) metabolite profiles of poplar plants which were inoculated with *Paenibacillus* sp. P22 showed a strongly altered C/N ratio directly pointing to a changed nitrogen assimilation pathway as a result of the endophyte-plant interaction. Further genes of nitrate assimilation in *Paenibacillus* sp. P22 were found, e.g. a nitrate reductase [NAD(P)H] large subunit [EC:1.7.1.4]. Furthermore, we were able to detect genes of the auxin-pathway, e.g. the tryptophan synthase beta chain [EC:4.2.1.20] suggesting growth-promoting effects by hormone secretion. Accordingly, the phytohormone auxin was detected in a gas chromatography-mass spectrometric analysis of metabolite profiles of the *Paenibacillus* sp. P22 isolate.

The poplar-endophyte-growth promoting effects were further investigated using poplar cuttings. In farming poplar is used as an energy crop in short-rotation culture using shoot cutting propagation. An inoculation experiment with shoot cuttings of different fast-growing poplar cultivars was conducted. Poplar cuttings grown under different conditions in the greenhouse showed that an inoculation with *Paenibacillus* sp. P22 after rooting led to higher biomass than those inoculated before rooting. More importantly, by inoculation with *Paenibacillus* sp. P22 root growth was stimulated in the early phases and shoot growth and length was significantly higher in the later stages (70 days). This is especially important for poplar as an energy crop in short-rotation plantation culture dependent on rapid growth of the cuttings.

Further, the impact of polyploidie on the proteome of poplar hybrids was investigated. The results showed significant changes between young and old leaves as well as among the ploidy levels themselves.

8.3 CURICULUM VITAE

Anne Mette Hanak

Personal data

Contact	Anne.mette.hanak@univie.ac.at
Place of birth	Vienna, Austria

Education

2007-2014	PhD Study of Botany (University of Vienna)
1998-2007	Study of Botany (University of Vienna)
09.06.1996	Final secondary school examinations (Matura)

Employments – scientific

2009 - 2014	PhD position (University of Vienna)
WS 2003 - WS 2007	Tutor of “Pflanzenanatomische Übungen” (University of Vienna)
WS 2003 - SS 2005	Tutor of “Biologische Einführungsübungen”(University of Vienna)
SS 2006 - SS 2009	Tutor of “Pflanzenanatomische Übungen für Fortgeschrittene (University of Vienna)
WS 2007 - SS 2013	Lector of “Pflanzenanatomie Übungen” (University of Vienna)
WS 2011 - WS 2012	Lector of “ Struktur der Pflanze” (University of Vienna)
SS 2012	Lector of “Pflanze, fertig los!” (University of Vienna, Children summer school)

Publications

Scientific journals

2013	Co-Author, Valledor, L., et al., Systemic cold stress adaption of <i>Chlamydomonas reinhardtii</i> , Mol. Cell Proteomics
2013	Hanak et al., Draft genome of poplar endophyte <i>Paenibacillus</i> sp. P22 , (submitted)
2013	Hanak A. M., Ulrich K. Ewald D., Weckwerth W., A novel endophyte increases root formation and growth in cuttings of poplar – a potential strategy for short-rotation poplar plantation , (manuscript in preparation)
2013	Hanak A. M., Fagner L., Ulrich K., Wawrosch C., Ewald D., Kopp B., Weckwerth W., Investigation of the Interaction of Endophytes and Poplar Plants in <i>in-vitro</i> Cultures and in Field Trials (submitted)

Conference presentations - posters

2012	Investigation of the Interaction of Endophytes and Poplar Plants in <i>in-vitro</i> Cultures and in Field Trials Hanak AM, Fagner L, Ulrich K, Wawrosch C, Ewald D, Kopp B and Weckwerth W 2 nd Symposium on Horticulture in Europe, France
2010	A Systems Biology Approach Combining Metabolomics, Proteomics, Growth Analyses and Cell Biology Investigating a Beneficial Poplar-Endophyte Interaction Hanak AM, Fagner L, Fuchs K, Kang Y-B, Ulrich K, Wawrosch C, Ewald D, Kopp B and Weckwerth W 5 th International Poplar Symposium – <i>Poplars and willows: from research models to multipurpose trees for a biobased society</i> , Orvieto, Italy

2010	Metabolomics in Poplar Research Fragner L, Hanak AM, Kang Y-B, Ulrich K, Fuchs K, Watzka M, Ewald D, Wawrosch C, Richter A, Wanek W, Kopp B and Weckwerth W <i>Metabolomics 2010 Conference</i> , Amsterdam, Netherlands
2009	Anatomical differences in adult plant organs of <i>Medicago truncatula</i> during drought- and salt-stress: symbiotic nitrogen fixation leads to stress alleviation Hanak AM and Wienkoop S COST FAO603 Europe, Nitra

Vienna, January 2014